MORPHO-MOLECULAR TAXONOMY AND SPECIES DIVERSITY OF NEMATODE-TRAPPING FUNGI IN YUNNAN PROVINCE, CHINA

FA ZHANG

DOCTER OF PHILOSOPHY
IN
BIOSCIENCES

SCHOOL OF SCIENCE
MAE FAH LUANG UNIVERSITY
2023

MORPHO-MOLECULAR TAXONOMY AND SPECIES DIVERSITY OF NEMATODE-TRAPPING FUNGI IN YUNNAN PROVINCE, CHINA

FA ZHANG

THIS DISSERTATION IS A PARTIAL FULFILLMENT OF THE REQUIREMENTS FOR THE DEGREE OF DOCTOR OF PHILOSOPHY IN BIOSCIENCES

SCHOOL OF SCIENCE
MAE FAH LUANG UNIVERSITY

2023

MORPHO-MOLECULAR TAXONOMY AND SPECIES DIVERSITY OF NEMATODE-TRAPPING FUNGI IN YUNNAN PROVINCE, CHINA

FA ZHANG

THIS DISSERTATION HAS BEEN APPROVED
TO BE A PARTIAL FULFILLMENT OF THE REQUIREMENTS
FOR THE DEGREE OF DOCTOR OF PHILOSOPHY
IN
BIOSCIENCES
2023

EXAMINATION COMMITTEE

.....CHAIRPERSON
(Assoc. Prof. Rajesh Jeewon, Ph. D.)

.....ADVISOR
(Saranyaphat Boonmee, Ph. D.)

.....EXAMINER
(Thilini Chethana Kandawatte Wedaralalage, Ph. D.)

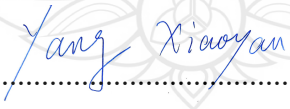

.....EXTERNAL EXAMINER
(Prof. Xiaoyan Yang, Ph. D.)

.....EXTERNAL EXAMINER
(Prof. Zong-Long Luo, Ph. D.)

ACKNOWLEDGEMENTS

As my graduate journey comes to a close, I am filled with gratitude for all the experiences I've had, both joyful and sorrowful, which have been the building blocks of my growth. Looking back over 13 years of academia, I consider myself incredibly fortunate for having met individuals who have significantly shaped my life. Through their scolding, whipping, encouragement and support, I gradually found the direction and meaning of life amidst confusion and anxiety, learning the true meaning of dedication.

I want to express my heartfelt gratitude to Prof. Kevin D. Hyde and Dr. Saranyaphat Boonmee. In 2017, I had the privilege of meeting Prof. Hyde. Not only did he provide me with the opportunity to study at Mae Fah Luang University, but he also offered me valuable guidance in my research. More importantly, Prof. Hyde taught me by example the importance of perseverance and the courage to explore and challenge in scientific research. His passion for scientific research deeply influenced me, making me more determined on my scientific journey. Dr. Boonmee has been the person who has helped me the most during my postgraduate studies. Since enrolling, the communication barrier arising language differences posed many challenges for Dr. Boonmee and me. However, she did not shun me; instead, she patiently guided and communicated with me. All my achievements were made possible through her patient assistance, with some manuscripts undergoing more than a dozen revisions under her guidance. These processes have helped me improve my writing skills and research capabilities. Dr. Boonmee's strict requirements for details and his deep dedication to research have benefited me greatly. With her guidance, I gradually overcame the language barrier and made certain achievements in scientific research. Her meticulous guidance and selfless sharing have allowed me to deeply understand the essence of scientific research and have made me more steadfast and courageous on the path of scientific research.

I am also especially grateful to my teachers, Prof. Yang Xiao-Yan and Prof. Xiao Wen! In September 2011, I entered university for my undergraduate studies with confusion, which caused me immense anxiety. Fortunately, joining Prof. Yang's research group changed everything for me. Prof. Yang has been the most crucial person in changing my life path and guiding me on my academic journey. She taught me microbiological experimental techniques and guided me through the process of writing research reports and papers. And more importantly, under her words and deeds, I gradually found the attitude that can make my heart peaceful (not to be satisfactory, but to have a clear conscience). This is the 13th year that Prof. Yang has guided me. Over these years, I have watched her hair gradually turn white as I grew up under her tutelage. Under Prof. Yang's guidance, encouragement and meticulous care, I gradually found the secret of a happy life, and also strengthened my determination to go on the road of scientific research. Benefiting from Prof. Yang's guidance, I was fortunate enough to meet the second mentor of my life, Prof. Xiao Wen. After graduating from my undergraduate studies in 2015, Prof. Xiao provided me with the opportunity to continue my studies at Institute of Eastern Himalayan Biodiversity Research. If Prof. Yang's care, support, and tolerance are akin to that of my mother, then Prof. Xiao's scolding and urging resemble more that of a stern yet wise father. When I was lost and hesitant, Prof. Xiao always knew when to scold me harshly or gently guide me forward. It is under his guidance that I learned how to face failure and uncertainty in life. During my time with Prof. Xiao and Prof. Yang, I was deeply impressed by their love for life and dedication to their work. Their towering figures have become the unwavering lighthouses in my life.

I extend my sincere thanks to Dali University (Institute of Eastern Himalaya Biodiversity Research) and Mae Fah Luang University (Center of Excellence in Fungal Research) for providing the platforms for study and research and for their support throughout. During my research, I received a thesis writing grant from Mae Fah Luang University (No. 0375, 80,000 THB), which greatly helped alleviate the issue of limited research funding. All the achievements and growth over the years have been made

possible under these two platforms. Additionally, I would like to thank all the classmates who helped me complete my research, such as Yang Yao-Quan, Zhou Fa-Ping, Li Zheng-Qiang, Yang Xin-Ju, Zhou Xin-Juan, and Deng Wei. They made significant contributions to fungal isolation, data collection and analysis, without which I would have had difficulty completing all the work on my own. In the process of writing and revising my articles, I received invaluable assistance from many individuals, such as Prof. Liu Xing-Zhong, Prof. Yu Ze-Fen, Prof. Jayarama D. Bhat, Prof. Rajesh Jeewon, Prof. Alexander R. Schmidt, Dr. Luo Zong-Long, Dr. Shang Qiu-Ju, Dr. Jutamart Monkai, and Dr. Sinang Hongsanan. Many of their suggestions have greatly improved the quality of my work.

In handling daily affairs, I also received selfless assistance from Dr. She Rong, Dr. Li Yan-Peng, and Dr. Zhao Cheng-Fa. The contributions of everyone was indispensable, enabling my research to progress smoothly. On the path of scientific research, I deeply appreciate the power of teamwork and have learned how to communicate and collaborate with people from different backgrounds. Thank you for your support and assistance, which have enabled me to make continuous progress in research and have provided me with valuable experience for my academic career.

I also want to thank my seniors and friends who have accompanied and helped me on this journey, including Dr. Luo Zong-Long, Dr. Jiang Hong-Bo, Dr. Li Jun-Fu, Dr. Huang Shi-Ke, Shen Hong-Wei, Ma Jian, Xu Rong-Ju, Fang Xue-Lan, Tang Xia, Wang Xin-Yu, Chen Gang, Ni Jun and Li Jing-Chao. With their companionship and guidance, I have spent seven fulfilling years of my postgraduate life. Thanks to all the teachers, classmates, and friends I have met during my PhD. Every exchange and discussion, every collaboration and assistance, has been invaluable to me. These valuable experiences have not only enriched my research life but also helped me grow into a more mature and comprehensive individual.

Finally, I want to sincerely thank my family, who are my strongest support. Regardless of the difficulties and challenges I face, my family always provides me with unconditional support and love. Their encouragement and understanding are essential driving forces that have enabled me to persist to the end and complete my studies. The love of my family has filled me with warmth and strength, serving as the cornerstone of my continuous progress.

Although my postgraduate journey is coming to an end, the path of scientific research is just beginning. In fact, all the above expressions of gratitude cannot fully repay their immense kindness. All I can do is to uphold their excellent qualities and continue to forge ahead on life's path. I will carry the knowledge, skills, enthusiasm, and sense of responsibility they have instilled in me, continuously explore the unknown, dare to innovate, and strive to make more meaningful contributions in my field of expertise. At the same time, I also hope to become a role model and guide for future generations, just as my mentors and predecessors have been for me.

Thank you, everyone, for being part of my journey.

Fa Zhang

Dissertation Title Morpho-Molecular Taxonomy and Species Diversity of Nematode-Trapping Fungi in Yunnan Province, China

Author Fa Zhang

Degree Doctor of Philosophy (Biosciences)

Advisor Saranyaphat Boonmee, Ph. D.

ABSTRACT

Among the approximately 160,000 described fungal species, about 0.1% possess the capability to form specialized trapping structures through vegetative hypha or conidia to capture nematodes for nutrient, these are known as Nematode-Trapping Fungi (NTF). Presently, over 180 NTF species produce eight types of trapping structures have been identified within *Zoopagomycota* (*Zoopagales*), *Basidiomycota* (*Polyporales* and *Agaricales*), and *Ascomycota* (*Orbiliomycetes*). Among them, NTF in *Orbiliomycetes* (ONTF) have emerged as a core group in NTF research due to they exhibit significant potential for application in the biological control of harmful nematodes, while also holding high research value in the theoretical studies on fungal evolution, regulation and balance of ecosystems.

The primary research objectives in the field of nematophagous fungi revolve around optimizing the utilization of NTF and unraveling their evolutionary processes. Understanding the diversity and phylogenetic relationships of ONTF serves as the foundational basis for achieving these core objectives. Therefore, this study selected Yunnan Province, China, known for its rich biodiversity, as the research area. Soil samples were collected from terrestrial forests, freshwater, and burned forests habitats. ONTF were isolated and identified. The aim is to explore ONTF diversity and discover new ONTF species

A total of 3929 isolates representing 91 ONTF species were isolated from 3788 samples. From 1710 terrestrial soil samples and 1710 freshwater sediment samples, 1832 strains representing 49 species and 1623 strains representing 42 species of ONTF were respectively isolated. In both habitats, *Arthrobotrys* is consistently dominant, with 1734 strains representing 40 species and 1536 strains representing 35 species, whereas the genera *Dactylellina* and *Drechslerella* were detected in lower numbers, with only 98 strains representing nine species and 60 strains representing seven species, respectively. A total of 474 strains representing 38 species of ONTF were isolated from 368 burnt forest soil samples, with the genus *Dactylellina* being the dominant group (264 strains, 22 species), follow by *Drechslerella* (115 strains, nine species) and *Arthrobotrys* (95 strains, seven species)

This study identified 42 new NTF species, accounting for 29% of all known NTF, indicating a substantial number of undiscovered ONTF resources in nature. Seven new *Arthrobotrys* species, one new *Dactylellina* species, and two new *Drechslerella* species were discovered from 1,710 terrestrial soil samples. Twelve new *Arthrobotrys* species were obtained from 1,710 freshwater sediment samples, suggesting that aquatic habitats contain a significant number of undiscovered NTF. Geographically, 77.3% (17 species) of the new species were found in the northwest of Yunnan Province (three parallel rivers region), indicating this area may be a hot-spot for NTF distribution. Furthermore, 20 new species of rare NTF (17 new *Dactylellina* species and three new *Drechslerella* species) were isolated from 368 burned forest soil samples. Finding so many new species in such a limeted samples suggesting that forest fires have a significant impact on ONTF and more rare microbial resources may be unearthed in burned forests.

The discovery of *Arthrobotrys blastospora* among the 42 new species holds significant importance for the evolutionary research of ONTF. *A. blastospora* produces yeast-like blastospores, which is distinct from all modern ONTFs and remarkably similar to the earliest fossil of carnivorous fungi (*Palaeoanellus dimorphus*). The identification of

this species not only confirms the authenticity of this fossil and its relationship with modern NTF but also provides crucial information for the evolutionary of NTF.

This study provides the new insights into the diversity and distribution of ONTF, laying the foundation for ecology and evolutionary on ONTF. Furthermore, the discovery of new ONTF species enriches the genetic resources available for the taxonomy and application, offering abundant materials for further investigation.

Keywords: 42 New Taxa, Burned Forest, Diversity, Nematophagous Fungi, *Orbiliomycetes*, Trapping Structure

TABLE OF CONTENTS

TABLE OF CONTENTS (continued)

TABLE OF CONTENTS (continued)

TABLE OF CONTENTS (continued)

TABLE OF CONTENTS (continued)

LIST OF TABLES

LIST OF FIGURES

LIST OF FIGURES (continued)

LIST OF FIGURES (continued)

LIST OF FIGURES (continued)

Figure **Page**

LIST OF FIGURES (continued)

LIST OF FIGURES (continued)

LIST OF FIGURES (continued)

LIST OF FIGURES (continued)

LIST OF FIGURES (continued)

LIST OF FIGURES (continued)

LIST OF FIGURES (continued)

LIST OF FIGURES (continued)

LIST OF FIGURES (continued)

CHAPTER 1

INTRODUCTION

1.1 Nematophagous Fungi

Nematodes and fungi are both important components of the soil ecosystem, directly or indirectly involved in nearly all ecological processes. They play a crucial role in maintaining the material, energy cycles and ecological balance of the soil ecosystem (Christensen, 1989; Dighton & White, Mekonen et al., 2017; Lazarova et al., 2021). The interaction between nematodes and fungi is complex. On one hand, some nematodes feed on fungi and the decomposition products of fungi serves as a source of nutrition for nematodes (Okada et al., 2005; Morris et al., 2014). On the other hand, in soil habitats with complex biological composition and intense competition for resources, fungi face intense nutritional competition pressure. Through a long process of adaptive evolution, certain soil fungi have acquired the ability to obtain nutrients from the most abundant soil animals, nematodes. Theses fungi are known as nematophagous fungi, which obtain nutrition by parasitizing, colonizing, poisoning, capturing and digesting nematodes, and serve as the primary regulatory factors for nematodes in ecosystems (Liu et al., 2009; Dackman et al., 2021). These fungi are widely distributed in almost all soil-related habitat, including the sediment from freshwater, marine and hot spring, the soil from forest and agricultural, animal feces, tree trunks and bird claws. etc. (Gray, 1983; Swe et al., 2009; Dackman et al., Freitas et al., Zhang et al., 2021; Zhang & Hyde, Liu et al., 2014).

As an important component of the natural world, parasitic nematodes such as root-knot nematodes, cyst nematodes, pine wood nematodes and intestinal parasitic nematodes cause significant annual losses to global agriculture, forestry, livestock farming and even aquaculture industries. There are over 4000 known species of plant-parasitic nematodes that pose threats to nearly all economic crops (Bernard et al., 2017;

Dayi, 2024). Traditional control methods, such as crop rotation and breeding for nematode-resistant varieties are time-consuming, labor-intensive, and often yield limited results (Rahman et al., 2007; Timper, 2014). Although chemical pesticides can rapidly eradicate nematodes with good efficacy, their broad spectrum of action (affecting not only parasitic nematodes but also harmless nematodes and even other soil organisms) leads to disruption of ecological balance, environmental pollution, pesticide residues and the emergence of nematode resistance (Lamberti et al., 2000; Haydock et al., 2006; Hussain et al., 2017). Relying on chemical pesticides for nematode control is not a sustainable solution in the long term. Therefore, the development of ecologically friendly and long-lasting nematode bio-control agents using natural enemies of nematodes, such as nematophagous fungi has gained widespread attention (Lamovšek et al., 2013; Braga & de Araújo, Norabadi et al., 2014; Stirling, 2018; Ahmad et al., 2021).

Among the approximately 160,000 described species of fungi, around 0.5% are nematophagous fungi (Yang et al., 2012; Herrera-Estrella et al., 2016; Yadav et al., 2023). As a highly specialized group within the fungal kingdom, the diversity and evolution of nematophagous fungi can provide valuable insights into the origin and evolution of fungi, making them an indispensable component in understanding the evolutionary history of fungi. Furthermore, the predatory ability of nematophagous fungi is often considered an adaptive evolution to nutrient-deficient habitats. Therefore, these highly specialized fungi are regarded as ideal group for studying adaptive evolution in biology (Yang et al., 2007, 2012). In conclusion, nematophagous fungi possess significant research value both in practical applications and theoretical studies.

Research on nematophagous fungi can be traced back to 180 years ago. In 1839, Corda established the genus *Arthrobotrys* with *Arthrobotrys superba* Corda as the type species (Corda, 1839). In 1850, Fresenius reported the second new species of this genus, *A. oligospora* Fresenius (Fresenius, 1850). In 1876, Sorokin observed that members of the genus *Arthrobotrys* could infect nematodes (Sorokin, 1876). In 1888, Zopf observed that members of *Arthrobotrys* could capture nematodes using adhesive networks, definitively establishing the relationship between these fungi and nematodes, marking the formal beginning of research on nematode-trapping fungi (Zopf, 1888). In 1874, Lohde observed that *Harposporium anguillulae* could penetrate the body wall of

Anguillule sp. and produce conidiophores and crescent-shaped conidia (Lohde, 1874), bringing endoparasitic fungi into the spotlight. However, research in this field stagnated for over 20 years until Sommerstorff reported *Zoophagus insidians* in 1911, which captures flagellates using adhesive spheres (Sommerstorff, 1911), and conducted a series of studies around *Zoophagus* (Gicklhorn, 1922; Arnaudow, 1923; Valkanov, 1931). During this period, due to methodological limitations, progress in studying nematophagous fungi was extremely slow. It was not until 1933 that Drechsler, with keen observational skills, discovered that placing chopped plant root pieces on a nutrient-poor culture medium favored the growth and reproduction of nematodes, inducing the germination and growth of nematophagous fungi (Drechsler, 1933ab), leading to the discovery of a series of nematophagous fungi using this method. Drechsler and Duddington's series of studies from 1933 to 1970 gradually unveiled the mystery of nematophagous fungi, revealing that they are not a rare group; rather, they are widespread in various ecosystems (Drechsler, 1934, 1937, 1940, 1944, 1946, 1947, 1952, 1954; Duddington, 1940, 1951, 1955).

With the gradual optimization of isolation methods, nearly a thousand species of nematophagous fungi have been reported. Based on their mechanisms of action on nematodes, they can be divided into four major categories.

1. Endoparasitic fungi, first reported by Lohde (Lohde, 1874), primarily parasitize nematodes or rotifers through their adhesive spores and ingested spores. The adhesive spores of these fungi can adhere to the surface of nematodes and invade their bodies. Some species can produce adhesive zoospores that are attracted to and move towards nematodes (Barron & Percy, 1975; Glockling & Beakes, 2000). The ingested spores are adapted to the feeding behavior of nematodes, germinate, kill and digest them inside their bodies after being fed by nematodes (Drechsler, 1946; Li et al., 2000; Wang et al., 2007). Some species can even produce metabolites that are attractive to nematodes, thus increasing their chances of being eaten. Endoparasitic fungi are a taxonomically heterogeneous group, with over 150 species reported in at least 25 genera in the *Ascomycota*, *Basidiomycota*, *Chytridiomycota*, *Zygomycota* and *Oomycota* (Zare et al., 2000; Van Vooren & Audibert, 2005; Li et al., Liang et al., 2006; Balazy et al., 2008; Kurihara et al., 2009; Evans et al., 2010).

2. Toxic fungi refer to a group of fungi that produce metabolites to poison nematodes (Li et al., 2000; Zhang et al., 2011). Currently, about 300 species of fungi have been reported to possess this ability, with nearly 200 species belonging to nearly 80 genera in the *Basidiomycota*, and over 90 species belonging to about 40 genera in the *Ascomycota* (Zhang et al., 2011). Meanwhile, there are about ten species in *Zygomycota* (Zhang et al., 2011). Nematocidal metabolites produced by these fungi are a major research topic in the field of nematophagous fungi. At present, approximately 250 nematocidal metabolites have been identified, including terpenes, macrolides, alkaloids, peptides, heterocycles, aromatics, fatty acids, quinones and alkynes (Zhang et al., 2011).

3. Opportunistic fungi (egg parasitic and female parasitic fungi) can parasitize nematode eggs, cysts and female (Liu et al., 2009; Zhang et al., 2011). In 1877, German scientist Kuhn discovered that the females of the sugar beet cyst nematode, *Heterodera schachtii*, were infected by a fungus, which he named *Tarichium auxiliare* (*Catenaria auxiliaria*), marking the first reported opportunistic fungus (Kühn, 1877). Currently, more than 400 species of opportunistic fungi have been found in over 80 genera across various taxonomic units (Li et al., 2000; Zhang et al., 2011). These fungi typically infect hosts that are immobile or have limited mobility, serving as unspecialized nematophagous fungi (Zhang et al., 2011). Their life cycle usually does not depend on nematodes, and they can survive independently in soil.

4. Nematode-trapping fungi refer to a group of fungi that can form specialized structures through vegetative hypha differentiation to capture nematodes (Li et al., 2000; Zhang & Mo, 2006; Zhang & Hyde, 2014). The first report of these fungi was made by Corda on *Arthrobotrys superba* (Corda, 1839), followed by Sorokin and Zopf's discovery of the predatory and prey relationship between the adhesive networks produced by *Arthrobotrys* and nematodes (Sorokin, 1876; Zopf, 1888). Since then, more and more species and trapping structures have been discovered. Currently, at least 180 species of nematode-trapping fungi have been found in *Ascomycota*, *Basidiomycota*, and *Zygomycota*. Approximately 80% of these species are predatory members of *Orbiliaceae*, *Orbiliomycetes* (Li et al., 2000; Zhang & Hyde, 2014; Jiang et al., 2017).

Due to the objective existence of fungal diversity and evolutionary complexity, the classification of the above four major groups is relative, and there is still significant debate when determining the classification of a particular species. For example, *Fusarium xiangyunensis* can adhere to nematodes with adhesive spores, as well as produce toxins to paralyze nematodes (Zhang et al., 2020); *Penicillium lilacinum* can parasitize nematode cysts and eggs, while also producing toxins that are lethal to nematodes (Girardi et al., 2022; Moliszewska et al., 2022); some species in the *Dactylellina* of nematode-trapping fungi produce non-constricting rings that can be defined as trapping structures when it not detached, but can also be defined as parasitic structures when detached from the stalk and attached to nematode body (Zhang & Mo, 2006; Zhang & Hyde, 2014).

In the terms of biological control of nematodes, most endoparasitic fungi are specialized parasites with a narrow host range. Their life cycle largely depends on the presence of the host nematodes or rotifers, making it difficult for these fungi to thrive in complex and dynamic soil environments (Jaffee et al., 1993; Nordbring-Hertz et al., 2001; Liu et al., 2009; Dackman et al., 2021). Therefore, the potential application of this group of fungi in nematode biological control is limited. The use of nematicidal metabolites produced by toxic fungi for nematode control essentially falls under chemical control, which may also face the problem of increased nematode resistance. Although toxic fungi show certain potential in the bio-control of nematodes, there are still many issues that need to be addressed in practical applications (Degenkolb & Vilcinskas, 2016; Nguyen et al., 2018). Opportunistic fungi do not strictly rely on nematodes for their life cycle and can survive independently in soil. However, these fungi generally infect weak or immobile female nematode or eggs and have weak ability to actively kill nematodes, making them unsuitable for developing specific bio-control agents against nematodes (Ashraf & Khan, 2005; Akhtar et al., 2015). However, many species of these fungi, such as *Paecilomyces lilacinus*, *Gliocladium roseum* and *Trichoderma harzianum*, not only can infect nematodes but also exhibit capabilities to suppress other pathogenic microorganisms and promote plant growth (Morales et al., 2011; Akladious & Abbas, 2014; Chen et al., 2023). Therefore, using them as raw materials for bio-fertilizers is a good choice. It is worth noting that almost all nematode-trapping fungi can live saprophytically or as predators in their habitats, and can

maintaining stable population sizes in most soil ecosystems (Liu et al., 2009; Singh & Pandey, 2014; Yang et al., 2020). NTF exhibit high species and trapping structural diversity, with strong predatory abilities, making them the most promising group for bio-control applications among nematophagous fungi (Pandit et al., 2014; Kang et al., 2019; Zhang et al., 2020).

Furthermore, from a theoretical research perspective, the evolution of nematophagous function and structure is one of the core research aspects on nematophagous fungi. Endoparasitic fungi heavily rely on nematodes, making their isolation difficult. In addition, their parasitic structures are single, and their species are scattered taxonomic distribution (Zhang et al., 2011). Therefore, their evolutionary research cannot be advanced in the short term and has not received much attention. As for toxic and opportunistic fungi, it is difficult to confirm which species, metabolites or functional structures are specifically evolved for nematodes. Consequently, the evolutionary research of their nematode-feeding function has been largely ignored. In contrast, nematode-trapping fungi have become the core representative group for the theoretical research of nematophagous fungi evolution due to their relatively mature isolation methods, diverse and sophisticated trapping structures specifically evolved for nematodes, rich species diversity and concentrated taxonomic distribution (Zhang & Mo, 2006; Zhang & Hyde, 2014). Both are from practical application and theoretical research perspectives, nematode-trapping fungi exhibit significant research value.

1.2 Nematode-Trapping Fungi (NTF)

Nematode-trapping fungi (NTF) represent a unique group of carnivorous, asexual fungi. Under the stress of long-term nutritional deficiency, their ancestors evolved a survival strategy of catching nematodes with specialized trapping structures to obtain nutrition (Yang et al., 2012; Zhang et al., 2023). Due to their excellent environmental adaptability and broad-spectrum nematode-trapping function, these fungi have become the most promising bio-control materials for pathogenic nematodes (Su et al., 2017; Lafta & Kasim, 2019; Moosavi & Zare, 2020). Furthermore, due to their rich species diversity, diverse nematode-trapping structures and concentrated

taxonomic distribution, this group of fungi has also gradually become a representative group for fungal adaptive evolution research, as well as the core group for nematophagous fungi research (Yang et al., 2012; Li et al., 2016; Yang et al., Zhang et al., 2020).

Since stepping onto the research stage in 1839, the study of NTF has gradually matured over more than 180 years of accumulation (Corda, 1839). Taxonomically, NTF comprise a heterogeneous group. Currently, over 180 NTF species belonging to *Zoopagomycota* (*Zoopagales*), *Basidiomycota* (*Polyporales* and *Agaricales*) and *Ascomycota*, have been discovered, producing eight types of trapping structures (Li et al., 2000; Swe et al., 2011; Jiang et al., 2017).

Zoopagaceae, *Cochlonemataceae*, *Helicocephalidaceae*, *Sigmoideomycetaceae*, and *Piptocephalidaceae* within *Zoopagomycota* (*Zoopagales*) all possess carnivorous capabilities to varying degrees (Fowler, 1970; Dayal, 1975; Morikawa et al., 1993; Gams & Zare, 2003). Among them, nematode-associated species are mainly concentrated in *Zoopagaceae* and *Cochlonemataceae*. Within *Zoopagaceae*, species with clear nematophagous functions are mainly concentrated in the genera *Stylopage*, *Zoopage*, and *Zoophagus*. They predominantly capture nematodes using adhesive hyphae or adhesive protrusions on the hyphae, representing typical nematode-trapping fungi (Drechsler, 1939, 1941; Saikawa, 2021). Carnivorous species within *Cochlonemataceae* are mainly distributed among the genera *Amoebophilus*, *Aplectosoma*, *Bdellospora*, *Cochlonema*, *Endocochlus* and *Euryancale*. They produce adhesive or ingested spores to parasitize nematodes and other soil-dwelling animals, thus being categorized as endoparasitic fungi (Tanabe et al., 2000; Saikawa, 2021; Rahman et al., 2023). In theory, *Zoopagales* is a highly specialized group of nematophagous fungi that should be the core group for studying the origin and evolution of carnivorous fungi. However, due to the fact that most species of this group of fungi are strictly predatory or parasitic, isolating and cultivating them for subsequent research is extremely difficult, and their biological and evolutionary studies are almost stalled (Liu et al., 2009; Benny et al., 2016; Moosavi & Zare, 2020).

Within the *Basidiomycota*, species with nematophagous capabilities are distributed among nearly 20 genera, with species that clearly capture nematodes using trapping structures mainly concentrated in *Agaricales* and *Polyporales* (Tzean & Liou, 1993; Sivanandhan et al., 2017). The typical representatives of NTF in *Agaricales* are

Hohenbuehelia (*Nematoctonus*), *Coprinus* and *Stropharia*. The former captures nematodes using small balls covered with adhesive substances, while the latter two capture nematodes using numerous spike-like structures forming a spiny ball (Luo et al., 2004, 2006; Koziak et al., 2007; Zouhar et al., 2013; Koziak et al., 2007). *Hyphoderma* is the only genus of NTF in *Polyporales*, and all *Hyphoderma* species catch nematodes with stephanocysts (a kind of spherical cells produced from hypha or conidia, with a ring of spiny structures at the base and covered with sticky material on the surface) (Liou & Tzean, 1992; Tzean & Liou, 1993; Jiang et al., 2017). In addition, numerous studies have reported that NTF in *Basidiomycota*, including those with clearly identified trapping structures, can produce rich metabolites with nematicidal activity. Therefore, compared with their nematode-trapping functions, they are more commonly studied as sources of nematocidal metabolites.

Nematode-trapping fungi within *Ascomycota* are the main constituents of NTF. Currently, 147 species have been discovered to produce five types of trapping structures: adhesive knobs (the relationship between stalked adhesive knobs and unstalked adhesive knobs is debatable), adhesive branches, non-constricting rings (usually occur together with adhesive knobs), non-constricting rings and adhesive networks (Figure 1.1). All 147 NTF species belong to the predatory members of *Orbiliaceae* (the sole family in *Orbiliomycetes*, the earliest diverging lineage in *Pezizomycotina*) (Cooke, 1965; Zhang & Mo, 2006; Zhang & Hyde, 2014; Quijada et al., 2020; Zhang et al., 2022abc, 2023ab, 2024; Yang et al., 2023). They exhibit both saprophytic and carnivorous lifestyles in their habitats (Liu et al., 2009). Due to this diverse survival strategy, NTF in *Orbiliomycetes* are often widely distributed in various habitats with high abundance, serving as important regulators of nematode populations in nature and excellent materials for developing nematode bio-control agents (Gronvold et al., 1993; Szabó et al., 2012; Saxena, 2018; Moosavi & Zare, Zhang et al., 2020). Furthermore, their high species and morphological diversity (trapping structures, conidia, etc.), well-established research methods and concentrated taxonomic distribution make them a core group for studying the origin and evolution of carnivorous fungi (Ahrén & Tunlid, 2003; Li et al., 2005; Yang et al., 2007, 2012; Su et al., 2017).

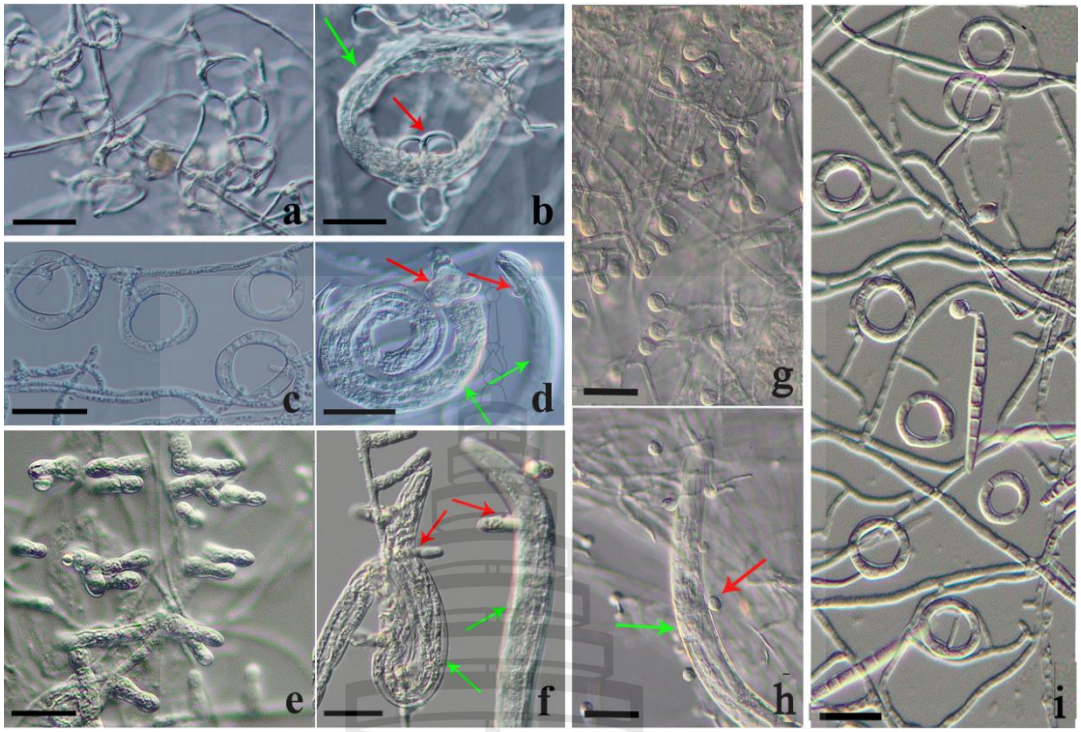

Figure 1.1 Trapping structures of nematode-trapping fungi in *Orbiliomycetes*. (a) Adhesive networks. (b) A nematode caught in adhesive networks. (c) Constricting rings. (d) Nematodes caught in constricting rings. (e) Adhesive branches. (f) Nematodes caught in adhesive branches. (g) Adhesive knobs. (h) A nematode caught in adhesive knobs. (i) Non-constricting rings and adhesive knobs. Bars: (a–i) = 20 μm. Red arrows point to trapping structures and green arrows point to captured nematodes

1.3 Nematode-Trapping Fungi in *Orbiliomycetes* (ONTF)

1.3.1 *Orbiliomycetes*

Orbiliomycetes is an early-diverging lineage within *Pezizomycotina*, *Ascomycota* (Pfister, 1997). It is a monoorder and monofamily groups (*Orbiliaceae*, *Orbiliales*) (Kimbrough, 1970). Research related to *Orbiliomycetes* can be traced back over 220 years (Persoon, 1801; Albertini & Schweinitz, 1805; Fries, 1815). Due to limited observation techniques at that time, researchers could only rely on macroscopic features such as the shape, color, texture and stalk of the apothecia to identify them. However, due to the objective existence of fungal diversity and convergent evolution, the identification methods based on macroscopic features often resulted in misclassification of *Orbiliomycetes* members into other groups such as *Helotiales*, *Phacidiales*, *Pezizales* or even *Basidiomycota* (Persoon, 1801; Fries, 1815; Baral et al., 2020). In 1932, Nannfeldt established *Orbiliaceae* based on the study of microscopic morphological characteristics. The family included three genera: *Orbilia*, *Hyalinia* and *Patinella*, and is characterized by its small, disc-shaped, waxy, translucent apothecia with bright colors, and colorless, tiny and usually single-celled ascospores (Nannfeldt, 1932). Before the 1990's, due to its unclear ecology and application value, *Orbiliaceae* was considered an unimportant ordinary group and received little systematic research attention. It was not until Pfister (1994) reported that the asexual generation of *Orbilia fimicola* belongs to the genus *Arthrobotrys* (a group of ONTF with sophisticated trapping structures and significant research and application value), that *Orbiliaceae* caught the attention of mycologists, and research in this field entered a new stage. In 1997, Pfister conducted DNA molecular phylogenetic studies and discovered that *Orbiliaceae* is a monophyletic group (Pfister, 1997). In 2003, Eriksson et al. found that *Orbiliaceae* and *Pezizales* are sister groups in molecular systematic, and they also discovered six informative nucleotides (CTAACC) on the SSU sequence that are present in all *Orbiliaceae* species but rare in other fungi (Eriksson et al., 2003). Based on these findings, *Orbiliaceae* was elevated to the order *Orbiliales*, and subsequently to the class *Orbiliomycetes* (Eriksson et al., 2003). Morphologically, the presence of highly refractive oil droplet-like structures called spore body (SB) within the

ascospores is the main distinguishing feature between *Orbiliomycetes* and other cup fungi (Baral et al., 2020).

Orbiliomycetes exhibit strong adaptability, being found in habitats ranging from deserts to grasslands and rainforests, from dead branches and fallen leaves to animal dung (Baral et al., 2020). Currently, the sexual-asexual relationships between *Orbiliomycetes* species and representative groups of NTF (*Arthrobotrys*, *Drechslerella*, *Dactylellina*) have been widely recognized (Pfister, 1994; Pfister & Liftik, 1995; Liu et al., 2005; Yu et al., 2006). It is precisely because of these relationships that significant progress has been made in the classification research of *Orbiliomycetes*. Eriksson, Baral, and Zhang believe that *Orbiliaceae* includes three sexual genera: *Hyalorbilia* Baral & G. Morson, *Orbilia* Frie and *Pseudorbilia* Zhang (Eriksson et al., 2003; Zhang et al., 2007; Baral et al., 2018). Subsequently, Baral proposed that *Orbiliaceae* should include seven sexual genera: *Amphosoma*, *Bryorbilia*, *Liladisca*, *Lilapila*, *Pseudorbilia*, *Hyalorbilia* and *Orbilia* (Baral et al., 2020). However, due to the high morphological diversity of anamorphic species within *Orbiliomycetes*, the taxonomic study of their anamorphic stage is much more complex. At present, more than 15 asexual genera have established sex-asexual relationship with *Orbiliomycetes* (Baral et al., 2020). Although there is no consensus on the taxonomic study of their asexual generations, as a highly specialized group within *Orbiliomycetes*, research on ONTF (*Orbiliomycetes* nematode-trapping fungi) is often conducted independently of other species in *Orbiliomycetes*.

1.3.2 Research History of Nematode-Trapping Fungi in *Orbiliomycetes*

As the core group of nematophagous fungi, research on ONTF is the focus of the entire study of nematophagous fungi. Its research history can be traced back to 1839 when Corda reported the first species, *Arthrobotrys superba* Corda, and established the genus *Arthrobotrys* (Corda, 1839). In 1850, Fresenius reported the second species of this genus *A. oligospora* Fresenius (Fresenius, 1850). At that time, both species were described as saprophytic fungi. In 1870, Woronin observed that the hyphae of *A. oligospora* would bend and merge into complex network structures, but the function of this structure was not clear yet (Voronin, 1870). In 1876, Sorokin discovered that this network structure could infect nematodes, and in 1888, Zopf confirmed that the network

structure produced by *A. oligospora* could catch nematodes, marking the start of ONTF research (Sorokin, 1876; Zopf, 1888). Subsequently, due to limitations in isolation methods, relevant research stagnated for a long time.

The rapid development of this group fungi can be attributed to the American scientist Drechsler (1933–1975). While studying the root-parasitic *Phycomycetes* and *Oomycetes* of higher plants, Drechsler cultured crushed diseased roots on a nutrient-poor medium (an environment conducive to the reproduction and growth of nematodes, and other small animals; the presence of nematodes promoted the germination and growth of nematophagous fungi), isolating and publishing a series of ONTF and endoparasitic fungi (Drechsler, 1933ab, 1934, 1937, 1940, 1944, 1946, 1947, 1952, 1954). Under Drechsler's guidance, scholars found that using a nutrient-poor medium supplemented with nematodes induction significantly increased the efficiency of ONTF isolation. Consequently, the method for ONTF isolation gradually improved, leading to extensive diversity surveys conducted by researchers worldwide, resulting in the discovery of numerous new species and predatory structures. These studies highlighted that ONTF is not a rare group, as they are widely distributed in various climates (from polar to tropical regions) and habitat types (forests, freshwater, marine environments, and hot springs) on diverse substrates (soil, sediments, decaying wood, tree trunks, bird claws, and animal feces) (Soprunov & Galiulina, 1951; Duddington, 1954; Kim et al., Zhang et al., 2001; Su et al., 2007; Mo et al., 2008; Swe et al., 2009; Kumar et al., 2011; Liu et la., 2014; Zhang et al., 2020). Subsequently, with the expansion of research teams, maturation of research methods and emergence of new technologies, ONTF research diversified into multiple directions. For example, the increasing threat of plant and animal pathogenic nematodes drove the large-scale screening of highly effective bio-control strains (Pandey, 1973; Graminha et al., 2005; Saxena, 2018); the discovery of two nematicidal compounds (oligospooron and 4,5-dihydrooligosporon) pioneered the study of nematicidal metabolites (Anderson et al., 1995); genomics and gene editing technologies advanced the research on fungal trapping mechanisms and engineered fungal strains (Ahman et al., 2002); the development of molecular biology techniques propelled ONTF systematics and evolutionary studies into core areas (Yang et al., 2007, 2012; Su et al., 2017). While the current research directions are diverse, almost all

studies can be summarized into three main questions: 1) Taxonomy and evolutionary; 2) Applications; 3) Diversity.

1.3.3 Taxonomy of Nematode-Trapping Fungi in *Orbiliomycetes*

Taxonomy is the fundamental basis for understanding organisms. The taxonomy of ONTF is one of the main research contents in this field. Similar to most other fungal, the taxonomy of ONTF has gone through a period of initial confusion, followed by the traditional taxonomy period based on comparative morphology and the recent molecular systematic taxonomy period. Initially, due to the high morphological diversity, the objective existence of convergent evolution and the lack of systematic comparative studies, ONTF species were scattered into 26 genera such as *Arthrobotrys*, *Anulosporium*, *Didymozoophaga*, *Dactylaria* and *Monacrosporiella* (Zhang & Mo, 2006; Zhang et al., 2022). By 1960, through systematic comparative morphology studies, ONTF was classified into three genera based on their morphology of conidia: *Arthrobotrys* produces ovoid, elliptical, pyriform, reniform, or digitate, 0–3-septate conidia, captures nematodes using adhesive networks, adhesive knobs and constricting rings; *Dactylella* produces cylindrical, clavate, lanceolate, or fusiform conidia with more than three septa evenly distributed, captures nematodes using adhesive networks, adhesive knobs, and non-constricting rings, also including species without trapping structures; *Monacrosporium* produces fusiform, elliptical, oval, obovate conidia with a super cell (the cell that are significantly larger than other cells), captures nematodes using adhesive networks, adhesive knobs, adhesive branches, non-constricting rings and constricting rings (Figure 1.2) (Zhang & Mo, 2006). Although this classification system largely resolved the confusion in ONTF classification, the scientific validity of this classification system has been a subject of controversy due to differences in emphasis on various morphological features among scholars, challenges in defining the morphological traits of certain species, and the question of whether a classification system based on morphological conidia can accurately reflect the natural phylogenetic relationships within this group. Researchers have started using molecular techniques such as restriction fragment length polymorphism (RFLP), random amplified polymorphic DNA (RAPD), and molecular phylogenetics to investigate the classification of ONTF (Pfister, 1997; Ahrén et al., 1998; Scholler et al., 1999; Yang et

al., 2007, 2012; Zhang & Hyde, 2014). Ahren et al. (1998) investigated the phylogenetic relationships of 15 ONTF species using 18S rDNA and suggested that the type of trapping structure is more meaningful for ONTF classification compared to conidia morphology. Scholler et al. (1999) supported the findings of Ahren et al. (1998) based on their study of ONTF phylogenetic relationships using 18S rDNA, 5.8S rDNA, and ITS sequences, and classifying ONTF into *Dactylellina* (characterized by adhesive knobs and non-constricting rings for capturing nematodes), *Gamsylella* (capture nematodes using unstalked adhesive knobs and adhesive branches), *Arthrobotrys* (producing adhesive networks to catch nematodes) and *Drechslerella* (producing constricting rings for capturing nematodes) (Scholler et al., 1999; Zhang & Hyde, 2014). Subsequent studies further emphasized the significant importance of trapping structures in the classification of ONTF and refined the taxonomy of ONTF. Currently, the classification system that divides ONTF into the genera *Arthrobotrys, Dactylellina* and *Drechslerella* based on the type of trapping structure is widely accepted (Li et al., 2005; Yang et al., 2007, 2012; Zhang et al., 2022, 2023).

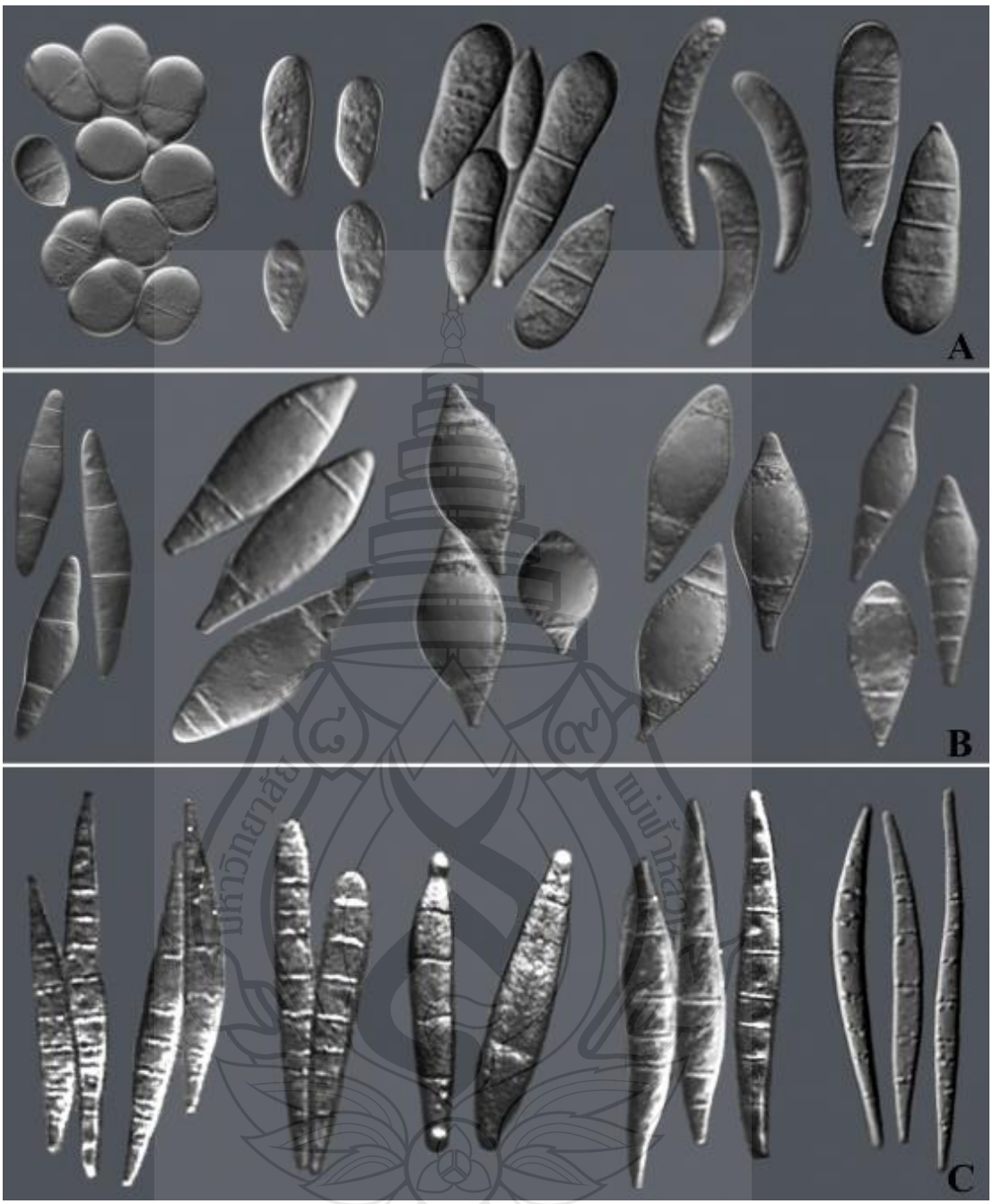

Figure 1.2 Conidia types of nematode-trapping fungi in *Orbiliomycetes*. (A) Arthrobotrys-shaped conidia represent the conidia type produced by *Arthrobotrys* species. (B) Monacrosporium-shaped conidia represent the conidia type produced by *Monacrosporium* species. (C) Dactylella-shaped conidia represent the conidia type produced by *Dactylella* species

Arthrobotrys was initially established by Corda (1839) with *A. superba* Corda as the type species. Its original generic diagnosis included clustered uniseptate conidia arising from nodes on conidiophores. Subsequently, more species were reported, and through comparative morphological studies, the generic diagnosis were revised to ovoid, elliptical, pyriform, reniform, or digitate, 0–3-septate conidia clusters growing on nodes or short denticles of conidiophores (Haard, 1968; Subramanian, Schenck et al., 1977; Zhang & Mo, 2006). Subsequent research using modern molecular biology techniques further revised the generic characteristics of *Arthrobotrys* to produce adhesive networks for capturing nematodes (Ahrén et al., 1998; Scholler et al., 1999; Li et al., 2005; Zhang & Hyde, 2014). Currently, a total of 74 *Arthrobotrys* species have been reported, making it the largest genus within ONTF (Li et al., 2000; Zhang & Mo, 2006; Swe et al., 2011; Liu et al., Zhang & Hyde, 2014; Zhang et al., 2022; Zhang et al., 2023ab). *Arthrobotrys* species also exhibits the greatest diversity in conidia morphology, which can be categorized into arthrobotrys-shaped, dactylellina-shaped and monacrosporium-shaped three types (Figure 1.2) (Zhang & Mo, 2006). Most *Arthrobotrys* species possess strong saprophytic ability, reproductive capacity and competitive ability, allowing them to rapidly establish dominance in various habitats (Mo et al., 2008; Wachira et al., 2009; Swe et al., 2009; Singh et al., 2014; Deng et al., 2023). Consequently, they exhibit significant potential for development in biological control applications.

Dactylellina was originally established by Morelet (1968) with *Da. leptospora* M. Morelet as the type species, and the genus was initially defined as producing elongate, fusiform conidia. Subsequently, Scholler et al. (1999) revised the generic characteristics based on phylogenetic analysis of multiple DNA fragments, redefining the genus to produce stalked adhesive knobs and non-constricting rings (occurring simultaneously with adhesive knobs) for nematode capture. Further molecular systematic studies further refined the generic characteristics to include adhesive knobs, adhesive branches and non-constricting rings for nematode capture (Li et al., 2005; Yang et al., 2007). Currently, *Dactylellina* comprises a total of 51 species (34 species catch nematodes with adhesive knobs, seven with adhesive branches, and ten with both adhesive knobs and non-constricting rings) (Li et al., 2006; Su et al., 2008; Zhang & Hyde, 2014; Kavitha et al., Zhang et al., 2020; Crous et al., 2022). The species of

Dactylellina exhibit various predatory structures, making them valuable in the evolutionary study of ONTF. Additionally, *Dactylellina* species generally demonstrate strong nematode predation abilities, indicating great potential for application in nematode bio-control (Ji et al., Yang et al., 2020; Kumar, 2024).

Drechslerella is the smallest genus within ONTF with 22 species. It was separated from *Monacrosporium* by Subrammanian based on the presence of filamentous appendages on the conidia of *Dr. Acrochaeta* (Subramanian, 1963). However, Liu and Zhang suggested that the filamentous appendage on the conidia are germ tubes of the conidia germination, which is also present in many *Arthrobotrys* and *Dactylellina* species. Therefore, this structure cannot serve as a valid taxonomic criterion, and *Drechslerella* is an invalid genus (Liu & Zhang, 1994). Subsequent molecular phylogenetic studies revealed that species producing constricting rings form a stable clade within ONTF. As a result, these species were classified under the genus *Drechslerella*, with the generic characteristics limited to producing constricting rings for nematode capture (Ahrén et al., 1998; Scholler et al., 1999; Li et al., 2005; Yang et al., 2012; Zhang & Hyde, 2014). Although most species within this genus exhibit weaker saprophytic ability, reproductive capacity and predatory ability, seemingly of limited value in nematode bio-control, the constricting ring produced by this genus catches nematode by mechanical force generated by the rapid expansion of the three cells that make up the ring. This unique capturing mechanism, distinct from the adhesive material-based capture of *Arthrobotrys* and *Dactylellina* species, makes *Drechslerella* a highly distinctive group within ONTF and an essential group for studying the origin and evolution of ONTF (Zhang & Mo, 2006; Zhang & Hyde, 2014).

1.3.4 Evolutionary Research of Nematode-Trapping Fungi in *Orbiliomycetes*

Similar to carnivorous and succulent plants, as highly specialized groups within the fungal kingdom, evolutionary study of ONTF is an indispensable aspect for understanding the entire fungal evolutionary history. Unraveling the evolutionary history of ONTF is also one of the research goals in this field. In synchrony with taxonomic studies, the evolutionary research of ONTF has gone through two phases based on solely morphology and combination of molecular phylogenetics analyses (Rubner, 1996; Li et al., 2000; Li et al., 2005; Yang et al., 2007, 2012). At present, all

evolutionary studies agree that trapping structures are crucial nutritional acquisition mechanisms for ONTF, and predatory function is an essential reason for the widespread distribution of ONTF. Thus, predatory structures are considered the most critical evolutionary feature of ONTF, with their evolution trend towards enhanced predatory ability (Rubner, 1996; Li et al., 2000; Li et al., 2005; Yang et al., 2007, 2012).

Based on the foundational assumptions, Rubner (1996) proposed that *Dactylella* species that do not form trapping structures are the ancestors of ONTF. Undifferentiated adhesive hyphae represent a primitive trapping structure, which then differentiates into adhesive knobs. Subsequently, adhesive knobs then evolved in two different directions to form non-constricting rings, constricting rings, and adhesive networks. Li et al. (2000) suggests that the evolutionary trend of trapping structures should involve enhanced predatory capability and simplified structures. Thus, adhesive hyphae are considered the most primitive trapping structure, followed by differentiation into adhesive networks, and then simplified into adhesive branches. Adhesive branches further simplifying into adhesive knobs. On the other hand, the tips of adhesive branches curve and fuse to form non-constricting rings and constricting rings. According to the evolutionary hypothesis of Li et al. (2000), adhesive networks represent a primitive trapping structure, while adhesive knobs and constricting rings are predatory structures with higher evolutionary status.

With the advancement of molecular biology, based on molecular phylogenetic studies, scholars have become increasingly convinced that trapping structures are the key feature in the evolution of ONTF. Consequently, three evolutionary hypotheses have been proposed. Li et al. (2005) suggest that adhesive knobs are the most primitive trapping structure, and evolving along two paths: (1) stalked knobs evolve into adhesive branches, two-dimensional adhesive networks and three-dimensional adhesive networks; (2) unstalked knobs evolve into adhesive branches—stalked knobs—non-constricting rings—constricting rings. In this hypothesis, adhesive networks and constricting rings are considered the trapping structures with highest evolutionary status. While Yang et al. (2007) argue that adhesive networks are a more primitive trapping structure, non-constricting rings and constricting rings are genetically distant and should not follow an adjacent sequence in evolution. Based on five protein-coding genes and two fossil records, Yang et al. (2012) estimated the differentiation time of

the main clades of ONTF and proposed that constricting rings and other four adhesive trapping structures had already differentiated in the early stages of evolution. Regarding the evolution of adhesive trapping structures, Yang et al. (2012) speculated that unstalked knobs and unicellular adhesive rings originated from adhesive ancestors. Unstalked knobs evolved into adhesive branches to increase adhesive surface and enhance trapping capabilities. Unicellular rings evolved in two directions to form adhesive networks and non-constricting rings, and non-constricting rings further evolved into stalked adhesive knobs.

Based on the above, it is evident that the evolutionary positions of different trapping structures are not consistent among the five hypotheses, and even entirely opposite. Moreover, none of the five evolutionary hypotheses align with the actual situation. For instance, three of these hypotheses consider non-constricting rings and constricting rings have similar morphologies, suggesting an adjacent evolutionary relationship between them (Rubner, 1996; Li et al., 2000; Li et al., 2005). However, current research shows significant differences in the mechanism of capturing nematodes between non-constricting rings and constricting rings, and phylogenetic studies have already suggested that these two trapping structures have differentiated significantly in the early stage of evolution, and their relatives are relatively distant, so they should not be evolutionally adjacent (Yang et al., 2007, 2012). Rubner (1996), Li et al. (2000) and Li et al. (2005) proposed that constricting rings occupy a higher evolutionary position. Based on the fundamental assumption that trapping structure is the main evolutionary feature of ONTF and the trend of ONTF evolution is the enhancement of predatory ability, the predatory capability of the constricting ring should be strong, and species that produce constricting ring should have a competitive advantage in survival, making them predominant in most habitats. However, *Drechslerella*, the genus that captures nematodes with constricting rings, has the fewest species within ONTF and is one of the rarest groups in the most of habitats (Swe et al., 2000; Mo et al., 2008; Singh et al., 2014; Zhang et al., 2020; Deng et al., 2023). Furthermore, the predatory ability of the constricting ring has been proven to be low (Graminha et al., 2005; Kumar et al., 2015). Rubner (1996), Li et al. (2005) and Yang et al. (2007) suggest that adhesive networks possess strong predatory abilities, thus implying a higher evolutionary position. However, both comparative genomics and

ultrastructural studies on trapping structures have indicated that adhesive networks have relatively weak predatory ability (Ji et al., 2020). Yang et al. (2012) propose that adhesive networks have weaker predatory ability and are a more primitive trapping structure. Based on the fundamental assumption that trapping structure is the main evolutionary feature of ONTF and the trend of ONTF evolution is the enhancement of predatory ability, we can infer from Yang et al. (2012)'s hypothesis that *Arthrobotrys* species, which produce adhesive networks have weaker competitive abilities and should be rare groups in most of habitats. However, the reality is that *Arthrobotrys* is the largest genus within ONTF and dominates the majority of habitats (Mo et al., 2008; Swe et al., 2009; Singh et al., 2014; Zhang et al., 2020; Deng et al., 2023).

Based on the above, we can see that in the case of scarce fossil records, it is difficult to solve the evolutionary problem of ONTF solely through morphological and molecular evolutionary studies. In fact, the evolution of organisms is a process of adapting to the environment, during which multiple traits undergo adaptive evolution in order to achieve broader dissemination of genetic information. The current patterns of biological abundance and diversity are actually the result of the combined effects of these evolutionary traits interacting with the environment.

Therefore, we believe that it is necessary to first understand the abundance and diversity of ONTF in their habitats, and therefore clarify the evolutionary traits of these fungi, identifying the patterns of variation in these traits among different species and combine these results with molecular phylogenetic studies, can we gradually explore the evolutionary rules of ONTF.

1.3.5 Biological Control Application of Nematode-Trapping Fungi in *Orbiliomycetes*

Nematodes are one of the most diverse and widely distributed animals on Earth, with approximately 30,000 described species, of which around 15,000 are parasitic (Hugot et al., 2001). These nematodes parasitize various plants and animals. In natural ecosystems, parasitic nematodes play an important role in regulating ecological balance and maintaining ecological stability (Yeates et al., 2009; Norton & Niblack, 2020). However, in artificial ecosystems, parasitic nematodes pose significant threats to various economically important species, causing extensive damage to agriculture,

forestry, and animal husbandry (Chitwood, 2003; Jones et al., 2013; Garcia-Bustos et al., 2019; Kim et al., 2020). Animal parasitic nematodes primarily inhabit the digestive tracts of poultry and livestock, reducing their reproductive capacity and meat, milk, and egg production and even causing death. This results in annual losses of over $80 billion to the livestock industry (Crofton, 1963; Hoste & Torres-Acosta, 2011; Comans-Pérez et al., 2021). Plant parasitic nematodes inhabit the roots, stems, leaves, flowers, fruits and seeds of living plants, causing reduced yields or even complete crop failure. Currently, over 4,000 species of plant parasitic nematodes have been reported to damage nearly all economic crops, including grains, soybeans and tobacco. Among them, root-knot nematodes and cyst nematodes cause particularly severe damage, resulting in annual economic losses exceeding $100 billion to agriculture (Williamson & Hussey; 1996; Midha, 1997; Nicol et al., 2011; Akers & McCrystal, 2014; Peiris et al., 2020). Pine wilt disease caused by pine wood nematodes is known as “non-smoking forest fire” or “forest cancer.” Since its appearance to China in 1982, it has infected millions of seedlings, destroyed tens of thousands of hectares of forests and causes annual economic losses exceeding $7 billion, which continue to increase year by year (Zhao et al., 2017; Lee et al., 2021). Whether they are animal or plant parasitic nematodes, their life cycle is closely related to soil (Jasmer et al., 2003; Vilela et al., 2016; Zarrin et al., 2017). Therefore, reducing the population density of parasitic nematodes in the soil is a key approach to their control.

Currently, the most efficient, convenient, and commonly used method for controlling parasitic nematodes is the use of highly toxic chemical pesticides such as Temik and Aldicarb (Husman et al., 1995; Moens & Hendrickx, 1998; Mueller, 2011). However, on one hand, the frequent use of chemical insecticides has led to the development of resistance in parasitic nematodes, creating a vicious cycle that can eventually lead to an embarrassing situation where no medicine is available (Trudgill, 1991; Fuller et al., 2008). On the other hand, the low specificity of highly toxic chemical insecticides not only kills parasitic nematodes but also has a significant impact on harmless nematodes and even other soil organisms, which seriously disrupting ecological stability and balance (Lechenet et al., 2014; Ahmad et al., 2022). Additionally, pesticide residue caused by chemical insecticides is an ecological and health issue that cannot be ignored (Dasika et al., 2012; Ali et al., 2021). Therefore, the

development of ecologically friendly nematode bio-control agents using natural enemies of nematodes, such as nematophagous fungi or bacteria is currently the most promising approach.

ONTF exhibits tremendous potential for biological control of nematodes due to its free-living lifestyle (both saprophytic and predatory nematodes), rich species diversity, diverse and efficient trapping structures, and global distribution (Zhang & Hyde, 2014; Jiang et al., 2017). Research on the application of ONTF in the control of parasitic nematodes can be traced back to around 1940. From 1940 to 1990, this field was still in its early stages, with no more than ten relevant studies conducted each year. However, since 1990, with the increasingly prominent harm of the use of highly toxic chemical pesticides, and people's awareness of ecological conservation and environmental health has been constantly strengthened, the use of ONTF for biological control of nematodes has received widespread attention, and the number of research reports has been increasing annually, with over 450 studies published in 2023. Initially, the main focus of research in this field was on selecting efficient bio-control strains in laboratory culture media environments, followed by evaluating the practical effects of these bio-control strains in field conditions (Yang et al., 2023). However, all studies have shown a common pattern: while most tested strains demonstrate satisfactory predatory capabilities in culture media environments, their actual effectiveness in the field is often discouraging (Yang & Zhang, 2014; Li et al., 2015; Stirling, Saxena, 2018). There are two main reasons for this problem: (1) Compared to other common microorganisms, ONTF grows slowly in soil, making it difficult to maintain a high population density and form dominant populations. (2) The interaction between ONTF and nematodes involves processes such as host recognition, trap induction, trap formation, capture and digestion, which are complex and time-consuming (Su et al., 2017; Vidal-Diez de Ulzurrun & Hsueh, 2018; Zhu et al., 2022).

Therefore, from the perspective of ecology, finding a method to maintain high population density of ONTF in soil and searching for efficient strains is the breakthrough for the successful application of ONTF. Solving these problems, however, depends on understanding natural abundance and diversity of ONTF.

1.3.6 Diversity Research of Nematode-Trapping Fungi in *Orbiliomycetes*

Even though research on ONTF has expanded to include systems evolution and molecular mechanisms based on modern molecular biology techniques, its diversity research remains a core work in this field and is a central basis for exploring the two major scientific questions in the field (evolutionary and application questions, as described in 1.3.4 and 1.3.5). To data, 147 ONTF species have been discovered, utilizing five or six trapping structures including adhesive networks, adhesive knobs (with the relationship between stalked and unstalked knobs still under debate), adhesive branches, non-constricting rings (usually occur together with adhesive knobs) and constricting rings to capture nematodes (Cooke, 1965; Zhang & Mo, 2006; Zhang & Hyde, 2014; Quijada et al., 2020; Zhang et al., 2022abc, 2023ab, 2024; Yang et al., 2023).

From a historical perspective, ONTF diversity research can be divided into three stages: (1) The nascent stage from 1839 to 1930, during which only five species were reported over nearly 90 years due to the limited practical application and theoretical research value of these fungi, as well as methodological constraints. (2) The period of rapid development from 1931 to 2009, characterized by gradual improvements in isolation methods by contributors such as Drechsler (1934, 1936, 1937, 1941, 1946), Duddington (1940, 1950, 1955), Eren (1965) and Pramer (1964). Concurrently, the demand for biological control of parasitic nematodes increased and the value of ONTF in fungal evolution studies became more prominent. This led to an explosion of reports on ONTF diversity, with nearly 90 species documented in an 80-year timeframe. (3) The bottleneck period from 2010 to 2020, with only four new species reported over a decade. This trend suggests that the exploration of new ONTF species has reached a plateau, and it is unlikely that many more new species will be discovered over time (Zhang et al., 2022). However, some scholars estimate that there may be over 8,000 species of nematophagous fungi in nature, with several hundred conservatively estimated for ONTF (Li et al., 2000). So, where are these undiscovered ONTF species?

From the perspective of habitat, ONTF is widely distribution globally due to its diverse ways of obtaining nutrients. Currently, the diversity of ONTF has been reported in various habitats in multiple regions. Soil, as the main habitat of ONTF, is the primary sample type for isolating ONTF. Numerous studies have confirmed that various types

of terrestrial soils such as farmland, forest, mines, and pastures contain rich ONTF resources (Soprunov & Galiulina, 1951; Kim et al., Zhang et al., 2001; Mo et al., 2008; Kumar et al., 2008; Liu et al., 2014; Zhang et al., 2020). Except for *A. dianchiensis* and the recently reported nine species, almost all species have distribution records in terrestrial soils (Mo et al., 2005; Zhang et al., 2022, 2023, 2024). Although there have been some reports on aquatic ONTF diversity, they are still insufficient compared to the terrestrial habitats (Hao et al., Mo et al., 2005; Tarigan et al., 2020). On the one hand, many nematodes exist in aquatic environments, and it is speculated that there should also be abundant ONTF, which has been proven by previous studies (Hao et al., Mo et al., 2005; Tarigan et al., 2020; Zhang et al., 2022, 2023). On the other hand, 13 ONTF species were initially isolated from aquatic environments, and ten of them are only recorded in aquatic environments, indicating that unique species may exist in aquatic habitats that are not found in terrestrial habitats (Mo et al., 2005; Zhang et al., 2022, 2023, 2024). Based on the above, we speculate that aquatic ONTF should be an important component of ONTF and should be considered in ONTF diversity research.

From an ecological perspective, different ONTF species often exhibit strong competitive relationships due to their similar nutrient acquisition strategies. In previous ONTF diversity studies, the species commonly isolated were predominantly from the *Arthrobotrys* genus, which uses adhesive networks to capture nematodes. These species typically possess strong competitive abilities (strong saprophytic and reproductive capacities) and become dominant in most habitats. While *Dactylellina* and *Drechslerella* species, which use adhesive knobs, adhesive branches, non-constricting rings, and constricting rings to capture nematodes generally have weaker competitive abilities (lower saprophytic and reproductive capacities). They are often suppressed by the dominant *Arthrobotrys* species, resulting in lower population densities and difficulties in isolation (Mo et al., 2008; Swe et al., 2009; Singh et al., Zhang & Hyde, 2014; Zhang et al., 2020; Deng et al., 2023). Therefore, removing the competitive suppression from the dominant *Arthrobotrys* species may be crucial for obtaining rarely ONTF species. In soil, *Arthrobotrys* with strong saprophytic and reproductive capacities typically occupy the nutrient-rich upper soil layers, while the rarer *Dactylellina* and *Drechslerella* are more commonly distributed in the lower soil layers (She et al., 2020; Dackman et al., 2021). This vertical distribution difference provides

a natural advantage for alleviating then competition suppression by dominant groups on rare taxa. Forest fires are common natural phenomena on Earth and serve as important regulatory factors in ecosystems (Giglio et al., 2006). During a fire, the surface temperature of the soil can reach 50–1500 °C, rapidly eliminating dominant groups in the upper soil layers (Bruns et al., 2020). Due to poor soil conductivity, rare ONTF in the lower soil layers are less affected and can be preserved. Therefore, forest fires provide an excellent natural mechanism for alleviating the competitive suppression of dominant species on rare species. Based on this, we speculate that rare ONTF may be discovered in burned forest.

From a geographical perspective, Yunnan Province in China is a region characterized by significant climate variations, minimal annual temperature differentials, abundant precipitation, and distinct and unevenly distributed wet and dry seasons. Geomorphologically, the region is characterized by the broom-shaped distributions of the Hengduan Mountains, Cangshan, Wuliang Mountains, Ailao Mountains, and other mountain ranges in the three parallel rivers fold belt area. The terrain descends in three major steps from west to east, with the highest point reaching 6740 meters and the lowest point at only 76.4 meters. Topographically, high mountains and valleys are interspersed, with fault basins, six major river systems, plateau lakes (37 in total), and various types of hot springs distributed throughout the area. On one hand, the diverse climate types and complex topography have fostered a rich variety of ecological environments, inevitably nurturing abundant biodiversity. On the other hand, the rugged terrain (such as the three parallel rivers region) and resulting geographical isolation play a crucial role in the formation of many species. Additionally, owing to the complex and rugged terrain of the region, some habitats in this area were not covered by glaciers during the fourth glaciation period, serving as refuges for numerous organisms and thereby fostering a variety of endemic species. In summary, selecting Yunnan as a research area for ONTF diversity offers unique geographical advantages. Building on this, multiple teams have conducted surveys of ONTF resources in Yunnan Province. For instance, researchers such as Zhang Ke-Qin and Liu Xing-Zhong have reported on the investigation and discovery of over ten new ONTF species in various regions of southwestern China, propelling the rapid development of ONTF research in China (Zhang & Mo, 2006; Zhang & Hyde, 2014). Investigations by Mo et al. (2008)

on ONTF in Pb-polluted soils have led the way in studying the adaptability of this group to extreme environments (Mo et al., 2006, 2008). These studies have all made significant contributions to our understanding of ONTF diversity. However, most of these studies have only covered specific areas of Yunnan, lacking systematic sampling surveys, and there is scarce research on ONTF in bio-diverse regions such as the three parallel rivers area.

In summary, taking Yunnan as the study area and considering aquatic, terrestrial and burnt forest ecosystems, systematic sampling survey on ONTF may be a necessary work to break through the research bottleneck of ONTF diversity and comprehensively understand ONTF diversity.

1.4 The Significance of This Study

1.4.1 The Research Value of Nematode-Trapping Fungi in *Orbiliomycetes*

In underdeveloped regions, crop yield reduction or even complete crop failure caused by parasitic nematodes is one of the factors contributing to social unrest. Even in developed areas, parasitic nematodes annually result in billions of dollars of economic losses in agriculture, forestry, and animal husbandry worldwide. With the emergence of pressing issues associated with the use of highly toxic chemical pesticides, such as environmental disruption and nematode resistance, the development of environmentally friendly bio-control agents utilizing the natural enemies of nematodes, specifically ONTF, represents the most promising approach to nematode control. Therefore, research on ONTF holds significant practical applications significance.

The life strategy of ONTF which captures nematodes for nutrient acquisition is believed to be an adaptive evolutionary outcome in response to nitrogen deficiency in their habitat. With its appropriate group size (three genera, 147 species), relatively mature isolation methods, and diverse morphological structures, ONTF is undoubtedly an excellent group for studying adaptive evolution in organisms. As a highly specialized group within the fungal kingdom, the origin and evolution of ONTF are also an indispensable part of understanding the evolutionary history of fungi. Therefore,

research on ONTF has tremendous theoretical significance in understanding adaptive evolution in organisms and the evolutionary history of fungi.

1.4.2 The Importance of This Study

Over the past 180 years, significant breakthroughs have been achieved in all aspects of the ONTF field thanks to the outstanding contributions of predecessors. However, in recent years, apart from the direction of molecular mechanisms of ONTF and nematode interactions, there has not been much progress in other research areas, suggesting that research on ONTF has reached a bottleneck period. Many scholars have gradually abandoned research in ONTF (especially the key fundamental direction of diversity research), which seriously hindering further development of ONTF field.

This study through a systematic exploration of the diversity of ONTF, not only provides guidance for diversity research of ONTF and potentially other fungal groups, but also in the process, introduces 36 new members to ONTF, offering fresh material for the taxonomy, evolution, and application research of ONTF, and it also provides solid information of natural diversity and abundance distribution for the subsequent evolution and application of ONTF.

1.5 Research Objective

1.5.1 To understand the distribution of abundance and diversity of *Orbiliomycetes* nematode-trapping fungi in Yunnan Province, China.

1.5.2 To isolate, identify and preserve a batch of nematode-trapping fungi and describe no less than ten new nematode-trapping fungi.

1.5.3 To explore the phylogenetic relationships of nematode-trapping fungi using more species.

1.6 Research Contents

This thesis consists of 11 chapters.

Chapter 1 is the general introduction, which begins with an overall introduction to nematophagous fungi, highlighting the particularity and importance of *Orbiliomycetes* nematode-trapping fungi (ONTF) among nematophagous fungi, as well as the practical application and theoretical significance of ONTF research. It then provides a comprehensive overview of the historical background of ONTF research, followed by a detailed review of four crucial research directions within the field of ONTF.

Chapter 2 reports on the diversity and distribution patterns of ONTF in Yunnan Province, which mainly consists of two sections. The first section details the diversity of ONTF from terrestrial soil and freshwater sediments, establishing that in normal habitats, *Arthrobotrys* is the dominant group, while *Dactylellina* and *Drechslerella* are rare. Furthermore, it analyzes the distribution patterns of ONTF across different habitat types, altitudes, latitudinal and longitudinal gradients within Yunnan Province. It specifically identifies the three parallel rivers region in northwest Yunnan as the core area for ONTF diversity. The second section explores the impact of forest fires on the community composition of ONTF, noting that forest fires significantly alter the community composition of ONTF and increase ONTF diversity. The study finds that rarer ONTF can be isolated from burned forests.

Chapter 3 introduces one novel nematode-trapping fungi *Fusarium xiangyunensis* (*Nectriaceae*) from freshwater sediment in Yunnan Province, China.

Chapter 4 introduces two new nematode-trapping fungi species *Dactylellina yushanensis* and *Da. cangshanensis* (*Orbiliaceae*) from burned forest in Yunnan Province, China.

Chapter 5 introduces two new nematode-trapping fungi *Drechslerella daliensis* and *Dr. xiaguanensis* (*Orbiliaceae*) from Yunnan Province, China.

Chapter 6 introduces six novel nematode-trapping fungi species that capture nematodes using adhesive networks.

Chapter 7 introduces a new nematode-trapping fungi from Yunnan, China *Arthrobotrys blastospora* (*Orbiliaceae*), which displays the morphological traits of mesozoic carnivorous fungi.

Chapter 8 introduces two novel nematode-trapping fungi species that capture nematodes using adhesive networks and three new nematode-trapping fungi catch nematodes with constricting rings.

Chapter 9 introduces five novel nematode-trapping fungi from freshwater habitats in Yunnan, China.

Chapter 10 introduces 15 novel rare nematode-trapping fungi from burned forest, and the effects of forest fires on microbial diversity are also discussed.

Chapter 11 provides the overall conclusion.

CHAPTER 2

DIVERSITY AND DISTRIBUTION OF *ORBILIOMYCETES* NEMATODE-TRAPPING FUNGI IN YUNNAN, CHINA

2.1 Introduction

The study of fungal diversity is a foundational element of mycological research. This work not only provides a scientific basis for the conservation and utilization of fungal resources but also establishes a framework for fungal ecology and evolutionary research (Hawksworth, 2004; Grube et al., 2017). Since the discovery of *Orbiliomycetes* nematode-trapping fungi (ONTF), the exploration of their diversity and distribution has been a core research focus in this field (Mo et al., 2008; Swe et al., 2009; Singh et al., Zhang et al., 2014). Over the last 180 years, 147 species across three genera of ONTF have been reported (Cooke, 1965; Zhang & Mo, 2006; Zhang & Hyde, 2014; Quijada et al., 2020; Zhang et al., 2022abc, 2023ab, 2024; Yang et al., 2023). Since 2010, the discovery of new ONTF has reached a plateau, with only four new ONTF species identified in the past decade (2010–2020) (Zhang et al., 2022). However, it is estimated that there could be over 8,000 nematophagous fungi in nature, potentially including hundreds of nematode-trapping fungi (Li et al., 2000). Therefore, understanding the diversity and distribution of ONTF and continuing to uncover unknown new species remain both a significant challenge and opportunity in this field.

ONTF are widely distributed across various habitats due to their unique survival strategies, including extreme environments such as heavy metal-contaminated soil, hot springs, and animal wastes (Gray, 1983; Swe et al., 2009; Dackman et al., Freitas et al., Zhang et al., 2021; Zhang & Hyde, Liu et al., 2014). Previous studies confirm the presence of a large number of nematodes and a rich diversity of ONTF in aquatic habitats (Hao et al., Mo et al., 2005; Tarigan et al., 2020; Zhang et al., 2022, 2023). However, compared to terrestrial habitats, the diversity of ONTF in aquatic habitats

remains underexplored. Among the known 147 ONTF species, the type strains of 13 species were isolated from aquatic habitats, and ten species (*Arthrobotrys blastospora*, *A. cibiensis*, *A. dianchiensis*, *A. eryuanensis*, *A. hengjiangensis*, *A. heihuiensis*, *A. hyrcanus*, *A. jinshaensis*, *A. yangbiensis*, and *A. yangjiangensis*) are exclusively found in aquatic habitats (Mo et al., 2005; Zhang et al., 2022, 2023, 2024). This suggests that aquatic habitats may harbor abundant and unique ONTF species. Therefore, in the studies of ONTF diversity, the significance of aquatic environments as crucial habitats for ONTF cannot be overlooked.

Similar to other fungal groups, different ONTF exhibit strong competitive interactions due to their similar modes of nutrient acquisition. In the three ONTF genera, species of the genus *Arthrobotrys* are predominant in most habitats due to their strong competitive abilities, whereas *Dactylellina* and *Drechslerella* are less competitive and thus rarer (Mo et al., 2008; Swe et al., 2009; Singh et al., Zhang & Hyde, 2014; Zhang et al., 2020; Deng et al., 2023). The competitive suppression exerted by more dominant *Arthrobotrys* species on the weaker *Dactylellina* and *Drechslerella* may be one reason for the low population densities and difficulty in isolating these rarer species. Removing the competitive suppression that *Arthrobotrys* exerts on *Dactylellina* and *Drechslerella* could be key to isolating rare ONTF species (*Dactylellina* and *Drechslerella*). In soil, *Arthrobotrys* species with strong saprophytic and reproductive capabilities typically occupy nutrient-rich upper soil layers, while the rarer *Dactylellina* and *Drechslerella* are found in lower layers (Rong et al., 2020; Dackman et al., 2021). This vertical distribution difference provides a natural advantage in relieving competitive suppression on rarer groups. Forest fires play a crucial role in ecosystem regulation (Giglio et al., 2006). The high temperatures generated during fires can rapidly eliminate *Arthrobotrys* from the soil surface, while the poorer thermal conductivity of the soil minimally affects the rarer ONTF in the lower layers. Thus, wildfires are an effective means of eliminating competitive suppression by dominant groups on the soil surface, potentially uncovering rare ONTF species from burned forests.

Yunnan Province, located in the southwestern border of China, is characterized by its unique and rugged terrain and a variety of climate types, exemplified by the three parallel rivers area. This diversity has fostered a rich array of ecological types and significant biodiversity, earning the region the title of kingdom of flora and fauna (Yang

et al., 2004; Basnet et al., 2019). The three parallel rivers area alone, constituting only 0.4% of the national territory, houses over 20% of the plant and animal species, earning it the reputation as a “world gene bank” (Li et al., 2001). Furthermore, the water system in Yunnan, comprising six major river systems and hundreds of tributaries, along with 37 plateau lakes, provides an excellent area for the study of aquatic ONTF. Additionally, Yunnan is a hotspot for forest fires, with 2,081 incidents occurring between 2010 and 2022, affecting over 220,000 hectares of forest (Fornacca et al., 2018). Thus, Yunnan also serves as an excellent area for pyroecology research.

In conclusion, this study focuses on Yunnan Province, China, covering both terrestrial and aquatic habitats, with systematically placed sampling sites to comprehensively understand the diversity of ONTF. By including the extreme environment of burned forests, aiming to understand the impact of forest fires on ONTF diversity and discover more additional new ONTF species.

2.2 Material and Methods

2.2.1 Study Area

Yunnan, located in Southwest China, spans from 21°8'32" to 29°15'8" in latitude and 97°31'39" to 106°11'12" in longitude. The collision and compression of the Eurasian Plate have shaped the geographical features of Yunnan, with mountain ranges such as the Hengduan Mountains, Wuliang Mountains, Ailao Mountains, and six major river systems and 37 plateau lakes outlining the basic geographical framework of the province. The terrain slopes from high northwest to low southeast, with altitudes ranging from 76 to 6,740 meters. The northwest of Yunnan is characterized by high mountains and deep valleys with rugged terrain, while the southeast comprises low mountains and rolling hills of the eastern and central Yunnan plateaus. The province encompasses a variety of climate types, such as tropical northern, subtropical southern, subtropical central, subtropical northern, warm temperate, mid temperate, and plateau climates (Owen, 2005). The diverse climate and complex topography foster rich biodiversity, earning the region titles such as the “kingdom of flora and fauna” and “world gene bank” (Li et al., 2001).

2.2.2 Sampling

2.2.2.1 Samples from terrestrial and aquatic habitats

Sampling sites: A total of 342 sampling sites were established across the province (Tables 2.1 to Table 2.3). Initially, 227 sites were set up across various ecosystems, altitudes, and latitudes (Figure 2.1 A). Considering the rich biodiversity in the three parallel rivers area, an additional 115 sampling sites were later added in this region (Figure 2.1 B).

Table 2.1 The number of sampling sites at different altitudes

Altitude (m)	**Below 1000**	**1000–1500**	**1500–2000**	**2000–2500**	**Above 2500**	**Total**
Number of sampling sites	75	73	81	79	34	342

Table 2.2 The number of sampling sites at different longitudes

Longitude (°)	**97–99**	**100–101**	**101–103**	**Above 103**	**Total**
Number of sampling sites	45	51	51	39	342

Table 2.3 The number of sampling sites at different latitudes

Latitude (°)	**21–23**	**23–25**	**25–26**	**26–27**	**Above 27**	**Total**
Number of sampling sites	36	68	62	130	46	342

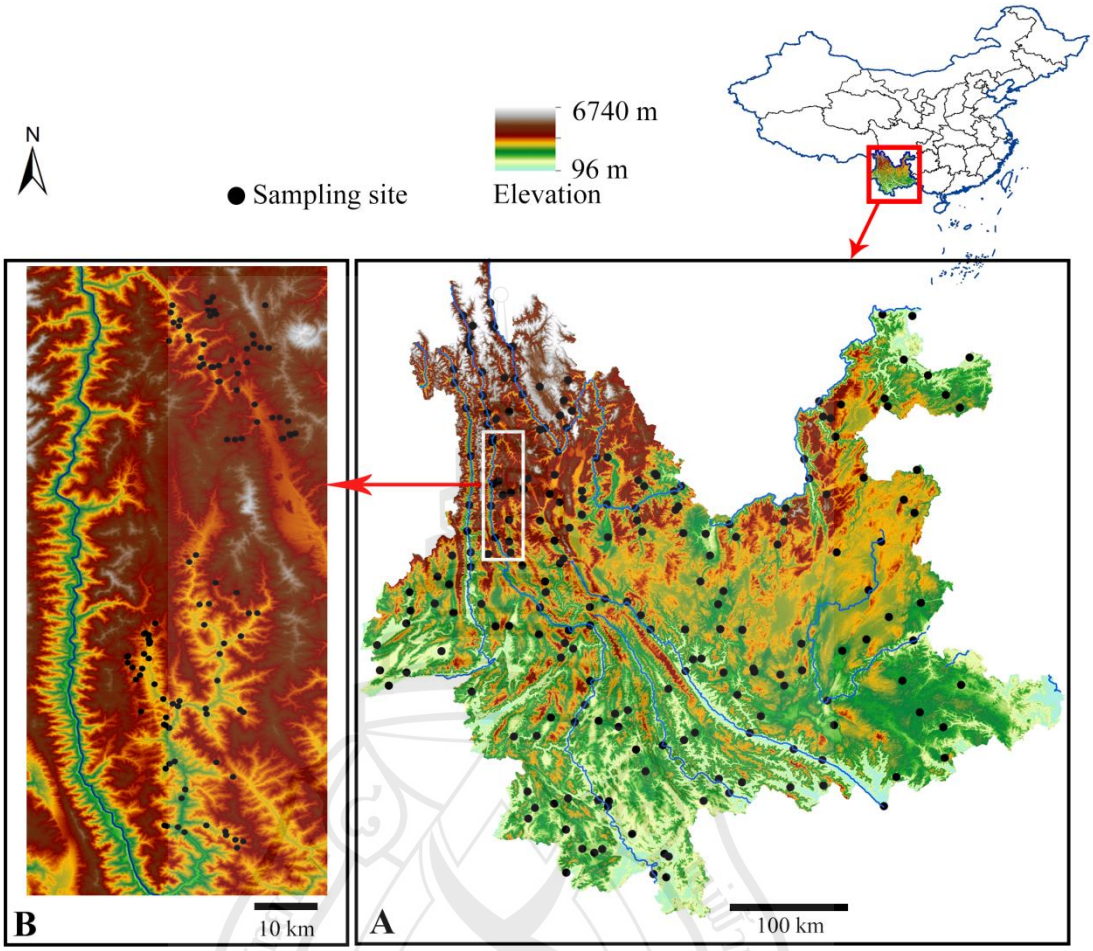

Figure 2.1 Sampling sites in Yunnan Province. (A) Yunnan Province with 227 sampling sites. (B) Yunlong and Lanping areas of the three parallel rivers region with 115 additional sampling sites

Sample collection: For each sampling site depicted in Figure 2.1, five 1×1 m squares (sampling squares, each square is spaced ten meters apart) were established both on land and in water (Figure 2.2 A). Within each square, five sampling points were set up, and terrestrial soil and freshwater sediment samples from 0–20 cm depth were collected using a 50 mm-diameter sterile soil borer and a Peterson bottom sampler, respectively. Samples from the five points were mixed to represent the composite sample of the square (Figure 2.2 B). Detailed sample information was recorded and sent back to the laboratory for further processing. The first batch of 227 sampling sites were collected from March to June 2017, and the second batch of 115 sampling sites were collected in October 2018.

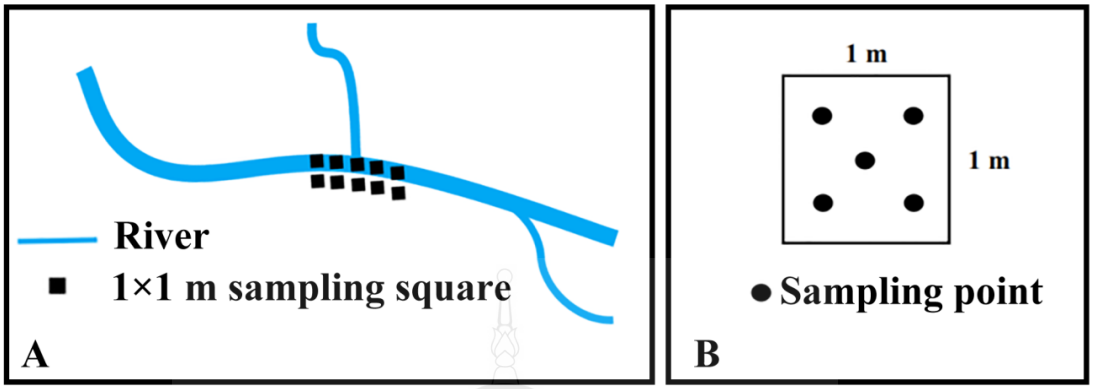

Figure 2.2 Schematic diagram of terrestrial soil and freshwater sediment sample collection. (A) Diagram of squares layout. (B) Diagram of sample collection.

2.2.2.2 Samples from three burned forests

Three burned forests in Dali City, Yunnan Province, which experienced wildfires at different times, were selected as study areas (Table 2.4). Twenty to 320 sampling squares (1×1 m) were established in both the burned areas and the adjacent unburned areas (The unburned areas were chosen to match the burned areas in terms of altitude, slope direction, and original vegetation type) (Figure 2.3).

Table 2.4 Burned forests information

Sample area	Coordinate	Ignition time	Burned area (acre)	Original vegetation	Sampling time	Number of sampling sites	Number of samples
Wanqiao	N 25°47'58" E 100°6'11"	May 2021	420	Yunnan pines	June 16, 2021	10	20
Yunlong	N 25°51'22" E 99°13'38"	March 2014	4200	Yunnan pines	March 6, 2018	160	320
Yushan	N 25°37'09" E 100°09'02"	April 2017	700	Yunnan pines	March 24, 2018	14	28

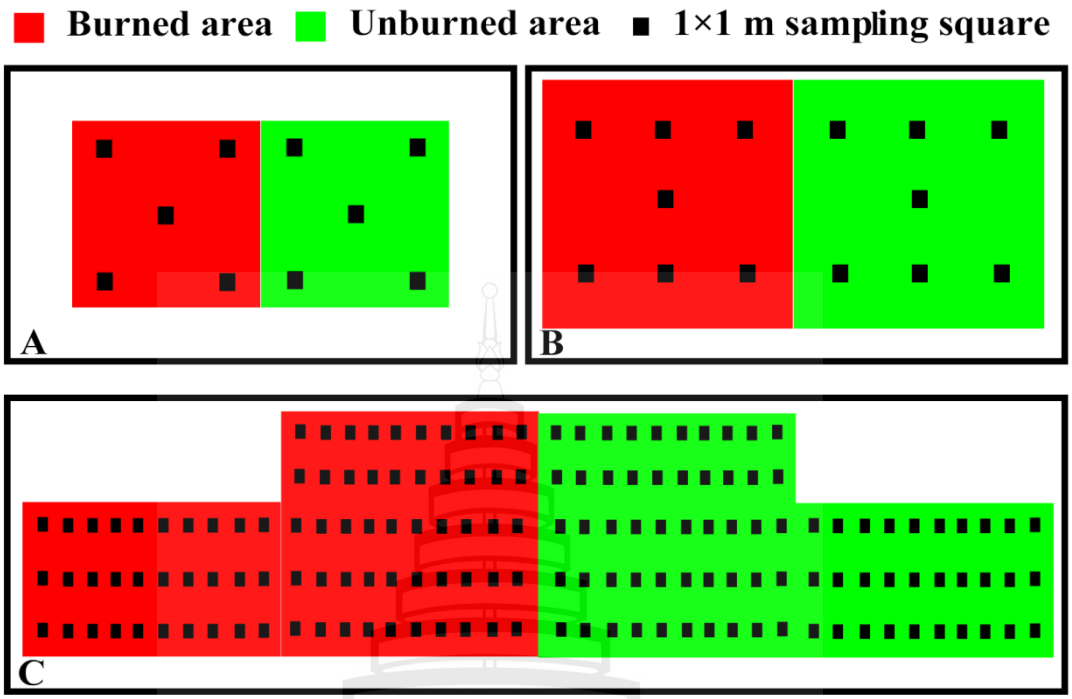

Figure 2.3 Schematic diagram of sampling squares in three burned forests. (A) Wanqiao burned forest. (B) Yushan burned forest. (C) Yunlong burned forest

Within each square, five sampling points were designated (Figure 2.2 B). A 50 mm-diameter sterile soil borer was used to collect soil core from each point, extracting up to a depth of 20 cm. Each soil core was subsequently divided into two segments (0–10 cm and 10–20 cm). Samples from the five different depths within a square were homogenized equally to form composite sample for that square (two composite samples per square, representing the upper and lower soil layers). After recording detailed sample information, these were transported back to the laboratory for further processing.

2.2.3 Isolation of *Orbiliomycetes* Nematode-Trapping Fungi (ONTF)

The Bellman funnel method (Staniland, 1954; Giuma & Cooke, 1972) was employed to isolate the nematodes (*Panagrellus redivivus* Goodey, free-living nematodes) cultured in oat meal medium. The nematode suspension was then adjusted to a concentration of 5000 nematodes per milliliter using sterile water.

The sample sprinkling and baiting nematodes methods were used for the isolation and purification of ONTF (Zhang & Hyde, 2014). Sterile toothpicks were used

to spread samples onto the surface of corn meal agar (CMA) plates, and 1 mL nematode suspension was added to the plates to promote the germination of ONTF. Three replicates of each sample were cultured at room temperature (17–29℃) for three to six weeks. During this period, the spores of ONTF were searched using a stereo-microscope, and then single spore was picked up with sterile toothpick and transferred onto fresh CMA plate. The plate was incubated at 26.5 °C for seven days and the process of single spore isolation was repeated until the pure culture was obtained.

2.2.4 Identification of *Orbiliomycetes* Nematode-Trapping Fungi (ONTF)

Morphological identification: The pure culture was inoculated onto CMA plates using sterile toothpicks and incubated at 26.5°C for seven to 20 days. After the culture entered the sporulation stage, a piece of transparent tape (1×1 cm) was used to stick the culture, which was then placed on the glass slide with 0.3% Melan stain to create a temporary slide. Morphological characteristics such as conidia, conidiophores, and chlamydospores were observed and measured using an Olympus BX53 microscope (Olympus Corporation, Tokyo, Japan). In addition, a piece of agar (2 × 2 cm) was removed from the center of fresh CMA plate with a sterile scalpel to prepare CMA observation well plate. The strain was inoculated into the CMA observation well plates and incubated at 26.5°C. After the mycelia covered the observation well, a drop of nematode suspension (approximately 200 nematodes) was added to the well and incubated at 26.5°C. The trapping structure was observed after 24–48 hours. Morphological identification was conducted according to relevant literature (Cooke, 1965; Zhang & Mo, 2006; Zhang & Hyde, 2014; Quijada et al., 2020; Zhang et al., 2022abc, 2023ab, 2024; Yang et al., 2023).

Molecular identification: All ONTF strains were identified through similarity comparison of ITS sequence via BLASTn search (https://blast.ncbi.nlm.nih.gov/) and multi-genes phylogenetic analysis (ITS, TEF and RPB2). The pure culture was inoculated on potato dextrose agar (PDA) plates and incubated at 26.5°C for 7–20 days. Fungal mycelia were collected with a sterile scalpel, and genomic DNA was extracted using a rapid fungal genomic DNA extraction kit following the manufacturer's instructions (Sangon Biotech, Limited, Shanghai, China). PCR amplification of ITS, TEF, and RPB2 fragments was performed using primers ITS4-ITS5 (White et al., 1990),

526F-1567R (O'Donnell et al., 1998), and 6F-7R (Liu et al., 1999), respectively (reaction systems and conditions are show in Figure 2.4 and Table 2.5). Agarose gel electrophoresis was employed to detect the PCR products, and then PCR products were sequenced by Biosune Biotechnology (BioSune Biotech, Limited, Shanghai, China) (ITS and RPB2 were sequenced using amplification primers, TEF was sequenced using primers 247F-609R (Yang et al., 2007)). The sequences were checked and assembled using SeqMan v. 7.0 (DNASTAR, Madison, WI, USA) (Swindell & Plasterer, 1997). The ITS sequences were compared against NCBI database using BLASTn (https://blast.ncbi.nlm.nih.gov/). Strains that exhibit a similarity of 98% or higher to known species in the database and are consistent with the results of morphological identification can be confirmed for their species name. Otherwise, a multi-genes phylogenetic analysis should be conducted as follows process.

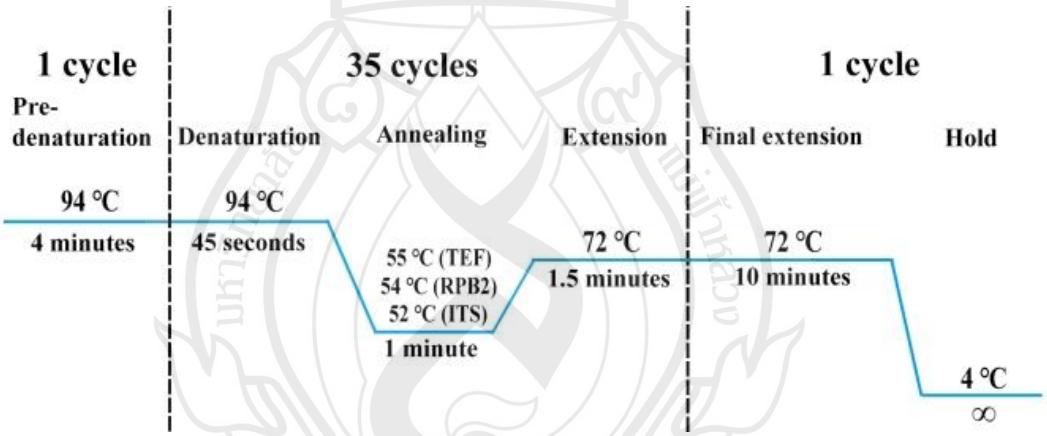

Figure 2.4 PCR amplification reaction condition of three genes

Table 2.5 PCR amplification reaction system of three fragments

Component	Volume
DNA template	2 uL
MgCl2 (25 mM)	3 μL
10×PCR buffer	5 μL
dNTPs (10 μM)	1 μL
Primer 1	2 μL
Primer 2	2 μL
Taq Polymerase	1 unit (1 μL)
ddH2O	34 μL
Total volume	**50 μL**

1. Generation of alignment files: ITS, TEF, and RPB2 sequences of related species were downloaded from NCBI based on BLASTn research results and relevant literature (Li et al., 2000; Zhang & Mo, 2006; Swe et al., 2011; Yang et al., 2012; Zhang & Hyde, 2014). Alignments of ITS, TEF and RPB2 sequences were generated using MAFFT v.7 (http://mafft.cbrc.jp/alignment/server/) (Katoh & Standley, 2013), followed by manual adjustment using Bioedit v7.2.3 (Hall, 1999) to improve accuracy. Finally, MEGA 6.0 (Tamura et al., 2013) was used to link the three alignments.

2. Selection of optimal nucleotide substitution models: The best nucleotide substitution models for ITS, TEF, and RPB2 were calculated under the AIC criterion using jModeltest v 2.1.10 (Posada, 2008).

3. Phylogenetic analysis: Maximum likelihood analysis (ML) was used to infer maximum likelihood phylogenetic trees via IQ-Tree v1.6.5 (Nguyen et al., 2014). The dataset was partitioned, and each gene was analyzed with the corresponding optimal substitution model. The bootstrap support values for each clade were calculated using 1000 repetitions rapid bootstraps (Felsenstein et al., 1985). MrBayes v. 3.2.6 (Huelsenbeck & Ronquist, 2001) was used to implement the Bayesian inference analysis. FastaConvert (Hall, 2007) was used to convert the combined alignment file into MrBayes-compatible NEXUS files, and following parameters were edited in the

MrBayes block in the NEXUS file. The dataset was partitioned according to the corresponding nucleotide substitution models, and six Markov chains were run for 10,000,000 generations, sampling a tree every 100 generations and discarding the first 25% of trees to calculate the posterior probabilities of the majority rule consensus tree.

4. Visualization of phylogenetic trees: The trees were visualized using FigTree v1.3.1 (Rambaut, 2010) and beautified using Microsoft PowerPoint (2013) and Adobe Photoshop CS6 software (Adobe Systems, San Jose, CA, USA).

2.2.5 Data Analyses

Data from each sampling site and sample were compiled using Excel (2016) for subsequent analysis.

2.2.5.1 ONTF diversity in terrestrial and aquatic habitats

Overall diversity of ONTF in Yunnan Province: (1) The species accumulation curves for 342 sampling sites were calculated using the 'specaccum' function in the 'vegan' package in R (R Core Team, 2014) to confirm the adequacy of sampling efforts. (2) The occurrence frequency of each genus and species was calculated (Occurrence Frequency, OF = Number of samples where a species/genus was found / Total number of samples × 100%), and bar charts were drawn using Excel (2016) to clarify the community composition of ONTF in Yunnan.

Terrestrial and aquatic differences of ONTF in Yunnan Province: (1) ONTF diversity data from terrestrial and aquatic samples were organized separately to assess diversity differences by counting species and strains found in terrestrial and aquatic samples. (2) Venn diagrams were created to delineate the uniqueness of ONTF in terrestrial and aquatic habitats.

Distribution Patterns of ONTF in Yunnan Province: (1) Information from Tables 2.1 to 2.3 was organized to compile ONTF data across different altitudes, longitudes, and latitudes. The species accumulation curves for various altitudes, longitudes, and latitudes were calculated using the 'specaccum' function in the 'vegan' package in R (R Core Team 2014) to identify patterns in ONTF diversity distribution. (2) The average number of ONTF strains obtained at each sampling sites at different altitudes, longitudes and latitudes were calculated to clarify the change law of ONTF biomass (e.g., for altitudes 0–1000 m, the average number of ONTF strains per site =

Total number of ONTF strains obtained at 75 sites within 0–1000m altitude / 75 sampling sites). (3) The occurrence frequency of species across different altitudes, longitudes, and latitudes was calculated to clarify community variations. (4) The number of ONTF species and strains detected at 342 sites was tallied, and the top 50 sites by species and strain counts were marked on maps using ArcGIS (Booth & Mitchell, 2001) to highlight the hotspot areas for ONTF distribution in Yunnan.

2.2.5.2 ONTF diversity in burned forests

The number of ONTF species and strains detected in burned and unburned areas within three study regions was tallied, and the proportions of *Arthrobotrys*, *Dactylellina*, and *Drechslerella* in different soil layers of the burned and unburned areas were calculated to assess the impact of fires on ONTF diversity.

2.3 Results

2.3.1 Diversity and Distribution of *Orbiliomycetes* Nematode-Trapping Fungi (ONTF) in Terrestrial and Aquatic Habitat in Yunnan Province

2.3.1.1 Overall diversity of ONTF in Yunnan Province

The species accumulation curves indicate that the number of ONTF species increased with the number of sampling sites. The curve began to plateau after reaching 300 sites, suggesting that the 342 sampling sites deployed provide comprehensive coverage of ONTF in Yunnan (Figure 2.5). From 342 sampling sites yielding 3420 samples, a total of three genera and 62 species comprising 3455 ONTF isolates were detected, with a site detection rate of 100% and a sample detection rate of 94.94%. The detected isolates included 3309 isolates of *Arthrobotrys* representing 46 species (19 new species), 80 isolates of *Dactylellina* representing nine species (one new species), and 66 isolates of *Drechslerella* representing seven species (two new species) (Table 2.6). *Arthrobotrys* had a detection rate of 91.08% and accounted for 95.51% of the total isolates, making it the dominant ONTF group in Yunnan Province (Figure 2.6).

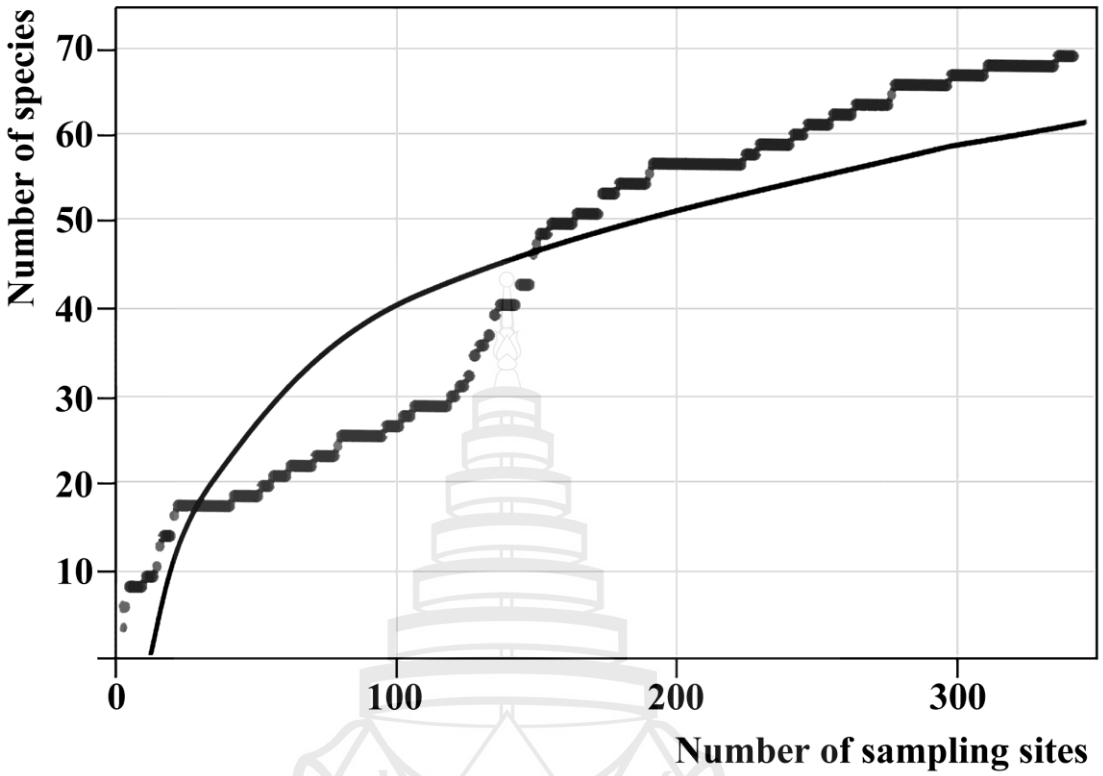

Figure 2.5 ONTF species accumulation curve for 342 sampling sites in Yunnan Province

Table 2.6 Detection of ONTF in Yunnan Province

Species	Number of strains	Number of samples	Occurrence frequency
Arthrobotrys oligospora	1352	1307	38.22%
Arthrobotrys musiformis	612	597	17.46%
Arthrobotrys conoides	592	560	16.37%
Arthrobotrys superba	134	132	3.86%
Arthrobotrys javanica	81	80	2.34%
Arthrobotrys thaumasia	67	65	1.90%
Arthrobotrys xiangyunensis	77	59	1.73%
Arthrobotrys vermicola	41	38	1.11%
Arthrobotrys eudermata	35	31	0.91%

Table 2.6 (continued)

Species	Number of strains	Number of samples	Occurrence frequency
Drechslerella dactyleoids	26	25	0.73%
Arthrobotrys reticulata	34	25	0.73%
Dactylellina ellipsospora	26	23	0.67%
Arthrobotrys obovata	27	23	0.67%
Arthrobotrys microscaphoides	29	21	0.61%
Arthrobotrys sphaeroides	24	20	0.58%
Arthrobotrys scaphoides	28	19	0.56%
Arthrobotrys cladodes	22	19	0.56%
Dactylellina drechsleri	23	17	0.50%
Arthrobotrys guizhouensis	18	14	0.41%
Drechslerella coelobrocha	14	11	0.32%
Arthrobotrys robusta	11	11	0.32%
Dactylellina parvicolla	9	9	0.26%
Arthrobotrys sinensis	9	9	0.26%
Arthrobotrys janus	9	9	0.26%
Drechslerella aphrobrocha	11	8	0.23%
Dactylellina gephyropaga	10	8	0.23%
Arthrobotrys pyriformis	8	8	0.23%
Dactylellina sichuanensis	8	7	0.20%
Drechslerella doedycoides	8	6	0.18%
Arthrobotrys megalospora	9	6	0.18%
Arthrobotrys flagrans	8	6	0.18%
Da. haptotyla	4	4	0.12%
Arthrobotrys tongdianensis sp.nov	6	4	0.12%
Arthrobotrys shuifuensis sp.nov	6	4	0.12%
Arthrobotrys multiformis	4	4	0.12%
Arthrobotrys dianchiensis	6	4	0.12%

Table 2.6 (continued)

Species	Number of strains	Number of samples	Occurrence frequency
Dactylellina dulongensis sp.nov	3	3	0.09%
Dactylellina cionopaga	3	3	0.09%
Arthrobotrys luzhangensis sp.nov	5	3	0.09%
Arthrobotrys jindingensis sp.nov	5	3	0.09%
Arthrobotrys hengjiangensis sp.nov	4	3	0.09%
Arthrobotrys eryuanensis sp.nov	4	3	0.09%
Drechslerella yunlongensis sp.nov	3	2	0.06%
Drechslerella stenobrocha	2	2	0.06%
Drechslerella pengdangensis sp.nov	2	2	0.06%
Arthrobotrys zhaoyangensis sp.nov	2	2	0.06%
Arthrobotrys yangjiangensis sp.nov	2	2	0.06%
Arthrobotrys weixiensis sp.nov	3	2	0.06%
Arthrobotrys tachengensis sp.nov	2	2	0.06%
Arthrobotrys luquanensis sp.nov	2	2	0.06%
Arthrobotrys lanpingensis sp.nov	2	2	0.06%
Arthrobotrys jinshaensis sp.nov	2	2	0.06%
Arthrobotrys jinpingensis sp.nov	3	2	0.06%
Arthrobotrys heihuiensis sp.nov	2	2	0.06%
Arthrobotrys gongshanensis sp.nov	2	2	0.06%
Arthrobotrys elegans	3	2	0.06%
Arthrobotrys cibiensis sp.nov	2	2	0.06%
Arthrobotrys blastospora sp.nov	2	2	0.06%
Dactylellina leptospora	1	1	0.03%
Dactylellina entomopaga	2	1	0.03%
Arthrobotrys yangbiensis sp.nov	2	1	0.03%
Arthrobotrys koreensis	2	1	0.03%
Total	**3455**	**3247**	**94.94%**

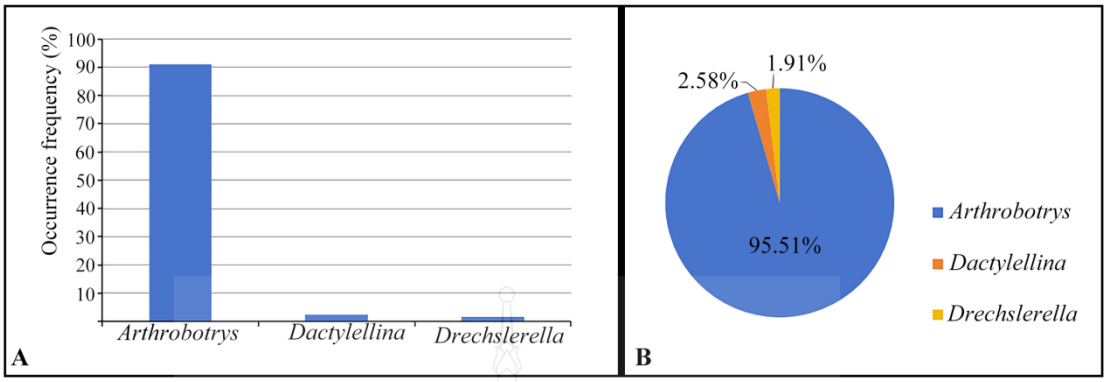

Figure 2.6 Community composition of ONTF in Yunnan Province. (A) Occurrence frequency of ONTF in Yunnan Province. (B) Strain composition of ONTF in Yunnan Province

2.3.1.2 Terrestrial and aquatic differences of ONTF in Yunnan Province

Three genera and 49 species comprising 1832 ONTF isolates were isolated from the 1710 terrestrial soil samples (including ten new species), whereas 1710 freshwater sediment samples yielded 42 species comprising 1623 isolates (including 12 new species). The detection rates and species count of terrestrial soil ONTF were higher than those of freshwater sediments, at 97.54% and 92.34%, respectively (Table 2.7). Twenty-nine species were common to both terrestrial soils and freshwater sediments, with each habitat hosting 20 and 13 unique species, respectively (Figure 2.7).

Table 2.7 ONTF detection in terrestrial soil and freshwater sediment samples

Sample type	Number of species	Number of strains	Number of samples	Occurrence frequency	Simpson' s index	Shannon index	Similar index
Terrestrial soil	49	1832	1668	97.54%	0.21	2.23	0.47
Freshwater sediment	42	1623	1579	92.34%	0.23	2.07	

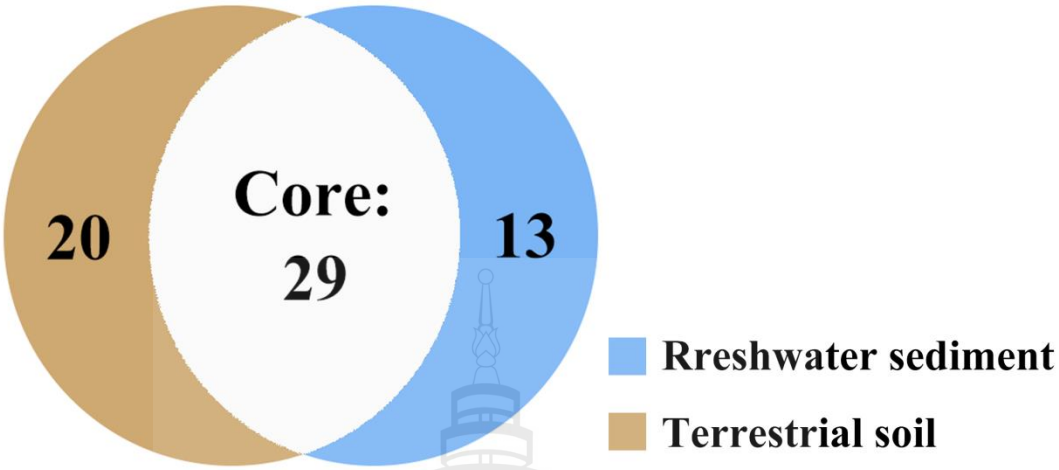

Figure 2.7 Common species in terrestrial soil and freshwater sediment. Brown indicates species endemic to terrestrial soil, blue indicates species endemic to freshwater sediment, 'core' represents the common species in both habitats

2.3.1.3 Distribution patterns of ONTF in Yunnan Province

Altitude distribution of ONTF: Despite only 34 sampling sites being located above 2500 meters altitude, species accumulation curves showed a plateauing trend across altitude ranges as the number of sites increased. The greatest number of ONTF species was recorded within the altitude range of 0–1000 meters with 42 species, and decreasing with increasing altitude (Figure 2.8). The detection rates and average number of isolates per site at different altitudes corresponded with the species count, decreasing with increasing altitude. The lowest detection rate (75.9%) and an average of only 7.4 isolates per site were recorded above 2500 meters (Figure 2.9 A). Only 11 of the 62 detected species were found across all five altitude ranges, with the number of unique species decreasing with increasing altitude (Figure 2.9 B).

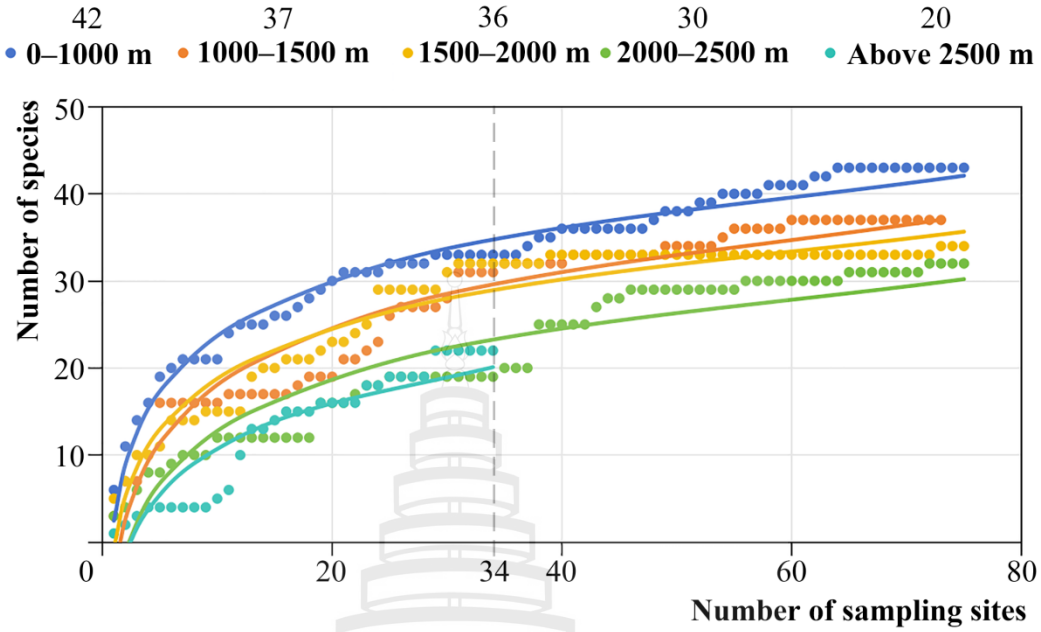

Figure 2.8 ONTF species accumulation curves at different altitudes in Yunnan Province. The number of species obtained in each altitude range is indicated above the legend

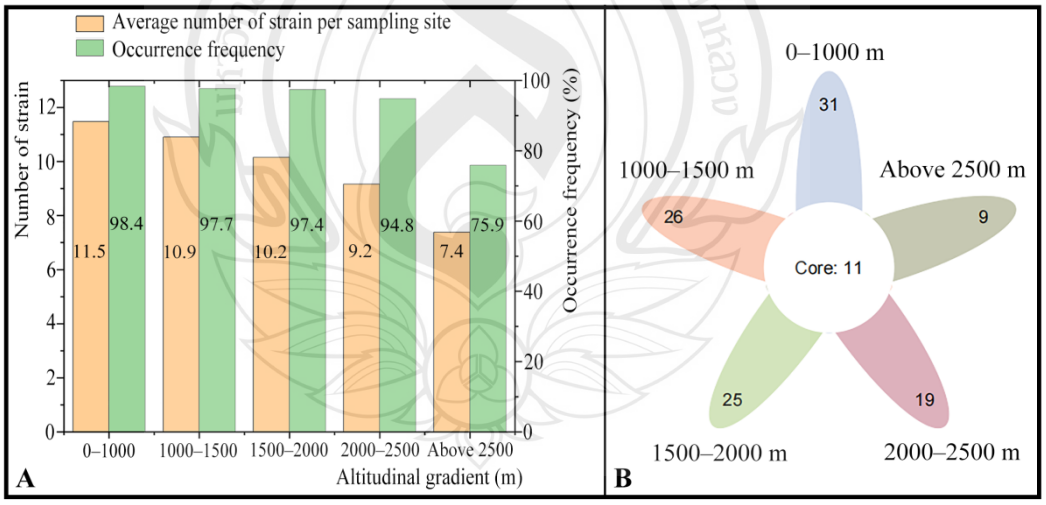

Figure 2.9 ONTF detection at different altitudes in Yunnan Province. 'Core' represents the common species in different altitudes

Longitude distribution of ONTF: Due to the unique topography in Yunnan Province, it was not possible to ensure adequate sampling sites across each longitude range. However, species accumulation curves indicate that the most species (38 species) were obtained between longitudes 97° and 99° (Figure 2.10). The ONTF detection rate and the average number of isolates per site were lowest within this longitude range, at 92% and 9.68 respectively (Figure 2.11 A). Seventeen of the 62 detected species were found across all five longitude ranges, with the number of unique species decreasing as longitude increased (Figure 2.11 B).

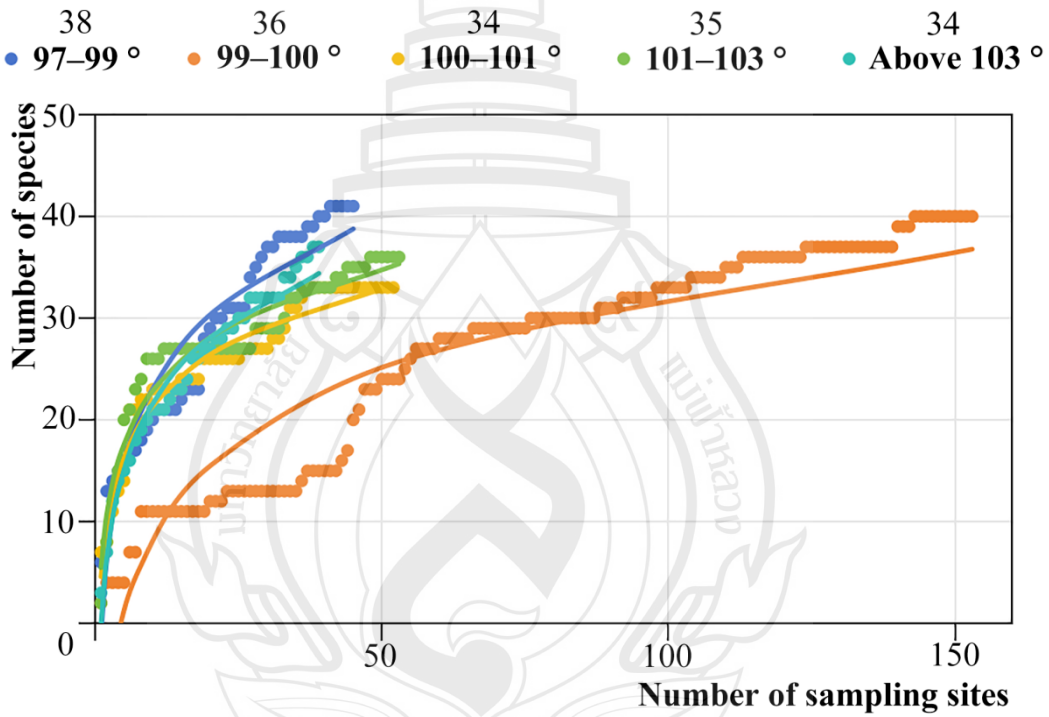

Figure 2.10 ONTF species accumulation curve at different longitude in Yunnan Province. The number of species obtained in each longitude range is indicated above

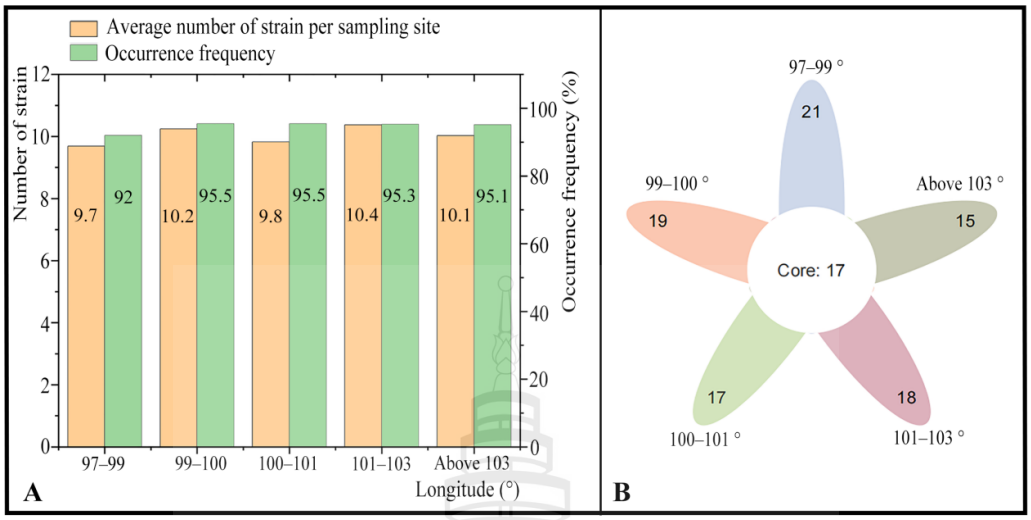

Figure 2.11 ONTF detection at different longitude in Yunnan Province. 'Core' represents the common species in different longitude

Latitude distribution of ONTF: similar to longitude data, insufficient sampling across latitude gradients resulted in unclear trends. However, species accumulation curves distinctly showed that the greatest number of ONTF species was obtained at latitudes above 27°, with 42 species detected both above and at 26–27° (Figure 2.12). Contrary to the species count, ONTF detection rates and the average number of isolates per site were lowest in the higher latitude areas, with detection rates and average isolates per site dropping to 89.78% and 9.43, respectively, above 27° (Figure 2.13 A). Twenty of the detected 62 species were found across all five latitude ranges, with the number of unique species generally increasing with latitude (Figure 2.13 B).

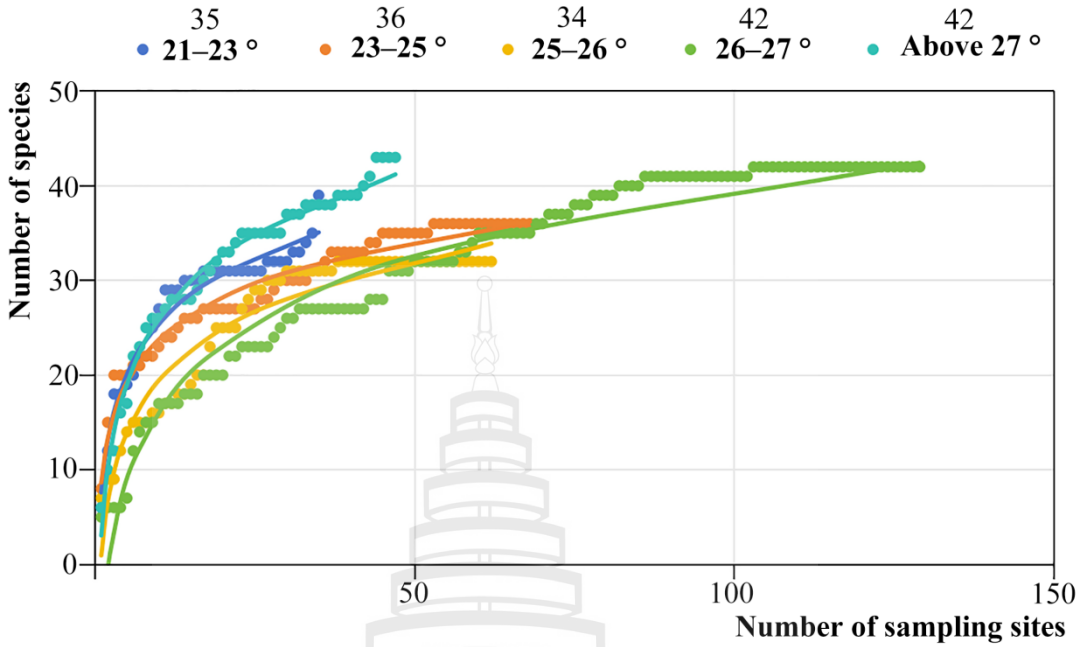

Figure 2.12 ONTF species accumulation curve at different latitude in Yunnan Province. The number of species obtained in each latitude range is indicated above

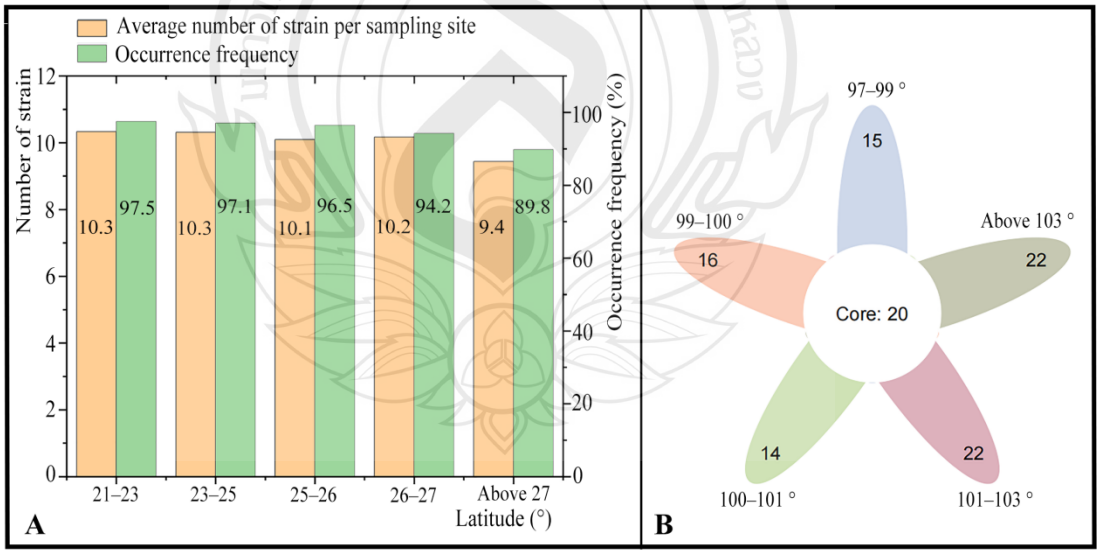

Figure 2.13 ONTF detection at different latitude in Yunnan Province. 'Core' represents the common species in different altitudes

ONTF hotspots in Yunnan Province: Among the top 50 sites with the highest number of species and strains, 44% (22 sites) and 52% (26 sites) were concentrated in the northwestern region of Yunnan, which constitutes less than 15% of the provincial area (the three parallel rivers area) (Figures 2.14 A, B). Furthermore, among the 22 new species isolated from this study, 77.3% (17 species) originating from this region (Figure 2.14 C).

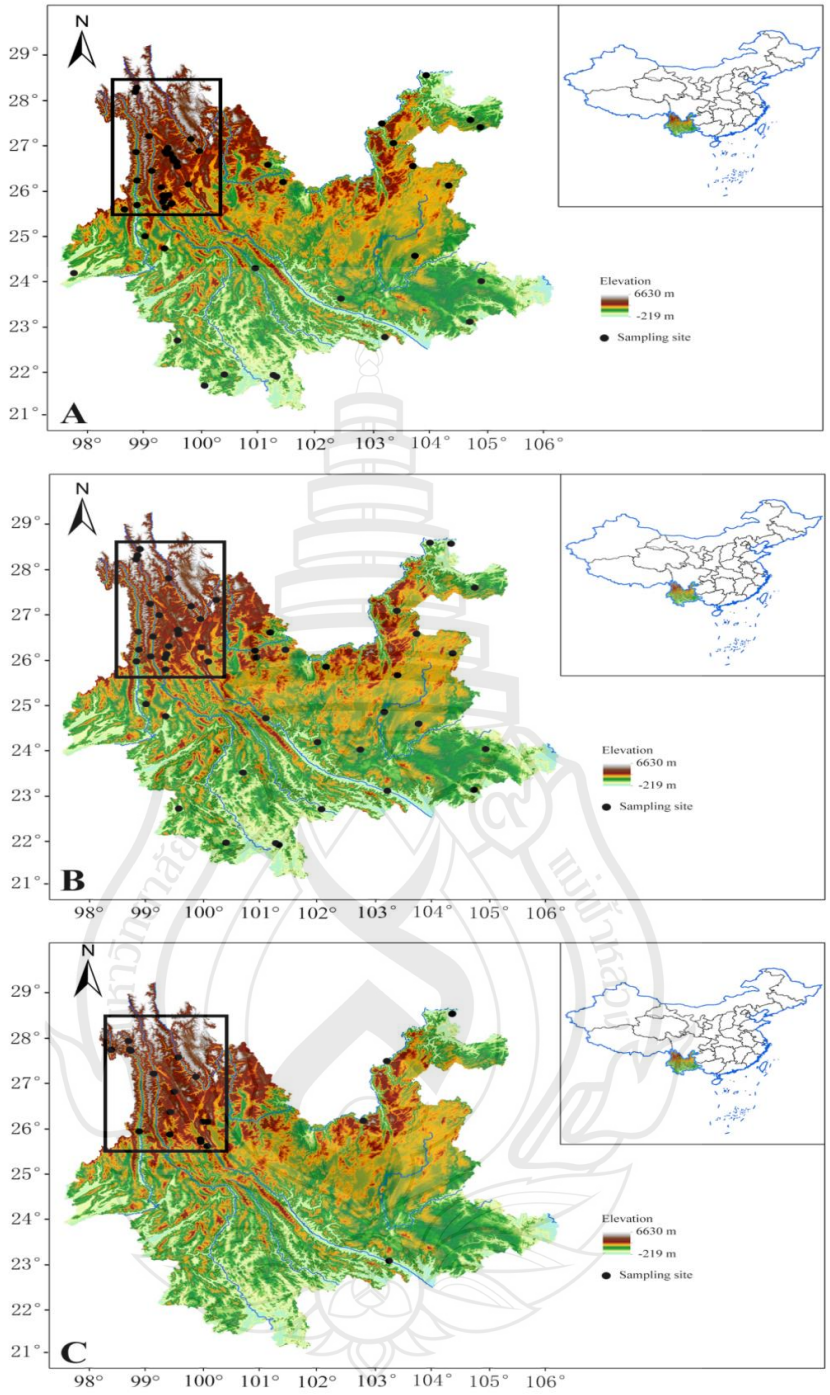

Figure 2.14 Distribution of ONTF new species and the top 50 sampling sites in number of species and strain. (A) The distribution of top 50 sampling sites with highest number of strains. (B) The distribution of top 50 sampling sites with highest number of species. (C). The distribution of sampling sites with new species

2.3.2 Diversity of *Orbiliomycetes* Nematode-Trapping Fungi (ONTF) in Burned Forests

2.3.2.1 Overall diversity of ONTF in burned forests

A total of 474 isolates representing 38 ONTF species, including 20 new species, were isolated from 184 sampling sites (368 samples) across three burned forests. The community of ONTF varied among the different burned forests. In the Wanqiao area, two genera and 14 species comprising 74 isolates were detected, including six *Arthrobotrys* species and eight *Dactylellina* species. Consistent with most normal habitats, *Arthrobotrys* maintained a dominant position with 61 isolates, while only 13 isolates of *Dactylellina* were found. In the Yushan area, 13 *Dactylellina* species totaling 20 isolates dominated, with *Arthrobotrys* contributing only four species and 16 isolates, and *Drechslerella* comprising four species and 12 isolates. In the Yunlong area, 24 species of *Dactylellina* with 231 isolates and nine *Drechslerella* species with 103 isolates were prominent, while *Arthrobotrys* was limited to five species and 18 isolates (Table 2.8).

Table 2.8 ONTF community composition on three burned forests

ONTF detection	Wanqiao			Yushan			Yunlong		
	Unburned area	Burned area	Total	Unburned area	Burned area	Total	Unburned area	Burned area	Total
Species counts	7	12	14	10	15	21	21	27	38
Strain counts	31	43	74	23	25	48	172	180	352
Arthrobotrys species counts	5	4	6	4	1	4	4	2	5
Arthrobotrys strain counts	33	28	61	14	2	16	14	4	18
OF of *Arthrobotrys*	100%	100%	100%	64.3%	14.3%	39.3%	5.6%	2.5%	4.1%
Dactylellina species counts	2	8	8	5	10	13	12	17	24
Dactylellina strain counts	2	11	13	6	14	20	127	104	231

Table 2.8 (continued)

ONTF detection	Wanqiao			Yushan			Yunlong		
	Unburned area	Burned area	Total	Unburned area	Burned area	Total	Unburned area	Burned area	Total
OF of *Dactylellina*	20%	60%	30%	35.7%	57.1%	46.4%	77.5%	57.5%	67.5%
Drechslerella species counts	0	0	0	1	4	4	5	8	9
Drechslerella strain counts	0	0	0	3	9	12	31	72	103
OF of *Drechslerella*	0	0	0	7.1%	42.9%	25.0%	17.5%	42.5%	30.3%

2.3.2.2 Impact of fire on ONTF community

Comparing the ONTF community between burned areas and adjacent unburned areas revealed a consistent trend across all three study regions. In terms of species number, the number of species detected in burned areas were significantly higher than those in unburned areas, with a general trend of a decrease in *Arthrobotrys* species and an increase in *Dactylellina* and *Drechslerella* species. In terms of isolate numbers, burned areas also had higher counts than unburned areas, with a general trend of a reduction in *Arthrobotrys* isolates and an increase in *Dactylellina* and *Drechslerella* isolates. Notably, in the Yushan area, the dominant group shifted from *Arthrobotrys* before the fire to *Dactylellina* after the fire (Figure 2.15).

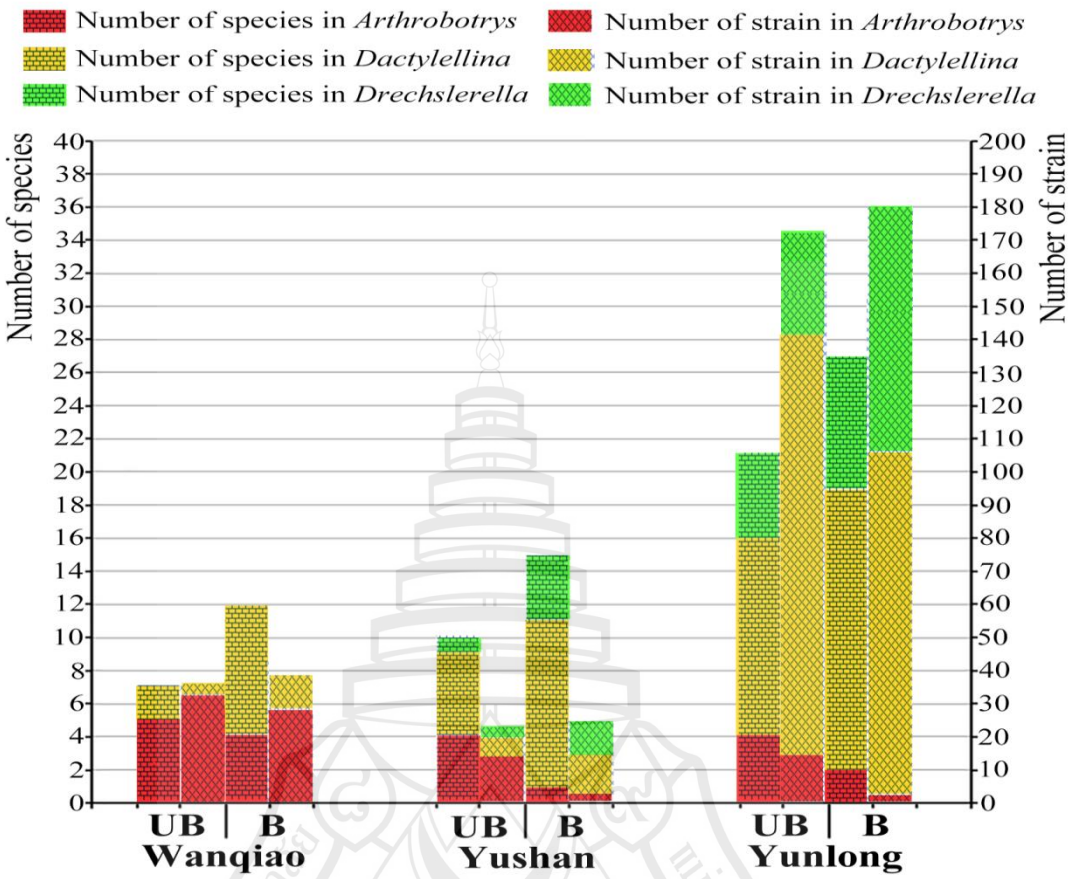

Figure 2.15 ONTF detection at three burned areas

Among different soil layers, in the unburned areas of all three study regions, *Arthrobotrys* had a higher detection rate in the upper soil layers, while *Dactylellina* and *Drechslerella* had higher deyection rates in the lower soil layers. After the fire, the detection rates of *Arthrobotrys* in both soil layers markedly decreased, while those of *Dactylellina* and *Drechslerella* significantly increased (Figure 2.16).

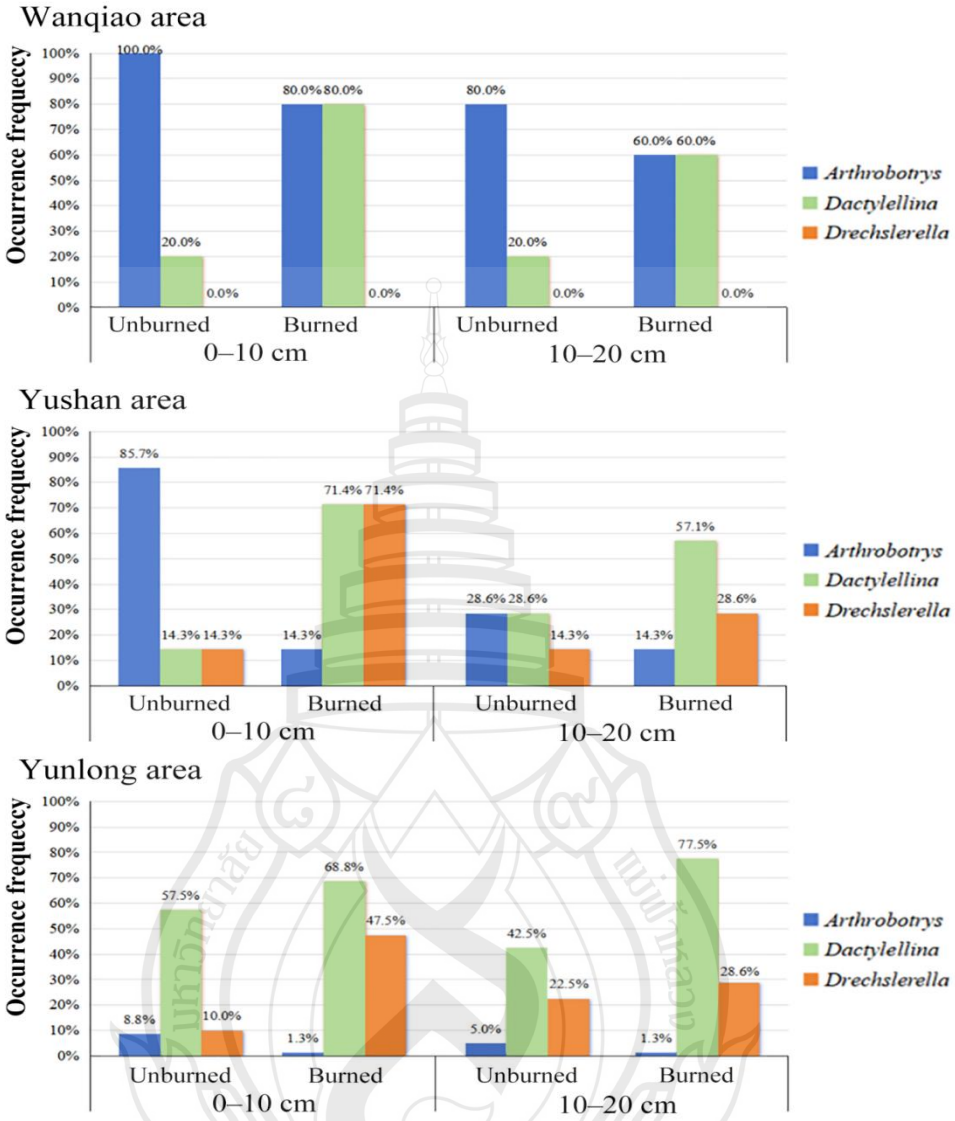

Figure 2.16 ONTF occurrence frequency (OF) at different soil layer in the three study areas. Numbers above the bars represent the OF value of different ONTF genera

2.4 Discussion

2.4.1 Diversity of *Orbiliomycetes* Nematode-Trapping Fungi (ONTF) in Terrestrial and Aquatic Habitats of Yunnan Province

This study isolated 3,455 strains of 62 ONTF species from 3,420 samples collected at 342 sites across Yunnan Province. The detection of ONTF at all sites with a sample detection rate of 94.94% illustrates the widespread and highly adaptable of ONTF, underscoring their significant diversity of ONTF in Yunnan.

The broad distribution of ONTF is commonly attributed to their predatory function, which enhances their environmental adaptability. Thus, current research on ONTF evolution focuses on the evolution of trapping structures, with the enhancement of predatory capabilities being a major evolutionary trend (Li et al., 2000; Li et al., 2005; Yang et al., 2007, 2012). According to this logic, species with stronger predatory abilities should be more widely distributed and abundant, while those with weaker predatory capabilities should be rarer and more narrowly distributed. However, in this study, regardless of the number of species or strains, the genus *Arthrobotrys*, known for weaker predatory capabilities, dominated, with a detection rate of 91.1% and accounting for 95.51% of all strains isolated. This paradox between reality and theory suggests that predatory traits, such as trapping structures and predation ability are not the sole factor influencing the wide distribution of ONTF. There must be other traits contributing significantly to their environmental adaptability. The evolutionary process of ONTF is essentially one of adaptive evolution; thus, traits related to environmental adaptation undoubtedly play a crucial role. Research focusing solely on the evolution of predatory traits risks overlooking the complexity of evolution and may not accurately reflect the real evolutionary processes or explain the current diversity of ONTF.

The discovery of new species provides crucial resources and foundational data for applications, conservation, taxonomy, evolution, and ecological studies. Since 2010, as the discovery of new ONTF species has become increasingly challenging, many researchers have presumed that no more new ONTF species remain to be discovered and have shifted focus away from diversity studies (Zhang et al., 2022). However, the

identification of 22 new species among the 62 species isolated in this study, accounting for 15% of the known ONTF, indicates that many undescribed ONTF await discovery.

Terrestrial soils, with higher detection rates, strain counts, and species numbers compared to freshwater sediments, and where ten new species were isolated, may be a stronghold for ONTF. This habitat type is crucial for ONTF diversity studies. The isolation of 42 ONTF species, including 13 unique and 12 new species from 1,710 freshwater sediment samples, demonstrates that aquatic habitats harbor a rich and unique ONTF diversity and are an essential component of ONTF diversity that should be integrated into future studies. Additionally, all 42 ONTF species isolated from aquatic habitats were from areas not deeper than two meters; previous research indicated no ONTF presence in waters deeper than four meters (Hao et al., 2005). However, numerous nematodes inhabit deeper waters (Ptatscheck & Traunspurger, 2020; de Jesús-Navarrete et al., 2022), suggesting other nematode-regulating agents might be present at these depths. Exploring and studying these elusive nematode-trapping microorganisms could provide valuable insights into the origins and evolutionary processes of carnivorous microorganisms and offer ideal materials for the bio-control of parasitic nematodes in aquatic habitats.

2.4.2 The Impact of Forest Fires on *Orbiliomycetes* Nematode-Trapping Fungi (ONTF) Diversity

Since 2010, research on new species of ONTF has entered a bottleneck phase, with more focus directed towards their predatory mechanisms, evolutionary development of predatory organs, and molecular mechanisms of trap formation. Hindered by the scarcity of species, especially in the genera *Dactylellina* and *Drechslerella*, many studies struggled to produce compelling results. Beyond our limited exploration of aquatic habitats and areas like the three parallel rivers region, what might we be overlooking? Could it be differences in survival strategies between ONTF genera or community distribution differences caused by these strategies?

Increasingly, microbial diversity surveys, whether based on high-throughput sequencing or pure culture techniques, tend to discover microorganisms that are abundant, predominantly surface-dwelling, or have strong saprophytic capabilities. Previous habitat surveys also identified more species from the genus *Arthrobotrys* (Mo

et al., 2008; Swe et al., 2009; Singh et al., Zhang & Hyde, 2014; Zhang et al., 2020; Deng et al., 2023), likely because these species possess stronger saprophytic capabilities, gaining a growth advantage in environments rich in organic matter. Another factor is the common practice of sampling only the top 10 cm of soil, potentially overlooking species residing in lower layers. This study hypothesizes that forest fires, by clearing ONTF from the upper soil layers, create ecological niches that are then occupied by ONTF residing in lower layers, thereby increasing soil ONTF diversity post-fire and facilitating the discovery of new species.

Indeed, this study alone identified 20 new species from just three burned forests, accounting for 20% of the species described. We also observed significant changes in the ONTF community structure post-fire, with *Datylellina* and *Drechslerella* species replacing the previously dominant *Arthrobotrys*. This confirms our hypothesis and suggests that many more ONTF species reside in the lower soil layers. The high temperatures and the insulating properties of the soil during fires provide the perfect opportunity for these lower-layer species to emerge. Moreover, many studies on post-fire biodiversity have found that moderate burning can promote greater biological diversity; for example, morels become more abundant post-fire (Larson et al., 2016), and plant diversity increases (Pausas & Ribeiro, 2017). These findings underscore that burned areas are ideal for research, particularly for discovering new species.

CHAPTER 3

Fusarium xiangyunensis (*NECTRIACEAE*), A REMARKABLE NEW SPECIES OF NEMATOPHAGOUS FUNGI FROM YUNNAN, CHINA

3.1 Introduction

Nematophagous fungi are an important, fascinating group, living in soil, plant debris, freshwater and marine sediments and animal wastes, which catch, parasitize and poison nematodes for nitrogen supplement (Swe et al., 2009; Lin et al., 2016). In general, these fungi are classified into four groups based on their nematicidal mechanisms: (1) nematode-trapping fungi which catch and kill nematodes with a variety of traps formed by mycelia. In this group, those predatory species of the family *Orbiliaceae* are well-known; (2) endoparasitic fungi which usually produce special spores (encysting, adhesive and ingested spores) which attach to and penetrate the cuticle of nematodes, such as *Harposporium anguillulae* and *Catenaria anguillulae*; (3) egg parasitic fungi which invade nematode eggs or females with hyphae tips, and (4) toxin-producing fungi which immobilize nematodes with toxic metabolites (Li et al., 2005; Zhang & Hyde, 2014). The first nematophagous fungus, *Arthrobotrys superba* Corda, was described in 1839. Now, at least 700 fungal species have been reported to have the ability to kill nematodes (Freitas et al., 2018). However, it is estimated that there are 6000–8000 species of nematophagous fungi not found remaining to be described (Drechsler, 1941; Pramer, 1964; Thorn & Barron, 1984; Li et al., 2000; Mcinnes, 2003; Yang et al., 2012).

The genus *Fusarium* (*Nectriaceae*) is a large complex of plant and animal pathogenic taxa, with a worldwide distribution. The genus was introduced by Link (1809) with *F. roseum* Link as type species. The primary character of this genus is the distinctive canoe or banana-shaped asexual conidia (Leslie & Summerell, 2006). Due

to the previous limitations of classification based on morphology, many species with similar characters were identified as a same species. In recent years, a multi-faceted approach has been used to classify the genus, with the *F. solani* species complex having been better resolved and new species having been introduced (Zhang et al., 2006; Short et al., 2013; Chehri, 2015, Guevara et al., 2016). Several metabolic compounds have been isolated and identified from *Fusarium* species (Brian et al., 1961; Blight & Grove, 1974; D'mello et al., 1999). In addition, some species of *Fusarium*, such as *F. oxysporum*, *F. moniliforme*, *F. sulphureum* and some species of *F. solani* complex, have ability to protect plants from nematodes by inducing plant resistance and killing nematodes (FSSC) (Mani & Sethi, 1984; Mathivanan et al., 1998; Zareen et al., 2001; Ciarmela et al., 2010; Maia et al., 2013).

In this study, we focused on the diversity of hot-spring inhabiting fungi, we found a species of *Fusarium* which is novel based on evidence from morphology and molecular data (ITS, TEF and RPB1). The species also has strong nematicidal activity in distilled water and on solid medium. Based on nematicidal mechanism, it was characterized as nematode-trapping fungi. In this paper, we described this new species and its nematicidal activity.

3.2 Material and Methods

3.2.1 Collection and Isolation

Water-logged soil samples were collected from Da-bo-na hot-spring, Xiangyun County, in Yunnan Province, China. The average annual water temperature of the hot-spring was 45 ℃ with a pH of 6.9. The samples were spread on corn meal agar (CMA) plates using a sterile toothpick and free-living nematodes added (*Panagrellus redivivus* Goodey) as baits to promote the germination of nematophagous fungi. After two weeks of incubation at room temperature, a fungus strain was found on the surface of soil samples and transferred to fresh CMA plates and incubated at 30 °C for growth of pure culture. The culture was deposited in China General Microbiological Culture Collection Center (CGMCC 3.19676) and duplicated in the microbiology lab at the School of Agriculture and Biology, Dali University, China (DLU11-1).

3.2.2 Morphological and Phylogenetic Analyses

The morphological characters of this strain were captured and measured with an Olympus BX51 microscope (Olympus Corporation, Japan). Total DNA was extracted from the mycelia grown on potato dextrose agar (PDA) medium according to the method of Jeewon et al. (2002). Primer pairs ITS4 and ITS5 (White et al., 1990) were used to amplify the complete ITS and 5.8S region, the translation elongation factor 1-atpha (TEF) gene was amplified with primer pair TEF-1 and TEF-2 (O'Donnell et al., 1998), and RPB1 gene was amplified with primer pair RPB1-DF2asc (Hofstetter et al., 2007) and RPB1-G2R (Stiller & Hall, 1997). PCR amplification was performed as follows: pre-denaturation at 94℃ for 3 minutes, followed by 35 cycles of denaturation at 94℃ for 45 seconds, annealing at 52℃ (ITS), 55℃ (TEF) for 1 minute, extension at 72℃ for 1 minute, and a final extension at 72℃ for 10 minutes. The PCR thermal program for RPB1 gene was amplified as initially 95°C for 5 minutes, followed by 35 cycles of denaturation for 1 minute at 95°C, annealing for 90 seconds at 55°C, elongation for 2 minutes at 72°C, and final extension for 10 minutes at 72°C. The PCR products were sequenced in forward and reverse directions.

Sequence data of related taxa were downloaded from NCBI (National Center for Biotechnology Information) based on the blast results and relevant publications (Aoki et al., 2003; O'Donnell et al., 2013; Nalim et al., 2011; Lombard et al., Chehri et al., 2015; Laurence et al., 2016; Shang et al., Šišić et al., 2018; Torbati et al., 2019) (Table 3.1). Three genes were aligned with MAFFT v.7 (Katoh & Standley, 2013; http://mafft.cbrc.jp/alignment/server/) and manually adjusted via BioEdit v7.2.3 (Hall, 1999) to improve the alignment respectively, then were combined with MEGA6.0 (Tamura et al., 2013). Phylogenetic trees were inferred with maximum likelihood (ML), maximum parsimony (MP) and Bayesian inference (BI) analyses.

The optimal substitution model of three genes were estimated with jModeltest v2.1.10 (Posada, 2008) respectively. The best-fit model is resulted as SYM+I+G model for ITS, TVM+I+G for TEF and TIMlef+I+G for RPB1 under the Akaike Information Criterion (AIC)

Bayesian Inference (BI) analysis was performed via the web CIPRES Science Gateway v. 3.3 (Miller et al., 2010) using MrBayes v. 3.2.6 on XSEDE. Posterior probabilities (PP) (Rannala & Yang, 1996; Zhaxybayeva & Gogarten, 2002). Six simultaneous Markov Chains were run from random trees for 10,000,000 generations and trees were sampled every 100th generation with total of 100,000 trees. The first 25% trees were discarded, and the remaining trees were used to calculate the posterior probabilities (PP) in the majority rule consensus tree.

Maximum likelihood (ML) analysis was performed using IQ-Tree v1.6.5 (Nguyen et al., 2014). The dataset was partitioned, and each gene was analyzed with corresponding model. The bootstrap replication was set as 1000 and *Nectria cinnabarina* CBS 256.47 was set as an out-group.

Maximum parsimony analysis (MP) was performed by PAUP v. 4.0b10 (Swofford, 2002) using the heuristic search option. Max-trees were set up at 1000 with all characters were treated as unordered and of equal weight. Gaps were treated as missing data and the branches of zero length were collapsed. All multiple equally parsimonious trees were saved. Bootstrap replicate was set as 1000, each with ten replicates of random stepwise addition of taxa (Hillis & Bull, 1993). The Kishino-Hasegawa tests (Kishino & Hasegawa, 1989) were obtained to determine the significantly different parsimonious trees under different optimality criteria.

The trees were shown with FigTree v1.3.1 (Rambaut, 2009) and Treeview (Page, 1996). The backbone tree was edited in Microsoft Power Point (2013) and Adobe Photoshop CS6 software (Adobe Systems, USA). Sequences derived from this study were deposited in GenBank (Table 3.1)

Table 3.1 GenBank accession numbers of isolates included in this study

Taxon	Strain No.	GenBank accession no.		
		ITS	TEF	RPB1
Fusarium acuminatum	PUF036	HQ165939	HQ165867	—
Fusarium ambrosium	NRRL 46583	KC691556	KC691528	KC691585
Fusarium asiaticum	NRRL 13818	—	AF212451	JX171459
Fusarium avenaceum	CBS 13818	—	HQ704078	—
Fusarium babinda	NRRL 25539	—	—	JX171519
Fusarium caeruleum	IR-1Sm-2-7-3-2	KP017789	—	—
Fusarium commune	NRRL 28387	—	HM057338	JX171525
Fusarium cuneirostrum	BF1117-13	KF530848	KF025649	—
Fusarium ensiforme	CPC 27191	LT746248	LT746200	—
Fusarium equiseti	NRRL 20697	GQ505683	GQ505594	JX171481
Fusarium falciforme	NRRL 32872	DQ094623	DQ247169	KC808313
Fusarium flocciferum	NRRL 45999	GQ505465	GQ505433	HM347195
Fusarium graminearum	NRRL 31084	—	HM744693	JX171531
Fusarium illudens	NRRL 22090	AF178393	AF178326	JX171488
Fusarium kelerajum	FRC S1837	JF433040	DQ247516	—
Fusarium keratoplasticum	NRRL 54963	—	KC808190	KC808265
Fusarium kurunegalense	FRC S1833	JF433036	DQ247511	—
Fusarium langsethiae	NRRL 53439	—	HM744691	KT597714
Fusarium lateritium	NRRL 52786	—	JF740854	JF741009
Fusarium lichenicola	NRRL 32434	DQ094444	DQ246977	HM347156
Fusarium mahasenii	FRC S1845	JF433045	DQ247513	—
Fusarium metavorans	NRRL 43489	DQ790528	DQ790484	HM347180
Fusarium neocosmosporiellum	NRRL 22468	DQ094318	AF178349	KC691616
Fusarium petroliphilum	NRRL 54995	KC808257	KC808215	KC808293
Fusarium phaseoli	CBS 265.5	MH856617	HE647964	—
Fusarium pseudensiforme	NRRL 46517	KC691584	KC691555	KC691615
Fusarium sarcochroum	NRRL 20472	—	—	JX171472
Fusarium solani	NRRL 32810	DQ094577	DQ247118	—
Fusarium solani	CBS 490.63	MH858333	JX435168	—
Fusarium solani f. sp. *batatas*	NRRL 22400	AF178407	—	—
Fusarium solani f. sp. *glycines*	NRRL 22823	AF178418	AF178356	—
Fusarium solani f. sp. *mori*	NRRL 22230	AF178420	AF178358	JX504709
Fusarium solani f. sp. *piperis*	CML 2187	MH879154	JX657677	—
Fusarium solani f. sp. *pisi*	CBS 123669	KM231796	KM231925	—
Fusarium solani f. sp. *robiniae*	NRRL 22161	AF178395	AF178330	JX504707
Fusarium solani f. sp. *xanthoxyli*	NRRL 22163	AF178394	AF178328	JX504708
Fusarium solani f. sp. *passiflorae*	IBFS09	FJ200222	JX524770	—

Table 3.1 (continued)

Taxon	Strain No.	GenBank accession no.		
		ITS	TEF	RPB1
Fusarium solani f. sp. *phalaenopsi*	RBG1806	KP768431	—	—
Fusarium solani f. sp. *eumartii*	Fs122	DQ164845	DQ164849	—
Fusarium solani f. sp. *radicicola*	MAFF 731042	AB513851	AB513841	—
Fusarium stilboides	NRRL 20429	—	—	JX171468
Fusarium striatum	CBS 101573	KM231798	KM231927	—
Fusarium torulosum	NRRL 52772	JF740926	JF740840	—
Fusarium tricinctum	NRRL 25481	HM068317	HM068307	JX171516
Fusarium venenatum	CBS 458.93	NR_156290	KM231942	—
Fusarium virguliforme	PPRI13441	KF648842	KF648850	—
Fusarium witzenhausenense	CBS 142480	MG250477	KY556525	—
Fusarium xiangyunensis	CGMCC3.19676	MH780923	MH992629	MH999281
Nectria cinnabarina	CBS 256.47	HM484692	—	—

3.2.3 Morphological and Phylogenetic Analyses

The nematode-infection process was observed in sterile water and on solid medium. In the sterile water assay, the conidia were harvested from pure culture with sterile distilled water, then 500 μL of rinsed conidia solution mixed with 100 nematodes (*P. redivivus*) in a sterile petri-dishes were incubated at room temperature. 500 μL of sterile distilled water mixed with 100 nematodes (*P. redivivus*) was maintained as control. The process of microconidia adhering and killing nematodes was observed and recorded using an Olympus BX51 microscope (Olympus Corporation, Japan).

In the solid medium assay, the strain was inoculated on fresh CMA plates (a square slot of 2×2 cm was created by removing the agar) and incubated at 30°C. When the mycelia were spread over the square slot, about 500 nematodes (*P. redivivus*) were added to the slot and observed by stereoscopic microscope one hour later. The process of microconidia adhering and killing nematodes was recorded with an Olympus BX51 microscope (Olympus Corporation, Japan).

3.3 Results

3.3.1 Phylogenetic Analysis

The alignment contained three genes (ITS, TEF and RPB1) from 49 species of *Fusarium* and *Nectria cinnabarina* CBS 256.47 was selected as the outgroup taxon. The dataset comprised 1,561 characters (ITS: 500, 78 gaps; TEF: 463, 67 gaps; RPB1: 598, no gaps), including 863 conserved characters, 687 variable characters and 536 parsimony-informative characters. Phylogenetic trees obtained from maximum likelihood (RAxML), maximum parsimony (MP) and Bayesian inference (BI) analyses show similar topologies, so the best scoring RAxML tree was selected to represent in here (Figure 3.1).

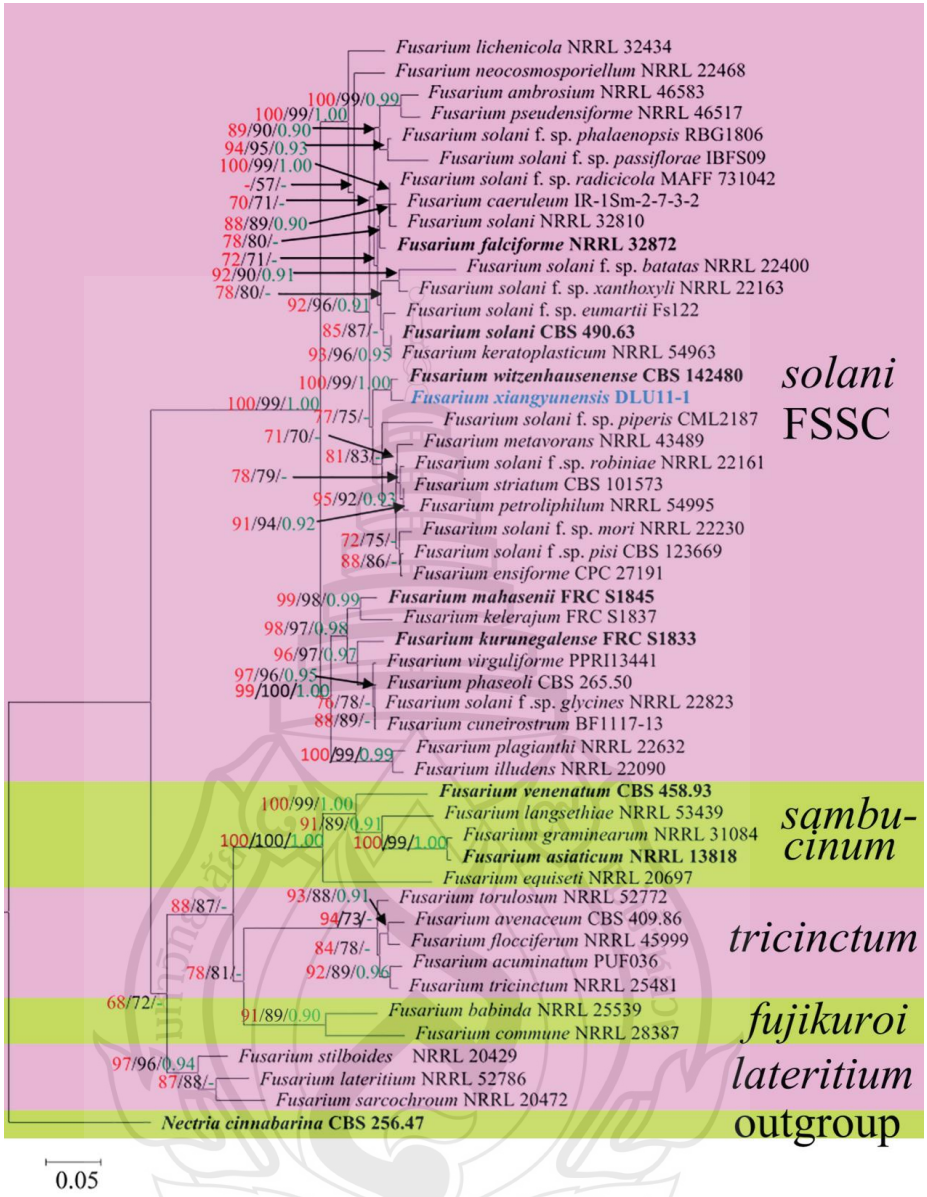

Figure 3.1 Maximum likelihood tree based on a combined ITS, TEF and RPB1 sequence data from 49 species of *Fusarium*. Bootstrap support values for maximum parsimony (red) and maximum likelihood (black) equal or greater than 50% are shown above the nodes and Bayesian posterior probabilities values (green) greater than 0.90 are also indicated above the nodes. The new isolates are in blue, ex-type strains are in bold. The tree is rooted to *Nectria cinnabarina* (CBS 256.47)

3.3.2 Taxonomy

Fusarium xiangyunensis F. Zhang, X.Y. Yang & K. D. Hyde, sp. nov. (Figure 3.2)

MycoBank number: MB 827515; Facesoffungi number: FoF 05669

Etymology: The species name "xiangyunensis" refers to the location where the sample was collected.

Material examined: CHINA, Yunnan Province, Xiangyun Country, Dabona Hot-spring, from hot-spring sediment, 11 June 2016, F. Zhang, YXY11-1, Holotype DLU11-1, ex-type living culture, CGMCC3.19676.

Saprobic on soil. *Isolation* grew fast on CMA, reaching a colony-diameter of 80 mm after six days incubation at 30°C. *Colonies* white, cottony at initial stage (1–9 days), later becoming usually green to bluish-brown (≥ 10 days). *Mycelia* colorless, composed of septate, branched, smooth. *Conidiophores* macronematous, mononematous, erect, flexuous, septate, unbranched or simple-branched at the base. *Conidiogenous cells* phialidic, cylindrical, with a minute collarette. *Conidia* two types: *Microconidia*, ellipsoidal, reniform, 8–25 × 3–6 μm., 0–1 septum in the middle, hyaline, smooth, developing in false, slimy chains. *Macroconidia* falciform, pod-shaped, falcate, straight or slightly curved, beaked at both ends, guttulate, 10–31 × 3.5–6.5 μm., 2–4 septate, hyaline, smooth. *Chlamydospores* spherical, ellipsoidal, in beaded-like chains, smooth to rough-walled, 5–10.5 μm. diameter.

Note: Based on phylogenetic analyses and morphological comparison, our isolate belongs to genus *Fusarium*. Phylogenetic analyses of combined ITS, TEF and RPB1 sequence data (Figure 3.1) show that *F. xiangyunensis* (CGMCC3.19676.) clusters with those species belonging to the *F. solani* species complex (FSSC) and grouped together with *F. witzenhausenense* with high support value (100% MP, 99% ML and 1.00 PP). There are 10 base pairs (no gaps) differences between *F. xiangyunensis* and *F. witzenhausenense* for ITS (two pairs) and TEF (eight pairs) sequences. Although both species could not be separated based on molecular data, they have a great difference in morphology, including the habitats, conidia characteristics and chlamydospore formation. *Fusarium witzenhausenense* was isolated from vascular tissue of infected hibiscus (*Hibiscus* sp.), while *F. xiangyunensis* was isolated from hot-spring waterlogged soil. Microconidia of *F. witzenhausenense* (6.2–22.5×3.1–6.1 μm.) are slightly smaller than those of *F. xiangyunensis* (8–25×3–6 μm.). Macroconidia of *F. witzenhausenense* are obtuse at both ends, while its in *F. xiangyunensis* they are tapered at both ends and beak-like, and are

smaller than *F. witzenhausenense* [*F. witzenhausenense*, 25.4–41.3×4.8–6.9 μm. versus 10–31×3.5–6.5 μm., *F. xiangyunensis*]. No chlamydospore formation was observed in *F. witzenhausenense*, whereas the chlamydospores of *F. xiangyunensis* are spherical to ellipsoidal and bead-like in appearance (Šišić et al., 2018). So, we propose this isolate to be a new species based on morphological data.

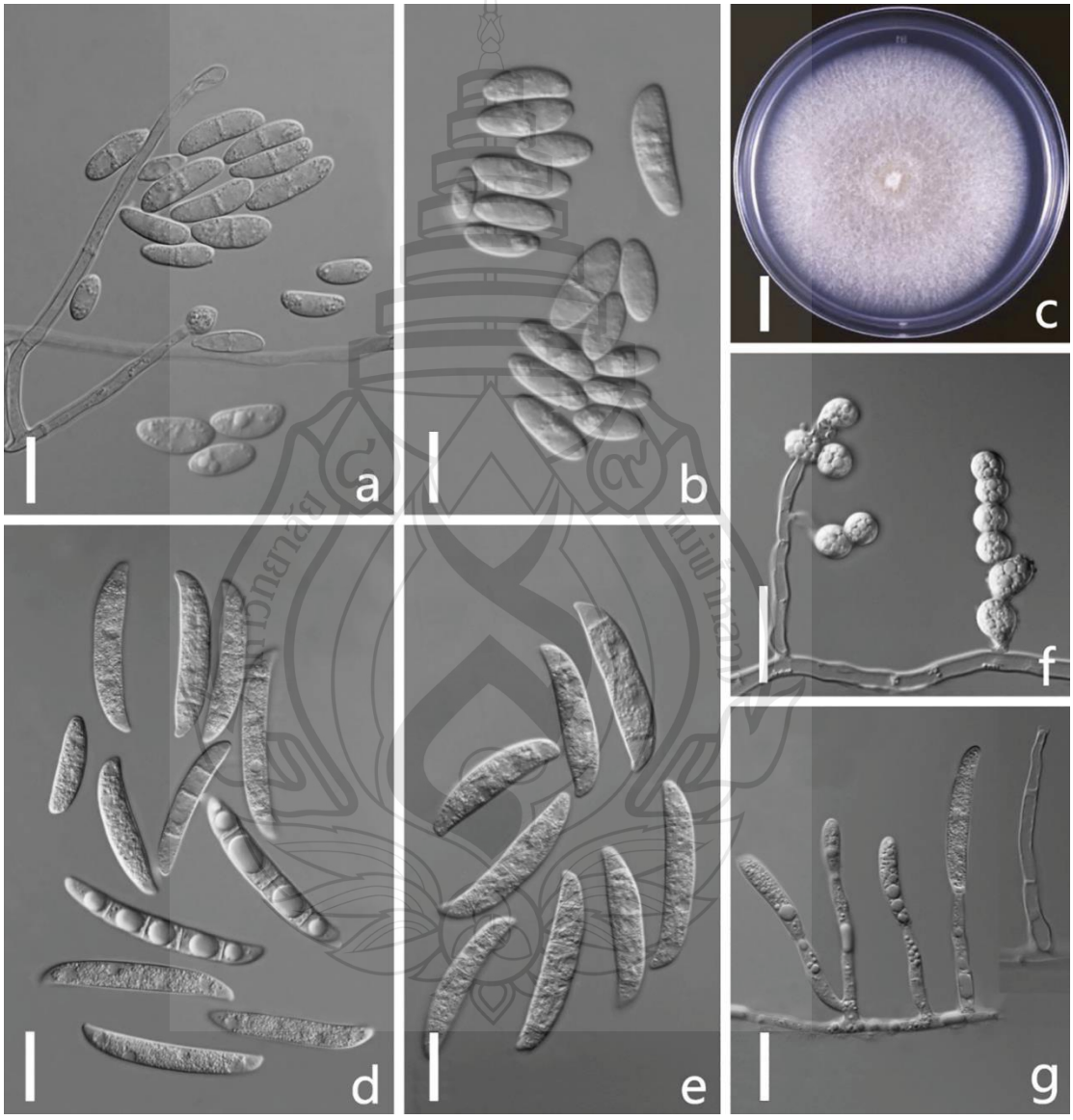

Figure 3.2 *Fusarium xiangyunensis* (CGMCC3.19676). (a, b) Microconidia. (c) Colony. (d, e) Macroconidia. (f) Chlamydospores. (g) Conidia developing on conidiophores. Scale bars: (a, b, d–g) = 10 μm., (c) = 10 mm.

3.3.3 Nematode Infection Process

All nematodes in sterile water or on solid medium with fungi were killed within two hours**.** When the nematodes contact with the conidia, the latter tightly adhered to the cuticle of nematodes. Then, the nematodes gradually got blackened, paralyzed and died. Finally, the mycelia invade the nematodes and digests them (Figure 3.3). Whereas, all nematodes in the control remained alive.

In addition, to confirm that the nematodes were killed by *Fusarium xiangyunensis*, several infected nematodes were transferred to fresh PDA plates with sterile toothpicks and incubated at 30°C for culture. Then, the sequence of ITS, TEF and RPB1 of the culture were obtained using the method described in above. The sequences were compared with the original sequences (the sequences first obtained for phylogenetic analysis), and found that there is just 1 bp (base pair) difference between them in TEF gene. Base on above, we can confirm that the nematodes were killed by *F. xiangyunensis*.

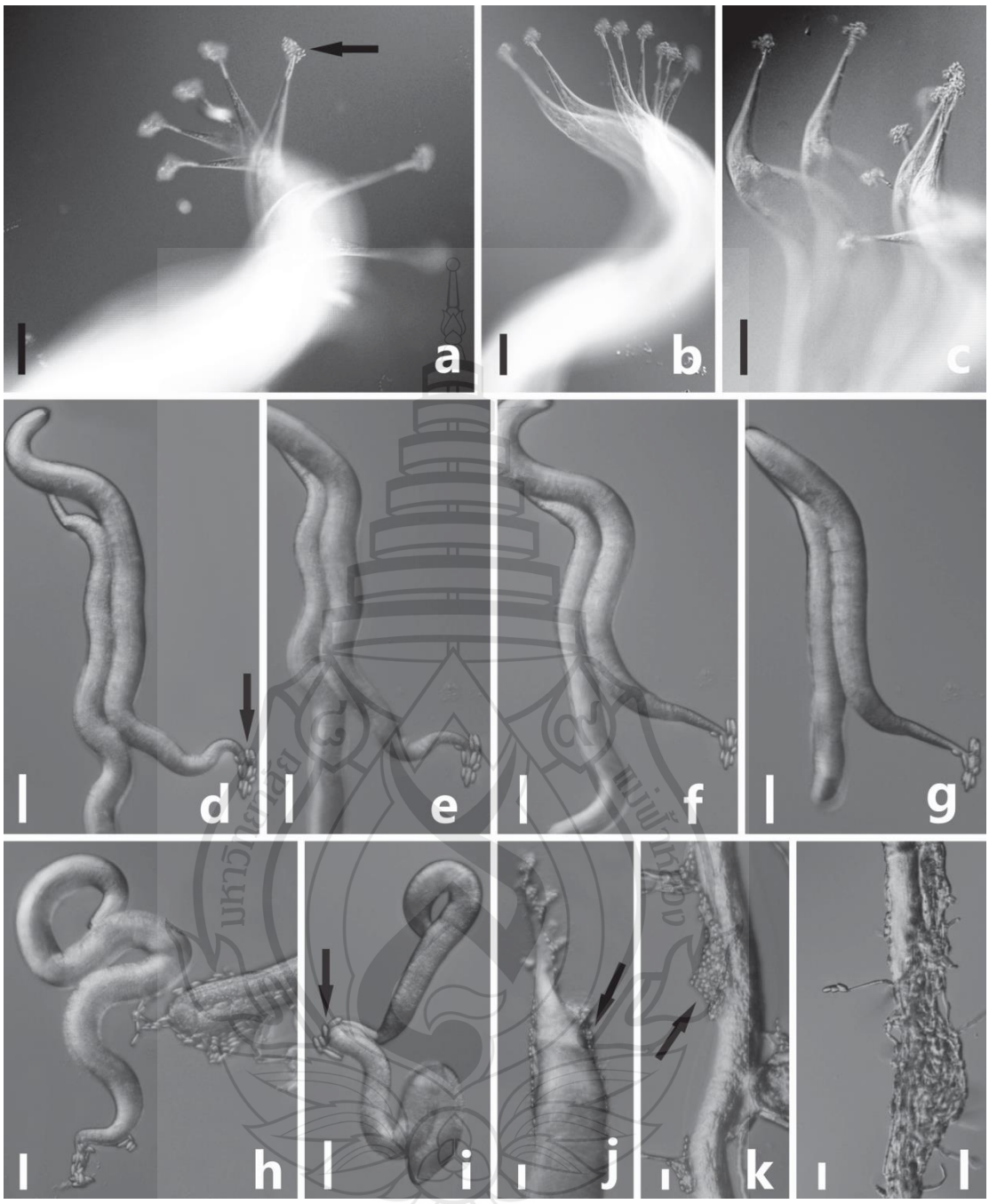

Figure 3.3 Nematode-killing process. (a–c) Nematode-trapping process in sterile water. (d–l) Nematode-trapping process on solid medium, note the nematode gradually blackened in d–g, note the fungus invading the cuticle of nematodes and mycelia filling the coelom in h–l. Arrow points to adhesive microconidia. Scale bars: (a–i) = 50 μm.

3.4 Discussion

With cottony, white to bluish-brown mycelia, macronematous, mononematous, erect, hyaline, septate, sparingly branched conidiophores, terminal, monophialidic conidiogenous cells with minute collarette, falcate and 3–4-septate, smooth, hyaline, guttulate, macroconidia and 0–1-septate, hyaline, smooth microconidia, *Fusarium xiangyunensis* is morphologically similar to *F. solani* reported in 1842 by KFP von Martius (Saccardo, 1880; Schroers et al., 2016). However, it is well known that *F. solani* is a species-complex and those strains identified as *F. solani* based on morphology. Initially, we identified our strain as *F. solani* based on its morphology. However, when the ITS, TEF and RPB1 genes were sequenced, the phylogenetic analysis showed that *F. xiangyunensis* clustered in one clade with *F. solani* species complex and was sister to *F. witzenhausenense*. Based on this, combined with comparative studies of morphology, we identified *F. xiangyunensis* as a new species.

Some species of *Fusarium* have been reported for their potential biological control of nematodes. Some strains of *F. oxysporum* can reduce the rot of excised banana roots caused by *Pratylenchus goodeyi* (Speijer & Sikora, 1993). Hallmann and Sikore (1994) reported that *Fusarium* species can reduce nematode diseases by inducing plant resistance, and at the same time, the species can also control nematode parasitism by reducing the penetration of J2 juveniles in plant roots. Many studies have shown that some species of *Fusarium*, such as *F. oxysporum, F. moniliforme, F. sulphureum* and the *F. solani* complex have ability to kill *Toxocara canis* eggs (a zoonotic geohelminth) (Mathivanan et al., 1998; Ciarmela et al., 2010; Maia et al., 2013). In addition, some species of *F. solani* complex can kill nematodes in fermentation broth (Mani & Sethi, 1984; Zareen et al., 2001). However, in the above studies, parasitism is not a mechanism used by these species. In this study, we found that *F. xiangyunensis* can infect and kill nematodes by adhering nematode cuticles through microconidia. Therefore, based on the nematicidal mechanism presented above, and a comparative study with other nematophagous fungi (Drechsler, 1968; Desai et al., 1972; Ciancio et al., 1988; Dijksterhuis et al., 1993; Khan et al., 2006; Maia et al., 2013), we classify this *Fusarium* species as an endoparasitic fungus.

Many studies reported that there are abundant nematophagous fungi (especially nematode-trapping fungi) live in water (Mo et al., 2005; Zhang et al., 2007; Swe et al., 2009). While, there have been no studies indicating how these fungi kill nematodes in water environment. This study discovered that a new species (*Fusarium xiangyunensis*) produces microconidia which can adhere and kill nematodes in sterile water. It infers that this strain can also kill nematodes in the natural water environment, and we speculate that other fungi with similar nematicidal mechanisms may also be able to control the population of nematodes in aquatic ecosystems. Therefore, this finding suggests more extensive studies to isolate nematophagous fungi from aquatic environments and further studies such as the experiment of nematode-infection process in natural water environment should be done.

CHAPTER 4

TWO NEW SPECIES OF NEMATODE-TRAPPING FUNGI (*Dactylellina*, *ORBILIACEAE*) FROM BURNED FOREST IN YUNNAN, CHINA

4.1 Introduction

Nematode-trapping fungi are a group of fungi which form trapping devices (adhesive networks, adhesive knobs, adhesive branches, non-constricting rings and constricting rings) to capture nematodes for nutrients (Barron, 1977; Li et al., 2006; Zhang & Hyde, 2014). They were broadly studied because of their special morphology, function and potential value on biological control of animal and plant parasitic nematodes (Linford et al., 1938; Jaffee et al., 1993; Wolstrup et al., 1996; Jaffee et al., 1998; Morton et al., 2003; Liu et al., Borai et al., Kumar et al., Swe et al., 2011; Vilela et al., 2012). Since 1839 the first nematode-trapping fungi species *Arthrobotrys superba* Corda was described (Corda, 1839), more than 100 species have been reported. Among them, the predatory species of *Orbiliaceae* family constitutes the majority (97 species) (Liu et al., Zhang & Hyde, 2014). Initially, these species were classified into more than 26 genera successively. After that, they were classified into *Arthrobotrys*, *Dactylella*, and *Monacroporium,* three genera based on morphology of conidia and conidiophores (Zhang & Mo, 2006). With the development of molecular biology, phylogenetic studies based on DNA sequence have revised the taxonomy system of this group again, the view that classified these species into *Arthrobotrys*, *Dactylellina*, and *Drechslerella*, three genera based on the types of trapping devices was proposed (Li et al., 2005; Yang et al., 2007; Zhang & Hyde, 2014).

The genus *Dactylellina* was first described by Morelet (1968) with *D. Leptospora* Drechsler. At that time, it was characterized by elongate, fusiform conidia, while microconidia rarely formed. Subsequently, Scholler et al. (1999) revised the characteristics of this genus to catch nematodes with stalked adhesive knobs or non-constricting rings, and moved all species with this trait into this genus. Furthermore, based on phylogenetic analysis, the characteristics of this genus were revised again to produce adhesive knobs, adhesive branches and non-constricting rings (Li et al., 2005; Yang et al., 2007). This revision has been accepted by many scholars. Until 2014, 28 species have been reported in this genus (Zhang & Hyde, 2014).

Recently, two species of nematode-trapping fungi were isolated from the burned forest, and identified as two new species of *Dactylellina* based on morphological and phylogenetic analysis. We describe them with illustrations herein.

4.2 Material and Methods

4.2.1 Samples Collection, Isolation and Morphology

Collection: soil samples were collected from the burned forest in Cangshan Mountain Dali City, Yunnan Province, China (geographical coordinates: N 25°37′09.37″, W 100°09′02.39″). After removing the fallen leaves from the soil surface, about 100 g of soil was collected and put into zip lock bag, the sample information was recorded. The sample was brought back to the laboratory and stored in the refrigerator at 4℃, and was processed within four days.

Isolation: the samples were sprinkled on corn meal agar (CMA) plates with sterile toothpicks. Then, free-living nematodes (*Panagrellus redivivus* Goodey) were added as baits to promote the germination of nematode-trapping fungi, three repetitions per sample. After three weeks of incubation at room temperature, the plates were observed under a stereo microscope to find the spores of nematode-trapping fungi. Following, a single spore was transferred to a new CMA plate using sterile toothpick, repeat this step until the pure culture was obtained.

Morphology: the strains were transferred to fresh CMA plates (a square slot 2×2 cm was created by removed the agar) and incubated at 26℃, when the mycelia overspread the square slot, about 500 nematodes (*P. redivivus*) were added to the slot to induce the formation of trapping devices, then type of trapping devices were checked under a stereo microscope. All morphological characters were captured and measured with an Olympus BX51 microscope (Olympus Corporation, Japan).

4.2.2 DNA Extraction, PCR Amplification and Sequencing

Total DNA were extracted from the mycelia grown on the potato dextrose agar (PDA) plates according to the method of Jeewon et al. (2002). Primer pairs ITS4-ITS5 (White et al., 1990), 526F-1567R (O'Donnell et al., 1998), 6F-7R (Liu et al., 1999) were used to amplify the ITS, TEF and RPB2 genes respectively. The PCR amplifications were performed as follows: pre-denaturation at 94 ℃ for 4 minutes, followed by 35 cycles of denaturation at 94℃ for 45 seconds, annealing at 52 ℃ (ITS), 55 ℃ (TEF) for 1 minute, extension at 72℃ for 1.5 minutes, and final extension at 72 ℃ for 10 minutes. The PCR thermal cycle program for RPB2 gene was performed as follows: 95 ℃ for 4 minutes, followed by 35 cycles of denaturation at 95 ℃ for 1 minutes, annealing at 54 ℃ for 1 minute, elongation at 72 ℃ for 2 minutes, and final extension at 72 ℃ for 10 minutes. The PCR products of ITS and RPB2 genes were sequenced in forward and reverse directions using the above PCR primers. The primer pair 247F-609R (Yang et al., 2007) was used to sequence TEF genes.

4.2.3 Phylogenetic Analysis

Based on morphological characteristics and the DNA sequence blast results from NCBI, we determined that these two new species belong to *Dactylellina*. So, all sequences of ITS, TEF and RPB2 of *Dactylellina* species were downloaded from GenBank (Table 4.1). Three genes were aligned with MAFFT v.7 (Katoh & Standley, 2013; http://mafft.cbrc.jp/alignment/server/) and manually adjusted via BioEdit v7.2.3 (Hall, 1999) to improve the alignment respectively, then were combined with MEGA 6.0 (Tamura et al., 2013). Phylogenetic trees were inferred with maximum likelihood (ML), maximum parsimony (MP) and Bayesian inference (BI) analyses.

The optimal substitution models of three genes were estimated with jModeltest v 2.1.10 (Posada, 2008) respectively. The best-fit models were resulted as GTR+I+G

model for ITS, TrN+I+G for TEF and TrNef+I+G for RPB2 under the Akaike Information Criterion (AIC).

Bayesian Inference (BI) analysis was performed via the web CIPRES Science Gateway v. 3.3 (Miller et al., 2010) using MrBayes v. 3.2.6 on XSEDE. Posterior probabilities (PP) (Rannala & Yang, 1996; Zhaxybayeva & Gogarten, 2002). Six simultaneous Markov Chains were run from random trees for 10,000,000 generations and trees were sampled every 100th generation with total of 100,000 trees. The first 25% trees were discarded and the remaining trees were used to calculate the posterior probabilities (PP) in the majority rule consensus tree.

Maximum likelihood (ML) analysis was performed using IQ-Tree v 1.6.5 (Nguyen et al., 2014). The dataset was partitioned and each gene was analyzed with corresponding model. The bootstrap replication was set as 1000 and *Dactylaria* sp. YNWS02-7-1was set as out-group.

Maximum parsimony analysis (MP) was performed by PAUP v. 4.0b10 (Swofford, 2002) using the heuristic search option. Maxtrees were set up at 1000 with all characters were treated as unordered and of equal weight. Gaps were treated as missing data and the branches of zero length were collapsed. All multiple equally parsimonious trees were saved. Bootstrap replicates were set as 1000, each with ten replicates of random stepwise addition of taxa (Hillis & Bull, 1993). The Kishino-Hasegawa tests (Kishino & Hasegawa, 1989) were obtained to determine the significantly different parsimonious trees under different optimality criteria.

The trees were shown with FigTree v1.3.1 (Rambaut, 2010) and Treeview (Page, 1996). The backbone tree was edited with Microsoft Power Point (2013) and Adobe Photoshop CS6 software (Adobe Systems, USA). Sequences derived from this study were deposited in GenBank (Table 4.1).

Table 4.1 GenBank accession numbers of isolates included in this study

Taxon	Strain No.	GenBank accession no.		
		ITS	TEF	RPB1
Dactylellina appendiculata	CBS 206.64	AF106531	DQ358227	DQ358229
Dactylellina arcuata	CBS 174.89	AF106527	DQ999852	DQ999799
Dactylellina asthenopaga	CBS 917.85	U51962	—	—
Dactylellina candida	YMF1.00036	AY965749	—	—
Dactylellina cangshanensis	CGMCC3.19714	MK372062	MN915115	MN915114
Dactylellina cionopaga	SQ27-3	AY773467	AY773409	AY773438
Dactylellina cionopaga	XJ03-9-3	AY773473	AY773415	AY773444
Dactylellina copepodii	CBS 487.9	U51964	DQ999835	DQ999816
Dactylellina drechsleri	CBS 549.63	DQ999819	DQ999840	DQ999810
Dactylellina ellipsospora	286	AY773449	AY773391	AY773420
Dactylellina ellipsospora	YNWS02-8-1	AY773458	AY773400	AY773429
Dactylellina entomopaga	CBS642.80	AY965758	DQ358228	DQ358230
Dactylellina formosana	CCRC 32740	U51956	—	—
Dactylellina gephyropaga	CBS585.91	AY965756	DQ999846	DQ999801
Dactylellina gephyropaga	CBS 178.37	U51974	DQ999847	DQ999802
Dactylellina haptospora	CBS 100520	DQ999820	DQ999850	DQ999814
Dactylellina haptotyla	SQ95-2	AY773470	AY773412	AY773441
Dactylellina haptotyla	XJ03-96-1	DQ999827	DQ999849	DQ999804
Dactylellina hertziana	CBS 395.93	AF106519	—	—
Dactylellina huisuniana	CCRC 33444	U51965	—	—
Dactylellina leptospora	SHY6-1	AY773466	AY773408	AY773437
Dactylellina lobata	CBS 329.94	KT215196	—	—
Dactylellina lobata	YMF1.00535	MF948399	—	MF948479
Dactylellina mammillata	CBS229.54	AY902794	DQ999843	DQ999817
Dactylellina mammillata	YMF1.00127	AY965751	—	—
Dactylellina parvicollis	XSBN22-1	AY804215	DQ999854	DQ999798
Dactylellina querci	6175	AY773453	AY773395	AY773424
Dactylellina robusta	CBS 110125	DQ999821	DQ999851	DQ999800
Dactylellina sichuanensis	YMF1.00023	AY902795	—	—
Dactylellina tibetensis	XZ04-92-1	DQ999833	DQ999848	DQ999803
Dactylellina varietas	YMF1.118	AY902805	—	—
Dactylellina yunnanensis	CBS615.95	AY965757	—	—
Dactylellina yushanensis	CGMCC3.19713	MK372061	MN915113	MN915112
Dactylaria sp.	YNWS02-7-1	AY773457	AY773399	AY773428

4.3 Results

4.3.1 Phylogenetic Analysis

The alignment contained ITS, TEF and RPB2 three genes from 29 species (34 strains). The dataset comprised 1878 characters (ITS: 502, TEF: 579 and RPB2: 797), including 841 conserved characters, 1006 variable characters and 686 parsimony-informative characters. Phylogenetic trees obtained from maximum likelihood (RAxML), maximum parsimony (MP) and Bayesian inference (BI) analyses shown similar topologies, so the best scoring RAxML tree was selected to represent in here (Figure 4.1).

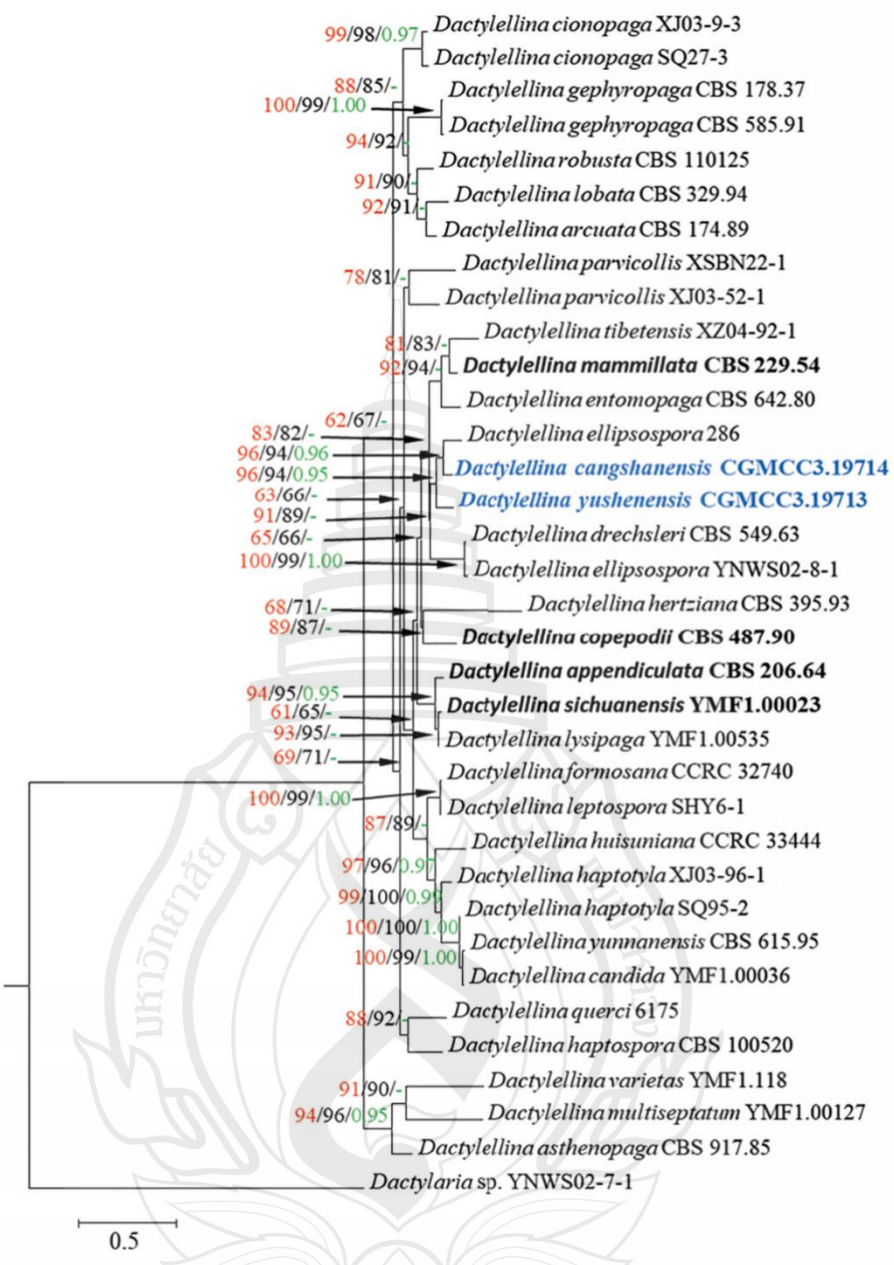

Figure 4.1 Maximum likelihood tree based on a combined ITS, TEF and RPB2 sequence data from 29 species of *Dactylellina*. Bootstrap support values for maximum parsimony (red) and maximum likelihood (black) equal or greater than 50% are shown above the nodes and Bayesian posterior probabilities values (green) greater than 0.90 are also indicated above the nodes. The new isolates are in blue, ex-type strains are in bold. The tree is rooted to *Dactylaria* sp. (YNWS02-7-1)

4.3.2 Taxonomy

Dactylellina cangshanensis F. Zhang, X.Y. Yang & K. D. Hyde, sp. nov. (Figure 4.2)

Index Fungorum number: IF555802; Facesoffungi number: FOF 05671

Etymology**:** The species name "cangshanensis" refers to the name of sample collection site: Cangshan Mountain, Dali City, Yunnan Province, China.

Material examined: CHINA, Yunnan Province, Dali City, burned forest in Cangshan Mountain, from burned forest soil, 25 July 2017, XJ. Zhou, YXY13-1. Holotype CGMCC 3.19714, ex-type living culture, DLU13-1.

Saprobic on soil. *Isolation* growing slowly on CMA, reaching a colony-diameter of 50 mm after 20 days incubation at 26°C. *Colonies* white, cottony. *Mycelium* colorless, septate, branched, smooth. *Conidiophores* hyaline, erect, septate, unbranched, 135–290 μm. long ($\bar{x}$ = 222.5 μm., n = 100), 2.5–4 μm. at the base ($\bar{x}$ = 3.2 μm., n = 100), gradually tapering upwards to a width of 1.5–2.5 μm. at the apex ($\bar{x}$ = 1.95 μm., n = 100), bearing a single conidium. *Conidia* broadly fusiform, spindle-shaped, some clavate or drop-shaped, hyaline, 23–48 × 7–13.5 μm. ($\bar{x}$ = 35.9 × 11.06 μm., n = 100), 2–4-septate, mostly 3 or 4-septate, the central cell is the largest, apex obtuse. *Chlamydospores* not observed. Capturing nematodes with adhesive knobs, producing trapping device spontaneously.

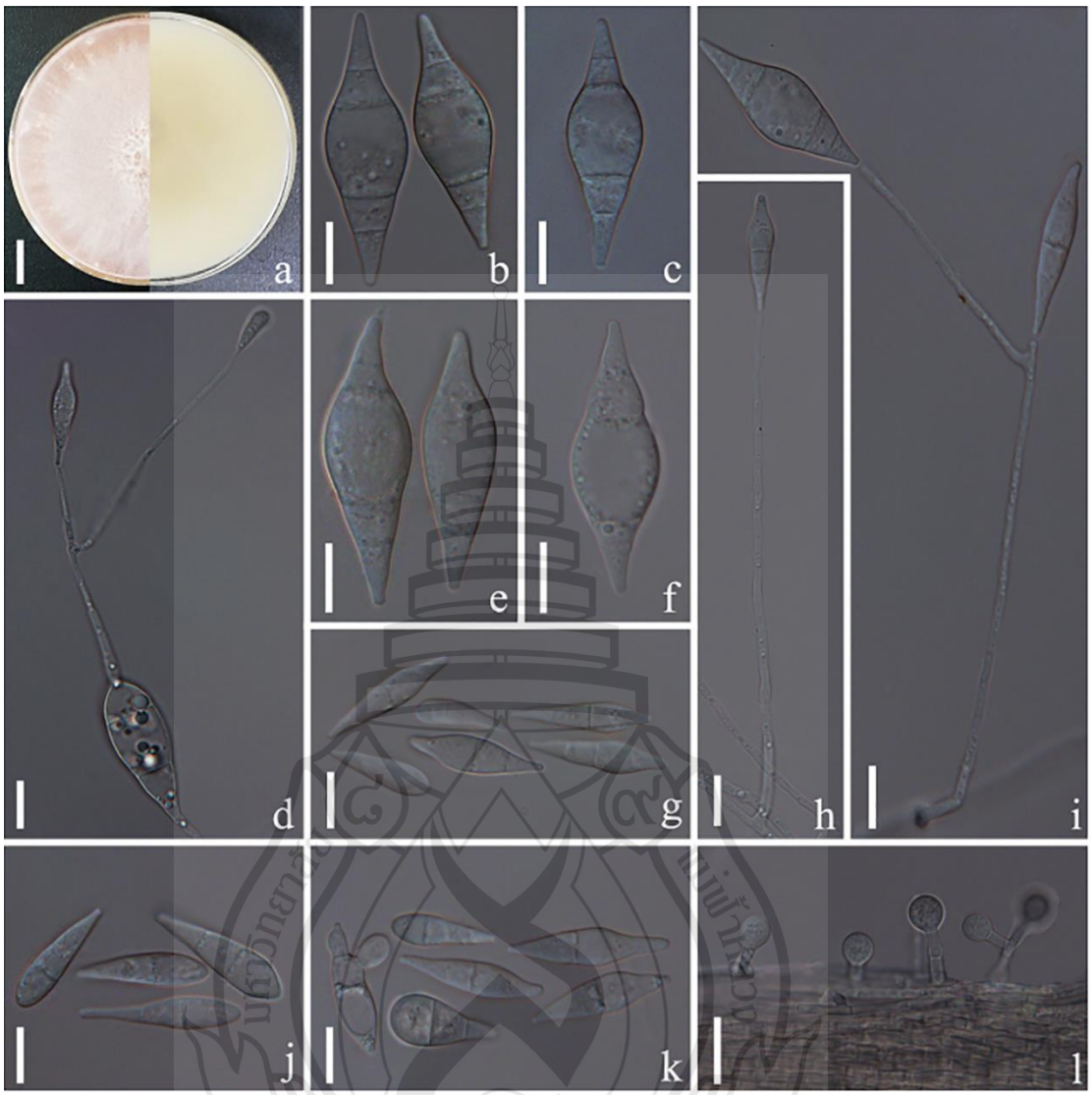

Figure 4.2 *Dactylellina yushanensis* (CGMCC3.19713). (a) Colony. (b, c, e, f) Macroconidia. d Micro-cycle conidiation. (g, j, k) Microconidia. (h, i) Conidiophore. (l) Trapping-device: adhesive knobs. Scale bars: (a) = 1.0 cm., (b–l) = 10 um.

Dactylellina yushanensis F. Zhang, X.Y. Yang & K. D. Hyde, sp. nov. (Figure 4.3)

Index Fungorum number: IF555801; Facesoffungi number: FOF 05670

Etymology: The species name “yushanensis” refers to the name of sample collection site: Yushan Mountain in Cangshan Mountain, Dali City, Yunnan Province, China. ($\bar{x}$ = 39.2 × 15.3 μm., n = 100)

Material examined: CHINA, Yunnan Province, Dali City, burned forest in Yushan Mountain in Cangshan Mountain, from burned forest soil, 25 July 2017, XJ. Zhou, YXY12-1. Holotype CGMCC3.19713, ex-type living culture, DLU12-1.

Saprobic on soil. *Isolation* grew slowly on CMA, reaching a colony-diameter of 50 mm after 35 days incubation at 26°C. *Colonies* white, cottony. *Mycelia* colorless, septate, branched, smooth, hyaline. *Conidiophores* hyaline, septate, erect, simple or geniculate branched, spore single grew in the apex or geniculate inflection point of conidiophore, 125–310 μm. long ($\bar{x}$ = 235.5 μm., n = 100), 2.5–5 μm. wide at the base ($\bar{x}$ = 3.5 μm., n = 100), gradually tapering upwards to a width of 1.8-3.0 μm. at the apex ($\bar{x}$ = 2.1 μm., n = 100). *Conidia* two types: *Macroconidia* spindle-shaped, hyaline, smooth, 30–48 × 7–15 μm. ($\bar{x}$ = 38.3 × 12.1 μm., n = 100), 2–4-septate, mostly 4-septate, the central cell is the largest, tapering at both ends. *Microconidia* fusiform, clavate or drop-shaped, hyaline, smooth, 16–40.5 × 3–8.5 μm. ($\bar{x}$ = 27 × 5.5 μm., n = 100), 1–3-septate, mostly 1-septate, grew on conidiophore or produce by macroconidia with the way of micro-cycle conidiation. *Chlamydospores* not observed. Capturing nematodes with adhesive knobs, producing trapping device spontaneously.

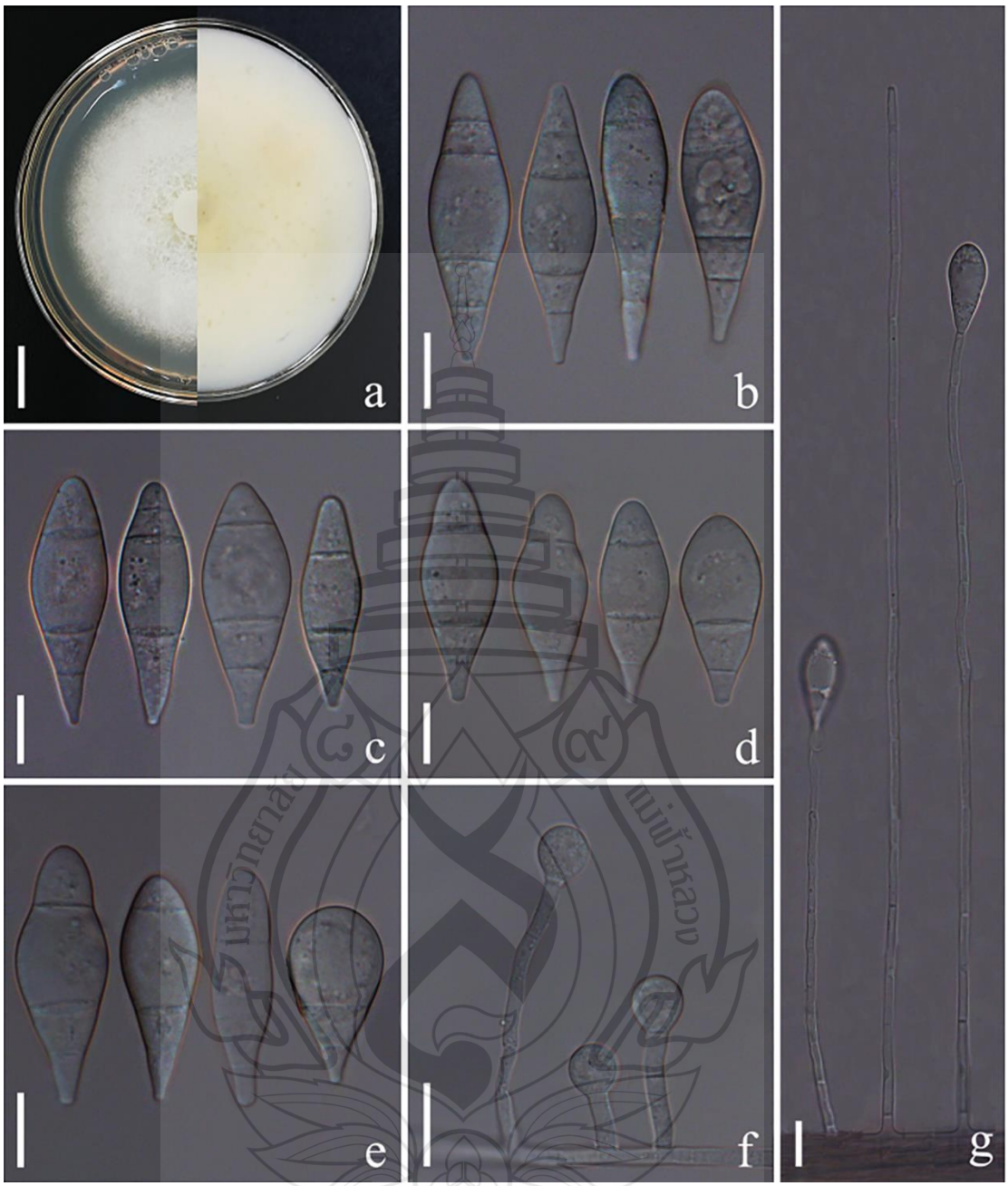

Figure 4.3 *Dactylellina cangshanensis* (CGMCC3.19714). (a) Colony. (b–e) Conidia. (f) Trapping-device: adhesive knobs. (g) Conidiophore. Scale bars: (a) = 1.0 cm., (b–g) = 10 um.

4.4 Discussion

Based on phylogenetic analysis (Figure 4.1), *Dactylellina cangshanensis* (CGMCC3.19714) cluster together with *D. ellipsospora* with high support value (96% MP, 94% ML and 0.96 PP). There are 122 base pairs are different between *D. cangshanensis* and *D. ellipsospora* 286 for combined sequences data (ITS: 22 pairs, TEF: 21 pairs, RPB2: 79 pairs). The morphology of this species is similar to *D. ellipsosporum.* But there are two distinct differences: first, the conidia of this species are more diverse in shape, some conidia are clavate or bottle-shaped except for the spindle shape, while the conidia of *D. ellipsosporum* Preuss are simple, mostly spindle-shaped with two septate both at the top and bottom. Second, the conidia of this species are smaller than the conidia of *D. ellipsosporum* [*D. cangshanensis*, 23–48 (35.9) × 7–13.5 (11.06) μm. versus 40–57.5 (48.3) × 10–17.5 (13) μm., *D. ellipsosporum*] (Cooke & Dickinson, 1965). Based on above, combined with phylogenetic analysis, we propose this isolate as a new species of *Dactylellina.*

Phylogenetic analysis (Figure 4.1) showed that *D. yushanensis* (CGMCC3.19713) cluster together with *D. ellipsospora* and *D. cangshanensis* with high support value (96% MP, 94% ML and 0.95 PP). There are 227 base pairs are different between *D.yushanensis* and *D.ellipsospora* 286 (ITS: 61 pairs, TEF: 31 pairs, RPB2: 135 pairs), and 189 base pairs are different between *D.yushanensis* and *D.cangshanensis* (ITS: 55 pairs, TEF: 31 pairs, RPB2: 103 pairs). The morphological characteristics of this species are clear, therefore can be distinguished from other species easily. Especially the macroconidia with tapering both ends. In *Dactylellina*, only the conidia of *D. ellipsospora* has similar feature, however, the conidia of this species are smaller than the conidia of *D. ellipsosporum* [*D. yushanensis*, 30–48 (38.3) × 7–15 (12.1) μm. versus 40–57.5 (48.3) × 10–17.5 (13) μm., *D. ellipsosporum*] (Cooke & Dickinson, 1965). In addition, the characteristics of fusiform, clavate or drop-shaped microconidia grew on conidiophore directly or produce by macroconidia with the way of micro-cycle conidiation and the conidiophore with geniculate branched of this species are unique in *Dactylellina*. Based on above, combined with phylogenetic analysis, we propose this strain as a new species of *Dactylellina.*

CHAPTER 5

Drechslerella daliensis AND *D. xiaguanensis* (*ORBILIALES, ORBILIACEAE*), TWO NEW NEMATODE-TRAPPING FUNGI FROM YUNNAN, CHINA

5.1 Introduction

Nematode-trapping fungi are important predators that capture nematodes by specialized trapping structures (Barron, 1977; Li et al., 2006; Swe et al., 2011; Zhang & Hyde, 2014). They play vital roles in maintaining energy balance and nutrient cycles in soil ecosystems and exhibit great potential for bio-control application in agricultural management (Cooke, 1962; Ulzurrun & Hsueh, 2018; Zhang et al., 2020a). Most nematode-trapping fungi belong to *Orbiliaceae*, which have been extensively studied due to their abundant species and sophisticated trapping devices (Linford et al., 1938; Jaffee et al., 1993; Wolstrup et al., 1996; Jaffee et al., 1998; Morton et al., 2003; Liu et al., 2009; El-Borai et al., Kumar et al., Swe et al., 2011; Vilela et al., 2012). Currently, 116 predatory species in *Orbiliaceae* have been reported (Glockling & Dick, 1994; Li et al., 2006; Wu et al., 2012; Li et al., 2013; Liu et al., Zhang & Hyde, 2014; Quijada et al., Zhang et al., 2020ab; Zhang et al., 2022). They are classified into three genera according to their types of trapping structure: (1) *Arthrobotrys* (67 species), catching nematodes using adhesive networks; (2) *Dactylellina* (34 species), capturing nematodes by adhesive knobs, adhesive branches and non-constricting rings; and (3) *Drechslelrella* (15 species), trapping nematodes with constricting rings (Scholler et al., 1999; Li et al., 2005; Yang et al., 2007; Zhang & Hyde, 2014).

Drechslerella was established by Subramanian (1963) with the type species *D. acrochaeta* (Drechsler) Subram. It is a small genus separated from *Monacrosporium*, based on conidia producing filamentous appendages at the apex, which are lacking in *Monacrosporium*. However, filamentous appendages are usually produced when

conidia germinate and are also commonly found in some species of *Arthrobotrys*. Therefore, Liu and Zhang (1994) treated *Drechslerella* as a synonym of *Monacrosporium*, based on their similar conidia morphology. Subsequently, the generic concept of nematode-trapping fungi in *Orbiliaceae* was revised, based on molecular phylogenetic analysis. *Drechslerella* is characterized by producing constricting rings to capture nematodes (Liou & Tzean, 1997; Pfister, 1997; Ahren et al., 1998; Scholler et al., 1999; Li et al., 2005). *Drechslerella* currently includes 15 accepted species, 13 of which have been reported in China (Zhang & Mo, 2006; Zhang & Hyde, 2014). They mainly occur in the soil or sediment of various ecosystems such as forests, mangroves, freshwater, brackish water, heavy metal polluted areas and even in tree trunks and animal feces (Jansson & Autery, 1961; Hao et al., 2005; Mo et al., 2006; Su et al., 2007; Swe et al., 2009; Zhang & Hyde, 2014; She et al., 2020; Zhang et al., 2020). In soil, *Drechslerella* species are mainly distributed in the upper litter and humus layer and closely related to the density of soil nematodes (Burges & Raw, 1967; Gray & Bailey, 1985; Zhang & Hyde, 2014). *Drechslerella* species lack nematodes mainly by the rapid expansion of the three cells that make up the constricting ring. This method of trapping nematodes mainly by mechanical force is significantly different from that of species in *Arthrobotrys* and *Dactylellina* (capture nematodes mainly with adhesive material) (Zhang & Mo, 2006; Zhang & Hyde, 2014). Therefore, *Drechslerella* is the most special genus amongst *Orbiliaceae* NTF and it is also a key group in studying the origin and evolution of carnivorous fungi.

The studies of nematode-trapping fungi have been poorly addressed in extreme habitats (Onofri & Tosi, 1992; Mo et al., 2008; Swe et al., 2008). Our previous research investigated the succession of nematode-trapping fungi after fire disturbance in forests in China (She et al., 2020). Four strains were isolated and identified as two new nematode-trapping fungi in *Orbiliaceae*. The aim of this study is to introduce these two new species, *D. daliensis* and *D. xiaguanensis*, based on morphology and phylogenetic evidence. The discovery of these two species increased the diversity of nematode-trapping fungi and provided more valuable materials for studying the evolution and origin of carnivorous fungi, as well as more potential species for the biological control of plant and animal parasitic nematodes.

5.2 Material and Methods

5.2.1 Samples Collection, Isolation and Morphology

The soil samples were collected from a burned forest in Cangshan Mountain, Dali City, Yunnan Province, China (geographical coordinates: N 100°07′44″, E 25°45′49″). The sampling site information has been described by She et al. (2020). About 100 g of soil was collected from 10–20 cm depth using a 35 mm-diameter soil borer. The soil sample was placed into a zip lock bag and samples were brought back to the laboratory and stored at 4°C until processing.

The soil samples were sprinkled on corn meal agar (CMA) plates with sterile toothpicks. Free-living nematodes (*Panagrellus redivivus* Goodey) were added as bait to promote the germination of nematode-trapping fungi. After three weeks of incubation at 26°C, the plates were observed under a stereo-microscope to find the spores of nematode-trapping fungi. A single spore was transferred to a fresh CMA plate using a sterile toothpick, repeating this step until the pure culture was obtained.

Fungal isolates were transferred to fresh potato dextrose agar plate (PDA) using a sterile toothpick and incubated at 26°C for colony characteristics observation. The pure cultures were transferred to fresh CMA observation plates (an observation well of 2×2 cm was made by removing the agar from the center of the CMA plate) and incubated at 26°C. When the mycelium overspread the observation well, about 500 nematodes (*P. redivivus*) were added to the well to induce the formation of trapping devices. The types of trapping devices were checked using a stereo-microscope. All morphological characters were captured and measured with an Olympus BX53 microscope (Olympus Corporation, Japan).

5.2.2 DNA Extraction, PCR Amplification and Sequencing

The genomic DNA was extracted from the mycelia grown on PDA plates according to the method described by Jeewon et al. (2002). The primer pairs ITS4-ITS5 (White et al., 1990), 526F-1567R (O'Donnell et al., 1998) and 6F-7R (Liu et al., 1999) were used to amplify the ITS, TEF and RPB2 genes, respectively. The PCR amplification was performed as follows: pre-denaturation at 94°C for 4 minutes, followed by 35 cycles of denaturation at 94°C for 45 seconds, annealing at 52°C (ITS),

55°C (TEF), 54°C (RPB2) for 1 minute, extension at 72°C for 1.5–2 minutes, and a final extension at 72°C for 10 minutes. The PCR products were purified with a DiaSpin PCR Product Purification Kit (Sangon Biotech Company, Limited, Shanghai, China). ITS and RPB2 genes were sequenced in forward and reverse directions using PCR primers and the TEF region was sequenced using the 247F-609R primer pair (Yang et al., 2007) (BioSune Biotech Company, Limited, Shanghai, China).

5.2.3 Phylogenetic Analysis

The sequences generated in this study were compared against the NCBI GenBank database using BLASTn (BLASTn; https://blast.ncbi.nlm.nih.gov/Blast.cgi/ PROGRAM=blastn&PAGE_TYPE=BlastSearch&LINK_LOC=blasthome; accessed on 16 July 2022). The morphological and BLASTn search results placed these two species in the genus *Drechslerella*. *Drechslerella* were searched in the Index Fungorum (http:// www.indexfungorum.org; accessed on 16 August 2022) and Species Fungorum (http:// www.speciesfungorum.org; accessed on 16 August 2022) and all relevant records were checked individually according to the relevant documents to ensure that all *Drechslerella* taxa were considered in this study (Li et al., 2013; Zhang & Hyde, 2014). All reliable ITS, TEF and RPB2 sequences of *Drechslerella* taxa were downloaded from the GenBank database (Table 5.1). The three datasets (including our two new species) were aligned using MAFFT online version (Madeira et al., 2022; https://www.ebi.ac.uk/Tools/msa/ mafft/), then manually adjusted and linked via BioEdit v.7.2.3 (Hall, 1999) and MEGA6.0 (Tamura et al., 2013). *Dactylaria* sp. YNWS02-7-1 and *Vermispora fusarina* YXJ02-13-5 were selected as outgroups (Yang et al., 2007). Phylogenetic trees were inferred with Maximum Likelihood (ML), Maximum Parsimony (MP) and Bayesian Inference analyses (BI).

Table 5.1 GenBank accession numbers of isolates included in this study

Taxon	Strain No.	GenBank accession no.		
		ITS	TEF	RPB1
Arthrobotrys conoides	YMF1.00009	MF948387	MF948544	MF948468
Arthrobotrys guizhouensis	YMF1.00014	MF948390	MF948547	MF948471
Arthrobotrys shizishanna	YMF1.00022	MF948392	MF948549	MF948473
Dactylaria sp.	YNWS02-7-1	AY773457	AY773399	AY773428
Dactylellina appendiculata	CBS 206.64	AF106531	DQ358227	DQ358229
Dactylellina copepodii	CBS 487.9	U51964	DQ999835	DQ999816
Dactylellina mammillata	CBS229.54	AY902794	DQ999843	DQ999817
Dactylellina yushanensis	CGMCC 3.19713	MK372061	MN915113	MN915112
Drechslerella anchonia	CBS109.37	AY965753	——	——
Drechslerella aphrobrocha	YMF1.00119	MF948397	——	MF948477
Drechslerella bembicodes	1.01429	MH179731	——	MH179835
Drechslerella brochopaga	701	AY773456	AY773398	AY773427
Drechslerella brochopaga	1.01829	MH179750	——	MH179852
Drechslerella brochopaga	CBS218.61	U51950	——	——
Drechslerella brochopaga	ATCC 96710	EF445987	——	——
Drechslerella brochopaga	DHP 212	U72609	——	——
Drechslerella brochopaga	BCRC 34361	FJ380936	——	——
Drechslerella brochopaga	H.B.9925	KT222412	——	——
Drechslerella brochopaga	H.B.9965	KT380104	——	——
Drechslerella brochopaga	6178	DQ656615	——	——
Drechslerella coelobrocha	FWY03-25-1	AY773464	AY773406	AY773435
Drechslerella coelobrocha	1.0148	MH179744	——	MH179847
Drechslerella dactyloides	1.00031	MH179690	MH179554	MH179799
Drechslerela dactyloides	expo-5	AY773463	AY773405	AY773434
Drechslerella dactyloides	1.00131	MH179705	——	MH179813
Drechslerella daliensis	CGMCC 3.20131	MT592896	OK556701	OK638157
Drechslerella daliensis	DLU22-1	OK643974	OK556700	OK638158
Drechslerella doedycoides	YMF1.00553	MF948401	——	MF948481
Drechslerella doedycoides	CBS 586.91	MH862283	——	——
Drechslerella doedycoides	CBS175.55	MH857432	——	——
Drechslerella effusa	YMF1.00583	MF948405	MF948557	MF948484
Drechslerella effusa	CBS 774.84	MH861835	——	——
Drechslerella hainanensis	YMF1.03993	KC952010	——	——
Drechslerella heterospora	YMF1.00550	MF948400	MF948554	MF948480
Drechslerella polybrocha	CBS 319.56	MH857657	——	——
Drechslerella polybrocha	CCRC 32872	U51973	——	——
Drechslerella polybrocha	DHP 133	U72606	——	——

Table 5.1 (continued)

Taxon	Strain No.	GenBank accession no.		
		ITS	TEF	RPB1
Drechslerella polybrocha	H.B.8317	KT222361	——	——
Drechslerella stenobrocha	YNWS02-9-1	AY773460	AY773402	AY773431
Drechslerella xiaguanensis	CGMCC 3.20132	MT592900	OK556699	OK638159
Drechslerella xiaguanensis	DLU23-1	OK643975	OK556698	OK638160
Drechslerella yunnanensis	1.01863	MH179759	——	MH179861
Drechslerella yunnanensis	YMF1.03216	HQ711927	——	——
Vermispora fusarina	YXJ02-13-5	AY773447	AY773389	AY773418

SYM+I+G, GTR+I+G and GTR+I+G models were selected as best-fit optimal substitution models for ITS, TEF and RPB2, respectively, via jModelTest v.2.1.10 (Posada, 2008) under the Akaike Information Criterion (AIC).

MrBayes v. 3.2.6. (Huelsenbeck & Ronquist, 2001) was used to perform the Bayesian Inference (BI) analysis. The multiple sequence alignment file was converted into the MrBayes compatible NEXUS file via Fasta Convert (Hall, 2005). The dataset was partitioned and the optimal substitution models of each gene were equivalently replaced to conform to the setting of MrBayes. Six simultaneous Markov Chains were run for 10,000,000 generations and trees were sampled every 100 generations (a total of 100,000 trees). The first 25% of trees were discarded and the remaining trees were used to calculate the posterior probabilities (PP) in the majority rule consensus tree. All the above parameters are edited into the MrBayes block in the NEX file.

IQ-Tree v.1.6.5 (Nguyen et al., 2014) was used to perform the Maximum Likelihood (ML) analysis. The dataset was partitioned and each gene was analyzed with its corresponding model. The rapid bootstrapping method with 1000 replicates (Felsenstein, 1985) was used to compute the bootstrap support values (BS).

Maximum Parsimony (MP) analysis was performed via the web CIPRES Science Gateway v. 3.3 (Miller et al., 2010; https://www.phylo.org) by PAUP 4. a168 on XSEDE using the heuristic search option with 1000 random sequence additions. Max-trees were set up at 5000 and no increase. Clade stability was assessed using a bootstrap analysis with 1,000 replicates (Felsenstein, 1985). Descriptive tree statistics tree length (TL), consistency index (CI), retention index (RI), rescaled consistency

index (RC) and homoplasy index (HI) were calculated for all trees generated under different optimality criteria. All the above parameters are edited into the PAUP block in the NEX file.

The trees were visualized with FigTree v.1.3.1 (Rambaut, 2009). The backbone tree was edited and reorganized by Microsoft PowerPoint (2013) and Adobe Photoshop CS6 software (Adobe Systems, USA). Sequences derived from this study were deposited in GenBank (Table 5.1).

5.3 Results

5.3.1 Phylogenetic Analyses

A total of 15 *Drechslerella* related taxa were listed in Index Fungorum (http:// www.indexfungorum.org; accessed on 16 August 2022) and Species Fungorum (http://www.speciesfungorum.org; accessed on 16 August 2022), representing 15 valid *Drechslerella* species. Among them, 13 species have available molecular data. The combined ITS, TEF and RPB2 sequence dataset contained 42 nematode-trapping taxa in *Orbiliaceae* (three *Arthrobotrys* species, four *Dactylellina* species and 35 *Drechslerella* taxa representing 15 species). The final dataset comprised 1939 characters (ITS = 591, TEF = 534 and RPB2 = 814), including 807 conserved characters, 1072 variable characters and 748 parsimony-informative characters. After Maximum Likelihood (ML) analysis, a best-scoring likelihood tree was obtained with a final ML optimization likelihood value of -7146.589745. For Bayesian analysis (BI), the first 25% of trees were discarded in a burn in period, the consensus tree was calculated with the remaining trees and the Bayesian posterior probabilities were evaluated with a final average standard deviation of the split frequency of 0.009547. Within Maximum Parsimony (MP) analysis, a strict consensus tree was obtained from the two equally most parsimonious trees (TL = 2817, CI = 0.471, RI = 0.514, RC = 0.296, HI = 0.404). The trees inferred by ML, MP and BI showed similar topologies. Therefore, the best-scoring ML tree was selected for presentation (Figure 5.1).

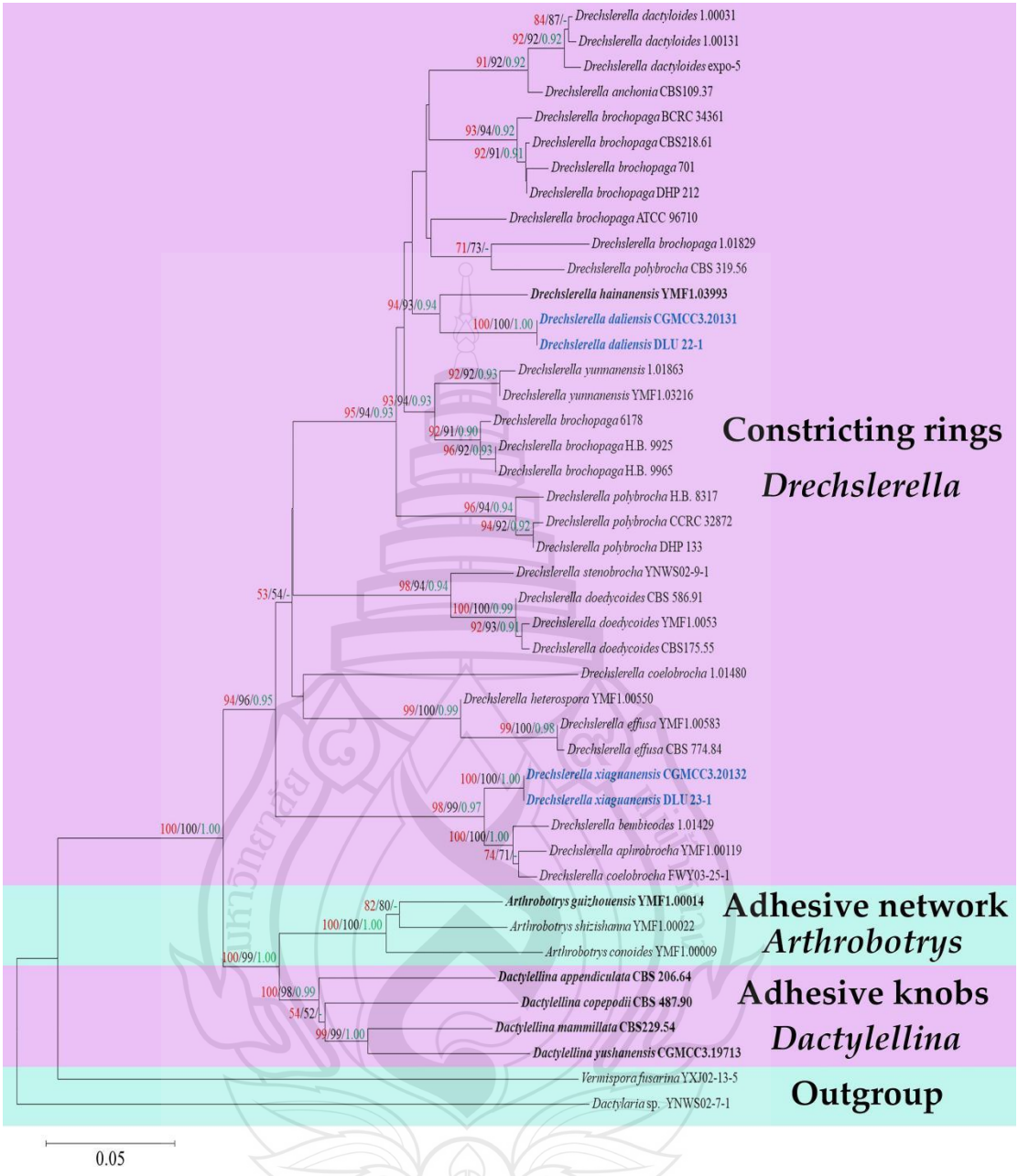

Figure 5.1 Maximum Likelihood tree, based on combined ITS, TEF and RPB2 sequence data from 42 nematode-trapping taxa in *Orbiliaceae*. Bootstrap support values for Maximum Parsimony (red) and Maximum Likelihood (black) equal or greater than 50% and Bayesian posterior probabilities values (green) greater than 0.90 are indicated above the nodes. New isolates are in blue, type strains are in bold

The phylogram inferred from the ITS+TEF+RPB2 dataset clustered 42 *Orbiliaceae* nematode-trapping fungi into two large clades according to their mechanisms for catching nematodes: (1) The genus *Drechslerella* that captures nematodes by mechanical force (Zhang & Hyde, 2014); (2) The genera *Arthrobotrys* and *Dactylellina* capture nematode by adhesive material (Zhang & Hyde, 2014). Our two new species *D. daliensis* and *D. xiaguanensis* clustered in *Drechslerella* with high statistical support. *Drechslerella. daliensis* forms a basal lineage closely nested with *D. hainanensis* (YMF1.03993) with 94% MPBS, 93% MLBS and 0.94 BYPP support. *Drechslerella. xiaguanensis* forms a sister lineage with *D. bembicodes* (1.01429), *D. aphrobrocha* (YMF1.00119) and *D. coelobrocha* (FWY03-25-1) with 98% MPBS, 99% MLBS and 0.97 BYPP support (Figure 5.1).

5.3.2 Taxonomy

Drechslerella daliensis Fa Zhang, Xiao-Yan Yang, Kevin D Hyde, sp. nov. (Figure 5.2)

Index Fungorum number: IF558120； Facesoffungi number: FOF 10565.

Etymology: The species name "*daliensis*" refers to the locality (Dali) of the type specimen.

Material examined: CHINA, Yunnan Province, Dali City, Cangshan Mountain, from burned forest soil, 25 July 2017, F Zhang. Holotype CGMCC3.20131. Isotype DLU22-1

Colonies white, cottony, slow-growing on PDA medium, reaching 50 mm diameter after 18 days at 26°C. *Mycelium* hyaline, septate, branched, smooth. *Conidiophores* 125– 335 µm. ($\bar{x}$ = 216.5 µm., n = 50) long, 3–6.5 µm. ($\bar{x}$ = 4.5 µm., n = 50) wide at the base, 2–3.5 µm. ($\bar{x}$ = 3 µm., n = 50) wide at the apex, hyaline, erect, septate, unbranched, bearing a single conidium at the apex. Conidia two types: *Macroconidia* 20–49.5 × 8.5–15 µm. ($\bar{x}$ = 38.5–12 µm., n = 50), hyaline, smooth, ellipsoid, broadly rounded at the apex, truncate at the base, 1–2-septate, mostly 2-septate. *Microconidia* 6.5–22 × 3.5– 7 µm. ($\bar{x}$ = 15.5–5 µm., n = 50), hyaline, smooth, clavate or bottle-shaped, broadly rounded at the apex, truncate at the base, 0–1-septate. *Chlamydospores* not observed. Capturing nematodes with three-celled *constricting rings*, in the non-constricted state, the outer diameter is 21–32 µm. ($\bar{x}$ = 26 µm., n =

50), the inner diameter is 12–21 µm. ($\bar{x}$ = 15.5 µm., n = 50), stalks 5.5–11 µm. ($\bar{x}$ = 8.5µm., n = 50) long and 4–6.5 µm. ($\bar{x}$ = 5µm., n = 50) wide (Figure 5.2).

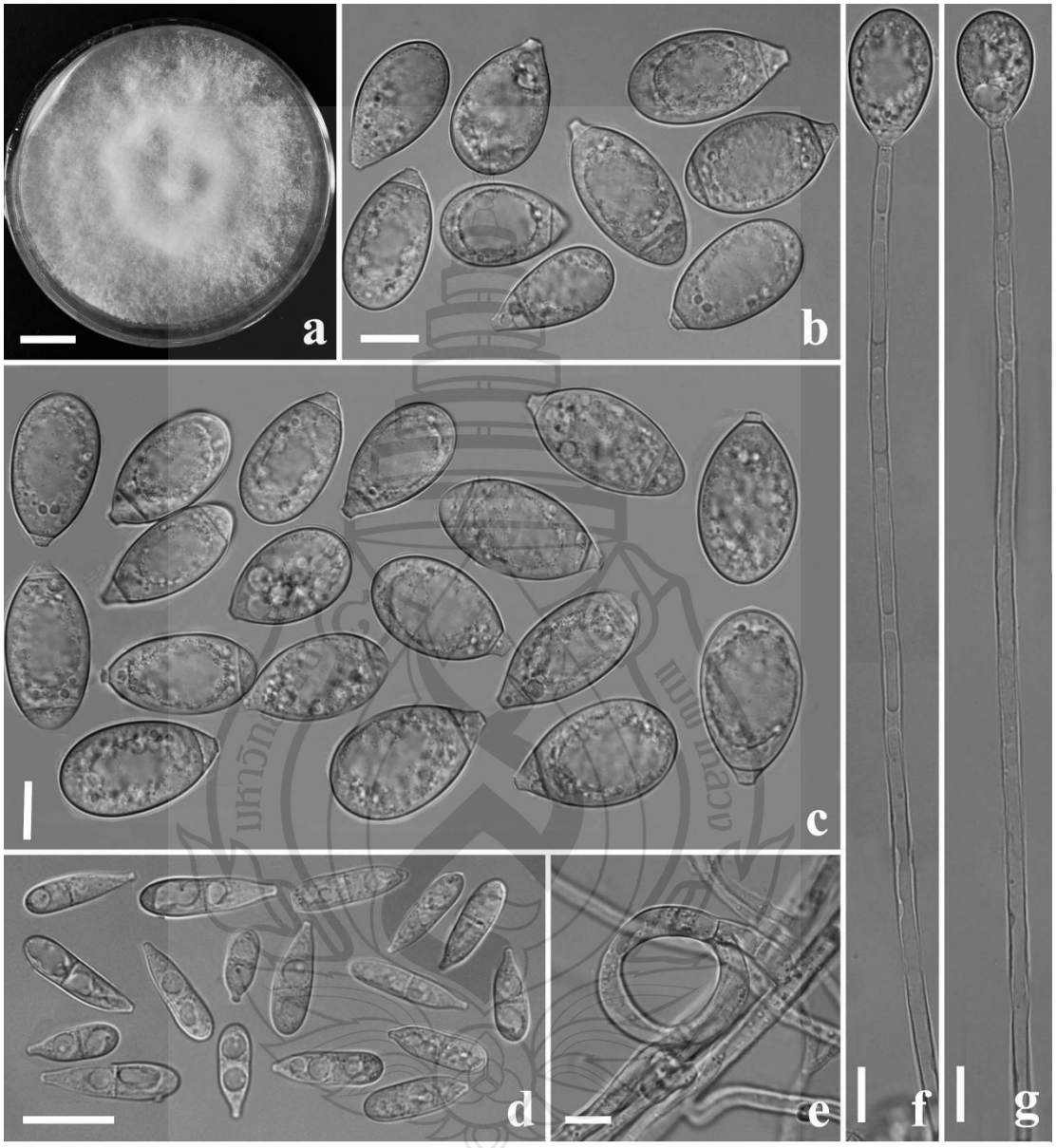

Figure 5.2 *Drechslerella daliensis* (CGMCC3.20131). (a) Culture colony. (b, c) Macroconidia. (d) Microconidia. (e) Constricting rings. (f, g) Conidiophores. Scale bars: (a) = 1 cm., (b–g) = 10 µm..

Drechslerella xiaguanensis Fa Zhang, Xiao-Yan Yang, Kevin D. Hyde, sp. nov. (Figure 5.3)

Index Fungorum number: IF55812; Facesoffungi number: FOF10566.

Material examined: CHINA, Yunnan Province, Dali City, Cangshan Mountain, from burned forest soil, 25 July 2017, F Zhang. Holotype CGMCC3.20132. Isotype DLU23-1

Colonies white, cottony, slow-growing on PDA medium, reaching 50 mm diameter after 15 days at 26 °C. *Mycelium* hyaline, smooth, septate, branched. *Conidiophores* 145– 315 µm. ($\bar{x}$ = 208.5 µm., n = 50) long, 3–6 µm. ($\bar{x}$ = 4 µm., n = 50) wide at the base, 2–3 µm. ($\bar{x}$ = 2.5 µm., n = 50) wide at the apex, hyaline, erect, septate, unbranched, bearing a single conidium at the apex. *Conidia* 33–52 × 9.5–28 µm. ($\bar{x}$ = 42.5–15.5 µm., n = 50), hyaline, smooth, fusiform, spindle-shaped, rounded and swollen at the both ends, 2–4- septate, mostly 3-septate, germinating tubes produced from both ends. *Chlamydospores* not observed. Capturing nematodes with three-celled *constricting rings*, in the non-constricted state, the outer diameter is 19–27.5 µm. ($\bar{x}$ = 24 µm., n = 50), the inner diameter is 12.5–20.5 µm. ($\bar{x}$ = 17 µm., n = 50), stalks 5–11.5 µm. ($\bar{x}$ = 9 µm., n = 50) long and 4.5–6 µm. ($\bar{x}$ = 5 µm., n = 50) wide (Figure 5.3).

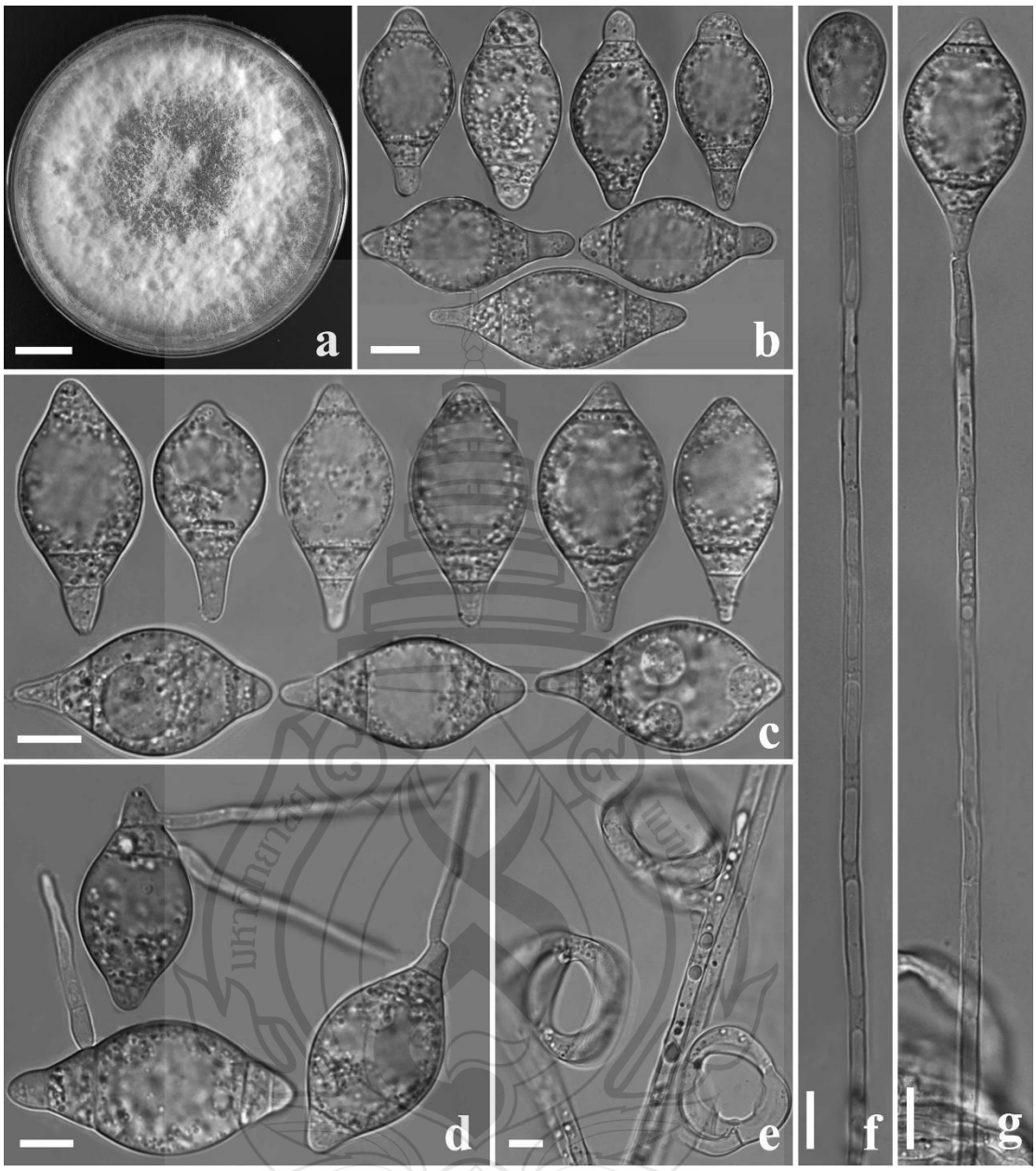

Figure 5.3 *Drechslerella xiaguanensis* (CGMCC3.20132). (a) Culture colony. (b, c) Conidia. (d) Germinating conidia. (e) Constricting rings. (f, g) Conidiophore. Scale bars: (a) = 1 cm. (b–g) = 10 µm.

5.4 Discussion

Drechslerella daliensis and *D. xiaguanensis* produce constricting rings to capture nematodes, which is consistent with the genus *Drechslerella* (Zhang & Hyde, 2014). The multi-genes phylogenetic analysis also confirmed that they are members of *Drechslerella*.

Phylogenetically, *D. daliensis* (CGMCC3.20131) forms a sister lineage to *D. hainanensis* (YMF 1.03993) with 97% MLBS, 96% MPBS and 0.95 BYPP support (Figure 5.1). A comparison of ITS nucleotide shows 10.15% difference (60/591 bp) between them. Morphologically, amongst 17 species in *Drechslerella* (plus our two new species), *D. daliensis*, *D. effusa*, *D. hainanensis* and *D. heterospora* produce ellipsoid 0–3 septate conidia (Li et al., 2013; Zhang & Hyde, 2014). The difference between *D. daliensis* and *D. effusa* is that the conidiophores of *D. daliensis* produce only a single conidium at the apex, while the conidiophores of *D. effusa* usually bear two or more conidia (Zhang & Hyde, 2014). *D. daliensis* can be easily distinguished from *D. heterospora* by their microconidia size and the apex characteristic of conidiophore: the microconidia of *D. daliensis* are significantly smaller than those of *D. heterospora* (6.5–22 × 3.5–7 µm. vs. 23–40 × 5.3–8 µm.), the conidiophores of *D. heterospora* usually swollen and spherical at the apex, while those of *D. daliensis* are not swollen. In addition, *D. daliensis* does not produce chlamydospores, while *D. heterospora* produces chlamydospores in chains (Zhang & Hyde, 2014). It is challenging to distinguish *D. daliensis* and *D. hainanensis* according to their shape characteristics. The difference between them is that the macroconidia of *D. daliensis* are thinner than those of *D. hainanensis* (20–49.5 × 8.5–15 µm. vs. 32.5–43 × 17– 25 µm.) and the microconidia are shorter than those of *D. hainanensis* (6.5–22 × 3.5–7 µm. vs. 18.2–22.8 × 4.2–5.3 µm.) (Li et al., 2013).

In the phylogenetic analysis, *D. xiaguanensis* (CGMCC3.20131) forms a sister lineage to *D. bembicodes* (1.01429), *D. aphrobrocha* (YMF1.00119) and *D. coelobrocha* (FWY03-25-1) with 100% MLBS, 100% MPBS and 1.00 BYPP support (Figure 5.3). Comparison of ITS nucleotide shows 2.6% (15/577 bp), 5.2% (30/577 bp) and 3.6% (20/556 bp) between *D. xiaguanensis* and *D. bembicodes*, *D. aphrobrocha*

and *D. coelobrocha*, respectively. Morphologically, they can be distinguished by their conidia size: the conidia of *D. xiaguanensis* are thinner than those of *D. bembicodes*, shorter than those of *D. coelobrocha* and smaller than those of *D. aphrobrocha* (*D. xiaguanensis* 33–52 (42.5)× 9.5–28 (15.5) µm. vs. *D. bembicodes* 36–43.2 (40) × 16.8–21.6 (20.5) µm. vs. *D. coelobrocha* 45.6–55.2 (49.5) × 16.8–21.6 (19.8) µm. vs. *D. aphrobrocha* 40–57.5 (51) × 15.5–35 (24.6) µm.). In addition, the cells at both ends of some conidia of *D. xiaguanensis* are swollen, while *D. bembicodes*, *D. aphrobrocha* and *D. coelobrocha* are not (Drechsler, 1950; Zhang & Mo, 2006; Zhang & Hyde, 2014). Based on the above, we propose *D. daliensis* and *D. xiaguanensis* as two new species of *Drechslerella*.

Among nematode-trapping fungi, species in *Arthrobotrys* are the dominant group in most ecosystems due to their strong reproductive and saprophytic ability, while the species in *Dactylellina* and *Drechslerella*, with weaker competitive abilities were rare (Jaffee et al., 1998; Hao et al., 2005; Elshafie et al., 2006; Su et al., 2007; Mo et al., Yang et al., 2008; Swe et al., Wachira et al., 2009; Yang et al., 2011). However, many species of *Dactylellina* and *Drechslerella* have been isolated from the burning forest in Cangshan, Yunnan (She et al., 2020). Among them, two new *Dactylellina* species (Zhang et al., 2020) and two new *Drechslerella* species (this paper) have been identified. We speculate that the reasons for this unusual phenomenon may be as follows: in normal habitat, *Arthrobotrys* species usually occupy the main living resources and are mainly distributed in the upper soil where humus, air and space are abundant due to their strong reproductive and saprophytic ability, while those species of *Dactylellina* and *Drechslerella* are mainly distributed in the lower soil where humus is scarce. When a fire occurs, *Arthrobotrys* species distributed in the upper soil are more vulnerable to the fire and are wiped out and then the habitat plaques form. In contrast, the rare species distributed in the lower layer are protected by the upper soil and preserved. In the subsequent recovery stage, these species can grow in large numbers and occupy the habitat plaque to form the dominant population in the area. Based on the above, we speculate that we would find more nematode-trapping fungi in burned forests. In addition, according to this principle, we speculate that other saprophytic fungi also have similar laws. Further research is underway and will be reported later.

CHAPTER 6

NEW *Arthrobotrys* NEMATODE-TRAPPING SPECIES (*ORBILIACEAE*) FROM TERRESTRIAL SOILS AND FRESHWATER SEDIMENTS IN CHINA

6.1 Introduction

Nematophagous fungi are a group of fungi that parasitize, capture, and poison nematodes and important balancing agents of the nematode population in nature (Linford et al., 1938; Jaffee et al., 1993; Zhang et al., 2001). They were divided into different groups according to their mode of action on nematodes: (1) nematode-trapping fungi capture nematodes with specialized hypha structure, (2) endoparasitic fungi infect nematodes with spores, (3) egg parasitic fungi invade nematode eggs and females with hypha tips, and (4) toxin-producing fungi produce toxins that paralyze and kill nematodes (Li et al., 2000; Zhang et al., 2001; Zhang & Hyde, 2014). Among these, nematode-trapping fungi have been the focus of related studies due to their highly specialized, sophisticated, and diverse trapping structures. Since Corda described the first nematode-trapping species (*Arthrobotrys superba* Corda) (Corda, 1839), more than 120 species have been discovered in *Zygomycota* (*Zoopagaceae*), *Basidiomycota* (*Nematoctonus*), and *Ascomycota* (*Orbiliomycetes*) over the past 180 years (Li et al., 2000; Kirk et al., 2008; Yang et al., 2012). Nematode-trapping fungi in *Zygomycota* (*Zoopagaceae*) are poorly understood due to their immature isolation and culture methods (Saikawa, 2011; Yang et al., 2012). All nematode-trapping fungi in *Basidiomycota* catch nematodes with adhesive knobs or adhesive spores, and all of them belong to *Nematoctonus* (Durschnerpelz, 1989; Poloczek & Webster, 1994; Thorn et al., 2000; Yang et al., 2012). All nematode-trapping fungi in the *Ascomycota* belong to *Orbiliaceae* (the only family of *Orbiliomycetes*), accounting for more than 80% of

all nematode-trapping fungi, which is a typical monophyletic group. They capture nematodes by producing constricting rings, adhesive networks, adhesive branches, adhesive knobs, and non-constricting rings (Swe et al., 2011; Zhang & Hyde, 2014).

Orbiliaceae nematode-trapping fungi have become the focus of studies on carnivorous fungi and also is a focus group of fungal evolutionists due to their unique survival strategies, diverse and complex trapping structures, abundant species, and relatively mature research methods (Jaffee et al., Ahrén et al., 1998; Li et al., 2005; Swe et al., 2011). At present, 103 species have been discovered (Zhang & Mo, 2006; Liu et al., Zhang & Hyde, 2014; Zhang et al., 2020). The history of its taxonomic research can be roughly divided into two periods: (1) from 1839 to about 1995, 26 genera were established to accommodate these species based on the morphological characteristics of conidia and conidiophores. With the subsequent discovery of more and more species, systematic comparative morphological studies were carried out, and the idea of dividing *Orbiliaceae* nematode-trapping fungi into *Arthrobotrys*, *Dactylella*, and *Monacrosporium* was proposed and widely accepted (Zhang & Mo, 2006). (2) Since 1995, with the development of molecular biology techniques, molecular phylogenetic studies based on DNA sequences, restriction fragment length polymorphism (RFLP), and random amplified polymorphic DNA (RAPD) indicate that species with the same trapping structure have closer phylogenetic relationships. Additionally, the idea that the types of trapping devices are more informative than conidia and conidiophores for the division of genera among *Orbiliaceae* nematode-trapping fungi was proposed. All *Orbiliaceae* nematode-trapping fungi are also classified into *Arthrobotrys*, *Dactylellina*, or *Drechserella* according to their types of trapping structure (Ahrén, 1998; Yang et al., 2012; Zhang & Hyde, 2014).

Arthrobotrys is the largest genus among *Orbiliaceae* nematode-trapping fungi. At present, 118 records of *Arthrobotrys* are listed in the Species Fungorum (http://www.speciesfungorum.org; (accessed on 6 March 2022)), which represent 59 accepted species (Li et al., 2000; Zhang & Mo, 2006; Swe et al., 2011; Yang et al., 2012; Zhang & Hyde, 2014). It was established by Corda (1839), with *A. superba* Corda as the type species. These taxa are characterized by regularly 1-septate conidia growing on the nodes or short denticles of conidiophores. At the time of its establishment, this genus was known for saprobic taxa (Corda, 1839; Fresenius, 1852). Zopf (1888) provided a

detailed description of a unique phenomenon in which *A. oligospora* produces adhesive networks to capture nematodes and clarified the relationship between *Arthrobotrys* and nematodes. In the following decades, due to the limitations of the available research techniques, the understanding of this group remained relatively poor. It was not until Drechsler and Duddington improved the isolation method that an increasing number of species were discovered (Drechsler, 1933, 1935, 1936, 1937, 1950, 1961, 1963; Duddington, 1950, 1951, 1954, 1955,1957). Because scholars attached different levels of importance to different morphological features, these species were parked in several genera such as *Didymozoophaga*, *Anilosporium*, and *Drechsleromyces* (Sherbakoff, 1933; Soprunov & Galiulina, 1951; Subramanian, 1977). Subsequently, scholars redefined the characteristics of the genus *Arthrobotrys* by systematic comparative morphological studies as follows: branched or simple conidiophores; obovoid, elliptic, pyriform, 0–3-septate conidia, growing asynchronously on the nodes or on short denticles of conidiophores; and including species that capture nematodes with adhesive networks, constricting rings, and adhesive knobs (Cooke & Dickinson, 1965; Castaner, Haard, 1968; McCulloch, Schenck et al., Subramanian, 1977; Chen et al., 2007). Subsequently, modern molecular biology techniques have been used to explore the taxonomy of *Orbiliaceae* nematode-trapping fungi and indicate that species with adhesive networks usually have similar molecular characteristics. Therefore, the main characteristic of *Arthrobotrys* was correspondingly changed to producing an adhesive network to capture nematodes (Ahrén et al., 1988; Li et al., 2005; Yang et al., 2012; Zhang & Hyde, 2014). In addition, *Arthrobotrys* is the most widely distributed nematode-trapping fungi and the dominant group in most habitats. They mainly occur in the soil or sediment of various ecosystems such as farmland, forests, mangroves, and freshwater, and they are also recorded in hot springs, animal waste, and tree trunks (Soprunov & Galiulina, 1951; Duddington, 1954; Liu et al., Zhang et al., 2001; Su et al., 2007; Mo et al., 2008; Swe et al., 2009; Kim et al., Kumar et al., 2011; Hastuti et al., 2018; Zhang et al., 2020). Most *Arthrobotrys* species have strong saprophytic and reproductive capacity and can quickly colonize in soil (Zhang et al., 2001; Zhang & Mo, 2006; Zhang & Hyde, 2014), so they are ideal materials for the development of parasitic nematode bio-control agents. At the same time, they are also a good group for the evolutionary studies of nematode-trapping fungi within the genus because of the

abundant species and obvious morphological differentiation of conidia and conidiophores (Zhang & Mo, 2006; Zhang & Hyde, 2014). The six new species described in this study enhance the diversity of nematode-trapping fungi, provide more materials for the biological control of parasitic nematodes, and add precious research objects for evolutionary studies of nematode-trapping fungi.

6.2 Material and Methods

6.2.1 Sampling, Fungal Isolation and Morphological Observation

The strains included in this study were isolated from terrestrial soil and freshwater sediment collected in Yunnan Province, China. Terrestrial soil samples were collected from 0–10 cm depth using a 35 mm-diameter soil borer after removing fallen leaves from the soil surface (Shepherd, 1955; Fowler, 1970; Farrell et al., 2006). Freshwater sediment samples were removed from the water with a Peterson bottom sampler (HL-CN, Wuhan Hengling Technology Company, Limited, Wuhan, China). The samples were placed into a zip-lock bag, and relevant site information were recorded. The samples were stored at 4℃ until processing.

Samples of 1–2 g of soil or sediment were spread on the surface of cornmeal agar (CMA) plates with sterile toothpicks. Approximately 5000 nematodes (*Panagrellus redivivus* Goodey, free-living nematodes) were added as bait to promote the germination of the nematode-trapping fungi (Drechsler, 1941; Duddington, 1955; Eren & Pramer, 1965; Zhang & Hyde, 2014). The plates were incubated at 26℃ for three weeks and then observed under a stereo-microscope; the spores of nematode-trapping fungi were transferred to fresh CMA plates using a sterile needle. This step was repeated until a pure culture was obtained (Li et al., 2000; Zhang & Hyde, 2014).

The pure cultures were transferred to fresh CMA plates with observation well (a square slot 2 × 2 cm created by removing agar in each plate) using a sterile needle and incubated at 26℃ until the mycelia spread beyond the well. Approximately 1000 living nematodes were placed in the well to induce the formation of the trapping device (Li et al., 2000; Zhang & Hyde, 2014). The types of trapping devices were checked

using a stereo-microscope. All micromorphological features were photographed and measured with an Olympus BX53 microscope (Olympus Corporation, Tokyo, Japan).

6.2.2 DNA Extraction, PCR Amplification and Sequencing

Total genomic DNA was extracted from mycelia grown on potato dextrose agar (PDA) plates using a rapid fungal genomic DNA isolation kit (Sangon Biotech Company, Limited, Shanghai, China). The ITS, TEF, and RPB2 regions were amplified with the primer pairs ITS4-ITS5 (White et al., 1990;), 526F-1567R (O'Donnell et al., 1998), and 6F-7R (Liu et al., 1999), respectively. The PCR amplification was performed as follows: pre-denaturation at 94℃ for 4 minutes; followed by 35 cycles of denaturation at 94℃ for 45 seconds; annealing at 52℃ (ITS), 55℃ (TEF), or 54℃ (RPB2) for 1 minutes, and extension at 72℃ for 1.5–2 minutes; with a final extension at 72℃ for 10 mnutes. The PCR products were purified with a DiaSpin PCR Product Purification Kit (Sangon Biotech Company, Limited, Shanghai, China). The purified PCR products of the ITS and RPB2 regions were sequenced in the forward and reverse directions using PCR primers, and the primer pair 247F-609R (Yang et al., 2007) was used to sequence the TEF genes (BioSune Biotech Company, Limited, Shanghai, China). SeqMan v. 7.0 (DNASTAR, Madison, WI, USA) (Swindell & Plasterer, 1997) was used to check, edit, and assemble the sequences. The sequences generated in this study were deposited in the GenBank database at the National Center for Biotechnology Information (NCBI; https://www.ncbi.nlm.nih.gov/, accessed on 26 February 2022), and the accession numbers are listed in Table 6.1.

Table 6.1 The GenBank accession numbers of the isolates included in this study

Taxon	Strain Number	GenBank Accession Number		
		ITS	TEF	RPB2
Arthrobotrys amerospora	CBS 268.83	NR 159625	—	—
Arthrobotrys anomala	YNWS02-5-1	AY773451	AY773393	AY773422
Arthrobotrys arthrobotryoides	CBS 119.54	MH857262	—	—
Arthrobotrys arthrobotryoides	AOAC	MF926580	—	—
Arthrobotrys botryospora	CBS 321.83	NR 159626	—	—
Arthrobotrys cladodes	1.03514	MH179793	MH179616	MH179893
Arthrobotrys clavispora	CBS 545.63	MH858353	—	—

Table 6.1 (continued)

Taxon	Strain Number	GenBank Accession Number		
		ITS	TEF	RPB2
Arthrobotrys conoides	670	AY773455	AY773397	AY773426
Arthrobotrys cookedickinson	YMF1.00024	MF948393	MF948550	MF948474
Arthrobotrys cystosporia	CBS 439.54	MH857384	—	—
Arthrobotrys dendroides	YMF1.00010	MF948388	MF948545	MF948469
Arthrobotrys dianchiensis	1.00571	MH179720	—	MH179826
Arthrobotrys elegans	1.00027	MH179688	—	MH179797
Arthrobotrys eryuanensis	CGMCC3.19715	MT612105	OM850307	OM850301
Arthrobotrys eryuanensis	YXY45	ON808616	ON809547	ON809553
Arthrobotrys eudermata	SDT24	AY773465	AY773407	AY773436
Arthrobotrys flagrans	1.01471	MH179741	MH179583	MH179845
Arthrobotrys gampsospora	CBS 127.83	U51960	—	—
Arthrobotrys globospora	1.00537	MH179706	MH179562	MH179814
Arthrobotrys guizhouensis	YMF1.00014	MF948390	MF948547	MF948471
Arthrobotrys indica	YMF1.01845	KT932086	—	—
Arthrobotrys iridis	521	AY773452	AY773394	AY773423
Arthrobotrys janus	Jan-85	AY773459	AY773401	AY773430
Arthrobotrys javanica	105	EU977514	—	—
Arthrobotrys jinpingensis	CGMCC3.20896	OM855569	OM850311	OM850305
Arthrobotrys jinpingensis	YXY101	ON808621	ON809552	ON809558
Arthrobotrys koreensis	C45	JF304780	—	—
Arthrobotrys lanpingensis	CGMCC3.20998	OM855566	OM850308	OM850302
Arthrobotrys lanpingensis	YXY80	ON808618	ON809549	ON809555
Arthrobotrys latispora	H.B. 8952	MK493125	—	—
Arthrobotrys longiphora	1.00538	MH179707	—	MH179815
Arthrobotrys luquanensis	CGMCC3.20894	OM855567	OM850309	OM850303
Arthrobotrys luquanensis	YXY87	ON808619	ON809550	ON809556
Arthrobotrys mangrovispora	MGDW17	EU573354	—	—
Arthrobotrys megalospora	TWF800	MN013995	—	—
Arthrobotrys microscaphoides	YMF1.00028	MF948395	MF948552	MF948476
Arthrobotrys multiformis	CBS 773.84	MH861834	—	—
Arthrobotrys musiformis	SQ77-1	AY773469	AY773411	AY773440
Arthrobotrys musiformis	1.03481	MH179783	MH179607	MH179883
Arthrobotrys nonseptata	YMF1.01852	FJ185261	—	—
Arthrobotrys obovata	YMF1.00011	MF948389	MF948546	MF948470
Arthrobotrys oligospora	920	AY773462	AY773404	AY773433
Arthrobotrys paucispora	ATCC 96704	EF445991	—	—
Arthrobotrys polycephala	1.01888	MH179760	MH179592	MH179862

Table 6.1 (continued)

Taxon	Strain Number	GenBank Accession Number		
		ITS	TEF	RPB2
Arthrobotrys pseudoclavata	1130	AY773446	AY773388	AY773417
Arthrobotrys psychrophila	1.01412	MH179727	MH179578	MH179832
Arthrobotrys pyriformis	YNWS02-3-1	AY773450	AY773392	AY773421
Arthrobotrys reticulata	CBS 550.63	MH858355	—	—
Arthrobotrys robusta	nefuA4	MZ326655	—	—
Arthrobotrys salina	SF 0459	KP036623	—	—
Arthrobotrys scaphoides	1.01442	MH179732	MH179580	MH179836
Arthrobotrys shizishanna	YMF1.00022	MF948392	MF948549	MF948473
Arthrobotrys shuifuensis	CGMCC3.19716	MT612334	OM850306	OM850300
Arthrobotrys shuifuensis	YXY48	ON808617	ON809548	ON809554
Arthrobotrys sinensis	105-1	AY773445	AY773387	AY773416
Arthrobotrys sphaeroides	1.0141	MH179726	MH179577	MH179831
Arthrobotrys superba	127	EU977558	—	—
Arthrobotrys thaumasia	917	AY773461	AY773403	AY773432
Arthrobotrys vermicola	629	AY773454	AY773396	AY773425
Arthrobotrys xiangyunensis	YXY10-1	MK537299	—	—
Arthrobotrys yunnanensis	AFTOL-ID 906	DQ491512	—	—
Arthrobotrys zhaoyangensis	CGMCC3.20944	OM855568	OM850310	OM850304
Arthrobotrys zhaoyangensis	YXY86	ON808620	ON809551	ON809557
Dactylaria higginsii	CBS 121934	KM009164	—	—
Dactylellina appendiculata	CBS 206.64	AF106531	DQ358227	DQ358229
Dactylellina copepodii	CBS 487.90	U51964	DQ999835	DQ999816
Dactylellina mammillata	CBS229.54	AY902794	DQ999843	DQ999817
Datylellina yushanensis	CGMCC3.19713	MK372061	MN915113	MN915112
Drchslerella coelobrocha	FWY03-25-1	AY773464	AY773406	AY773435
Drchslerella dactyloides	expo-5	AY773463	AY773405	AY773434
Drchslerella stenobrocha	YNWS02-9-1	AY773460	AY773402	AY773431
Drechslerella brochopaga	701	AY773456	AY773398	AY773427
Orbilia jesu-laurae	LQ59a	MN816816	—	—
Vermispora fusarina	YXJ02-13-5	AY773447	AY773389	AY773418

6.2.3 Phylogenetic Analysis

The sequences generated in this study were compared against the NCBI GenBank database using BLASTn (https://blast.ncbi.nlm.nih.gov/, accessed on 11 February 2022). The BLASTn search results and the morphological features of these six species indicated

that they belong to the genus *Arthrobotrys*. This genus was searched in the Species Fungorum (http://www.speciesfungorum.org, accessed on 13 February 2022), and all relevant records were checked individually according to the relevant documents to ensure that all *Arthrobotrys* taxa were considered in this study (Li et al., 2000; Zhang & Mo, 2006; Swe et al., 2011; Yang et al., 2012; Zhang & Hyde, 2014). All reliable ITS, TEF, and RPB2 sequences of *Arthrobotrys* taxa were downloaded from GenBank database (Table 6.1). Three genes were aligned using the online program MAFFT v.7 (http://mafft.cbrc.jp/alignment/server/, accessed on 15 February 2022) (Katoh & Standley, 2013) and manually adjusted using BioEdit v7.2.3 (Hall, 1999); they were then linked with MEGA 6.0 (Tamura et al., 2013). *Vermispora fusarina* YXJ13-5 and *Dactylaria higginsii* CBS 121934 were selected as outgroups. Phylogenetic trees were inferred via maximum likelihood (ML), maximum parsimony (MP), and Bayesian inference (BI) analyses.

The SYM+I+G, GTR+I+G, and GTR+I+G models were selected via jModelTest v2.1.10 (Posada, 2008) as the best-fit optimal substitution models for ITS, TEF, and RPB2, respectively, for maximum likelihood (ML) and Bayesian inference (BI) analysis.

Maximum likelihood (ML) analysis was implemented using IQ-Tree v1.6.5 (Nguyen et al., 2014). The dataset was partitioned, and each gene was analyzed with the corresponding model. The statistical bootstrap support values (BS) were computed using rapid bootstrapping with 1000 replicates (Felsenstein et al., 1985).

PAUP 4. a168 on XSEDE (Swofford, 2001) in the CIPRES Science Gateway v. 3.3 web resource was used to generate the maximum parsimony (MP) analysis. Trees were inferred using the heuristic search option with TBR branch swapping and 1000 random sequence additions. Max-trees were set up at 5000 and no-increase. Clade stability was assessed via a bootstrap analysis with 1000 replicates (Felsenstein, 1985). Tree length (TL), consistency index (CI), retention index (RI), rescaled consistency index (RC), and homoplasy index (HI) values were calculated for all trees generated under different optimality criteria. All of the above parameters were edited into the PAUP block in the NEX file.

Bayesian inference (BI) analysis was conducted with MrBayes v. 3.2.6. (Huelsenbeck & Ronquist, 2001). The multiple sequence alignment file was converted into a MrBayes-compatible NEXUS file using FastaConvert (Hall, 2007). The dataset was partitioned, and the optimal substitution models of each gene were equivalently replaced to

conform to the setting of MrBayes. Six simultaneous Markov chains were run for 10,000,000 generations, and trees were sampled every 100 generations. The first 25% of the trees were discarded, and the remaining trees were used to calculate the posterior probabilities (PP) in the majority rule consensus tree. All of the above parameters were edited in the MrBayes block in the NEX file.

The tree was visualized with FigTree v1.3.1 (Rambaut, 2010). The backbone tree was edited and reorganized using Microsoft PowerPoint (2013) and Adobe Photoshop CS6 software (Adobe Systems, San Jose, CA, USA).

6.3 Results

6.3.1 Phylogenetic Analysis

A total of 118 *Arthrobotry* related taxa were listed in the Species Fungorum (http:// www.speciesfungorum.org/ (accessed on 6 March 2022)), representing 59 valid *Arthrobotrys* species. Among them, 51 species had confirmed molecular data. Therefore, the combined ITS, TEF, and RPB2 alignment dataset contained 64 *Arthrobotrys* isolates representing 57 *Arthrobotrys* species (plus our 12 isolates and six new species) and other related species in *Orbiliaceae* (*Dactylellina*: four species and *Drechslerella*: four species). The final dataset comprised 1918 characters (551 for ITS, 547 for TEF, and 820 for RPB2), among which 872 bp were constant, 1004 bp were variable, and 748 bp were parsimony informative. The maximum likelihood analysis of a best-scoring tree was performed with a final ML optimization likelihood value of −6304.618465. Within the MP analysis, a strict consensus MP tree was obtained from the three most equally parsimonious trees (TL = 3443, CI = 0.546, RI = 0.510, RC = 0.298, HI = 0.419). For the Bayesian analysis (BI), the consensus tree was calculated with the remaining 75% of trees, and the Bayesian posterior probabilities were evaluated with a final average standard deviation of the split frequency of 0.009254. Although the trees inferred by ML, MP, and BI showed slightly different topologies in some clusters, all trees showed that all six species clustered together with known *Arthrobotrys* species, with distinct divergence from other species. The best-scoring ML tree was selected for presentation (Figure 6.1).

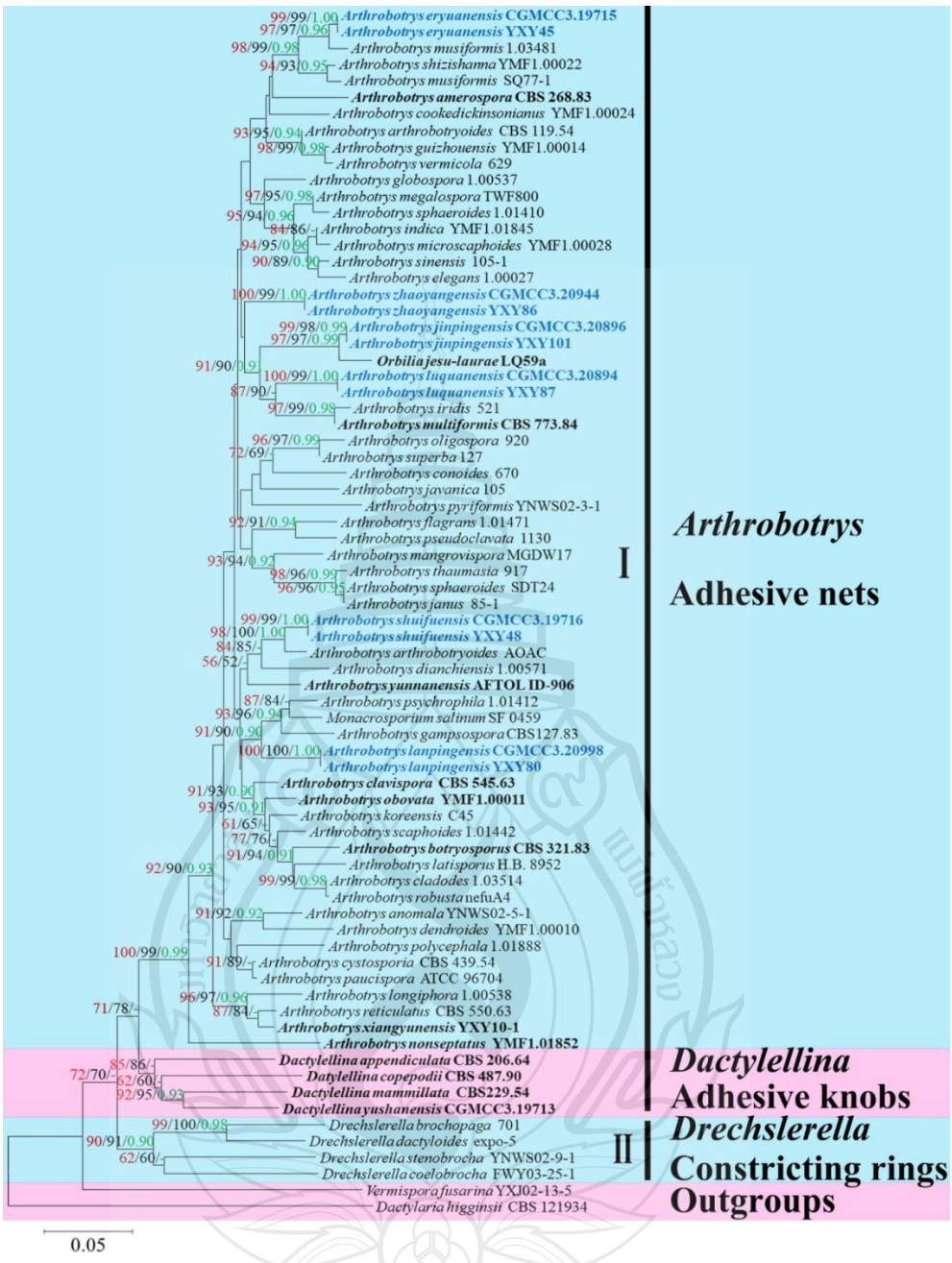

Figure 6.1 Maximum likelihood tree based on a combined ITS, TEF, and RPB2 sequence from 65 species of *Orbiliaceae* nematode-trapping fungi. Bootstrap support values for maximum likelihood (red) and maximum parsimony (black) greater than 50% and Bayesian posterior probabilities values (green) greater than 0.90 are indicated above the nodes. The new isolates are in blue; type strains are in bold. The tree is rooted by *Vermispora fusarina* YXJ13-5 and *Dactylaria higginsii* CBS 121934

The phylogram inferred from the ITS+TEF+RPB2 dataset showed these six species clustered in *Arthrobotrys*. Among these species, *Arthrobotrys eryuanensis* clustered together with *A. musiformis* and *A. shizishanna* with 98% MPBS, 99% MLBS, and 0.98 BYPP support. *Arthrobotrys jinpingensis* and *A. shuifuensis* were sisters to *Orbilia jesu-laurae* and *A. arthrobotryoides*, respectively, with high support values (95% MPBS, 95%MLBS, 0.95 BYPP). *Arthrobotrys luquanensis* formed a basal lineage with *A. iridis* and *A. multiformis* with 87% MPBS and 90% MLBS support. *Arthrobotrys lanpingensis* clustered together with *A. psychrophila*, *A. salinum*, and *A. gampsospora* with 91% MPBS, 90% MLBS, and 0.90 BYPP support. The phylogenetic position of *Arthrobotrys zhaoyangensis* was uncertain, but this species showed significant divergence from known species.

6.3.2 Taxonomy

Arthrobotrys eryuanensis F. Zhang & X.Y. Yang sp. nov. (Figure 6.2).

Index Fungorum number: IF556938; Facesoffungi number: FoF 10760

Etymology: The species name "eryuanensis" refers to the name of the sample collection site: Eryuan County, Dali City, Yunnan Province, China.

Material examined: CHINA, Yunnan Province, Dali City, Eryuan County, Xihu Lake, N 26°9′8.77″, E 99°57′17.03″, from freshwater sediment, 20 June 2014, F. Zhang. Holotype CGMCC3.19715, preserved in the China General Microbiological Culture Collection Center. Ex-type culture DLUCC 14-1, preserved in the Dali University Culture Collection.

Colonies on PDA white, cottony, growing rapidly, reaching 50 mm diameter after 7 days in the incubator at 26°C. *Mycelium* partly superficial, partly immersed, composed of septate, branched, smooth hyphae. *Conidiophores* 110–308 µm. ($\bar{x}$ = 213.5 µm., n = 50) long, 2.5–4.5 µm. ($\bar{x}$ = 3.2 µm., n = 50) wide at base, gradually tapering upwards to apex, 1.5–3 µm. ($\bar{x}$ = 2.2 µm., n = 50) wide at apex, erect, septate, branched, hyaline, producing 2–10 short polylactic denticles at apex, with each denticle bearing a single holoblastic conidium. *Conidia* two types: *Macroconidia* 18–44.5 × 5–11.5 µm. ($\bar{x}$ = 28.4 × 8.7 µm., n = 50), clavate to elongate pyriform, some slightly curved, wider rounded at apex, narrower towards the lower with truncate at base, 1-septate, septum median to sub-median, hyaline, guttulate. *Microconidia* 7.5–28 × 4–11 µm. ($\bar{x}$ = 17.6 × 8.6 µm., n = 50),

sub-globose to clavate, obovoid, wider rounded at apex, truncate at papillate bulged base, aseptate, hyaline, guttulate. *Chlamydospores* 7–18.5 × 3.5–8 µm. ($\bar{x}$ = 10.7 × 5.8 µm., n = 50), cylindrical, hyaline, in chains when present, sometimes guttulate, slightly verrucose-walled. Captures nematodes with adhesive networks.

Additional specimen examined: CHINA, Yunnan Province, Dali City, Eryuan County, Xihu Lake, N 26°9′8.77″, E 99°57′17.03″, from freshwater sediment, 20 June 2014, F. Zhang. Living culture YXY45.

Notes: Phylogenetically, *Arthrobotrys eryuanensis* clusters together with *A. shizishanna* and *A. musiformis* with high support values (98% MLBS, 99% MPBS, 0.99 BYPP). *Arthrobotrys eryuanensis* was 6.7% (39/586 bp) and 5.3% (26/486 bp) different from *A. shizishanna* and *A. musiformis* in ITS sequence. Morphologically, *A. eryuanensis* can be easily distinguished from *A. shizishanna* in shape, size, septation, and numbers of conidia and conidiophores (Liu & Zhang, 2003). It is more similar to *A. musiformis* in the morphology of its macroconidia (Zhang & Mo, 2006; Zhang & Hyde, 2014). Their differences are as follows: (1) *A. musiformis* produces one type of conidia, most of which are curved, while *A. eryuanensis* produces two types of conidia. Macroconidia is 1-septate, partly curved and partly symmetrical, and microconidia is aseptate and truncate at the base with a papillate bulge. (2) The conidiophores of *A. musiformis* are unbranched, while most of those in *A. eryuanensis* are branched.

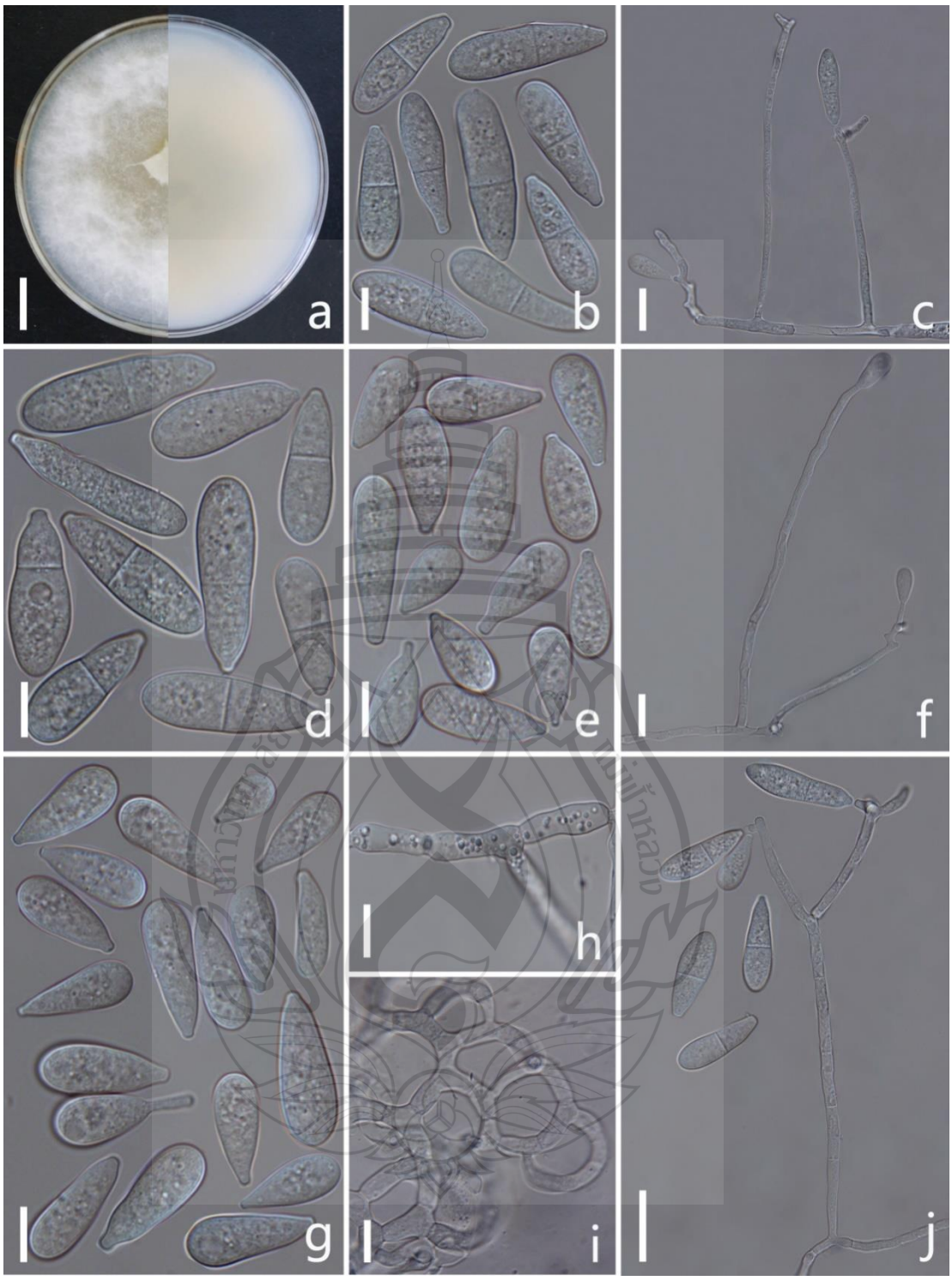

Figure 6.2 *Arthrobotrys eryuanensis* (CGMCC3.19715). (a) Colony. (b, d) Macroconidia. (e, g) Microconidia. (c, f, j) Conidiophores. (h) Chlamydospores. (i) Trapping device: adhesive networks. Scale bars: (a) = 1 cm., (b, d, e, g–i) = 10 µm., (c, f, j) = 20 µm.

Arthrobotrys jinpingensis F. Zhang & X.Y. Yang sp. nov. (Figure 6.3)

Index Fungorum number: IF 556018; Facesoffungi number: FoF 10761.

Etymology: The species name “jinpingensis” refers to the name of the sample collection site: Jinping County, Gejiu City, Yunnan Province, China.

Material examined: CHINA, Yunnan Province, Gejiu City, Jinping County, N 23°4′54.80″, E 103°12′40.80″, from terrestrial soil, 19 April 2017, F. Zhang. Holotype CGMCC3.20896, preserved in the China General Microbiological Culture Collection Center. Ex-type culture DLUCC 21-1, preserved in the Dali University Culture Collection.

Colonies on PDA white, cottony, growing rapidly, reaching 60 mm diameter after 10 days in the incubator at 27°C. *Mycelium* partly superficial, partly immersed, composed of septate, branched, smooth hyphae. *Conidiophores* 225–509 µm. ($\bar{x}$ = 348.2 µm., n = 50) long, 3–8.5 µm. ($\bar{x}$ = 4.9 µm., n = 50) wide at base, gradually tapering upwards to apex, 1.5–3 µm. ($\bar{x}$ = 2.1 µm., n = 50) wide at apex, erect, septate, unbranched, hyaline, producing several separate nodes by the repeated elongation of conidiophores, with each node bearing 2–11 polylactic conidia. *Conidia* 11–26.5 × 6.5–14.5 µm. ($\bar{x}$ = 18.6 × 10.8 µm., n = 50), sub-globose, oval to obovoid, obpyriform, wider rounded at apex, narrow towards with truncate at base, sometimes with a bud-like projection at base, 0 or 1-septate, hyaline, rough to smooth-walled. *Chlamydospores* 7–18.5 × 5.5–9.5 µm. ($\bar{x}$ = 13.3 × 7.4 µm., n = 50), cylindrical, ellipsoidal, in chains, hyaline, guttulate, rough-walled. Captures nematodes with adhesive networks.

Additional specimen examined: CHINA, Yunnan Province, Gejiu City, Jinping County, N 23°4′54.80″, E 103°12′40.80″, from terrestrial soil, 19 April 2017, F. Zhang. Living culture YXY101.

Notes: Phylogenetically, *Arthrobotrys jinpingensis* forms a sister lineage to *Orbilia jesulaurae* with 97% MLBS, 97% MPBS, 0.99 BYPP support. There is 2.5% (15/600 bp) difference in their ITS sequences. However, the conidiophores of *A. jinpingensis*is are unbranched, producing several separate nodes by repeated elongation, while the conidiophores of *O. jesu-laurae* are branched and produce only one node at apex. In addition, some conidia of *A. jinpingensis* have a bud-like projection at base, while the conidia of *O. jesu-laurae* do not (Quijada et al., 2020).

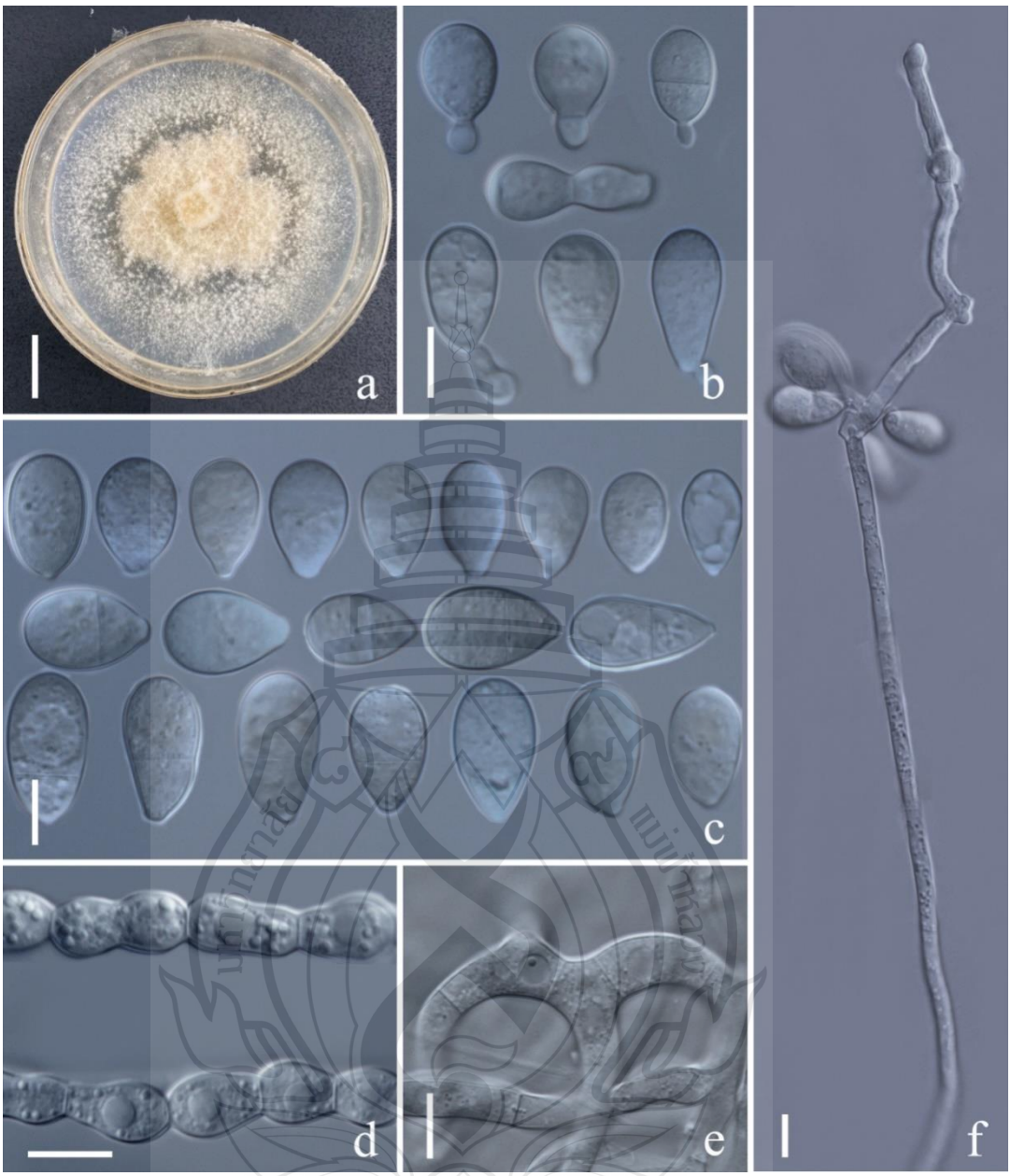

Figure 6.3 *Arthrobotrys jinpingensis* (CGMCC3.20896). (a) Colony. (b, c) Conidia. (d) Chlamydospores. (e) Trapping device: adhesive networks. (f) Conidiophore. Scale bars: (a) = 1 cm., (b–f) = 10 µm.

Arthrobotrys lanpingensis F. Zhang & X.Y. Yang sp. nov. (Figure 6.4).

Index Fungorum number: IF559021; Facesoffungi number: FoF 10762.

Etymology: The species name “lanpingensis” refers to the name of the sample collection site: Lanping County, Nujiang City, Yunnan Province, China.

Material examined: CHINA, Yunnan Province, Nujiang City, Lanping County, N 26°22′13.50″, E 99°23′0.20″, from freshwater sediment, 16 May 2015, F. Zhang. Holotype CGMCC3.20998, preserved in the China General Microbiological Culture Collection Center. Ex-type culture DLUCC 18-1, preserved in the Dali University Culture Collection.

Colonies on PDA white, cottony, growing rapidly, reaching 50 mm diameter after 10 days in the incubator at 27°C. *Mycelium* partly superficial, partly immersed, composed of septate, branched, smooth hyphae. *Conidiophores* 241–503 µm. ($\bar{x}$ = 307.5 µm., *n* = 50) long, 3.5–7 µm. ($\bar{x}$ = 4.7 µm., n = 50) wide at base, gradually tapering upwards to apex, 2–3.5 µm. ($\bar{x}$ = 2.4 µm., n = 50) wide at apex, erect, septate, unbranched, hyaline, bearing a single holoblastic conidium at apex. *Conidia* 31–55 × 13.5–24.5 µm. ($\bar{x}$ = 45.4 × 19.7 µm., n = 50), obovoid, cuneiform to slightly pyriform, upper cell wider than lower cell, apex rounded, widest at median cell, tapering towards the narrow and subacute with truncate base, 1-septate when immature, becoming 3-septate at maturity (2 at base and 1 at apex), hyaline, minutely guttulate, smooth-walled. *Chlamydospores* 8–27 × 8–25 µm. ($\bar{x}$ = 17.4 × 14.5 µm., n = 50), globose to sub-globose or ellipsoidal, growing in chains, hyaline, guttulate, rough-walled. Capturing nematodes with adhesive networks.

Additional specimen examined: CHINA, Yunnan Province, Nujiang City, Lanping County, N 26°22′13.50″, E 99°23′0.20″, from freshwater sediment, 16 May 2015, F. Zhang. Living culture YXY80.

Notes: Phylogenetically, *Arthrobotrys lanpingensis* formed a sister lineage to *A. psychrophila*, *A. salinum* and *A. gampsospora* with 91% MLBS, 90% MPBS, and 0.90 BYPP support. *Arthrobotrys lanpingensis* was 9.3% (56/602 bp), 6.4% (32/503 bp), and 8.7% (50/576 bp) different from *A. gampsospora*, *A. psychrophile*, and *A. salinum* in ITS sequences, respectively. Morphologically, *A. lanpingensis* is most similar to *A. guizhouensis* in their sub-fusiform conidia. However, *A. guizhouensis* produces two types of conidia, while *A. lanpingensis* produces only one type of conidia. In addition, most conidia of *A. lanpingensis* are 3-septate, whereas the conidia of *A. guizhouense* are 2-septate, and the conidia of *A. lanpingensis* are significantlysmaller than those of *A. guizhouensis* [*A. lanpingensis*, 31.1–55.2 (45.4) × 13.5–24.3 (19.7) µm. versus *A. guizhouensis*, 30.5–71.5 (52.7) × 18.5–28.5 (23.9) µm.] (Zhang & Mo, 2006; Zhang & Hyde, 2014).

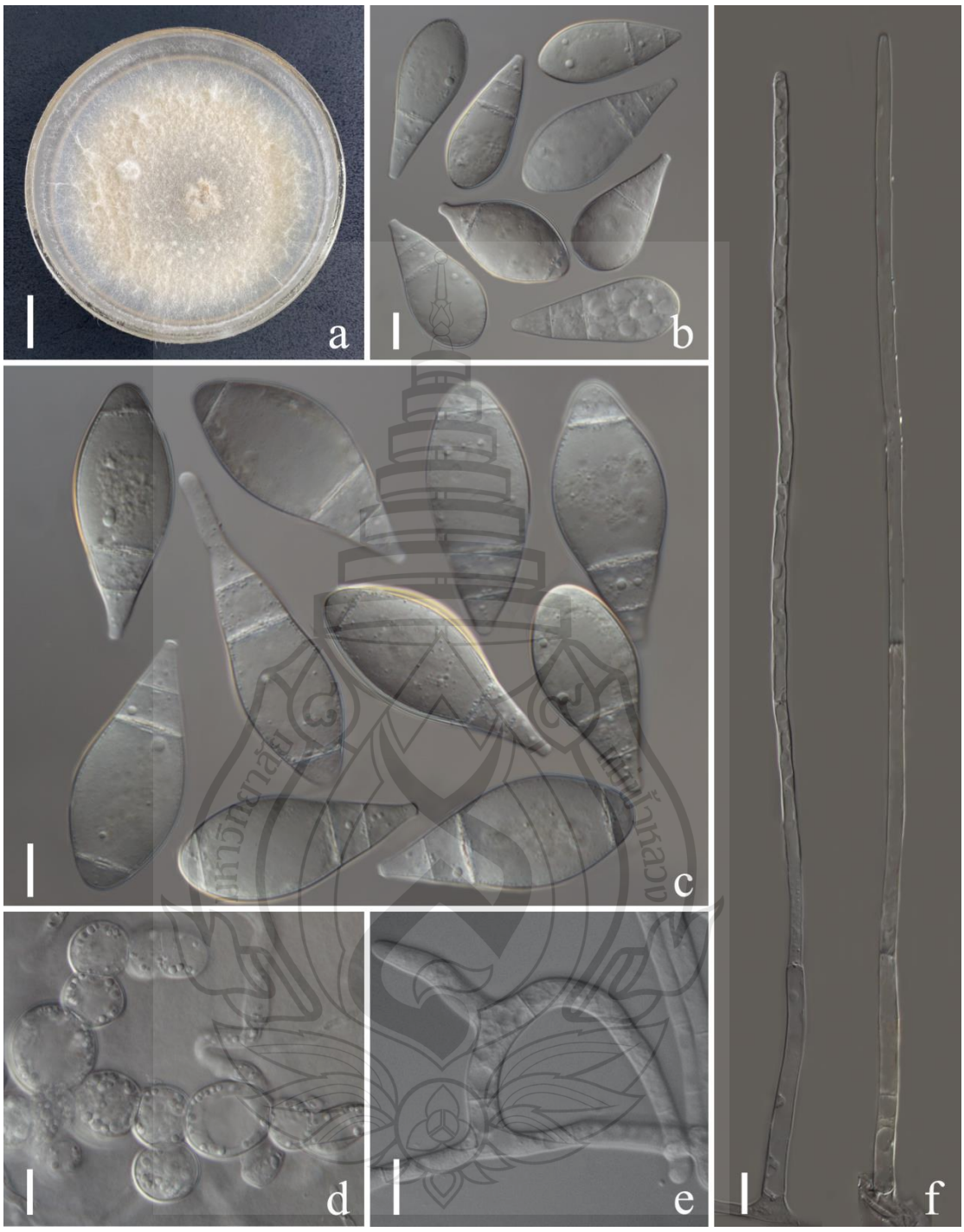

Figure 6.4 *Arthrobotrys lanpingensis* (CGMCC3.20998). (a) Colony. (b, c) Conidia. (d) Chlamydospores. (e) Trapping device: adhesive networks. (f) Conidiophores. Scale bars: (a) = 1 cm., (b–f) = 10 µm.

Arthrobotrys luquanensis F. Zhang & X.Y. Yang sp. nov. (Figure 6.5).

Index Fungorum number: IF 557884; Facesoffungi number: FoF 10763.

Etymology: The species name “luquanensis” refers to the name of the sample collection site: Luquan County, Kunming City, Yunnan Province, China.

Material examined: CHINA, Yunnan Province, Kunming City, Luquan County, N 26°10′33.20″, E 102°45′43.50″, from terrestrial soil, 24 May 2017, F. Zhang. Holotype CGMCC3.20894, deposited in the China General Microbiological Culture Collection Center. Ex-type culture DLUCC 19-1, deposited in the Dali University Culture Collection.

Colonies on PDA white, cottony, growing rapidly, reaching 55 mm diameter after 10 days in the incubator at 27°C. *Mycelium* partly superficial, partly immersed, composed of septate, branched, smooth hyphae. *Conidiophores* 216–522 µm. ($\overline{x}$ = 346.5 µm., *n* = 50) long, 2.5–6.5 µm. ($\overline{x}$ = 4.3 µm., n = 150) wide at base, gradually tapering upwards to apex, 1.5–3.5 (2.3) µm. ($\overline{x}$ = 2.3 µm., n = 50) wide at apex, erect, septate, unbranched, hyaline, bearing a single holoblastic conidium at apex. *Conidia* 28–53.5 × 17–2.5 µm. ($\overline{x}$ = 40.9 × 26.3 µm., n = 50), sub-globose to widely ovate, with largest cell located at supra-median towards and rounded apex, tapering towards the subacute with truncate at base, 1–2-septate, mostly located at base, sometimes 3-septate (with 2 septa located at basal part and 1 at apex), hyaline, smooth-walled. *Chlamydospores* 6.5–17.5 × 6–14 µm. ($\overline{x}$ = 11.2 × 9.1 µm., n = 50), globose to sub-globose, ellipsoidal, in chains, hyaline, guttulate, rough-walled. Captures nematodes with adhesive networks.

Additional specimen examined: CHINA, Yunnan Province, Kunming City, Luquan County, N 26°10′33.20″, E 102°45′43.50″, from terrestrial soil, 24 May 2017, F. Zhang. Living culture YXY87.

Notes: The phylogenetic analyses revealed that *Arthrobotrys luquanensis* is related to *A. multiformis* and *A. iridis*. *Arthrobotrys luquanensis* was 9.5% (56/590 bp) and 8% (47/589 bp) different from *A. multiformis* and *A. iridis* in ITS sequences, respectively. In morphology, *A. luquanensis* is similar to *A. cookedickinson* and *A. sphaeroides* in simple conidiophores and sub-fusiform or obovate conidia (Castaner, 1968; Zhang & Mo, 2006; Chen et al., 2007; Zhang & Hyde, 2014), whereas the conidia of *A. luquanensis* are wider than those of *A. cookedickinson* [*A. luquanensis*, 28.1–53.3 (40.9) × 17–32.4 (26.3) µm. versus *A. cookedickinson*, 30–52.5 (42) × 15–22.5 (17.5) µm.] and bigger than those of *A.*

sphaeroides [*A. luquanensis*, 28.1–53.3 (40.9) × 17–32.4 (26.3) µm. versus *A. sphaeroides*, 20–44 (32) × 17–25 (20.4) µm.].

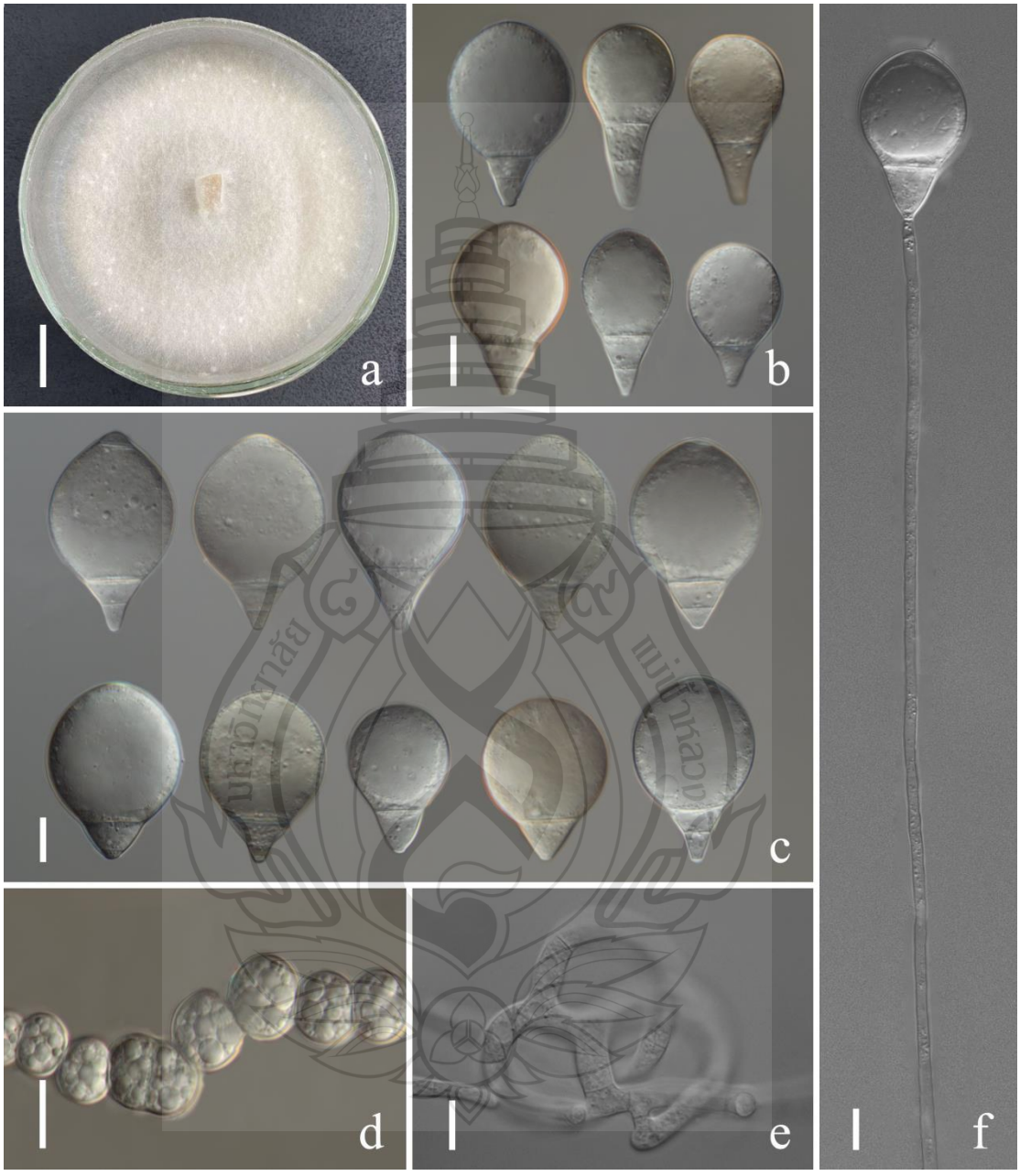

Figure 6.5 *Arthrobotrys luquanensis* (CGMCC3.20894). (a) Colony. (b, c) Conidia. (d) Chlamydospores. (e) Trapping device: adhesive networks. (f) Conidiophore. Scale bars: (a) = 1 cm., (b–f) = 10 µm.

Arthrobotrys shuifuensis F. Zhang & X.Y. Yang sp. nov. (Figure 6.6).

Index Fungorum number: IF556937; Facesoffungi number: FoF 10764.

Etymology: The species name “shuifuensis” refers to the name of the sample collection site: Shuifu County, Zhaotong City, Yunnan Province, China.

Material examined: CHINA, Yunnan Province, Zhaotong City, Shuifu county, N 28°32′31.80″, E 104°19′9.50″, from terrestrial soil, 16 June 2017, F. Zhang. Holotype CGMCC3.19716, deposited in the China General Microbiological Culture Collection Center. Ex-type culture DLUCC 15-1, deposited in the Dali University Culture Collection.

Colonies on PDA initially white and turned to pink tinged after 2 weeks, cottony, rapidly growing, reaching 50 mm diameter after 9 days in the incubator at 26℃. *Mycelium* partly superficial, partly immersed, composed of septate, branched, smooth hyphae. *Conidiophores* 105–305 µm. ($\overline{x}$ = 218.2 µm., n = 50) long, 3–5 µm. ($\overline{x}$ = 3.8 µm., n = 50) wide at base, gradually tapering upwards to apex, 1.5–3.5 µm. ($\overline{x}$ = 2.5 µm., n = 50) wide at apex, erect, septate, unbranched or rarely branched, hyaline, producing several separate nodes by repeated elongation of conidiophores, with each node consisting of 2–8 papilliform bulges and bearing polylactic conidia. *Conidia* 17–36 × 5–12.5 µm. ($\overline{x}$ = 27.2 × 8.2 µm., n = 50), oblong or capsule-shaped, narrower towards the lower and pointed base, 1-septate, median septum, hyaline, rough-walled. *Chlamydospores* 6–18 × 3–7.5µm. ($\overline{x}$ = 9.7 × 8.2 µm., n = 50), cylindrical, in chains, hyaline, rough-walled. Capturing nematodes with adhesive networks.

Additional specimen examined: CHINA, Yunnan Province, Zhaotong City, Shuifu County, N 28°32′31.80″, E 104°19′9.50″, from terrestrial soil, 16 June 2017, F. Zhang. YXY48.

Notes: Phylogenetic analysis showed that *Arthrobotrys shuifuensis* is the closest species to *A. arthrobotryoides*, there are 9.6% (57/596 bp) differences in ITS sequence between them. Morphologically, this species is similar to *A. arthrobotryoides* in their capsule-shaped, 1- septate conidia, whereas the conidia of *A. shuifuensis* are significantly longer than those of *A. arthrobotryoides* [*A. shuifuensis*, 17–36 (27.2) µm. versus *A. arthrobotryoides* 20–22 µm.]. In addition, the conidiophores of *A. arthrobotryoides* are unbranched and produces a continuous irregularly swollen node at apex, while the conidiophores of *A. shuifuensis* are branched, producing several

separate nodes with the repeated elongation of the conidiophores (Zhang et al., 1996; Zhang & Mo, 2006).

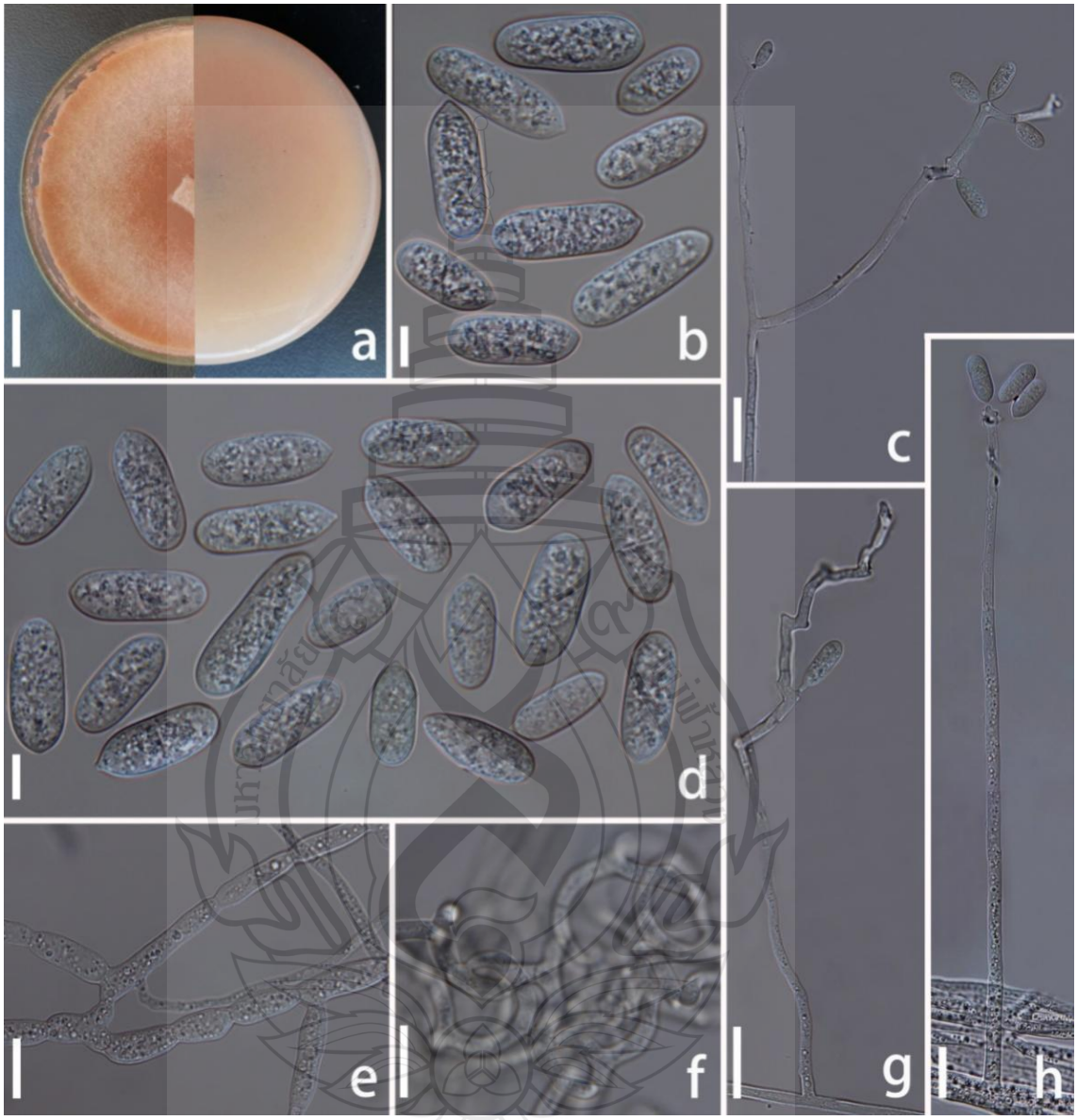

Figure 6.6 *Arthrobotrys shuifuensis* (CGMCC3.19716). (a) Colony. (b, d) Conidia. (e) Chlamydospores. (c, g, h) Conidiophores. (f) Trapping device: adhesive networks. Scale bars: (a) = 1 cm., (b, d, e) = 10 µm., (c, f–h) = 20 µm.

Arthrobotrys zhaoyangensis F. Zhang & X.Y. Yang sp. nov. (Figure 6.7).

Index Fungorum number: IF 556055; Facesoffungi number: FoF 10765.

Etymology: The species name "zhaoyangensis" refers to the name of the sample collection site: Zhaoyang County, Zhaotong City, Yunnan Province, China.

Material examined: CHINA, Yunnan Province, Zhaotong City, Zhaoyang County, N 27°29′43.20″, E 103°10′22.50″, from freshwater sediment, 14 April 2015, F. Zhang. Holotype CGMCC3.20944, deposited in the China General Microbiological Culture Collection Center. Ex-type culture DLUCC 20-1, deposited in the Dali University Culture Collection.

Colonies on PDA white, cottony, growing rapidly, reaching 48 mm diameter after 10 days in the incubator at 27°C. *Mycelium* partly superficial, partly immersed, composed of septate, branched, smooth hyphae. *Conidiophores* 207–498 µm. ($\bar{x}$ = 316.5 µm., n = 50) long, 3–9.5 µm. ($\bar{x}$ = 5.9 µm., n = 50) wide at base, gradually tapering upwards to apex 2–4 µm. ($\bar{x}$ = 2.6 µm., n = 50) wide at apex, erect, septate, unbranched, hyaline, bearing a single holoblastic conidium at apex. *Conidia* 25.5–52 × 14–32 µm. ($\bar{x}$ = 35.4 × 22.9 µm., n = 50), sub-globose, obovoid to obpyriform, wider at median towards supra-median, rounded at apex, tapering towards narrow with subacute and truncate base, 1–3-septate, mostly 3-septate (2 septa at base and 1 at apex), hyaline, rough to smooth-walled. *Chlamydospores* 12.5–31.5 × 6.6–12.5 µm. ($\bar{x}$ = 19.2 × 9.4 µm., n = 50) cylindrical, globose or ellipsoidal, in chains, hyaline, guttulate. Captures nematodes with adhesive network.

Additional specimen examined: CHINA, Yunnan Province, Zhaotong City, Zhaoyang County, N 27°29′43.20″, E 103°10′22.50″, from freshwater sediment, 14 April 2015, F. Zhang. Living culture YXY86.

Notes: Phylogenetic analysis revealed that the systematic position of *Arthrobotrys zhaoyangensis* is uncertain but showed significant distinction from known species. *A. zhaoyangensis* is most similar to *A. sinensis* and *A. sphaeroides*. *A. zhaoyangensis* can be distinguished from *A. sinensis* and *A. sphaeroides* by bigger conidia [*A. zhaoyangensis*, 25.3–52.1 (35.4) × 14–31.8 (22.9) µm. versus *A. sinensis* 23.5–30 (27.6) × 17–25 (20) µm., versus *A. sphaeroides* 20–44(32) × 17–25(20.4) µm.]. In addition, these three species differ slightly in the number of septation on conidia; *A. zhaoyangensis* produces 1–3-septate

conidia (mostly 3-septate), while the conidia of *A. sinensis* are 2-septate; *A. sphaeroides* sometimes produces aseptate conidia (Lindau et al., 1904; Castaner, 1968).

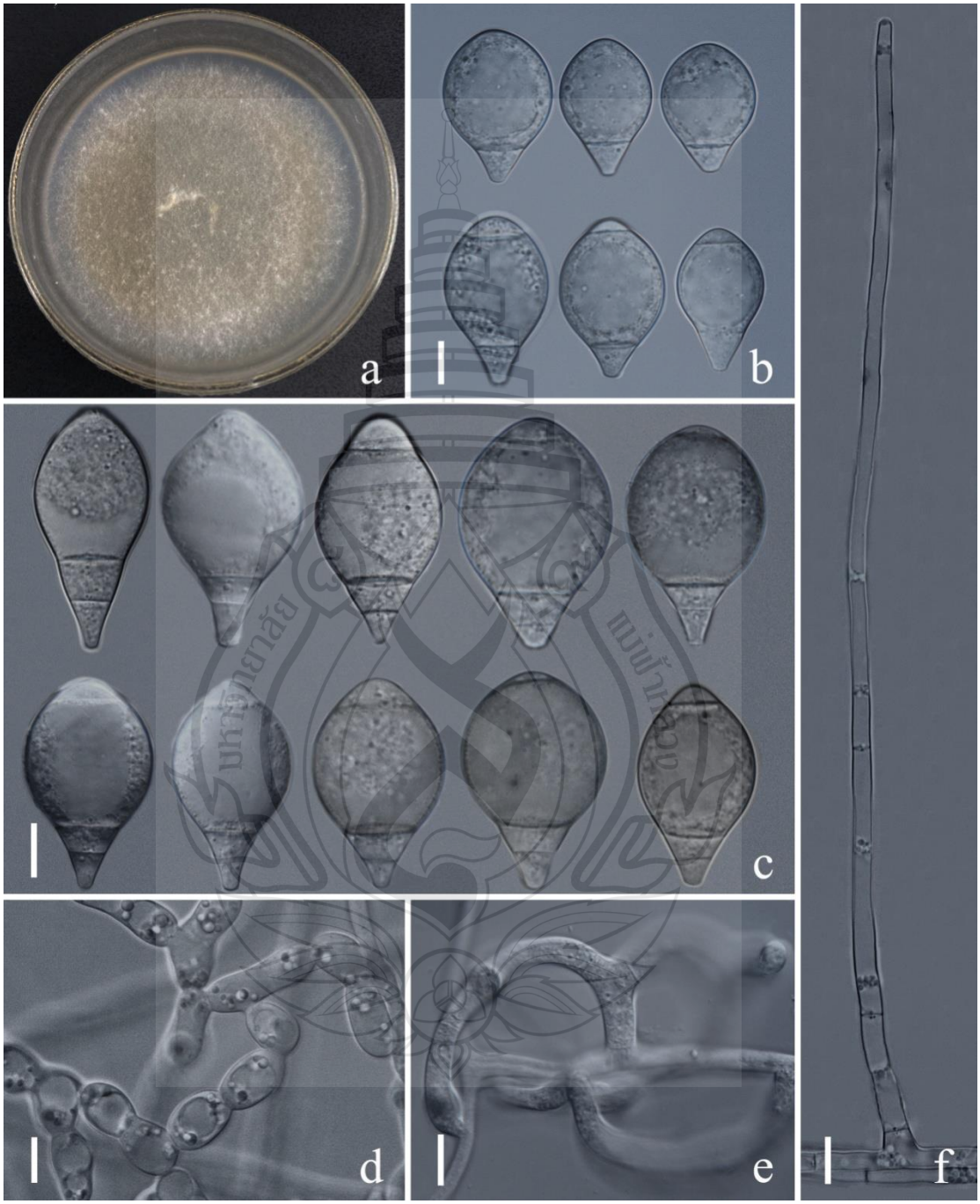

Figure 6.7 *Arthrobotrys zhaoyangensis* (CGMCC3.20944). (a) Colony. (b, c) Conidia. (d) Chlamydospore. (e) Trapping device: adhesive network. (f) Conidiophores. Scale bars: (a) = 1 cm., (b–f) = 10 µm.

6.4 Discussion

In this phylogenetic analysis, 65 species of nematode-trapping fungi used in this study were clustered into two large clades according to their mechanisms of catching nematodes. Clade I contained species that catch nematodes with adhesive trapping devices (adhesive nets and knobs). Clade II contained species that catch nematodes with active traps (constricting rings). Within clade I, species were clustered into two clades according to their trap types: one clade contained all species that produce adhesive nets, and the other contained those species that produce adhesive knobs. The results were consistent with previous studies (Scholler et al., 1999; Li et al., 2005; Yang et al., 2007, 2012) and again emphasized the importance of different types of trapping devices in the division of genera among nematode-trapping fungi. At the genus level, the taxonomy of *Orbiliaceae* nematode-trapping fungi remains an open question, especially in *Arthrobotrys*, which contains the greatest number of species. Morphologically, 61 species of *Arthrobotrys* can be divided into different groups according to the morphologies of their conidiophores and conidia (Zhang & Mo, 2006); however, phylogenetic studies have not supported this division; many phylogenetic clades show low support values, and the phylogenetic position of some *Arthrobotrys* species are unclear. The reason for this dilemma is the lack of molecular data for many species, and the existing data cannot provide a stable phylogenetic placement. Therefore, to thoroughly analyses the taxonomy of nematode-trapping fungi, we should use more comprehensive molecular data in future studies.

The emergence of molecular phylogenetic methods has led to unprecedented breakthroughs in the study of fungal taxonomy. Phylogenetic studies based on only a few molecular barcodes cannot provide sufficient and reliable information for the definition of fungal species; therefore, morphological descriptions of each species are still extremely important (Jeewon & Hyde, 2016; Chethana et al., 2021). However, a significant problem facing fungal taxonomy studies is that the description of species is too shallow (Meier et al., 2022). This problem is particularly prominent in *Orbiliaceae* nematode-trapping fungi and is mainly reflected in two aspects. (1) The descriptions of some morphological characteristics are too indistinct. Among six described species in

this study, only *A. eryuanensis* and *A. shuifuensis* could be easily distinguished from known species based on their distinct morphological characteristics. The remaining four species required more detailed characteristics (such as the size of conidia) to be identified from known species. When mycologists measure the size of conidia, they are accustomed to uniformly calculating the size data of conidia with different shapes and septate numbers, and the sizes of these conidia usually show significant differences. This causes the size range of conidia to be too extensive for effective comparisons of different species (Zhang & Mo, 2006; Zhang & Hyde, 2014). (2) There are too few morphological features that can be used for species identification; although the description of a species includes many features, such as its trap type, conidia, chlamydospores, and hyphae, only the trap type, conidia, and conidiophores can be used for species identification (Zhang & Mo, 2006; Zhang & Hyde, 2014). As an increasing number of new species are established, it is difficult to distinguish some similar species based on these three characteristics only. In conclusion, we should screen all potential morphological features in future studies to identify more features with significance for species identification. On the other hand, we should establish a unified standard morphological feature description model to facilitate comparisons between different species.

After the first nematode-trapping fungus was established in 1839 (Corda, 1839), the history of studies on the diversity of nematode-trapping fungi can be divided into three periods. In the nursery period, from 1839 to 1929, due to the limitation of separation methods, only five species were discovered over 90 years. In the rapid development period, from 1931 to 2009, the separation method improved gradually with the contributions of Drechsler (1936,1937), and nearly 90 species were described over 80 years. From 2010 to 2019, only three species were discovered over 10 years (http://www.speciesfungorum.org (accessed on 6 March 2022)). These data indicated that the excavation of nematode-trapping fungi seems to have reached a plateau, and over time, it is unlikely that many new species will be discovered. However, in recent years, we have investigated nematode-trapping fungi in Yunnan Province and collected ten new species (four previously published and six reported in this study) (Zhang et al., 2020), which indicates that there are still many nematode-trapping fungi in nature that have not been discovered. Previous studies on the diversity of nematode-trapping fungi

have mainly focused on soil habitat, whereas there have been considerably fewer investigations of aquatic nematode-trapping fungi (Serra et al., 2017; Hastuti et al., 2018; She et al., 2020). However, three of the six new species described in this paper are from freshwater sediment, suggesting that aquatic habitats may also be important sources of nematode-trapping fungi and should not be ignored in future studies.

CHAPTER 7

Arthrobotrys blastospora SP. NOV. (*ORBILIOMYCETES*): A LIVING FOSSIL DISPLAYING MORPHOLOGICAL TRAITS OF MESOZOIC CARNIVOROUS FUNGI

7.1 Introduction

The origin and evolution of life are the core of biological research (Kennedy & Norman, 2005). As primary decomposers in nature, fungi play a vital role in the circulation of matter and energy in ecosystems (Gleason & Lilje, 2009; Krauss et al., 2011; Grossart et al., 2019). Studying fungal evolution is integral to understanding the origin and evolution of life. In nature, most fungi are saprophytic, symbiotic, and parasitic, while a few fungi feed on micro-animals such as nematodes, rhizopods, rotifers, and mites (carnivorous fungi) (Liu et al., 1996, 2009; Barron, 1990, 2012). This survival strategy of feeding on other microorganisms is generally considered an adaptive evolution of fungi to allow them to adapt to nitrogen deficiency (Liu et al., 2009; Yang et al., 2012). The study of the origin and evolution of carnivorous fungi is crucial for understanding the history of fungal evolution. More than 80% of carnivorous fungi in the whole fungal kingdom belong to *Orbiliaceae* (*Orbiliomycetes, Ascomycota*) (Li et al., 2000; Yang et al., 2012). These fungi capture nematodes with various trapping structures. Modern molecular phylogenetic and morphological studies have divided all *Orbiliomycetes* carnivorous species into three genera according to type of trapping structure. *Drechslerella* captures nematodes using constricting rings, *Arthrobotrys* produces adhesive networks, and *Dactylellina* captures nematodes with adhesive branches, adhesive knobs, and non-constricting rings (Ahrén et al., 1998; Yang et al., 2007; Zhang & Hyde, 2014). Although such studies have revealed the phylogenetic relationship among these fungi, the evolutionary hypothesis of *Orbiliomycetes*

carnivorous fungi is still controversial (Rubner, 1996; Liou & Tzean, 1997; Ahrén et al., 1998; Scholler et al., 1999; Li et al., 2000, 2005; Yang et al., 2007, 2012).

Fossils hold the key that nature provided us to breakthrough in the study of the origin and evolution of life (Kukalova-Peck, 1978; Gingerich et al., 1983; Thaler, 1986; Flynn, 2007). However, compared with animals and plants, most fungi are tiny and do not have solid tissue structures to form fossils and be discovered by humans. Therefore, understanding the origin and evolution of fungi is very difficult. Excitingly, a few fossils that might be related to carnivorous fungi have been discovered. Jansson and Poinar found several conidia that resembled modern carnivorous fungi and several nematodes with appendages (the morphology of which is similar to adhesive spores or adhesive knobs produced by carnivorous fungi) attached to their bodies and fungal mycelium in their bodies in approximately 26-million-year-old amber (Jansson & Poinar, 1986). Schmidt et al. (2007, 2008) discovered the oldest relatively complete and clear fossil of a possible carnivorous fungus (*Palaeoanellus dimorphus*) in approximately 100-million-year-old amber, which caused a stir in the research on carnivorous fungi. Unfortunately, no species similar to this fossil has been found in the modern ecosystem so far. It has therefore been unclear whether this fossil is an ancestor of modern carnivorous fungi (Schmidt et al., 2008; Swe et al., 2011; Zhang & Hyde, 2014) because the character combination found in this fossil was distinct from any extant taxa.

During our large-scale survey of carnivorous fungi in the three parallel rivers region in China, two extraordinary carnivorous fungal isolates were discovered from 8698 carnivorous fungal strains isolated from 3617 soil samples and identified as a new species of the *Orbiliomycetes* carnivorous fungi. Fascinatingly, the morphological characteristics of this species are different from other modern carnivorous fungi and are strikingly similar to the carnivorous fossil fungus (*Palaeoanellus dimorphus*) discovered by Schmidt et al. (2007, 2008), according to which we speculate that this new species is a relict descendant of *P. dimorphus*. The discovery of this new species suggests that *P. dimorphus* is a possible ancestor of *Orbiliomycetes* carnivorous fungi and provides more accurate information for the evolutionary study of this group of fungi.

7.2 Material and Methods

7.2.1 Sample Collection

The two carnivorous fungal strains were isolated from two freshwater sediment samples in the Nujiang River Basin, the core area of the three parallel rivers. The sample numbers were EOS-1 (N 27°43′14.60″, E 98°41′30.20″) and EMS-2 (N 27°24′33.20″, E 98°49′34.70″). The freshwater sediment samples were removed from the water with a Peterson bottom sampler (HL-CN, Wuhan Hengling Technology Company, Limited, Wuhan, China). The samples were placed into zip lock bags and stored at 4℃ until processing.

7.2.2 Fungal Isolation

Three to five g of freshwater sediment sample was sprinkled on the surface of cornmeal agar plates (CMA) with sterile toothpicks. Roughly 5000 nematodes (*Panagrellus redivivus* Goodey, free-living nematodes) were added as bait to induce the germination of carnivorous fungi (Duddington, 1955; Zhang & Hyde, 2014). The plates were incubated at 26℃ for three weeks and then observed under a stereo-microscope. A sterile needle was used to transfer a single spore of carnivorous fungi to fresh CMA plates. This step was repeated until a pure culture was attained (Ahrén et al., 1998; Zhang & Hyde, 2014).

7.2.3 Morphological Observation

The pure culture was transferred to fresh potato dextrose agar plates (PDA) using a sterile needle and incubated at 26℃ to observe the color and texture of the colony. The pure culture was transferred to the fresh observation well CMA plates (a 2 × 2 cm observation well was created by removing agar from each plate) using a sterile needle. It was incubated at 26℃ until the mycelia overspread the well. Then, approximately 1000 living nematodes (*P. redivivus*) were added to the well to induce the formation of the trapping structure. The trapping structure in the observation well and the conidiophores extending from the wall of the observation well were photographed with an Olympus BX53 microscope (Olympus Corporation, Tokyo, Japan) and Keyence VHX-6000 super deep scene 3D microscope (Keyence

Corporation, Osaka, Japan), respectively. A sterile cover glass was obliquely inserted into the fresh CMA plates. Then, strains were inoculated on the plates at 26℃. The cover glass was removed after the mycelia covered it and was then placed on the glass slide with 0.3% Melan stain to make a temporary slide (Zhang & Hyde, 2014). The morphological characteristics of conidia and conidiophores were measured and photographed by an Olympus BX53 microscope (Olympus Corporation, Tokyo, Japan).

7.2.4 DNA Extraction, PCR Amplification, and Sequencing

The strain was inoculated in PDA plates at 26 C for ten days. The mycelium was collected using a sterile scalpel. A rapid fungal genomic DNA isolation kit (Sangon Biotech, Limited, Shanghai, China) was used to extract the total genomic DNA. The primer pairs ITS4-ITS5 (White et al., 1990), 526F-1567R (O'Donnell et al., 1998), and 6F-7R (Liu et al., 1999) were used to amplify the ITS, TEF, and RPB2 regions. The PCR amplification was performed in a 50 µL reaction system (2 uL DNA template, 3 µL 25 mM MgCl2, 5 µL 10 × PCR buffer, 1 µL 10 µm. dNTPs, 2 µL each primer, 1 unit Taq Polymerase, and 34 uL ddH2O) under the following PCR conditions: pre-denaturation at 94℃ for 4 minutes; followed by 35 cycles of denaturation at 94℃ for 45 s; annealing at 52℃ (ITS), 55℃ (TEF), or 54℃ (RPB2) for 1 minute; and extension at 72℃ for 1.5–2 minutes, with a final extension at 72℃ for 10 minutes. A DiaSpin PCR Product Purification Kit (Sangon Biotech, Limited, Shanghai, China) was used to purify the PCR products. The purified PCR products of the ITS and RPB2 regions were sequenced in the forward and reverse directions using PCR primers, and the primer pair 247F-609R was used to sequence the TEF gene (BioSune Biotech, Limited, Shanghai, China). SeqMan v. 7.0 [30] was used to check, edit, and assemble the sequences. The sequences generated in this study were deposited in the GenBank database (NCBI, https://www.ncbi.nlm.nih.gov/ (accessed on 2 December 2022)).

7.2.5 Phylogenetic Analysis

The sequences generated in this study were deposited in the NCBI Genbank database (Table 7.1) and compared against the database using BLASTn (https://blast.ncbi.nlm.nih. gov/ (accessed on 1 December 2022)) to determine the attribution of the new isolates. The ITS, TEF, and RPB2 sequences of all reliable taxa of the corresponding genus and partial taxa of the related genus were downloaded (Table 7.1)

according to the BLASTn search results and relevant publications (Yang et al., 2007; Zhang & Mo, 2006; Zhang & Hyde, 2014; Zhang et al., 2022). Three genes were aligned using the online program MAFFT v.7 (http://mafft.cbrc.jp/alignment/server/ (accessed on 3 December 2022)) (Katoh et al., 2013), manually adjusted using BioEdit v7.2.3 (Hall, 1999), and then linked using MEGA6.0 (Vu et al., 2019). *Vermispora fusarina* YXJ02-13-5 was selected as an outgroup. Phylogenetic trees were inferred via maximum likelihood (ML) and Bayesian inference (BI) analyses.

Table 7.1 The GenBank accession numbers of the isolates included in this study

Taxon	Strain Number	GenBank Accession Number		
		ITS	TEF	RPB2
Arthrobotrys amerospora	CBS 268.83	NR_159625	—	—
Arthrobotrys anomala	YNWS02-5-1	AY773451	AY773393	AY773422
Arthrobotrys arthrobotryoic	CBS 119.54	MH857262	—	—
Arthrobotrys arthrobotryoic	AOAC	MF926580	—	—
Arthrobotrys blastospora	CGMCC 3.20940	OQ332405	OQ341651	OQ341649
Arthrobotrys blastospora	ZA173	OM956088	OQ341650	OQ341648
Arthrobotrys botryospora	CBS 321.83	NR_159626	—	—
Arthrobotrys cladodes	1.03514	MH179793	MH179616	MH179893
Arthrobotrys clavispora	CBS 545.63	MH858353	—	—
Arthrobotrys conoides	670	AY773455	AY773397	AY773426
Arthrobotrys cookedickinso	YMF1.00024	MF948393	MF948550	MF948474
Arthrobotrys cystosporia	CBS 439.54	MH857384	—	—
Arthrobotrys dendroides	YMF1.00010	MF948388	MF948545	MF948469
Arthrobotrys dianchiensis	1.00571	MH179720	—	MH179826
Arthrobotrys elegans	1.00027	MH179688	—	MH179797
Arthrobotrys eryuanensis	CGMCC 3.19715	MT612105	OM850307	OM850301
Arthrobotrys eudermata	SDT24	AY773465	AY773407	AY773436
Arthrobotrys flagrans	1.01471	MH179741	MH179583	MH179845
Arthrobotrys gampsospora	CBS 127.83	U51960	—	—
Arthrobotrys globospora	1.00537	MH179706	MH179562	MH179814
Arthrobotrys guizhouensis	YMF1.00014	MF948390	MF948547	MF948471
Arthrobotrys indica	YMF1.01845	KT932086	—	—
Arthrobotrys iridis	521	AY773452	AY773394	AY773423
Arthrobotrys janus	85-1	AY773459	AY773401	AY773430
Arthrobotrys javanica	105	EU977514	—	—
Arthrobotrys jindingensis	CGMCC 3.20985	OP236810	OP272511	OP272515
Arthrobotrys jinpingensis	CGMCC 3.20896	OM855569	OM850311	OM850305
Arthrobotrys koreensis	C45	JF304780	—	—
Arthrobotrys lanpingensis	CGMCC 3.20998	OM855566	OM850308	OM850302
Arthrobotrys latispora	H.B. 8952	MK493125	—	—
Arthrobotrys longiphora	1.00538	MH179707	—	MH179815
Arthrobotrys luquanensis	CGMCC 3.20894	OM855567	OM850309	OM850303

Table 7.1 (continued)

Taxon	Strain Number	GenBank Accession Number		
		ITS	TEF	RPB2
Arthrobotrys mangrovispor	MGDW17	EU573354	—	—
Arthrobotrys megalospora	TWF800	MN013995	—	—
Arthrobotrys microscaphoic	YMF1.00028	MF948395	MF948552	MF948476
Arthrobotrys multiformis	CBS 773.84	MH861834	—	—
Arthrobotrys musiformis	SQ77-1	AY773469	AY773411	AY773440
Arthrobotrys musiformis	1.03481	MH179783	MH179607	MH179883
Arthrobotrys nonseptata	YMF1.01852	FJ185261	—	—
Arthrobotrys obovata	YMF1.00011	MF948389	MF948546	MF948470
Arthrobotrys oligospora	920	AY773462	AY773404	AY773433
Arthrobotrys paucispora	ATCC 96704	EF445991	—	—
Arthrobotrys polycephala	1.01888	MH179760	MH179592	MH179862
Arthrobotrys pseudoclavata	1130	AY773446	AY773388	AY773417
Arthrobotrys psychrophila	1.01412	MH179727	MH179578	MH179832
Arthrobotrys pyriformis	YNWS02-3-1	AY773450	AY773392	AY773421
Arthrobotrys reticulata	CBS 201.50	MH856589.1	—	—
Arthrobotrys robusta	nefuA4	MZ326655	—	—
Arthrobotrys salina	SF 0459	KP036623	—	—
Arthrobotrys scaphoides	1.01442	MH179732	MH179580	MH179836
Arthrobotrys shizishanna	YMF1.00022	MF948392	MF948549	MF948473
Arthrobotrys shuifuensis	CGMCC 3.19716	MT612334	OM850306	OM850300
Arthrobotrys sinensis	105-1	AY773445	AY773387	AY773416
Arthrobotrys sphaeroides	1.01410	MH179726	MH179577	MH179831
Arthrobotrys superba	127	EU977558	—	—
Arthrobotrys thaumasia	917	AY773461	AY773403	AY773432
Arthrobotrys tongdianensis	CGMCC 3.20942	OP236809	OP272509	OP272513
Arthrobotrys vermicola	629	AY773454	AY773396	AY773425
Arthrobotrys xiangyunensis	YXY10-1	MK537299	—	—
Arthrobotrys yunnanensis	AFTOL-ID 906	DQ491512	—	—
Arthrobotrys zhaoyangensis	CGMCC 3.20944	OM855568	OM850310	OM850304
Dactylellina appendiculata	CBS 206.64	AF106531	DQ358227	DQ358229
Datylellina cionopogum	SQ27-3	AY773467	AY773409	AY773438
Dactylellina copepodii	CBS 487.90	U51964	DQ999835	DQ999816
Datylellina gephyropagum	CBS178.37	U51974	DQ999847	DQ999802
Datylellina haptotylum	SQ95-2	AY773470	AY773412	AY773441
Datylellina haptotylum	XJ03-96-1	DQ999827	DQ999849	DQ999804
Dactylellina leptosporum	SHY6-1	AY773466	AY773408	AY773437
Dactylellina mammillata	CBS229.54	AY902794	DQ999843	DQ999817
Dactylellina yushanensis	CGMCC 3.19713	MK372061	MN915113	MN915112
Drechslerella brochopaga	701	AY773456	AY773398	AY773427
Drechslerella dactyloides	expo-5	AY773463	AY773405	AY773434
Drechslerella effusa	YMF1.00583	MF948405	MF948557	MF948484
Drechslerella heterospora	YMF1.00550	MF948400	MF948554	MF948480
Drechslerella stenobrocha	YNWS02-9-1	AY773460	AY773402	AY773431
Orbilia jesu-laurae	LQ59a	MN816816	—	—
Vermispora fusarina	YXJ02-13-5	AY773447	AY773389	AY773418

The GTR + I + G, SYM + I + G, and GTR + I + G models were selected as the best-fit optimal substitution models of ITS, TEF, and RPB2, respectively, via jModelTest v 2.1.10 (Posada, 2008).

IQ-Tree v 1.6.5 (Nguyen et al., 2015) was used to implement the maximum likelihood (ML) analysis. The dataset was partitioned, and each gene was analyzed with the corresponding optimal substitution model. The statistical bootstrap support values (BS) were computed using rapid bootstrapping with 1000 replicates (Felsenstein, 1985).

A Bayesian inference (BI) analysis was conducted with MrBayes v. 3.2.6 (Huelsenbeck & Ronquist, 2001) Fasta Convert (Hall, 2007) was used to convert the multiple sequence alignment file into a MrBayes compatible NEXUS file. The dataset was partitioned, and the optimal substitution models of each gene were equivalently replaced to conform to the setting of MrBayes. Six simultaneous Markov chains were run for 10,000,000 generations, and trees were sampled every 100 generations. The first 25% of the trees were discarded, and the remaining trees were used to calculate the posterior probabilities (PP) in the majority rule consensus tree. The above parameters were edited in the MrBayes block in the NEX file. The trees were visualized with FigTree v1.3.1 (Rambaut, 2010). The backbone tree was edited using Microsoft PowerPoint (2013) and Adobe Photoshop CS6 software (Adobe Systems, San Jose, CA, USA).

7.3 Results

7.3.1 Phylogenetic Analysis

Both new fungal isolates were placed in the *Arthrobotrys* (*Orbiliaceae*, *Orbiliomycetes*) genus according to their type of trapping structure (Ahrén et al., 1998; Yang et al., 2007; Zhang & Hyde, 2014) and the BLASTn search results of ITS, TEF, and RPB2 genes. Therefore, all *Arthrobotrys* species with valid sequence data (62 isolates representing 59 species) (Zhang et al., 2022) and other related taxa in *Orbiliomycetes* (nine isolates representing eight *Dactylellina* species and five isolates representing five *Drechslerella* species) were included in this phylogenetic analysis (Table 7.1). The final dataset contained 77 ITS, 51 TEF, and 54 RPB2 sequences. The

combined DNA dataset comprised 1909 characters (570 for ITS, 531 for TEF, and 708 for RPB2), among which 858 bp are constant, 982 bp are variable, and 770 bp are parsimony informative. After maximum likelihood (ML) analysis, the best-scoring likelihood tree was obtained with a final ML optimization likelihood value of -6867.586931. The Bayesian analysis (BI) evaluated the Bayesian posterior probabilities with a final average standard deviation of the split frequency of 0.009098. The trees generated by maximum likelihood (ML) and Bayesian analysis (BI) showed similar topologies, so the best-scoring ML tree was selected for presentation (Figure 7.1).

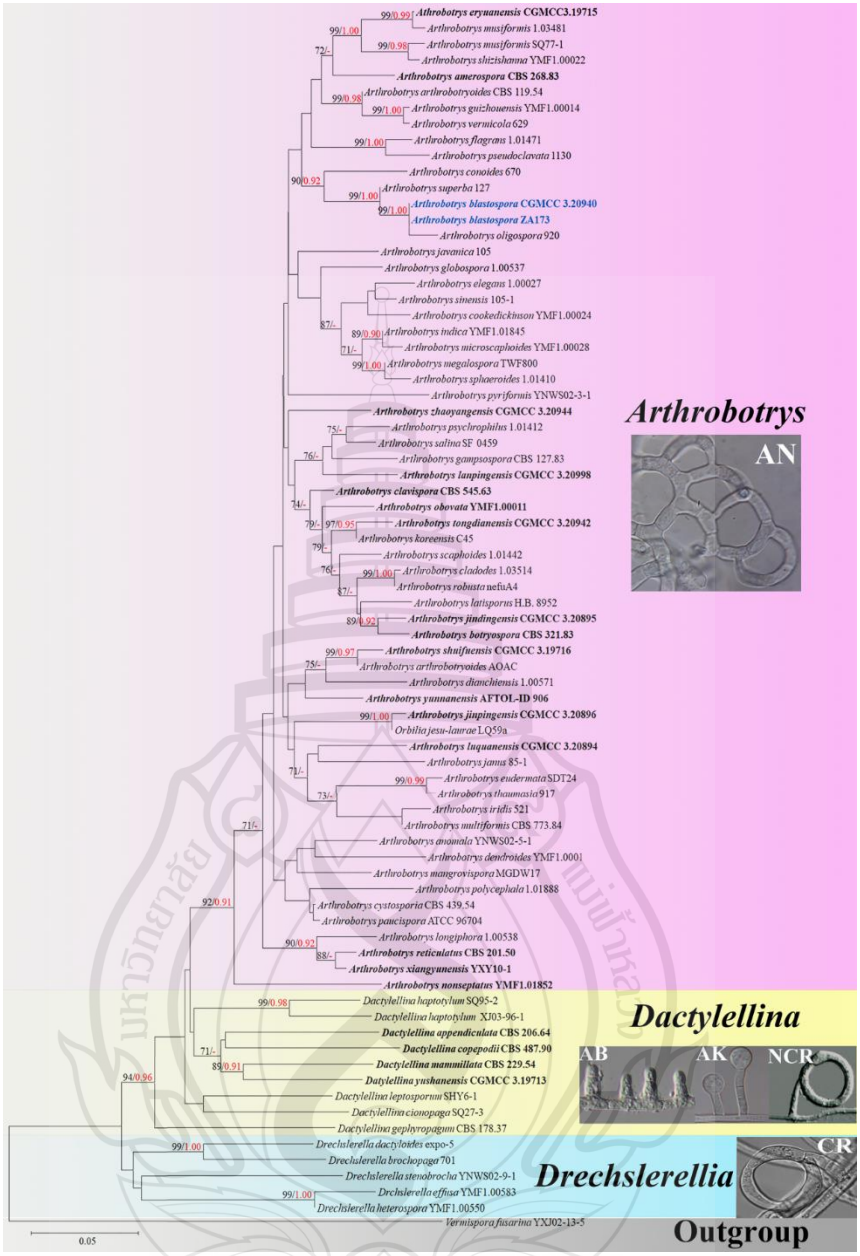

Figure 7.1 Maximum likelihood tree based on combined ITS, TEF, and RPB2 sequence data from 72 *Orbiliaceae* (*Orbiliomycetes*) carnivorous species. Bootstrap support values for maximum likelihoods (black) equal to or greater than 70% and Bayesian posterior probability values (red) equal to or greater than 0.90 are indicated above the nodes. The new isolates are in blue and the type strains are in bold. The genus name and trapping structure corresponding to each clade are indicated on the right. AN, adhesive networks; AB, adhesive branches; AK, adhesive knobs; NCR, non-constricting rings; CR, constricting rings

The phylogenetic analysis showed that the tested 72 *Orbiliaceae* (*Orbiliomycetes*) carnivorous species were clustered into three clades according to their types of trapping structure. All species catch nematodes with adhesive networks clustered together stably. Both new fungal isolates were placed in *Arthrobotrys* and formed a basal lineage with *A. oligospora* and *A. superba* with 99% MLBS and 1.00 BYPP (Figure 7.1).

7.3.2 Taxonomy

Arthrobotrys blastospora F. Zhang and X.Y. Yang sp. nov. (Figures 7.2, 7.3a, 7.4b, 7.5a).

Index Fungorum number: IF900162; Facesoffungi number: FoF 14034

Etymology: The species name "blastospora" refers to the most prominent feature of this species, i.e., the production of blastospores.

Materials examined: CHINA, Yunnan Province, Nujiang City, Nujiang River, N 27°43′14.60″, E 98°41′30.20″, from freshwater sediment, 18 May 2014, F. Zhang. Holotype CGMC 3.20940, preserved in the China General Microbiological Culture Collection Center. Ex-type culture DLUCC 27-1, preserved in the Dali University Culture Collection.

Colonies white, cottony, and rapidly growing on the PDA medium, reaching 50 mm diameter after 7 days at 26°C. *Mycelia* 2.5–6 µm. wide, hyaline, septate, branched, and smooth. *Conidiophores* 110–625 µm. ($\bar{x}$ = 341.5 µm., n = 100) long, 4–6.5 µm. ($\bar{x}$ = 5 µm., n = 100) wide at the base, gradually tapering upwards to a width of 3–6 µm. ($\bar{x}$ = 4 µm., n = 100) at the apex, hyaline, erect, septate, unbranched, produced by hyphae or directly by spore germination. This species produces hyaline, yeast-like *blastospores*, which usually cluster on the tuberculous bulges on the upper half of the conidiophores. A conidium is produced on the conidiophore first; then, a second conidium is formed from the right apex, or occasionally the side apex, of the first conidium, thus continuously producing a chain of blastospores. There is a septum between the two conidia, which tend to separate from each other after maturation. *The exfoliated blastospores* 13.5 − 62.5 × 7.5 − 16 ($\bar{x}$ = 25.6 × 10.5 µm., n = 300) µm., globose, and elliptic to long elliptic, with zero or one septum. *Chlamydospores* not observed. Capturing nematodes with the adhesive networks in the early stages of its formation usually consists of a single adhesive hypha ring (Figure 7.2) (Zhang & Hyde, 2014).

Additional specimens examined: CHINA, Yunnan Province, Nujiang City, Nujiang River, N 27°43′14.60″, E 98°41′30.20″, from freshwater sediment, 20 May 2014, F. Zhang. Living culture ZA173.

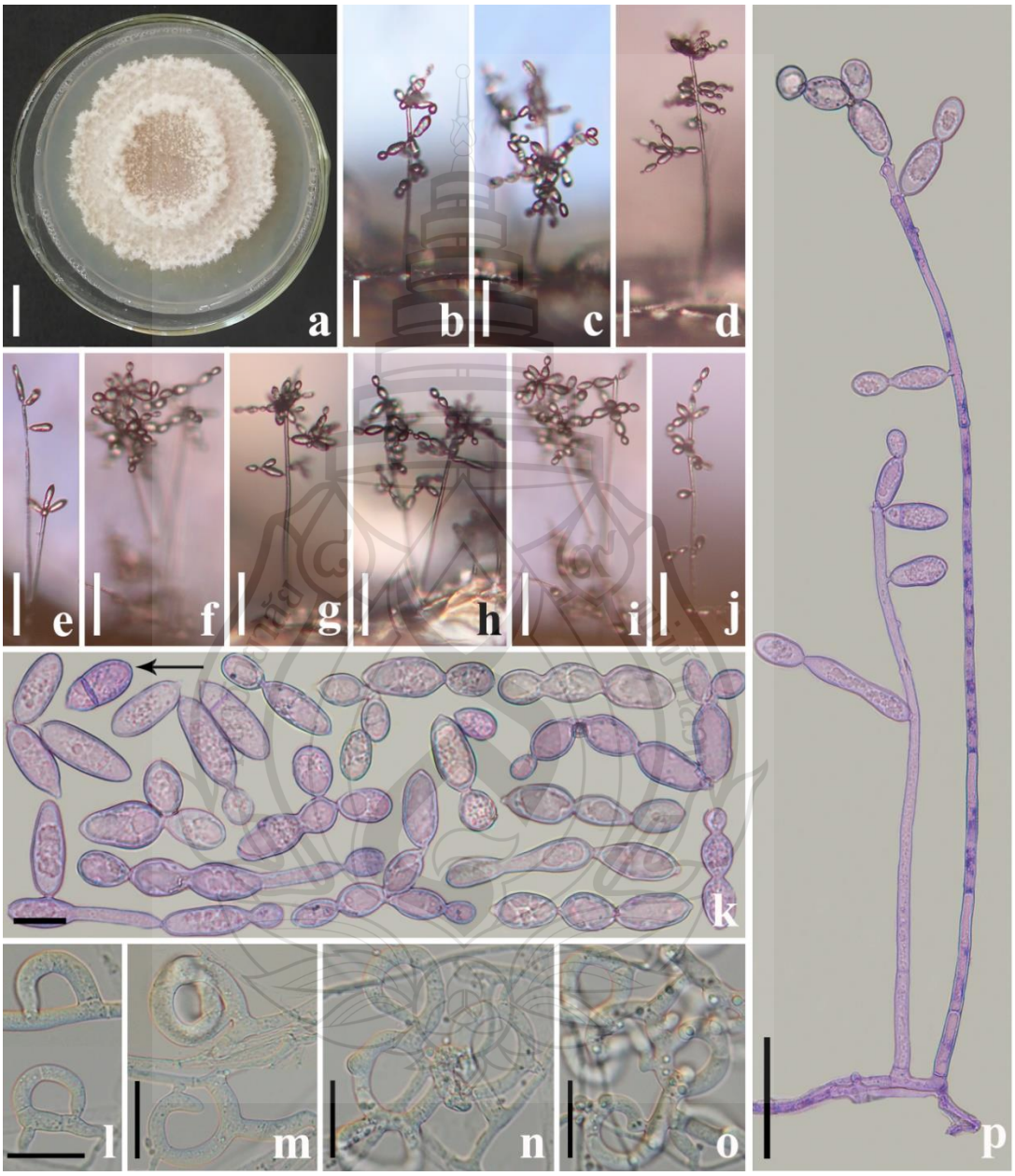

Figure 7.2 *Arthrobotrys blastospora* (CGMCC 3.20940). (a) Colony. (b–j) Conidiophores and blastospores. (k) Blastospores. (l–**o**) Trapping structure: adhesive networks. (p) Conidiophores. Scale bars: (a) = 1 cm., (b–j) = 10 µm., (k–o) = 20 µm., (p) = 100 µm.

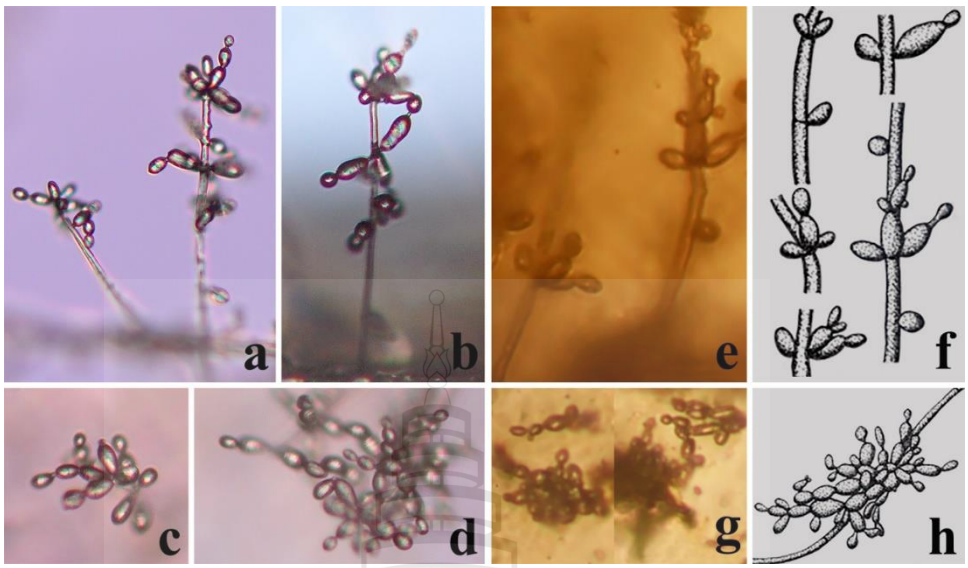

Fgure 7.3 Blastospores and conidiophores of fossil and extant carnivorous fungi. (a, b) Conidiophores of *Arthrobotrys blastospora*. (c, d) Blastospores of *Arthrobotrys blastospora.* (e, f) Conidiophores of the fossil *Palaeoanellus dimorphus.* (g, h) Blastospores of the fossil *Palaeoanellus dimorphus,* reprinted with permission from Ref. (Schmidt et al., 2008). 2023, John Wiley and Sons

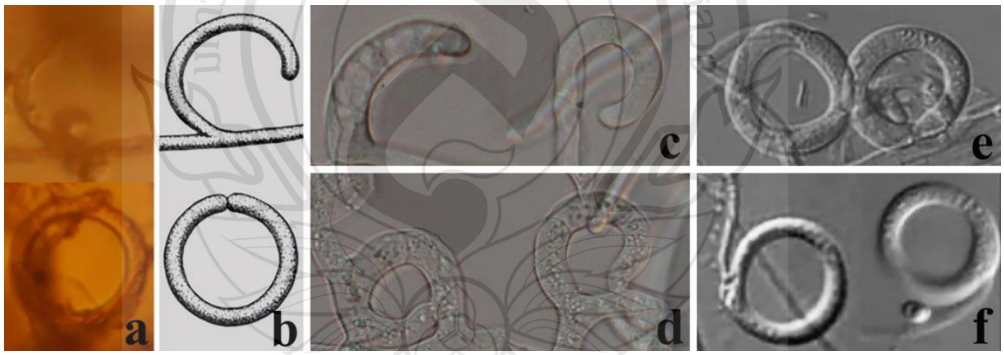

Figure 7.4 Trapping structure of fossil and extant carnivorous fungi. (a, b) Trapping structure of *Palaeoanellus dimorphus*: unicellular adhesive hyphal rings, reprinted with permission from Ref. (Schmidt et al., 2008). 2023, John Wiley and Sons. (c, d) The early stages of adhesive networks produced by *Arthrobotrys blastospora*: single adhesive hyphae rings. (e, f) Trapping structure of some *Dactylellina* species: nonconstricting rings (Zhang & Hyde, 2014)

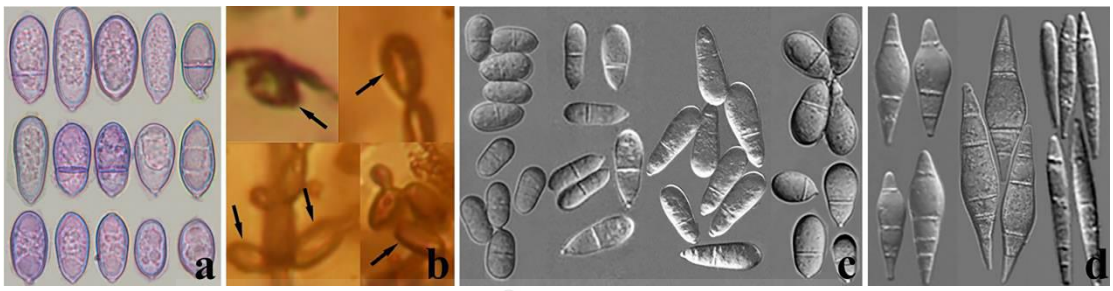

Figure 7.5 Conidia of several carnivorous fungi. (a) The single conidia formed by the separation of the blastospore of *Arthrobotrys blastospora*. (b) The single conidia produced by *Palaeoanellus dimorphus*, reprinted with permission from Ref. (Schmidt et al., 2008). 2023, John Wiley and Sons. (c) The conidia produced by some *Arthrobotrys* species (Zhang & Mo, 2006). (d) The conidia produced by most of the *Dactylellina* species (Zhang & Mo, 2006)

7.4 Discussion

7.4.1 New Species of *Arthrobotrys*

Arthrobotrys blastospora catches nematodes with adhesive networks, which is consistent with the main characteristics of *Arthrobotrys*, *Orbiliaceae* (the largest genus of modern carnivorous fungi (Ahrén et al., 1998; Yang et al., 2007; Swe et al., 2011; Zhang & Hyde, 2014). Our phylogenetic analysis based on ITS, TEF, and RPB2 substantiated that *A. blastospora* is a member of *Arthrobotrys*. Phylogenetically, *A. blastospora* forms the sister lineage to *A. oligospora* (Figure 7.1). However, the conidia of all modern carnivorous fungi in *Orbiliomycetes* are individually born in clusters or singly on the conidiophores, which is significantly different from the catenulate blastospores produced by *A. blastospora* (Zhang & Mo, 2006; Zhang & Hyde, 2014). Therefore, we identified *A. blastospora* as a new species of *Arthrobotrys*.

7.4.2 *Palaeoanellus Dimorphus* Is an Ancient Ancestor of Modern *Orbiliomycetes* Carnivorous Fungi

Similar to carnivorous plants, as a highly specialized group in the fungal kingdom, carnivorous fungi are a model for the study of adaptive fungal evolution; their

evolution is also a critical node in the study of fungal evolution. Such studies rely heavily on the discovery of fossil fungi. Schmidt et al. (Schmidt et al., 2007, 2008) found the earliest and best-preserved fossil of carnivorous fungi (*P. dimorphus*) in approximately 100-million-year-old amber from Southwestern France. *Palaeoanellus dimorphus* produced blastospores which were generated in whorls on small projections of conidiophores and also produced unicellular adhesive hyphal rings to trap nematodes (Figures 7.3, 7.4) (Schmidt et al., 2007, 2008). However, no structure directly connecting the blastospores to unicellular adhesive hyphal rings was illustrated by Schmidt et al. (Schmidt et al., 2007, 2008). Therefore, whether the blastospores and unicellular adhesive hyphal rings in this fossil actually represent a single fossil species has been a controversial topic due to their unusual combination (Thorn et al., 2008; Schmidt et al., 2009). In addition, the fossil was not considered an ancestor of modern carnivorous fungi but as belonging to an extinct lineage because no blastospore-producing carnivorous fungi were found in modern ecosystems (Schmidt et al., 2007, 2008; Swe et al., 2011; Zhang & Hyde, 2014). *Arthrobotrys blastospora* reported in this study produced yeast-like blastospores on the small projections of conidiophores and captured nematodes with adhesive networks (a single adhesive hypha ring structure at the initial stage of its formation) (Figure 7.2) (Zhang & Mo, 2006). The discovery of this species confirms the existence of an extant species in nature that produces both specialized nematode-trapping structures and blastospores. Furthermore, *A. blastospora* and *P. dimorphus* share strong similarities with regard to the morphological characteristics of conidia, conidiophores, and the manner of catching nematodes with adhesive materials (Figures 7.3, 7.4). Accordingly, we infer that *A. blastospora* is closely related to *P. dimorphus* and maintained traits of Mesozoic carnivorous fungi, and *P. dimorphus* may be an ancient ancestor of modern *Orbiliomycetes* carnivorous fungi.

Similar to other fungi, convergent evolution has also been observed in carnivorous fungi; for example, some species of *Dactylellina* (*Orbiliaceae, Orbiliomycetes, Ascomycota*) and some species of *Nematoctonus* (*Agaricomycetes, Pleurotaceae, Basidiomycota*) trap nematodes with stalked adhesive knobs (Nordbring-Hertz et al., 2006). Therefore, we also cannot rule out the possibility of convergent evolution between *A. blastospora* and *P. dimorphus*, which resulted in the sharing of

similar characteristics, while having a distant genetic relationship. However, given the scarcity of carnivorous fungi in the fungal kingdom (Yang et al., 2012; Zhang & Hyde, 2014) and the high similarity of several different structures (conidia, conidiophores, and trapping structures) between *A. blastospora* and *P. dimorphus* (Figures 7.3, 7.4) (Schmidt et al., 2007, 2008), we speculate that it is less likely that two species would have evolved such similar traits with only a distant genetic relationship.

7.4.3 The Possible Ancestral Position of *Palaeoanellus Dimorphus*

Among *Orbiliomycetes* carnivorous fungi, all species are divided into two main groups according to their mechanisms of trapping nematodes. One is the genus *Drechslerella*, which first diverged from other carnivorous species and produces constricting rings to capture nematodes with the mechanical force generated by the expansion of the cells that make up the rings. Another contains all species in the genera *Arthrobotrys* and *Dactylellina*, which catch nematodes with adhesive traps (Figure 7.1) (Ahrén et al., 1998; Yang et al., 2007; Zhang & Hyde, 2014). *Palaeoanallus dimorphus* produced unicellular hyphal rings, which possibly produced a sticky secretion used to capture nematodes (Schmidt et al., 2007, 2008). This structure is similar to those species in *Arthrobotrys* and *Dactylellina* in the manner of trapping nematodes (capture of nematodes performed mainly with adhesive material), but it is quite different from the *Drechslerella* species, which capture nematodes by mechanical force. Therefore, we speculate that *P. dimorphus* is more related to *Arthrobotrys* and *Dactylellina*, and that *P. dimorphus* may be the common ancestor of *Arthrobotrys*, *Dactylellina*, or *Arthrobotrys* and *Dactylellina*.

Generally accepted, modern *Orbiliomycetes* carnivorous fungi originated from saprophytic fungi without a trapping structure (Rubner, 1996; Liou & Tzean, 1997; Ahrén et al., 1998; Scholler et al., 1999; Li et al., 2000; Li et al., 2005; Yang et al., 2012). Their evolution from possessing no trapping structure to complex trapping structures, such as modern adhesive trapping structures, was undeniably a course of gradual complexity. The structural complexity of unicellular adhesive hyphal rings produced by *P. dimorphus* is lower than that of most modern adhesive trapping structures. Therefore, unicellular adhesive hyphal rings may be considered an intermediate stage in the evolution of structural complexity and the common ancestor

of all adhesive trapping structures (*Arthrobotrys* and *Dactylellina*). However, based on phylogenetic analysis of multiple genes and molecular clock theory, Yang et al. (2012) inferred that the adhesive trapping structures of modern *Orbiliomycetes* carnivorous fungi originated about 246 million years ago and further evolved around 198–208 million years ago. In contrast, *P. dimorphus* was found in the amber from 100 million years ago (Schmidt et al., 2007, 2008). Therefore, it can be inferred that the unicellular adhesive hyphal rings produced by *P. dimorphus* are probably not the ancestor of all the modern adhesive-trapping structures (*Arthrobotrys* and *Dactylellina*).

Phylogenetically, *A. blastospora* forms a sister lineage to *A. oligospora* and *A. superba* (Figure 7.1). Combined with the morphological similarities between *A. blastospora* and *P. dimorphus*, we can infer that *P. dimorphus* is closely related to the *Arthrobotrys* species. Concerning morphology, the following aspects can also support the close relationship between *P. dimorphus* and *Arthrobotrys*: (1) *P. dimorphus* produced unicellular adhesive hypha rings to capture nematodes (Schmidt et al., 2007, 2008). This structure is morphologically similar to the single ring stage of adhesive networks produced by *Arthrobotry* species (Figure 7.4) (Zhang & Mo, 2006). (2) The formation of the unicellular adhesive hypha rings produced by *P. dimorphus* initiated with a branch which was first generated on the vegetative mycelia, then the branch was curved and fused with the mycelia to form a ring (Schmidt et al., 2007, 2008). This process is highly similar to the formation process of adhesive networks produced by *Arthrobotrys* species (Zhang & Mo, 2006) (Figure 7.4). (3) The blastospores produced by *A. blastospora* are easily separated from each other to form non-septate and 1-septate elliptic conidia. The blastospores produced by *P. dimorphus* also had this characteristic. The non-septate or 1-septate conidia formed by the separation of blastospores are morphologically similar to those of many species in *Arthrobotrys* (Figure 7.5) (Zhang & Mo, 2006; Zhang & Hyde, 2014). (4) Among *Arthrobotrys* species, except *A. blastospora*, a few conidia of *A. oligospora* and *A. conoides* also have a similar morphology to blastospores (Figure 7.6), which suggests that the formation of blastospores may be an ancestral characteristic of *Arthrobotrys*, or an inherent feature of other *Arthrobotrys* species, but it is rarely developed or not developed in culture and thus, it has been overlooked so far. This phenomenon further illustrated the close relationship between *P. dimorphus* and *Arthrobotrys*.

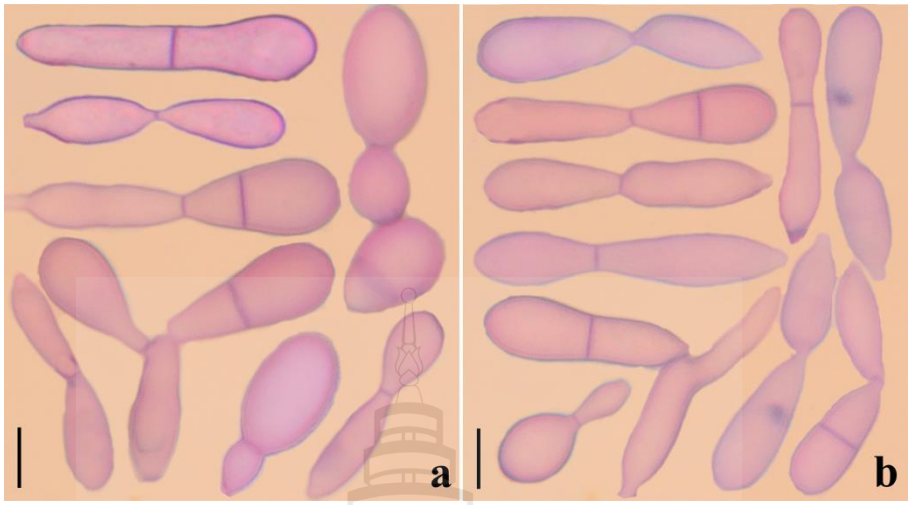

Figure 7.6 Blastospores of some *Arthrobotrys* species. (a) The blastospores produced by *A. oligospora*. (b) The blastospores produced by *A. conoides*. Scale bars = 10 μm.

By contrast, *Dactylellina* demonstrates similarities to *P. dimorphus* only in the aspect of trapping structure: a few species in *Dactylellina* produce a single ring covered with adhesive material (non-constricting ring) to capture nematodes, which is formed by producing a branch from the vegetative mycelia, and then the branch is curved and fused to form a ring (Zhang & Mo, 2006). This structure is similar to the unicellular adhesive hyphal rings produced by *P. dimorphus* in the morphology and formation process (Figure 7.4).

In summary, considering that *P. dimorphus* and *Arthrobotrys*share a reproductive structure (conidia) and nutritional structure (trapping structure) morphology, we speculate that *P. dimorphus* is more likely to be the ancestor of *Arthrobotrys*

7.4.4 The Necessity of Strengthening the Research on Carnivorous Fungi in the Three Parallel Rivers

The two *A. blastospora* strains were isolated from the core area of the three parallel rivers region in China. This region is located in the southwest of the Heng Duan Mountains where mountains alternate with valleys, the terrain is highly diverse, and the region combines tropical, subtropical, temperate, and alpine cold climate types (Li et

al., 2001; Feng et al., 2016). The complex terrain and climate create rich ecosystems and make the region one of the most diverse in the world (Lin et al., 2018; Basnet et al., 2019). Glaciers did not cover this region during the Quaternary glaciation due to its unique mountain and deep valley landform, particularly its geographical position, formation and evolutionary process. Therefore, this region is a significant refuge for many ancient species, and it is the center of species distribution and the differentiation of many biological groups (Sun, 2002; Su & Li, 2003; Wang et al., 2005; Li, Zhang et al., 2009). According to statistics, 34 species of Chinese national protected plants, 600 species of endemic plants, and 20 species of relict plants are distributed in this region (Fu, 1987; Zhou, 2010). This situation renders it possible to find the relict species of carnivorous fungi in this region and suggests that there may be precious living fossils of other groups living in this region. In addition, *P. dimorphus* was found in the amber from Southwestern France (Schmidt et al., 2007, 2008) and *A. blastospora* was isolated from Southwestern China, more than 11,000 km from each other. This indicates that Palaeoanellus-type fungi were widely distributed and numerous in the past, giving rise to the extant genera of *Oribiliomycetes.*

CHAPTER 8

MORPHOLOGICAL AND PHYLOGENETIC CHARACTERIZATION OF FIVE NOVEL NEMATODE-TRAPPING FUNGI (*ORBILIOMYCETES*) FROM YUNNAN, CHINA

8.1 Introduction

Nematode-trapping fungi (NTF) are a group of fungi that can produce unique structures (trapping structures) to capture nematodes (Zhang & Mo, 2006; Swe et al., 2011; Zhang & Hyde, 2014). They have attracted much attention for over 180 years since Corda (1839) reported the first species (*Arthrobotrys superba* Corda) because of their unique survival strategy, excellent application potential in nematode control, and significance of maintaining the balance of nematode populations in the ecosystem (Drechsler, 1933; Wang et al., 2014; Yang et al., 2023). *Orbiliomycetes* NTF is the research focus of NTF due to their abundant species, diversified trapping structures, and mature research methods (Li et al., 2000; Yang et al., 2012; Zhang & Hyde, 2014). Currently, 119 *Orbiliomycetes* NTF species have been reported and divided into *Arthrobotrys*, *Dactylellina*, and *Drechslerella* based on their trapping structures according to modern molecular biology research (Pfister, 1997; Ahrén et al., 1998; Scholler et al., 1999; Yang et al., 2007).

Arthrobotrys, the most widespread and diverse (67 species) genus among *Orbiliomycetes* NTF, was established by Corda (1839) with A. *superba* Corda, which is characterized by 1-septate conidia growing in clusters on the nodes of the conidiophores. With the improvement in the isolation method, more species were discovered, and the characteristic of *Arthrobotrys* was revised as producing obovoid, elliptic, pyriform.

0–3-septate conidia on the nodes or short denticles of the conidiophores (Cooke & Dickinson, 1965; Schenck et al., 1977; Zhang & Mo, 2006; Chen et al., 2007).

However, the taxonomy system based on these characteristics still needs to be clarified due to confusion caused by scholars attaching different importance to morphological features. The development of molecular biology has brought a significant breakthrough in the taxonomic study of NTF. Methods such as restriction fragment length polymorphism (RFLP), random amplified polymorphic DNA (RAPD), and molecular phylogenetics have gradually clarified the importance of the trapping structure in NTF classification (Pfister, 1997; Ahrén et al., 1998; Scholler et al., 1999; Yang et al., 2007). Accordingly, the main characteristic of *Arthrobotrys* has also been revised again to produce adhesive networks to capture nematodes (Zhang & Hyde, 2014). Species in *Arthrobotrys* are essential materials for developing bio-control agents for plant and animal parasitic nematodes because of their excellent competition, adaptation, and reproductive ability (Soliman et al., 2021; Júnior et al., 2021).

Drechslerella is the smallest genus (17 species) among *Orbiliomycetes* NTF, which separated from *Monacrosporium* by *Subrammanian* with Dr. acrochaeta (Drechsler) *Subram* as the type species based on conidia producing filamentous appendages at the apex (Subramanian, 1963). However, Liu and Zhang (1994) pointed out that the filamentous appendage is not a stable and valid feature because it is formed by conidia germination, which is common in many *Arthrobotrys* and *Dactylellina* species (Liu & Zhang, 1996). Accordingly, *Drechslerella* is considered to be an invalid genus. Subsequently, the taxonomy of NTF was studied based on molecular phylogenetic analysis. All species produce constricting rings clustered into a monophyletic clade named *Drechslerella*, characterized by producing constricting rings composed of three cells and locking nematodes via the rapid expansion of the three cells (Pfister, 1997; Ahrén et al., 1998; Scholler et al., 1999; Yang et al., 2007; Zhang & Hyde, 2014). This method of capturing nematodes mainly via mechanical force significantly differs from species in *Arthrobotrys* and *Dactylellina* (mainly capturing nematodes with adhesive material) (Zhang & Mo, 2006; Zhang & Hyde, 2014). Therefore, *Drechslerella* is a unique genus among *Orbiliomycetes* NTF and a key group in the origin and evolution study of carnivorous fungi.

NTF is a crucial node in fungal evolution and a good material for studying fungal adaptive evolution. The discovery of new species contributes to the development of related research and provides more materials for developing bio-control agents of

parasitic nematodes. This research aims to report five new NTF species and list a key species of *Drechslerella* that has been studied less.

8.2 Material and Methods

8.2.1 Sample Collection

Terrestrial soil and freshwater sediment samples involved in this study were collected from Yunnan Province, China. The detailed collection methods are the same as Zhang et al. (2022).

8.2.2 Fungal Isolation

The soil sprinkling technique and baited plates method (Drechsler, 1941; Duddington, 1955; Eren & Pramer, 1965; Zhang & Hyde, 2014) were used to incubate nematode-trapping fungi (NTF) in the soil samples. The single-spore isolation method was used to obtain the pure culture of NTF. The details of the above three methods are the same as Zhang et al. (2022).

8.2.3 Morphological Observation

The observation well and nematode baiting methods (Gao et al., 1996) were used to induce the trapping structure of NTF in accordance with Zhang et al. (2022). All micromorphological features, such as conidia, conidiophore, trapping structure, and chlamydospores, were photographed and measured with an Olympus BX53 differential interference microscope (Olympus Corporation, Tokyo, Japan).

8.2.4 DNA Extraction, PCR Amplification, and Sequencing

The total genomic DNA of isolates was extracted from the mycelia grown on potato dextrose agar (PDA) plates using a rapid fungal genomic DNA isolation kit (Sangon Biotech Company, Limited, Shanghai, China). The ITS, TEF, and RPB2 regions were amplified with the primer pairs ITS4-ITS5 (White et al., 1990), 526F-1567R (O'Donnell et al., 1998), and 6F-7R (Liu et al., 1999), respectively. The PCR amplification was performed according to Zhang et al. (2022). A DiaSpin PCR Product Purification Kit (Sangon Biotech Company, Limited, Shanghai, China) was used to purify the PCR products according to the user manual. The purified PCR products of

the ITS and RPB2 regions were sequenced in the forward and reverse directions using PCR primers, and TEF genes were sequenced using the primer pair 247F-609R (Ahrén et al., 1998) (BioSune Biotech Company, Limited, Shanghai, China).

Sequences were checked, edited, and assembled via SeqMan v. 7.0 (Swindell & Plastere, 1997). The sequences generated in this study were deposited in the GenBank database at the National Center for Biotechnology Information (NCBI; https://www.ncbi.nlm.nih.gov/; accessed on 20 March 2023).

8.2.5 Phylogenetic Analysis

BLASTn search (BLASTn; https://blast.ncbi.nlm.nih.gov/; accessed on 11 March 2023) was used to compare the sequences generated in this study against the NCBI GenBank database. The BLASTn search results and the morphological features (trapping structure) of these five species indicated that they belong to the genus Arthrobotrys and Drechslerella. Therefore, all Arthrobotrys and Drechslerella taxa were searched in Species Fungorum (http://www.speciesfungorum.org; accessed on 12 March 2023) and checked individually according to the relevant documents to ensure that all Arthrobotrys and Drechslerella taxa were considered in this study (Ahrén et al., 1998; Li et al., 2000; Zhang & Mo, 2006; Swe et al., 2011; Yang et al., 2012; Li et al., 2013; Zhang & Hyde, 2014; Zhang et al., 2020, 2022ab; Yang et al., 2023). All reliable ITS, TEF, and RPB2 sequences of Arthrobotrys and Drechslerella taxa were downloaded from the GenBank database (Table 8.1). Online program MAFFT v.7 (http://mafft.cbrc.jp/alignment/server/; accessed on 15 March 2023) (Katoh & Standley, 2013) was used to generate the alignments of three genes, BioEdit v 7.2.3 (Hall, 1999) was used to manually adjust the three alignments, and the three alignments were then linked with MEGA 6.0 (Tamura et al., 2013). Vermispora fusarina YXJ 02-13-5 and Vermispora leguminaceae AS 6.0291 were set as outgroups. Phylogenetic trees were inferred via maximum likelihood (ML) and Bayesian inference (BI) analyses.

Table 8.1 GenBank accession numbers involved in this study

Taxon	Strain Number	GenBank accession Number		
		ITS	TEF	RPB2
Arthrobotrys amerospora	CBS 268.83	NR_159625	—	—
Arthrobotrys anomala	YNWS02-5-1	AY773451	AY773393	AY773422
Arthrobotrys arthrobotryoides	CBS 119.54	MH857262	—	—
Arthrobotrys arthrobotryoides	AOAC	MF926580	—	—
Arthrobotrys botryospora	CBS 321.83	NR_159626	—	—
Arthrobotrys cladodes	1.03514	MH179793	MH179616	MH179893
Arthrobotrys clavispora	CBS 545.63	MH858353	—	—
Arthrobotrys conoides	670	AY773455	AY773397	AY773426
Arthrobotrys cookedickinson	YMF 1.00024	MF948393	MF948550	MF948474
Arthrobotrys cystosporia	CBS 439.54	MH857384	—	—
Arthrobotrys dendroides	YMF 1.00010	MF948388	MF948545	MF948469
Arthrobotrys dianchiensis	1.00571	MH179720	—	MH179826
Arthrobotrys elegans	1.00027	MH179688	—	MH179797
Arthrobotrys eryuanensis	CGMCC 3.19715	MT612105	OM850307	OM850301
Arthrobotrys eudermata	SDT24	AY773465	AY773407	AY773436
Arthrobotrys flagrans	1.01471	MH179741	MH179583	MH179845
Arthrobotrys gampsospora	CBS 127.83	U51960	—	—
Arthrobotrys globospora	1.00537	MH179706	MH179562	MH179814
Arthrobotrys gongshanensis	CGMCC 3.23753	OM801277	OM809162	OM809163
Arthrobotrys guizhouensis	YMF 1.00014	MF948390	MF948547	MF948471
Arthrobotrys hengjiangensis	CGMCC 3.24983	OQ946587	OQ989312	OQ989302
Arthrobotrys hengjiangensis	XA190	OQ946586	OQ989311	OQ989301
Arthrobotrys indica	YMF 1.01845	KT932086	—	—
Arthrobotrys iridis	521	AY773452	AY773394	AY773423
Arthrobotrys janus	85-1	AY773459	AY773401	AY773430
Arthrobotrys javanica	105	EU977514	—	—
Arthrobotrys jindingensis	CGMCC 3.20895	OP236810	OP272511	OP272515
Arthrobotrys jinpingensis	CGMCC 3.20896	OM855569	OM850311	OM850305
Arthrobotrys koreensis	C45	JF304780	—	—
Arthrobotrys lanpingensis	CGMCC 3.20998	OM855566	OM850308	OM850302
Arthrobotrys latispora	H.B. 8952	MK493125	—	—
Arthrobotrys longiphora	1.00538	MH179707	—	MH179815
Arthrobotrys lunzhangensis	CGMCC 3.20941	OK643973	OM621809	OM621810
Arthrobotrys luquanensis	CGMCC 3.20894	OM855567	OM850309	OM850303
Arthrobotrys mangrovispora	MGDW17	EU573354	—	—
Arthrobotrys megalospora	TWF800	MN013995	—	—
Arthrobotrys microscaphoides	YMF 1.00028	MF948395	MF948552	MF948476

Table 8.1 (continued)

Taxon	Strain Number	GenBank accession Number		
		ITS	TEF	RPB2
Arthrobotrys multiformis	CBS 773.84	MH861834	—	—
Arthrobotrys musiformis	SQ77-1	AY773469	AY773411	AY773440
Arthrobotrys musiformis	1.03481	MH179783	MH179607	MH179883
Arthrobotrys nonseptata	YMF 1.01852	FJ185261	—	—
Arthrobotrys obovata	YMF 1.00011	MF948389	MF948546	MF948470
Arthrobotrys oligospora	920	AY773462	AY773404	AY773433
Arthrobotrys paucispora	ATCC 96704	EF445991	—	—
Arthrobotrys polycephala	1.01888	MH179760	MH179592	MH179862
Arthrobotrys pseudoclavata	1130	AY773446	AY773388	AY773417
Arthrobotrys psychrophila	1.01412	MH179727	MH179578	MH179832
Arthrobotrys pyriformis	YNWS02-3-1	AY773450	AY773392	AY773421
Arthrobotrys reticulata	CBS 550.63	MH858355	—	—
Arthrobotrys robusta	nefuA4	MZ326655	—	—
Arthrobotrys salina	SF 0459	KP036623	—	—
Arthrobotrys scaphoides	1.01442	MH179732	MH179580	MH179836
Arthrobotrys shizishanna	YMF 1.00022	MF948392	MF948549	MF948473
Arthrobotrys shuifuensis	CGMCC 3.19716	MT612334	OM850306	OM850300
Arthrobotrys sinensis	105-1	AY773445	AY773387	AY773416
Arthrobotrys sphaeroides	1.01410	MH179726	MH179577	MH179831
Arthrobotrys superba	127	EU977558	—	—
Arthrobotrys thaumasia	917	AY773461	AY773403	AY773432
Arthrobotrys tongdianensis	CGMCC 3.20942	OP236809	OP272509	OP272513
Arthrobotrys vermicola	629	AY773454	AY773396	AY773425
Arthrobotrys weixiensis	CGMCC 3.24984	OQ946585	OQ989310	OQ989300
Arthrobotrys weixiensis	FA675	OQ946584	OQ989309	OQ989299
Arthrobotrys xiangyunensis	YXY10-1	MK537299	—	—
Arthrobotrys yunnanensis	YMF 1.00593	AY50993	—	—
Arthrobotrys zhaoyangensis	CGMCC 3.20944	OM855568	OM850310	OM850304
Dactylellina cangshanensis	CGMCC 3.19714	MK372062	MN915115	MN915114
Dactylellina copepodii	CBS 487.90	U51964	DQ999835	DQ999816
Dactylellina mammillata	CBS 229.54	AY902794	DQ999843	DQ999817
Dactylellina yushanensis	CGMCC 3.19713	MK372061	MN915113	MN915112
Drechslerela dactyloides	expo-5	AY773463	AY773405	AY773434
Drechslerella anchonia	CBS 109.37	AY965753	—	—
Drechslerella aphrobrocha	YMF 1.00119	MF948397	—	MF948477
Drechslerella bembicodes	1.01429	MH179731	—	MH179835

Table 8.1 (continued)

Taxon	Strain Number	GenBank accession Number		
		ITS	TEF	RPB2
Drechslerella brochopaga	CBS 218.61	U51950	—	—
Drechslerella brochopaga	BCRC 34361	FJ380936	—	—
Drechslerella coelobrocha	FWY03-25-1	AY773464	AY773406	AY773435
Drechslerella dactyloides	1.00031	MH179690	MH179554	MH179799
Drechslerella daliensis	CGMCC 3.20131	MT592896	OK556701	OK638157
Drechslerella doedycoides	YMF 1.00553	MF948401	—	MF948481
Drechslerella doedycoides	CBS 175.55	MH857432	—	—
Drechslerella effusa	YMF 1.00583	MF948405	MF948557	MF948484
Drechslerella effusa	CBS 774.84	MH861835	—	—
Drechslerella hainanensis	YMF 1.03993	KC952010	—	—
Drechslerella heterospora	YMF 1.00550	MF948400	MF948554	MF948480
Drechslerella pengdangensis	CGMCC 3.24985	OQ946589	OQ989314	OQ989304
Drechslerella pengdangensis	DL53	OQ946588	OQ989313	OQ989303
Drechslerella polybrocha	CCRC 32872	U51973	—	—
Drechslerella polybrocha	DHP 133	U72606	—	—
Drechslerella polybrocha	H.B. 8317	KT222361	—	—
Drechslerella stenobrocha	YNWS02-9-1	AY773460	AY773402	AY773431
Drechslerella tianchiensis	CGMCC 3.24986	OQ946591	OQ989316	OQ989306
Drechslerella tianchiensis	XJ353	OQ946590	OQ989315	OQ989305
Drechslerella xiaguanensis	CGMCC 3.20132	MT592900	OK556699	OK638159
Drechslerella yunlongensis	CGMCC 3.20946	OM956086	OQ989318	OQ989308
Drechslerella yunlongensis	YL402	OQ946592	OQ989317	OQ989307
Drechslerella yunnanensis	1.01863	MH179759	—	MH179861
Drechslerella yunnanensis	YMF 1.03216	HQ711927	—	—
Orbilia jesu-laurae	LQ59a	MN816816	—	—
Orbilia orientalis	H.B.9925	KT222412	—	—
Orbilia orientalis	H.B.9965	KT380104	—	—
Orbilia pseudopolybrocha	YMF 1.02660	NR_172380	—	—
Orbilia tonghaiensis	YMF 1.03006	NR_172397	MF948570	MF948496
Vermispora fusarina	YXJ02-13-5	AY773447	AY773389	AY773418
Vermispora leguminacea	AS 6.0291	DQ494376	—	—

The best-fit optimal substitution models of ITS, TEF, and RPB2 were selected as GTR+I+G, TrN+I+G, and GTR+I+G via jModelTest v2.1.10 (Posada, 2008) under the Akaike Information Criterion (AIC).

Maximum likelihood (ML) analysis was implemented using IQ-Tree v1.6.5 according to Zhang et al. (2022). The statistical bootstrap support values (BS) were computed using rapid bootstrapping with 1000 replicates (Felsenstein, 1985)

Bayesian inference (BI) analysis was conducted with MrBayes v. 3.2.6 (Huelsenbeck & Ronquist, 2001) according to Zhang et al. (2022). The remaining 75% of trees were used to calculate the posterior probabilities (PP) in the majority rule consensus tree.

FigTree v1.3.1 (Rambaut, 2010) was used to visualize the trees. The backbone tree was edited and reorganized using Microsoft PowerPoint (2013) and Adobe Photoshop CS6 software (Adobe Systems, San Jose, CA, USA).

8.3 Results

8.3.1 Phylogenetic Analysis

The combined ITS, TEF, and RPB2 alignment dataset consisted of 104 ITS sequences, 60 TEF sequences, and 67 RPB2 sequences from 66 *Arthrobotrys* taxa representing 62 valid species (plus our two new species), 32 *Drechslerella* taxa representing 21 valid species (plus our three new species), other related taxa in *Orbiliaceae* (*Dactylellina*: four species), and two outgroup taxa. The final dataset comprised 2038 characters (627 for ITS, 822 for RPB2, and 542 for TEF), among which 900 bp were constant, 1087 bp were variable, and 886 bp were parsimony informative. A best-scoring maximum likelihood tree was performed with a final ML optimization likelihood value of −6158.611237. Within the Bayesian analysis (BI), the Bayesian posterior probabilities were evaluated with a final average standard deviation of the split frequency of 0.009264. The trees inferred by ML and BI showed slightly different topologies in some clusters, but both trees showed that all tested nematode-trapping fungi were clustered into two large clades, and five new species showed distinct divergence from known species. The best-scoring ML tree was selected to present herein (Figure 8.1), and the Bayesian majority rule consensus tree (BI) was also attached in the Supplementary Materials.

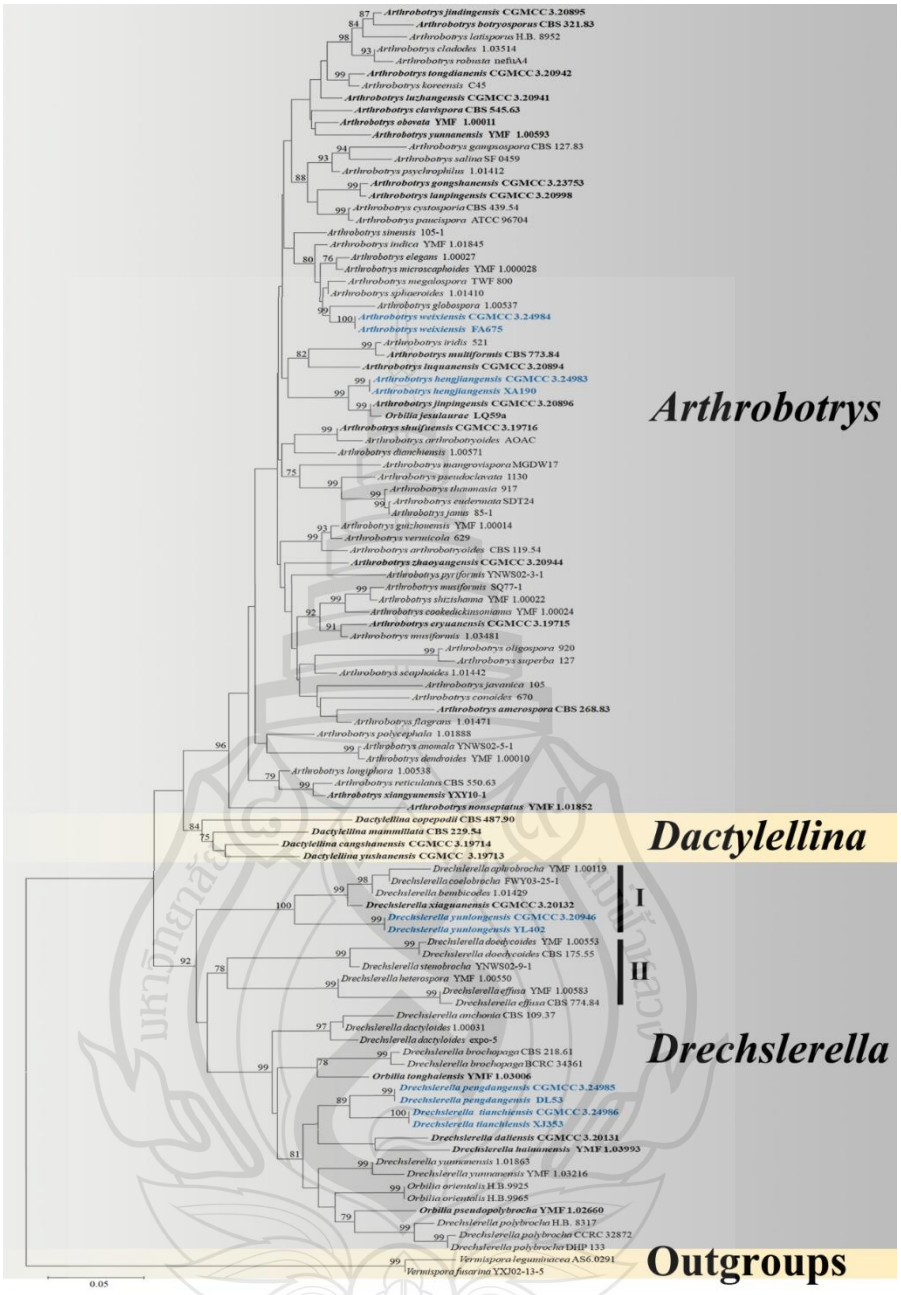

Figure 8.1 Maximum likelihood tree based on a combined ITS, TEF and RPB2 sequence from 87 species of *Orbiliaceae* nematode-trapping fungi. Bootstrap support values equal to or greater than 70% are indicated above the nodes. The new isolates are in blue; type strains are in bold. The tree is rooted by *Vermispora fusarina* YXJ02-13-5 and V. *leguminacea* AS 6.0291

The phylogenetic tree inferred from the ITS, TEF, and RPB2 combined dataset placed five pairs of new isolates in Arthrobotrys and *Drechslerella. Arthrobotrys hengjiangensis* sp. nov. clustered with A. *jinpingensis* and *Orbilia jesu-laurae* with 99% MLBS and 0.98 BYPP support. *Arthrobotrys weixiensis* sp. nov. was sister to A. *globospora* with 99% MLBS, 1.00 BYPP support. *Drechslerella pengdangensis* sp. nov. and Dr. tianchiensis sp. nov. were clustered together (89% MLBS). *Drechslerella yunlongensis* sp.nov. was clustered with four other species that produce fusiform conidia (100% MLBS, 1.00 BYPP, Figure 8.1).

8.3.2 Taxonomy

Arthrobotrys hengjiangensis F. Zhang & X.Y. Yang sp. nov. (Figure 8.2).

Index *Fungorum* number: IF900409; *Facesoffungi* number: FOF14151.

Etymology: The species name "*hengjiangensis*" refers to the name of sample collection site: Hengjiang County, Zhaotong City, Yunnan Province, China.

Material examined: CHINA, Yunnan Province, Zhaotong City, Hengjiang County, Hengjiang River, N 28°32′31.8″, E 104°19′09.5″, from freshwater sediment, 12 July 2014, F. Zhang. Holotype CGMCC 3.249834, preserved in the China General Microbiological Culture Collection Center. Ex-type culture DLUCC 34-1, preserved in the Dali University Culture Collection.

Colonies on PDA: initially white and turned to pale pink or yellowish after 2 weeks, cottony, growing rapidly, reaching 60 mm diameter after 10 days at 26 °C. Mycelium: partly superficial, partly immersed, composed of septate, branched, smooth, and hyaline. Conidiophores: 182.5–343 µm. ($\bar{x}$ = 268.4 µm., n = 50) long, 3–5.5 µm. ($\bar{x}$ = 3.7 µm., n = 50) wide at the base, gradually tapering upwards to the apex with 2.5–3.5 µm. ($\bar{x}$ = 2.7 µm., n = 50) wide, erect, septate, unbranched or sometimes branched, producing a node at the apex or several separate nodes by repeated elongation of conidiophores, each node consisting of 3–8 papilliform bulges and bearing 3–8 conidia. Conidia: 14.5–29.5 × 9.5–18 µm. ($\bar{x}$ = 19.9 × 12.7 µm, n = 50), obpyriform or drop-shaped, rounded at the apex, tapering towards narrow with tapering base, 0–2-septate (mostly 0 or 1-septate), and hyaline. Chlamydospore 7–14 × 5–10 µm. ($\bar{x}$ = 9.5 ×7.6 µm, n = 50), cylindrical, globose or ellipsoidal, hyaline, and in chains when present. Nematodes were captured with adhesive networks.

Additional specimen examined: CHINA, Yunnan Province, Zhaotong City, Hengjiang County, Hengjiang River, N 28°32′31.8″, E 104°19′09.5″, from freshwater sediment, 12 July 2014, F. Zhang. Living culture XA190.

Notes: Phylogenetically, *Arthrobotrys hengjiangensis* clusters together with A. *jinpingensis* and *Orbilia jesu-laurae* with 99% MLBS, 0.98 BYPP support. *Arthrobotrys hengjiangensis* was 4.3% (27/626 bp) and 3.2% (20/620 bp) different from A. *jinpingensis* and *Orbilia jesu-laurae* in ITS sequences. Morphologically, these three species are similar in their conidia shape and the nodes of conidiophores (Quijada et al., 2020; Zhang et al., 2022). However, A. *hengjiangensis* can be distinguished from A. *jinpingensis* by its wider conidia [A. *hengjiangensis*, 9.5–18 (12.7) µm. versus A. *jinpingensis*, 6.5–14.5 (10.8) µm.], 2-septate conidia with tapering base, and branched conidiophores (Zhang et al., 2022). The difference between A. *hengjiangensis* and O. *jesu-laurae* is that the conidiophores of O. *jesu-laurae* branched at the apex. In contrast, the conidiophores of A. *hengjiangensis* branched in the middle and upper parts. In addition, *Orbilia jesu-laurae* does not produce 2-septate conidia, while A. *hengjiangensis* does. Furthermore, the conidia produced by A. *hengjiangensis* have a more pointed base than those of O. *jesu-laurae*. The conidia of O. jesu-laurae are often slightly constricted at the septum, while those of A. *hengjiangensis* do not (Quijada et al., 2020).

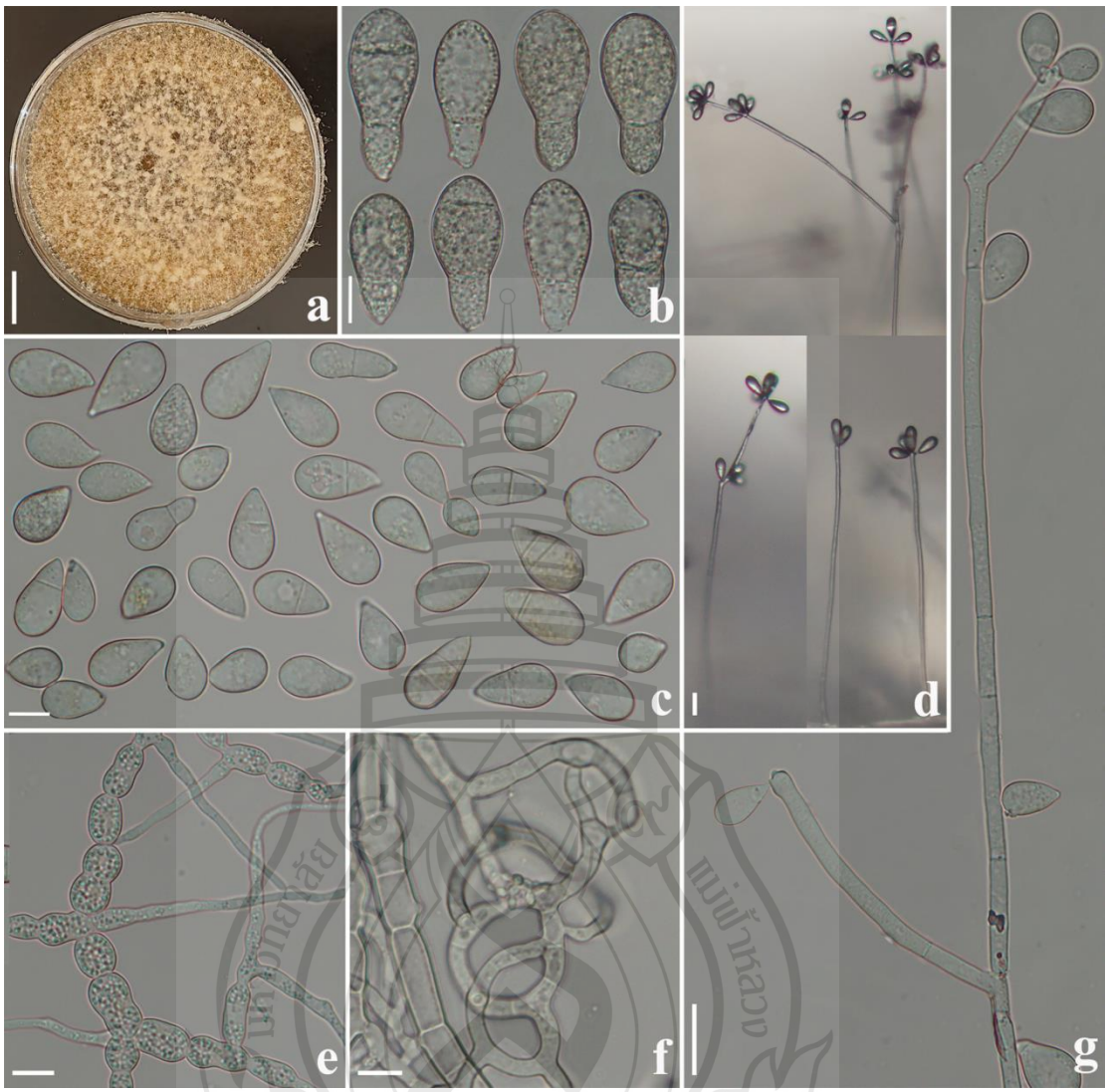

Figure 8.2 *Arthrobotrys hengjiangensis* (CGMCC 3.24983). (a) Colony. (b, c) Conidia. (e) Chlamydospores. (f) Trapping structure: adhesive networks. (d, g) Conidiophores. Scale bars: (a) = 1 cm., (b, c, e, f) = 10 µm., (d, g) = 20 µm.

Arthrobotrys weixiensis F. Zhang & X.Y. Yang sp. nov. (Figure 8.3).

Index *Fungorum* number: IF900410; *Facesoffungi* number: FOF14152.

Etymology: The species name “weixiensis” refers to the name of sample collection site: Weixi County, Diqing City, Yunnan Province, China.

Material examined: CHINA, Yunnan Province, Diqing City, Weixi County, N 27°12′40.3″, E 99°05′24.2″, from terrestrial soil, 26 July 2014, F. Zhang. Holotype CGMCC3.24984, preserved in the China General Microbiological Culture Collection

Center. Ex-type culture DLUCC 35-1, preserved in the Dali University Culture Collection.

Colonies on PDA: white, cottony, growing rapidly, reaching 55 mm diameter after 9 days in the incubator at 26 °C. Mycelium: partly superficial, partly immersed, composed of septate, branched, smooth, and hyaline. Conidiophores 165–364.5 µm. ($\bar{x}$ = 253.4 µm., n = 50) long, 2.5–5 µm. ($\bar{x}$ = 3.4 µm., n = 50) wide at the base, gradually tapering upwards to the apex 1.5–3 µm. ($\bar{x}$ = 2.2 µm., n = 50) wide, erect, septate, unbranched, hyaline, producing 1–3 short denticles at the apex, and each denticle bearing a single conidium. Conidia: two types: I-type conidia: 22.5–39 × 14–27.5 µm. ($\bar{x}$ = 27.8 × 17.7 µm, n = 50), drop-shaped or obovate, rounded at the apex, tapering towards narrow with subacute and truncate base, 1–2-septate (mostly 1-septate, usually located at the base), hyaline, with the largest cell located at the apex. II-type conidia: 30.5–48 × 14–27 µm. ($\bar{x}$ = 36.7 × 19.5 µm, n = 50), fusiform, rounded at the apex, tapering towards narrow with subacute and truncate base, 1–2-septate (mostly 2-septate, usually located at both ends of the conidia), and hyaline, with the largest cell located at the middle of the conidia. Chlamydospore: 6–24 × 3.5–24 µm. ($\bar{x}$ = 13.9 × 9.1 µm, n = 50), cylindrical, globose or ellipsoidal, hyaline or yellowish, and in chains when present. Nematodes were captured with adhesive networks.

Additional specimen examined: CHINA, Yunnan Province, Diqing City, Weixi County, N 27°12′40.3″, E 99°05′24.2″, from terrestrial soil, 26 July 2014, F. Zhang. Living culture FA675.

Notes: Phylogenetically, *Arthrobotrys weixiensis* forms a sister lineage to A. *globospora* (99% MLBS, 1.00 BYPP). There are 13.2% (64/484 bp) differences between them in ITS. Morphologically, the conidia shape of A. weixiensis and A. *globospora* are similar. They can be distinguished by their conidia size. The conidia of A. weixiensis are significantly larger than those of A. globospora [A. weixiensis, 30.5–48 (36.7) × 14–25 (19.5) µm. versus A. globospora, 25–37.5 (30) × 15–22.5 (18) µm.]. In addition, the conidiophore of A. globospora bears only a single conidium, while the conidiophore of A. weixiensis bears 1–3 conidia (Zhang & Mo, 2006; Zhang & Hyde, 2014).

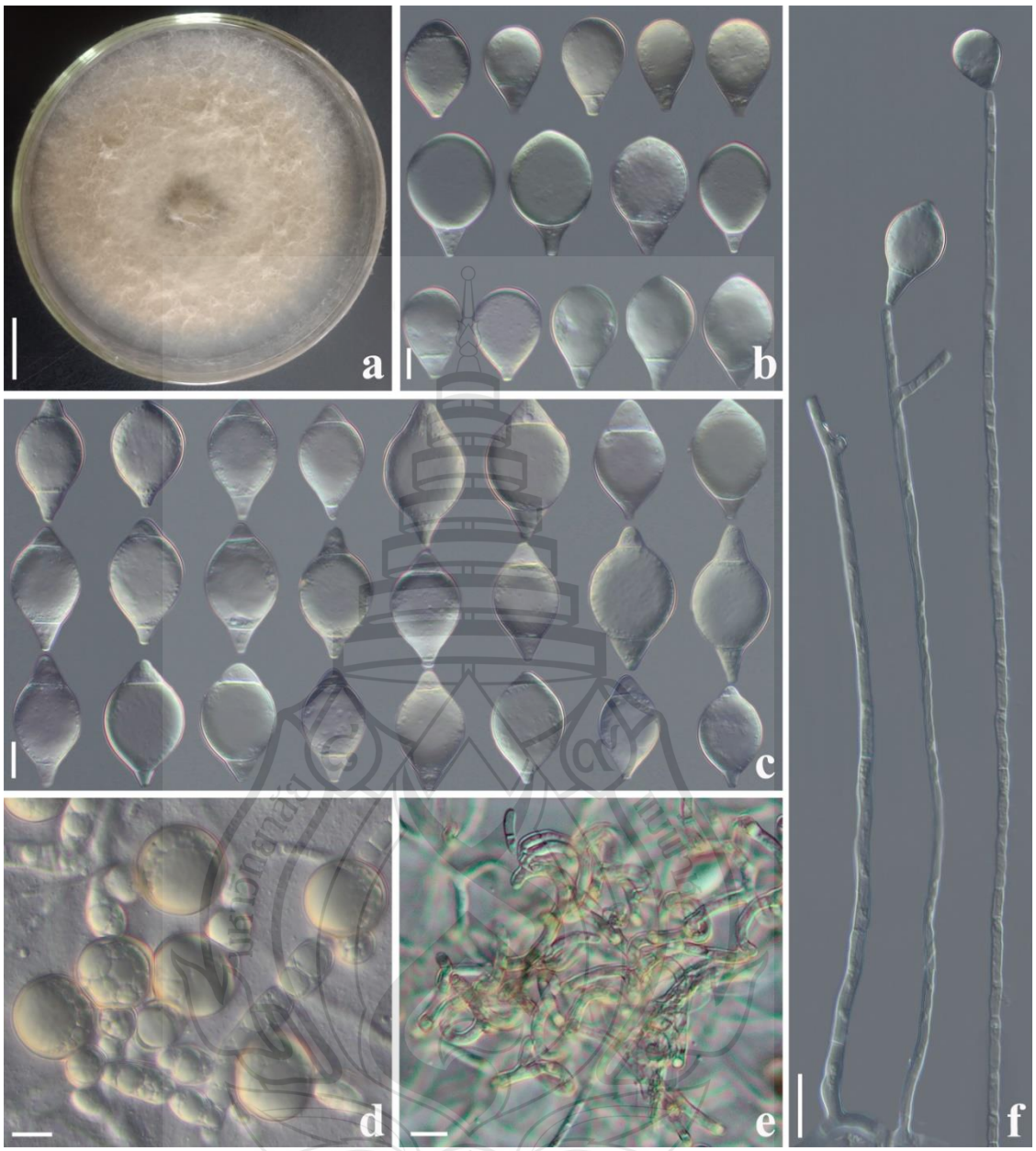

Figure 8.3 *Arthrobotrys weixiensis*. (CGMCC 3.24984). (a) Colony. (b, c) Conidia. (d) Chlamydospores. (e) Trapping structure: adhesive networks. (f) Conidiophores. Scale bars: (a) = 1 cm., (b–e) = 10 μm., (f) = 20 μm.

Drechslerella pengdangensis F. Zhang & X.Y. Yang sp. nov. (Figure 8.4).

Index *Fungorum* number: IF900411; *Facesoffungi* number: FOF14153.

Etymology: The species name “pengdangensis” refers to the name of sample collection site: Pengdang County, Nujiang City, Yunnan Province, China.

Material examined: CHINA, Yunnan Province, Nujiang City, Pengdang County, N 27°56′16.88″, E 98°39′8.71″, from terrestrial soil, 4 May 2018, F. Zhang. Holotype CGMCC 3.24985, preserved in the China General Microbiological Culture Collection Center. Ex-type culture DLUCC 37-1, preserved in the Dali University Culture Collection.

Colonies on PDA: white, cottony, growing slowly, reaching 40 mm diameter after 15 days in the incubator at 26 °C. Mycelium: partly superficial, partly immersed, composed of septate, branched, smooth, and hyaline. Conidiophores: 195.5–355 µm. ($\bar{x}$ = 273.4 µm., n = 50) long, 2.5–5 µm. ($\bar{x}$ = 3.5 µm., n = 50) wide at the base, gradually tapering upwards to the apex 2.5–4 µm. ($\bar{x}$ = 2.4 µm., n = 50) wide, erect, septate, unbranched, and bearing a single conidium at the knob-like apex. Conidia: 30–45 × 17–27 µm. ($\bar{x}$ = 38 × 22.4 µm, n = 50), ellipsoidal to sub-fusiform, rounded at the apex, tapering towards narrow with truncate at the base, 1–2-septate (mostly 2-septate), hyaline, with the largest cell located at the middle or apex of the conidia, where the base cell is tiny. Chlamydospore: not observed. Nematodes were captured with constricting rings; in the non-constricted state, the outer diameter is 19–28.5 µm. ($\bar{x}$ = 24 µm., n = 50), and the inner diameter is 13–22.5 µm. ($\bar{x}$ = 20.1 µm., n = 50).

Additional specimen examined: CHINA, Yunnan Province, Nujiang City, Pengdang County, N 27°56′16.88″, E 98°39′8.71″, from terrestrial soil, 4 May 2018, F. Zhang. Living culture DL53.

Notes: Phylogenetically, *Drechslerella pengdangensis* forms a sister lineage with another new species (*Drechslerella tianchiensis*) reported in this study, with 89% MLBS support. There are 15% (128/853 bp) differences in ITS sequence between them. Morphologically, Dr. pengdangensis can be easily distinguished from Dr. tianchiensis in the shape of the conidia and single conidiophore. *Drechslerella pengdangensis* is similar to Dr. doedycoides in their ellipsoidal to sub-fusiform conidia and simple conidiophore with knob-like apex (Zhang & Mo, 2006; Zhang & Hyde, 2014). However, Dr. doedycoides produces 3-septate conidia, while Dr. pengdangensis never. Moreover, the base cell of conidia produced by Dr. pengdangensis is significantly smaller than those of Dr. Doedycoides (Zhang & Mo, 2006; Zhang & Hyde, 2014).

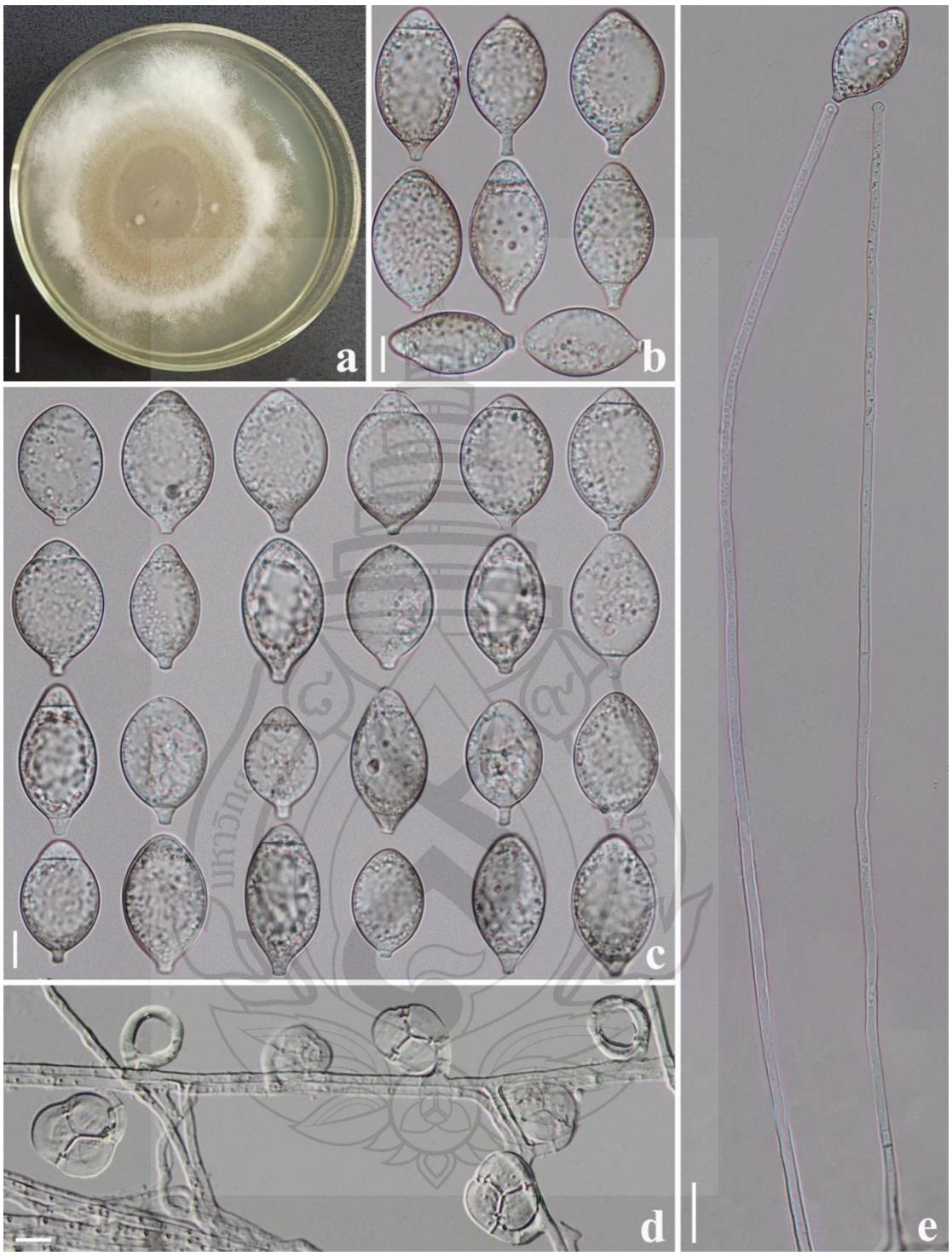

Figure 8.4 *Drechslerella pengdangensis* (CGMCC 3.24985). (a) Colony. (b, c) Conidia. (d) Trapping structure: constricting rings. (e) Conidiophores. Scale bars: (a) = 1 cm., (b–d) = 10 µm., (e) = 20 µm.

Drechslerella tianchiensis F. Zhang & X.Y. Yang sp. nov. (Figure 8.5).

Index *Fungorum* number: IF900412; *Facesoffungi* number: FOF14154.

Etymology: The species name “tianchiensis” refers to the name of sample collection site: Tianchi Nature Reserve, Yunlong County, Dali City, Yunnan Province, China.

Material examined: CHINA, Yunnan Province, Dali City, Yunlong County, Tianchi Nature Reserve, N 25°51′22.50″, E 99°13′38.43″, from burned forest soil, 28 May 2018, F. Zhang. Holotype CGMCC 3.24986, preserved in the China General Microbiological Culture Collection Center. Ex-type culture DLUCC 38-1, preserved in the Dali University Culture Collection.

Colonies on PDA white, cottony, growing slowly, reaching 40 mm diameter after 15 days in the incubator at 26 °C. Mycelium partly superficial, partly immersed, composed of septate, branched, smooth, hyaline. *Macroconidiophores* 186.5–305.5 µm. ($\bar{x}$ = 248.1 µm., n = 50) long, 2.5–5 µm. ($\bar{x}$ = 3.6 µm., n = 50) wide at the base, gradually tapering upwards to the apex with 1.5–3 µm. ($\bar{x}$ = 2.2 µm., n = 50) wide, erect, septate, hyaline, unbranched or producing 1–2 short branches near the apex, each branch bearing a single conidium. Microconidiophores 137.5–245.5 µm. ($\bar{x}$ = 183.7 µm., n = 50) long, 2–4 µm. ($\bar{x}$ = 3.2 µm., n = 50) wide at the base, gradually tapering upwards to the apex with 1.5–3 µm. ($\bar{x}$ = 1.8 µm., n = 50) wide, erect, septate, hyaline, unbranched, producing 3–12 short denticles near the apex, each denticles bearing a single conidium. Conidia two types: *Maroconidia* 30–41 × 14.5–24 µm. ($\bar{x}$ = 36.2 × 18.7 µm, n = 50), ellipsoidal, rounded at the apex, tapering towards narrow with truncate base, 1–2-septate (mostly 2-septate), hyaline, with a largest cell located at the middle or apex of the conidia. *Miroconidia* 16–26.5 × 4.5–11.5 µm. ($\bar{x}$ = 21.6 × 6 µm, n = 50), clavate or cylindrical, rounded at the apex, tapering towards narrow with truncate base, 0–1-septate (mostly 1-septate), hyaline. Chlamydospore not observed. Capturing nematodes with constricting rings, in the non-constricted state, the outer diameter is 20.5–27.5 µm. ($\bar{x}$ = 24.7µm., n = 50), the inner diameter is 14.5–22 µm. ($\bar{x}$ = 19.3µm., n = 50).

Additional specimen examined: CHINA, Yunnan Province, Dali City, Yunlong County, Tianchi Nature Reserve, N 25°51′22.50″, E 99°13′38.43″, from burned forest soil, 28 May 2018, F. Zhang. Living culture XJ353.

Notes: Phylogenetically, *Drechslerella tianchiensis* formed a sister lineage with Dr. pengdangensis (89% MLBS). Morphologically, Dr. tianchiensis is similar to Dr. hainanensis and the asexual morph of *Orbilia pseudopolybrocha* in their shape of macroconidia and microconidia. The difference between Dr. tianchiensis and *Orbilia pseudopolybrocha* is that the macro-conidiophore of the latter is simple and bears a single conidium, while some macro-conidiophore of Dr. tianchiensis produces 1–2 short branches near the apex and bears 1–2 conidia. The conidia of Dr. tianchiensis are significantly larger than those of O. *pseudopolybrocha* (Dr. tianchiensis, 30–41 (36.2) × 14.5–24 (18.7) µm. versus O. *pseudopolybrocha*, 26–30 × 16–22.2 µm.) (Zhang et al., 2022). *Drechslerella tianchiensis* can be easily distinguished from Dr. hainanensis by its 1–2-branch macro-conidiophore and wider microconidia (Dr. tianchiensis, 16–26.5 (21.6) × 4.5–11.5 (6) µm. versus Dr. hainanensis, 18.2–22.8 × 4.2–5.3 µm.) (Zhang et al., 2022).

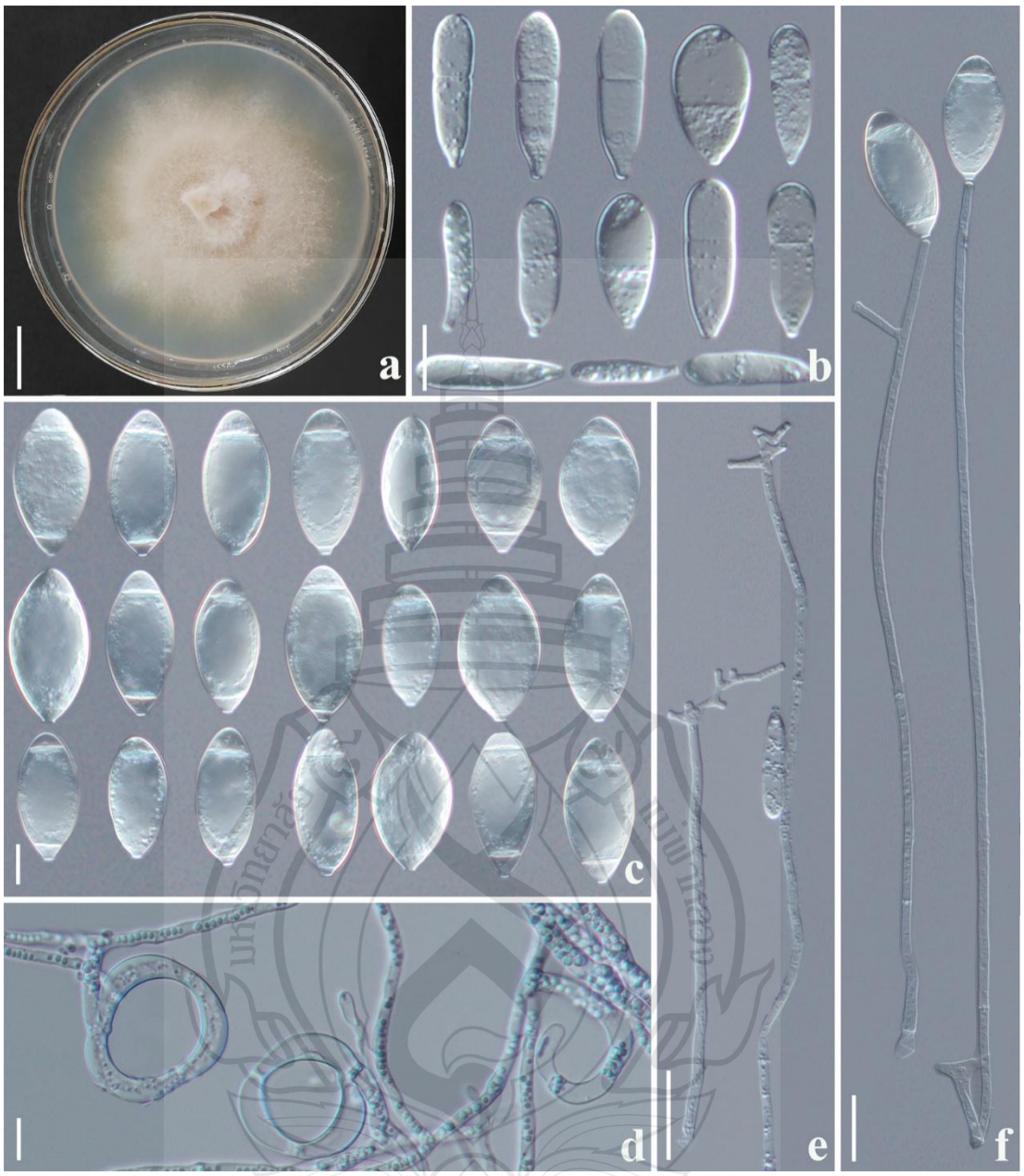

Figure 8.5 *Drechslerella tianchiensis* (CGMCC 3.24986). (a) Colony. (b) Microconidia. (c) Macroconidia. (d) Trapping structure: constricting rings. (e) Microconidiophores. (f) Macroconidiophores. Scale bars: (a) = 1 cm., (b–d) = 10 µm., (e, f) = 20 µm.

Drechslerella yunlongensis F. Zhang & X.Y. Yang sp. nov. (Figure 8.6).

Index *Fungorum* number: IF900413; *Facesoffungi* number: FOF14155.

Etymology: The species name “yunlongensis” refers to the name of sample collection site: Yunlong County, Dali City, Yunnan Province, China.

Material examined: CHINA, Yunnan Province, Dali City, Yunlong County, N 25°52′27.91″, E 99°22′19″, from terrestrial soil, 3 June 2018, F. Zhang. Holotype CGMCC 3.20946, preserved in the China General Microbiological Culture Collection Center. Ex-type culture DLUCC 39-1, preserved in the Dali University Culture Collection.

Colonies on PDA: white, cottony, growing slowly, reaching 45 mm diameter after 15 days in the incubator at 26 °C. Mycelium: partly superficial, partly immersed, composed of septate, branched, smooth, and hyaline. Conidiophores: 164–331 µm. ($\bar{x}$ = 239.8 µm., n = 50) long, 2.5–5 µm. ($\bar{x}$ = 3.3 µm., n = 50) wide at the base, gradually tapering upwards to the apex 1.5–3µm. ($\bar{x}$ = 2.1 µm., n = 50) wide, erect, septate, unbranched, hyaline, bearing a single conidium at the apex. Conidia: 36–54 × 17–27 µm. ($\bar{x}$ = 47 × 23.6 µm, n = 50), drop-shaped or fusiform, rounded at the apex, tapering towards narrow with truncate base, 1–4-septate (mostly 4-septate), hyaline, with the largest cell located at the apex or middle of the conidia. Chlamydospore: 5–14 × 5.5–10 µm. ($\bar{x}$ = 8.7 ×7.1 µm, n = 50), cylindrical, globose or ellipsoidal, hyaline, and in chains when present. Nematodes were captured with constricting rings; in the non-constricted state, the outer diameter was 19.5–27 µm. ($\bar{x}$ = 23.1 µm., n = 50), the inner diameter was 15–21.5 µm. ($\bar{x}$ = 18.9µm., n = 50).

Additional specimen examined: CHINA, Yunnan Province, Dali City, Yunlong County, N 25°52′27.91″, E 99°22′19″, from terrestrial soil, 3 June 2018, F. Zhang. Living culture YL402.

Notes: The phylogenetic analysis clustered *Drechslerella yunlongensis* with the other four fusiform conidia-producing species (99% MLBS, 1.00 BYPP). *Drechslerella yunlongensis* was 9.8% (55/559 bp), 8.1% (40/496 bp), 9.1% (51/559 bp), and 7.9% (47/596 bp) different from Dr. aphrobrocha, Dr. bembicodes, Dr. coelobrocha, and Dr. xiaguanensis in ITS, respectively. Morphologically, Dr. yunlongensis is also similar to these four species. However, the conidia of Dr. yunlongensis are bigger than those of Dr. bembicodes and Dr. xiaguanensis (Dr. yunlongensis, 36–54 (47) × 17–27 (23.6)

µm. versus Dr. bembicodes, 36–43.2 (40) × 16.8–21.6 (20.5) µm. versus Dr. xiaguanensis, 33–52 (42.5) × 9.5–28 (15.5) µm.); moreover, Dr. bembicodes produces obovoid, 1-septate microconidia, while Dr. yunlongensis does not; the conidia of Dr. xiaguanensis are mostly 3-septate, while the conidia produced by Dr. yunlongensis are mostly 4-septate (Zhang & Mo, 2006; Zhang & Hyde, 2014; Zhang et al., 2022). The difference between Dr. yunlongensis and Dr. aphrobrocha is that Dr. aphrobrocha produces mostly 3-septate conidia, while Dr. yunlongensis produces mostly 4-septate conidia; the conidia of Dr. yunlongensis are smaller than that of Dr. aphrobrocha due to its smaller apical cell (Dr. yunlongensis, 36–54 (47) × 17–27 (23.6) µm. versus Dr. aphrobrocha, 40–57.5 (51) × 15.5–35 (24.6) µm.) (Zhang & Mo, 2006; Zhang & Hyde, 2014). Drechslerella yunlongensis can be distinguished from Dr. coelobrocha by its wider conidia (Dr. yunlongensis, 17–27 (23.6) µm. versus Dr. coelobrocha, 16.8–21.6 (19.8) µm.), and shorter base and apical cells (Zhang & Mo, 2006; Zhang & Hyde, 2014). Furthermore, Dr. yunlongensis produces cylindrical or ellipsoidal chlamydospores, while none of the four closely related species produces chlamydospores (Zhang & Mo, 2006; Zhang & Hyde, 2014; Zhang et al., 2022).

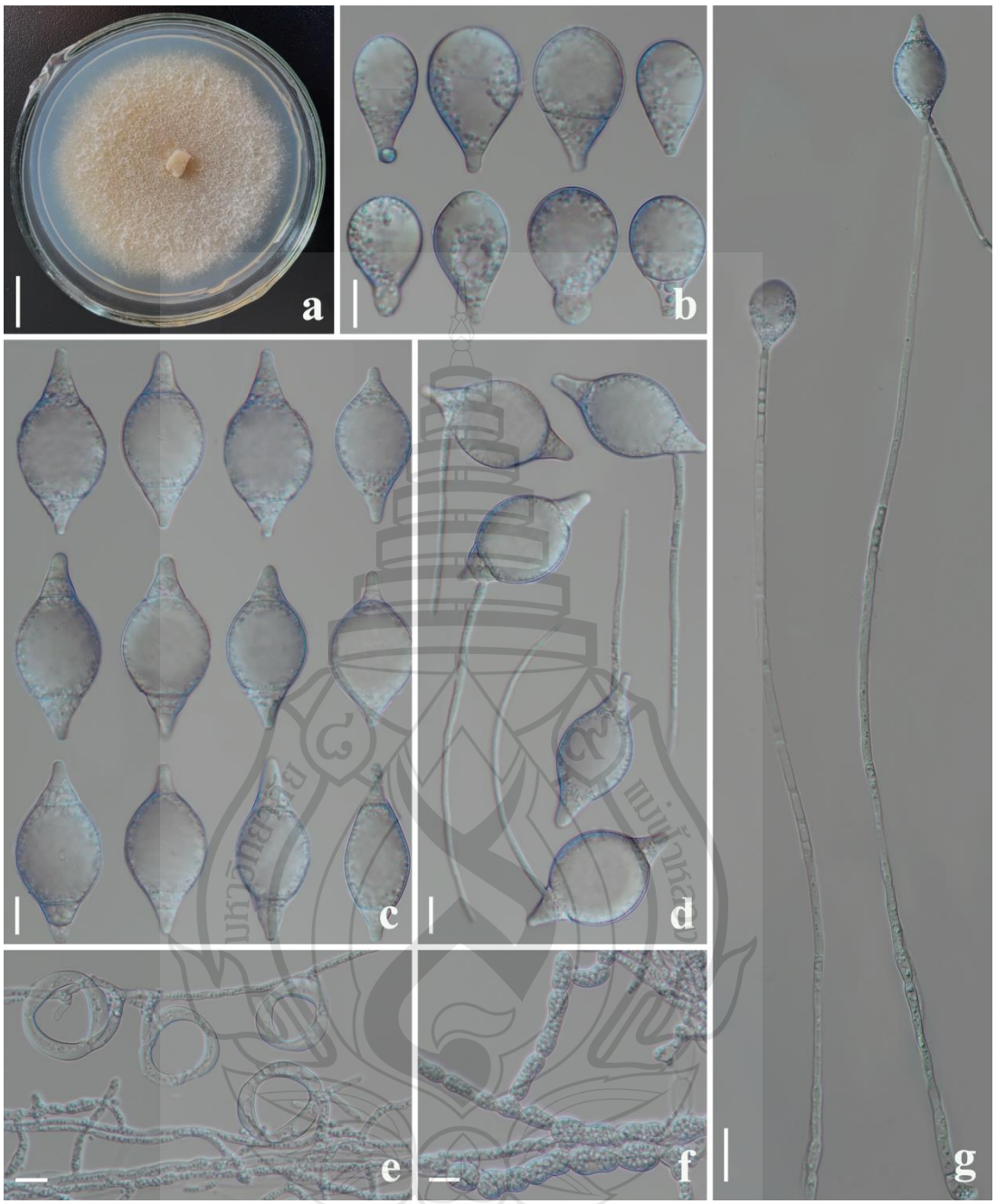

Figure 8.6 *Drechslerella yunlongensis* (CGMCC 3.20946). (a) Colony. (b, c) Conidia. (d) Germinating conidia. (e) Trapping structure: constricting rings. (f) Chlamydospores. (g) Conidiophores. Scale bars: (a) = 1 cm., (b–d) = 10 µm., (e, f) = 20 µm.

8.4 Discussion

Both the phylogenetic analysis in this study and previous studies divided NTF into two main clades based on the mechanisms by which they catch nematodes (the genus *Drechslerella* produces constricting rings to capture nematodes with mechanical force, and the genera *Arthrobotrys* and *Dactylellina* catch nematodes with adhesive traps) (Pfister, 1997; Ahrén et al., 1998; Scholler et al., 1999; Yang et al., 2007). These results again emphasized the significance of trapping structure for species division and evolution. Different from previous studies, this study failed to cluster *Dactylellina* species into a stable cluster, possibly due to insufficient DNA data. We believe that as more DNA data are used, we will find more morphological or physiological features that match phylogenetic studies.

The evolution of nematode-trapping fungi (NTF) is one crucial node to understanding the history of fungal evolution because of its unique morphological characteristics and survival strategy (Corda, 1839; Drechsler, 1933; Zhang & Mo, 2006; Zhang & Hyde, 2014). Currently, the main focus of the evolution research on NTF is the evolution of the trapping structure (Ahrén et al., 1998; Li et al., 2000, 2005). However, on the one hand, the phylogenetic clade of *Drechslerella* in this study showed that some species with similar conidia morphology cluster stably into one branch, such as species in clade I producing fusiform conidia and species in clade II producing ellipsoidal conidia (Figure 8.1). Moreover, in the whole NTF, species that produce the same trapping structure can easily be divided into different groups according to their conidia. For example, *Drechslerella* species can be divided into two groups according to the presence or non-presence of super-cell in their conidia, and all *Arthrobotrys* species can be divided into three groups according to their conidia shape (Zhang & Mo, 2006). In addition to the law above, as the most critical reproductive structure in the asexual generation of fungi, conidia should have crucial evolutionary significance in theory. Based on the above, conidia may also be an essential evolutionary feature for NTF and an important basis for the NTF classification. Similarly, are other structures or physiological characteristics of NTF experiencing the same problems as conidia (which have important evolutionary or taxonomic significances but have been neglected)? In conclusion, the evolution of organisms is a process of interaction

between organisms and the environment. The evolution of a single structure (trapping structure) cannot represent the evolution of the NTF species. The excessive focus on the evolution of a single structure while ignoring the characteristics of the whole species may lead to the mistake of the blind man feeling the elephant.

The compilation logic of the key of *Drechslerella* species is that species are first roughly classified by those features that can be used to identify species and are easily distinguishable, such as whether the conidia produce a super-cell or not, the shape of the conidia (fusiform, elliptical, cylindrical, digitate, etc.), whether the conidiophore is branched or not, and the number of conidia on the conidiophore. Then, species are further classified by those features that can be used for species identification but require further measurement and observation, such as the detailed feature of macroconidia (number and position of the septum and the size of the macroconidia). Finally, morphologically similar species are distinguished by those characteristics that are uncertain whether they can be used for species identification but are differences between different species, such as the presence and features of microconidia, the detailed feature of the apex of the conidiophore, and the features of the chlamydospore. Even identifying *Drechslerella* species requires those morphological features that are not known to be valid, so how difficult would it be to identify the more complex *Arthrobotrys* and *Dactylellina* species based on these features alone? Therefore, follow-up research needs to systematically study all potential morphological characteristics to find more reliable characteristics for species identification.

Most of the sexual generations of *Orbiliomycetes* nematode-trapping fungi are members of *Orbilia* (Zhang & Hyde, 2014). However, due to the morphological conservation of the sexual generations, there exists a phenomenon wherein one sexual species corresponds to several morphologically different asexual species (Mo et al., 2005). Additionally, with the implementation of the one fungus, one name policy (Norvell, 2011; Wingfield et al., 2012), asexual NTFs need to use sexual names when discovering their sexual generation (*Orbilia* sp.). This results in these different asexual species sharing the same sexual species name (Mo et al., 2005), which further leads to confusion in the classification system and relevant data in some databases (such as Genebank, https://www.ncbi.nlm.nih.gov/nuccore/?term=Orbilia+auricolor (accessed on 3 April 2023)). For this reason, we suggest that when reporting a pair of sexual and

asexual species, it is necessary to discuss the difference between the sexual generation and known sexual species and, more importantly, consider the distinction between the asexual generation and known asexual generation. The naming of this pair of sexual and asexual species should be carefully evaluated separately, giving sexual and asexual generations different species names if necessary.

CHAPTER 9

MULTILOCUS PHYLOGENY AND CHARACTERIZATION OF FIVE UNDESCRIBED AQUATIC CARNIVOROUS FUNGI (*ORBILIOMYCETES*)

9.1 Introduction

Nematode-trapping fungi (NTF) are a group of fungi that possess a unique trapping structure to capture nematodes for nutrition (Barron, 1977; Zhang & Mo, 2006; Swe et al., 2011; Zhang & Hyde, 2014). NTF in *Orbiliomycetes* are considered the core representatives of NTF due to their rich species diversity, and intricate and diverse trapping structures, as well as their important role in maintaining ecological balance and their potential value in the bio-control of harmful nematodes (Yang et al., 2007; Zhang & Hyde, 2014; Jiang et al., 2017; Soliman et al., 2021). Currently, this group of fungi includes 125 species from three genera: *Arthrobotrys* (73 species) which captures nematodes using adhesive networks; *Dactylellina* (35 species), the genus that captures nematodes with adhesive branches, non-constricting rings, and adhesive knobs; and *Drechslerella* (17 species) which catches nematodes using constricting rings (Ahrén et al., 1998; Yang et al., 2007; Zhang & Hyde, 2014).

These fungi are widely distributed in various habitats because of their unique survival strategy. They are commonly found in the soils from farmlands, forests, and even heavy metal-contaminated areas (Mo et al., 2008; Singh & Pandey, Zhang & Hyde, 2014; Zhang et al., 2020), as well as in sediments from marine, freshwater, and even hot springs (Hao et al., 2005; Swe et al., 2009; Liu et al., 2014). But compared to the well-studied terrestrial ecosystems, the diversity of NTF in freshwater habitats remains insufficiently studied (Hao et al., 2005; Tarigan et al., Zhang et al., 2022). Previous studies have confirmed the existence of a rich diversity of NTF in freshwater ecosystems, which is reasonable given the abundance of nematodes in aquatic environments (Hao et al., 2004,

2005). Meanwhile, the diverse array of nematodes in aquatic habitats includes parasitic species that pose threats to aquatic crops and fisheries (González-Solís & Jiménez-García, 2006; Tahseen, 2012). So, studying aquatic NTF resources is an important part of NTF diversity research and bio-control of harmful aquatic nematodes. Additionally, the study on aquatic NTF also provides a valuable entry point for investigating fungal adaptive evolution, as aquatic NTF originate from their terrestrial counterparts.

In the past ten years, we have investigated the NTF in the six major watersheds in Yunnan Province and successfully isolated ten strains, which were identified as five novel members of *Arthrobotrys*. This paper provides a comprehensive account of these species, offering new material for the bio-control research of harmful nematodes and the study of fungal aquatic adaptive evolution.

9.2 Material and Methods

9.2.1 Samples Collection

All freshwater sediment samples involved in this study were collected using a Peterson bottom sampler (HL-CN, Wuhan Hengling Technology Company, Limited, Wuhan, China). The samples were placed into plastic zip-lock bags to preserve moisture. Collecting sites, date, and collector were recorded (Table 9.1). The samples were stored at 4°C and processed within a week.

Table 9.1 Samples information involved in this study

Sample Source	Sampling Location	Sampling Date	Number of Samples
Cibi Lake	N 26°9′7.14″ E 99°56’32.72″	4 June 2013	25
Heihui River	N 25°37′4.13″, E 100°1′52.06″	6 April 2018	10
Jinsha River	N 27°8′50.56″, E 99°49′39.43″	9 July 2014	10
Yangbi River	N 25°42′37.94″, E 99°54′52.15″	4 April 2018	10
Yangjiang River	N 25°45′52.11″, E 99°54′46.43″	14 May 2018	10

9.2.2 Fungal Isolation

Nematodes (*Panagrellus redivivus* Goodey, free-living nematodes) cultured on oatmeal medium (Zhang & Hyde, 2014) were isolated using the Baermann funnel method (Staniland, 1954) and the concentration of the nematodes was adjusted with sterile water to 3000–5000 nematodes per milliliter. The soil sprinkling technique was used to disperse the sediment sample onto the surface of corn meal agar plates (CMA) (Zhang & Hyde, 2014) and 1 mL of nematode suspension was added to promote the germination of NTF. The plates were incubated at room temperature (14–28°C) for about three weeks and a stereo-microscope was used to observe the plates to search for the NTF spores. The single-spore isolation method was used for the isolation and purification of the NTF (Zhang & Hyde, 2014).

9.2.3 Morphological Observation

The isolates were inoculated onto potato dextrose agar (PDA) (Zhang & Hyde, 2014) plates and cultured at 26°C for colony observation. The isolate was transferred to CMA observation plates (creating an observation well by removing a 2 × 2 cm piece of agar from the center of the CMA plate and obliquely inserting a sterile cover glass into the surface of the medium) and incubated at 26°C (Zhang et al., 2023). After the observation

well was covered by the mycelia, about 1000 nematodes (*P. redivivus*) were added as bait to induce the production of traps. The types of traps were checked and photographed using an Olympus BX53 microscope (Olympus Corporation, Tokyo, Japan). When the mycelia had spread over the cover glass, the cover glass was removed with tweezers and a temporary slide made with sterile water (Su et al., 2006). An Olympus BX53 microscope (Olympus Corporation, Tokyo, Japan) was used to photograph and measure the morphological characteristics such as conidia, conidiophores, and chlamydospores.

9.2.4 Collection of DNA Molecular Data

The mycelia grown on PDA plates was used to extract genomic DNA, as described by Zhang et al. (Zhang et al., 2022). The primer pairs ITS4-ITS5 (White et al., 1990), 526F-1567R (O'Donnell et al., 1998), and 6F-7R (Liu et al., 1999) were used to amplify the ITS, TEF, and RPB2 regions, respectively, under the reaction system and conditions described in the previous study (Zhang et al., 2023). The PCR products were sent to BioSune Biotech Company Limited (Shanghai, China) for purification and sequencing (TEF genes were sequenced using the 247F-609R (Yang et al., 2007) primer pair and ITS and RPB2 regions were sequenced with PCR primers).

The generated sequences were carefully examined, edited, and assembled using SeqMan v. 7.0 (Swindell & Plasterer, 1997). All sequences obtained in this study have been submitted to the GenBank database (NCBI; https://www.ncbi.nlm.nih.gov/; accessed on 29 November 2023) for deposition.

9.2.5 Phylogenetic Analysis

The sequences generated in this study were compared with the GenBank database using BLASTn (https://blast.ncbi.nlm.nih.gov/; accessed on 9 November 2023). Our five species were placed within *Arthrobotrys* according to the BLASTn search and their trapping structures (Zhang & Hyde, 2014). Consequently, relevant publications (Zhang & Mo, 2006; Yang et al., 2007; Zhang & Hyde, 2014; Zhang et al., 2022, 2023; Masigol et al., 2022) and the BLASTn search results were used to retrieve all reliable ITS, TEF, and *RPB2* sequences of *Arthrobotrys* taxa from the GenBank database (Table 9.2). Three genes were aligned via the online program MAFFT v. 7 (http://mafft.cbrc.jp/alignment/server/; accessed on 14 November 2023) (Katoh & Standley, 2013). MEGA6.0 (Tamura et al., 2013) was used to adjust and link the three alignments.

Table 9.2 GenBank accession numbers involved in this study

Taxon	Strain Number	GenBank accession Number		
		ITS	TEF	RPB2
Arthrobotrys amerospora	CBS 268.83	NR_159625	——	——
Arthrobotrys anomala	YNWS02-5-1	AY773451	AY773393	AY773422
Arthrobotrys arthrobotryoides	AOAC	MF926580	——	——
Arthrobotrys blastospora	CGMCC 3.20940	OQ332405	OQ341651	OQ341649
Arthrobotrys botryospora	CBS 321.83	NR_159626	——	——
Arthrobotrys cibiensis	DLUCC 109	OR880379	OR882792	OR882797
Arthrobotrys cibiensis	EY10	OR902195	OR882787	OR882802
Arthrobotrys cladodes	1.03514	MH179793	MH179616	MH179893
Arthrobotrys clavispora	CBS 545.63	MH858353	——	——
Arthrobotrys conoides	670	AY773455	AY773397	AY773426
Arthrobotrys cookedickinson	YMF 1.00024	MF948393	MF948550	MF948474
Arthrobotrys cystosporia	CBS 439.54	MH857384	——	——
Arthrobotrys dendroides	YMF 1.00010	MF948388	MF948545	MF948469
Arthrobotrys dianchiensis	1.00571	MH179720	——	MH179826
Arthrobotrys elegans	1.00027	MH179688	——	MH179797
Arthrobotrys eryuanensis	CGMCC 3.19715	MT612105	OM850307	OM850301
Arthrobotrys eudermata	SDT24	AY773465	AY773407	AY773436
Arthrobotrys flagrans	1.01471	MH179741	MH179583	MH179845
Arthrobotrys gampsospora	CBS 127.83	U51960	——	——
Arthrobotrys globospora	1.00537	MH179706	MH179562	MH179814
Arthrobotrys gongshanensis	CGMCC 3.23753	OM801277	OM809162	OM809163
Arthrobotrys guizhouensis	YMF 1.00014	MF948390	MF948547	MF948471
Arthrobotrys heihuiensis	DLUCC 108-1	OR880378	OR882791	OR882796
Arthrobotrys heihuiensis	Y710	OR902194	OR882786	OR882801
Arthrobotrys hengjiangensis	CGMCC 3.24983	OQ946587	OQ989312	OQ989302
Arthrobotrys hyrcanus	IRAN 3650C	MH367058	OP351540	——
Arthrobotrys indica	YMF 1.01845	KT932086	——	——
Arthrobotrys iridis	521	AY773452	AY773394	AY773423
Arthrobotrys janus	85-1	AY773459	AY773401	AY773430
Arthrobotrys javanica	105	EU977514	——	——
Arthrobotrys jindingensis	CGMCC 3.20895	OP236810	OP272511	OP272515
Arthrobotrys jinpingensis	CGMCC 3.20896	OM855569	OM850311	OM850305
Arthrobotrys jinshaensis	DLUCC 133	OR880381	OR882794	OR882799
Arthrobotrys jinshaensis	MA142	OR902197	OR882789	OR882804
Arthrobotrys koreensis	C45	JF304780	——	——
Arthrobotrys lanpingensis	CGMCC 3.20998	OM855566	OM850308	OM850302

Table 9.2 (continued)

Taxon	Strain Number	GenBank accession Number		
		ITS	TEF	RPB2
Arthrobotrys latispora	H.B. 8952	MK493125	——	——
Arthrobotrys longiphora	1.00538	MH179707	——	MH179815
Arthrobotrys lunzhangensis	CGMCC 3.20941	OK643973	OM621809	OM621810
Arthrobotrys luquanensis	CGMCC 3.20894	OM855567	OM850309	OM850303
Arthrobotrys mangrovispora	MGDW17	EU573354	——	——
Arthrobotrys megalospora	TWF800	MN013995	——	——
Arthrobotrys microscaphoides	YMF 1.00028	MF948395	MF948552	MF948476
Arthrobotrys multiformis	CBS 773.84	MH861834	——	——
Arthrobotrys musiformis	SQ77-1	AY773469	AY773411	AY773440
Arthrobotrys musiformis	1.03481	MH179783	MH179607	MH179883
Arthrobotrys nonseptata	YMF 1.01852	FJ185261	——	——
Arthrobotrys obovata	YMF 1.00011	MF948389	MF948546	MF948470
Arthrobotrys oligospora	920	AY773462	AY773404	AY773433
Arthrobotrys paucispora	ATCC 96704	EF445991	——	——
Arthrobotrys polycephala	1.01888	MH179760	MH179592	MH179862
Arthrobotrys pseudoclavata	1130	AY773446	AY773388	AY773417
Arthrobotrys psychrophila	1.01412	MH179727	MH179578	MH179832
Arthrobotrys pyriformis	YNWS02-3-1	AY773450	AY773392	AY773421
Arthrobotrys reticulata	CBS 550.63	MH858355	——	——
Arthrobotrys robusta	nefuA4	MZ326655	——	——
Arthrobotrys salina	SF 0459	KP036623	——	——
Arthrobotrys scaphoides	1.01442	MH179732	MH179580	MH179836
Arthrobotrys shizishanna	YMF 1.00022	MF948392	MF948549	MF948473
Arthrobotrys shuifuensis	CGMCC 3.19716	MT612334	OM850306	OM850300
Arthrobotrys sinensis	105-1	AY773445	AY773387	AY773416
Arthrobotrys sphaeroides	1.01410	MH179726	MH179577	MH179831
Arthrobotrys superba	127	EU977558	——	——
Arthrobotrys thaumasia	917	AY773461	AY773403	AY773432
Arthrobotrys tongdianensis	CGMCC 3.20942	OP236809	OP272509	OP272513
Arthrobotrys vermicola	629	AY773454	AY773396	AY773425
Arthrobotrys weixiensis	CGMCC 3.24984	OQ946585	OQ989310	OQ989300
Arthrobotrys xiangyunensis	YXY10-1	MK537299	——	——
Arthrobotrys yangbiensis	DLUCC 36-1	OR880382	OR882795	OR882800
Arthrobotrys yangbiensis	Y678	OR902198	OR882790	OR882805
Arthrobotrys yangjiangensis	DLUCC 124	OR880380	OR882793	OR882798
Arthrobotrys yangjiangensis	YB19	OR902196	OR882788	OR882803

Table 9.2 (continued)

Taxon	Strain Number	GenBank accession Number		
		ITS	TEF	RPB2
Arthrobotrys yunnanensis	YMF 1.00593	AY50993	——	——
Arthrobotrys zhaoyangensis	CGMCC 3.20944	OM855568	OM850310	OM850304
Dactylellina cangshanensis	CGMCC 3.19714	MK372062	MN915115	MN915114
Dactylellina copepodii	CBS 487.90	U51964	DQ999835	DQ999816
Dactylellina mammillata	CBS 229.54	AY902794	DQ999843	DQ999817
Dactylellina yushanensis	CGMCC 3.19713	MK372061	MN915113	MN915112
Drechslerella coelobrocha	FWY03-25-1	AY773464	AY773406	AY773435
Drechslerella dactyloides	expo-5	AY773463	AY773405	AY773434
Drechslerella daliensis	CGMCC 3.20131	MT592896	OK556701	OK638157
Drechslerella heterospora	YMF 1.00550	MF948400	MF948554	MF948480
Drechslerella stenobrocha	YNWS02-9-1	AY773460	AY773402	AY773431
Drechslerella xiaguanensis	CGMCC 3.20132	MT592900	OK556699	OK638159
Orbilia jesu-laurae	LQ59a	MN816816	——	——
Orbilia tonghaiensis	YMF 1.03006	NR_172397	MF948570	MF948496
Vermispora fusarina	YXJ02-13-5	AY773447	AY773389	AY773418
Vermispora leguminacea	CGMCC 6.0291	NR_173249	——	——

The best-fit optimal substitution models for ITS (GTR + I + G), TEF (SYM + I + G), and RPB2 (SYM + I + G) were calculated using jModelTest v. 2.1.10 (Posada, 2008).

Two *Vermispora* species (*V. fusarina* (YXJ02-13-5) and *V. leguminacea* (CGMCC 6.0291)) were set as outgroups. IQ-Tree v. 1.6.5 (Nguyen et al., 2015) and MrBayes v. 3.2.6 (Huelsenbeck & Ronquist, 2001) were used to infer the phylogenetic trees using maximum likelihood (ML) and Bayesian inference (BI) methods. The related parameter settings are the same as in the previous study (Zhang et al., 2023).

The trees were visualized via FigTree v. 1.3.1 (Rambaut, 2010) and edited using Microsoft PowerPoint v. 2016 (Microsoft, Washington, USA) and Adobe Photoshop CS6 software (Adobe Systems, California, USA).

9.3 Results

9.3.1 Phylogenetic Analysis

The combined ITS, TEF, and RPB2 alignment dataset consisted of 88 sequences of ITS, 62 sequences of TEF, and 64 sequences of RPB2 from *Arthrobotrys* 75 taxa, representing 69 valid species (plus our five new species), other related taxa in *Orbiliomycetes* (*Dactylellina* four taxa and *Drechslerella* seven taxa), and two outgroup taxa. The final dataset comprised 2000 characters (585 for ITS, 832 for RPB2, and 583 for TEF), among which 900 base pair (bp) are constant, 1087 bp are variable, and 886 bp are parsimony-informative.

The best-scoring ML tree was generated with a final ML optimization likelihood value of −6817.314758. Bayesian analysis (BI) was used to evaluate the Bayesian posterior probabilities with a final average standard deviation of the split frequency of 0.009092. Both ML and BI trees consistently grouped all tested nematode-trapping fungi into three major clades and five new species exhibited distinct divergence from known species. Therefore, the ML tree was chosen for presentation (Figure 9.1).

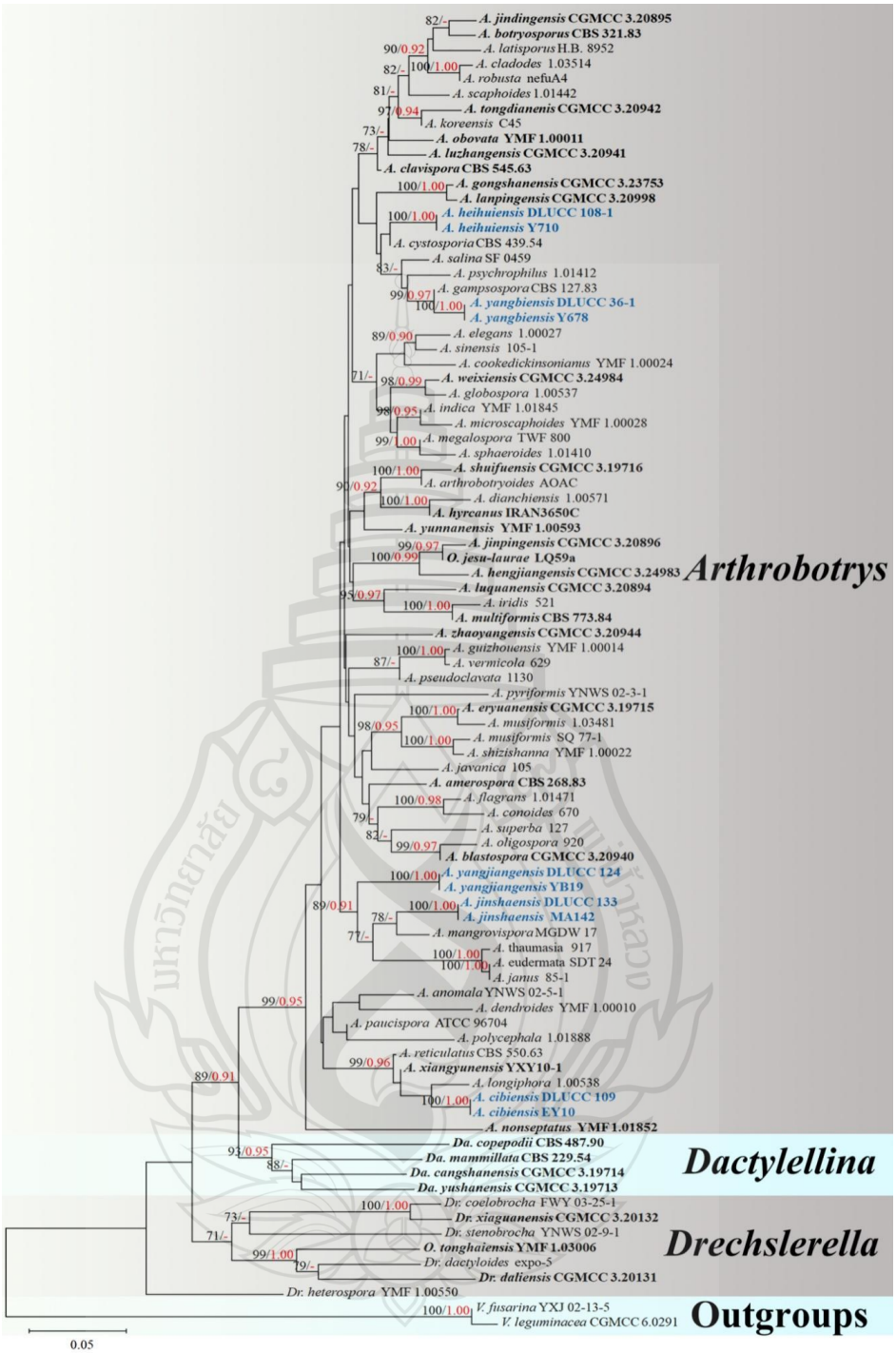

Figure 9.1 The maximum likelihood tree inferred from a combined ITS, TEF, and RPB2 dataset. The black and red numbers in front of the node indicate Bootstrap support values for maximum likelihood equal or greater than 70% and Bayesian posterior probabilities values equal or greater than 0.90, respectively. Our new isolates are in blue and the type strains are in bold

The phylogenetic tree inferred from the ITS, TEF, and *RPB2* combined dataset placed five new species in *Arthrobotrys*. The phylogenetic position of *A. heihuiensis* is uncertain but clearly diverges from known species. The two isolates of *A. yangbiensis* formed a distinct lineage basal to *A. gampsospora* with 99% MLBS and 0.97 BYPP support. Furthermore, *A. yangjiangensis* and *A. jinshaensis* clustered together with *A. mangrovispora, A. thaumasia, A. eudermata*, and *A. janus* with 89% MLBS and 0.91 BYPP support. *Arthrobotrys cibiensis* formed a distinct lineage basal to *A. longiphora, A. xiangyunensis*, and *A. reticulatus* with 99% MLBS and 0.96 BYPP support (Figure 9.1).

9.3.2 Taxonomy

Arthrobotrys cibiensis F. Zhang, S. Boonmee, and X.Y. Yang sp. nov. (Figure 9.2)

Index Fungorum number: IF901486; Facesoffungi number: FOF14174

Etymology: The species name "*cibiensis*" refers to the name of the sample collection site: Cibi Lake, Eryuan County, Dali City, Yunnan Province, China.

Material examined: China, Yunnan Province, Dali City, Eryuan County, Cibi Lake, N 26°9′7.14″, E 99°56′32.72″, from freshwater sediment, 4 June 2013, F. Zhang. Holotype CGMCC 3.20970, preserved in the China General Microbiological Culture Collection Center. Ex-type culture DLUCC 109, preserved in the Dali University Culture Collection. Additional specimen examined: China, Yunnan Province, Dali City, Eryuan County, Cibi Lake, N 26°9′7.14″, E 99°56′32.72″, from freshwater sediment, 4 June 2013, F. Zhang. Living culture EY10, preserved in germplasm resources center of Institute of Eastern-Himalaya Biodiversity Research, Dali University.

Culture characteristics: *Colonies* on PDA white, cottony, reaching 60 mm diameter after 10 days at 26°C. *Hypha* composed of septate, branched, smooth, and hyaline. *Conidiophores* erect, septate, hyaline, unbranched, bearing a single conidium at the apex, 145–315.5 µm. long ($\bar{x}$ = 234.4 µm., n = 50), 4.5–7.5 µm. ($\bar{x}$ = 5.6 µm., n = 50) wide at the base, and 2–4 µm. ($\bar{x}$ = 3.1 µm., n = 50) wide at the apex. *Conidia* smooth-faced and hyaline, rounded at the apex and truncated at the base, 26.5–46 × 13.5–23 µm. ($\bar{x}$ = 37.1 × 17.7 µm, n = 50), immature having drop-shaped, obovate, with a super cell (the cell in the conidia significantly larger than other cells) at the apex and one to three septa (mostly two-septate) at the base of the conidia; mature conidia sub-fusiform, 2–3-septate (mostly three-septate, one septum at the apex and two septa at the base), with a super cell at the

middle of the conidia. Conidia germinate from the small cells at both ends and the super cells never germinate. Catching nematodes with *adhesive networks*. *Chlamydospores* 9–35.5 × 6.5–13 µm. ($\bar{x}$ = 16.2 × 10.1 µm, n = 50), smooth-faced and hyaline, cylindrical, globose or ellipsoidal, hyaline, and in chains when present.

Notes: The phylogenetic analyses revealed that *A. cibiensis* are grouped within a clade of *A. longiphora*, *A. reticulatus*, and *A. xiangyunensis* with 99% MLBS and 0.96 BYPP support (Figure 9.1). A comparison of the ITS nucleotides indicates that *A. cibiensis* differs from *A. longiphora* (11.8% (56/473 bp)), *A. reticulatus* (3.0% (25/834 bp)), and *A. xiangyunensis* (3.1% (24/768 bp)), respectively. However, *A. cibiensis* produces conidia with no more than three septa, while *A. longiphora*, *A. xiangyunensis*, and *A. reticulatus* produce four or five-septate conidia. In addition, the conidia of *A. cibiensis* are significantly smaller than these three species (*A. cibiensis*, 26.5–46 (37.1) × 13.5–23 (17.7) µm. versus *A. longiphora*, 40–90 (54) × 15–27.5 (18) µm. versus *A. xiangyunensis*, 27–72 (55.8) × 14.5–28.5 (21.9) µm. versus *A. reticulatus*, 50–65 × 20–25 µm.) (Peach, 1950; Liu et al., Zhang & Hyde, 2014).

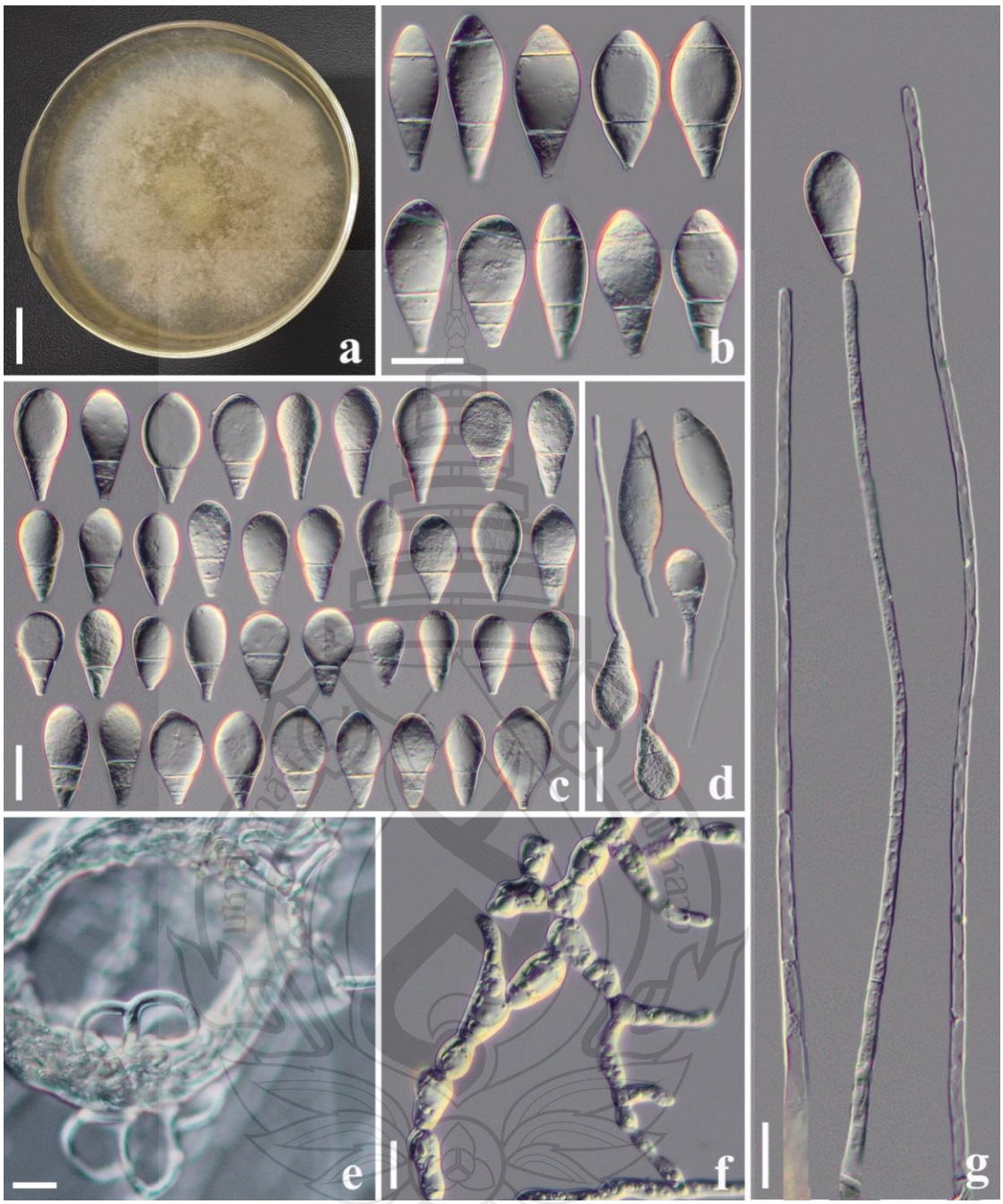

Figure 9.2 *Arthrobotrys cibiensis* (CGMCC 3.20970). (a) Colony. (b) Mature conidia. (c) Immature conidia. (d) Germinating conidia. (e) Adhesive networks. (f) Chlamydospores. (g) Conidiophores. Scale bars: (a) = 1 cm., (b–g) = 20 μm.

Arthrobotrys heihuiensis F. Zhang, S. Boonmee, and X.Y. Yang sp. nov. (Figure 9.3)

Index Fungorum number: IF901485; Facesoffungi number: FOF14175

Etymology: The species name "*heihuiensis*" refers to the Heihui River, the alias of the Yangbi River, where the species was first collected.

Material examined: China, Yunnan Province, Dali City, Yangbi County, Heihui River, N 25°37′4.13″, E 100°1′52.06″, from freshwater sediment, 6 April 2018, F. Zhang. Holotype CGMCC 3.20967, preserved in the China General Microbiological Culture Collection Center. Ex-type culture DLUCC 108-1, preserved in the Dali University Culture Collection. Additional specimen examined: China, Yunnan Province, Dali City, Yangbi County, Heihui River, N 25°37′4.13″, E 100°1′52.06″, from freshwater sediment, 6 April 2018, F. Zhang. Living culture Y710, preserved in germplasm resources center of Institute of Eastern-Himalaya Biodiversity Research, Dali University.

Culture characteristics: *Colonies* on PDA white, cottony, reaching 55 mm diameter after 10 days at 26°C. *Hypha* composed of septate, branched, smooth, hyaline. *Conidiophores* erect, septate, unbranched or occasionally producing a long branch, each branch produces several clusters of short denticles (1–3 denticles, mostly 1) by repeated elongation, each short denticle bear a single conidium, 360–720 µm. long ($\bar{x}$ = 561.3 µm., n = 50), 3.5–6.5 µm. ($\bar{x}$ = 5 µm., n = 50) wide at the base, 1.5–3.5 µm. ($\bar{x}$ = 2.3 µm., n = 50) wide at the apex. *Conidia* two types: *macroconidia* 31–56 × 6.5–14.5 µm. ($\bar{x}$ = 45.4 × 11.5 µm, n = 50), hyaline, clavate or sub-fusiform, rounded at the apex, constricted and truncated at the base, 2–5-septate (mostly three-septate, one septum at the apex and two septa at the base), with a super cell at the middle. *Microconidia* 18.5–26.5 × 5–9.5 µm. ($\bar{x}$ = 20.2 × 6.7 µm, n = 50), hyaline, smooth-faced, clavate or drop-shaped, rounded at the apex and truncated at the base, 0–2-septate (mostly zero or one-septate), producing with micro-cycle conidiation. Macroconidia germinate from the small cells at both ends, and the super cells never germinate. Catching nematodes with *adhesive networks*. *Chlamydospores* 7–30 × 6–12.5 µm. ($\bar{x}$ = 16.2 × 9.3 µm, n = 50), hyaline, smooth-faced, cylindrical, globose or ellipsoidal, in chains when present.

Notes: Phylogenetically, *A. heihuiensis* is sister to *A. cystosporia* but lacking in statistical support (Figure 9.1). Of all *Arthrobotrys* species, the morphological characteristics of *A. heihuiensis* are relatively unique and only *A. scaphoides* may be confused with *A. heihuiensis* but there are several obvious differences between them: (1)

the conidia of *A. heihuiensis* usually scattered on the short denticles of the conidiophores, while the conidia of *A. scaphoides* are usually clustered on the node of the short branch produced by conidiophores; and (2) *A. scaphoides* produces five or six-septate conidia, while the conidia of *A. heihuiensis* have no more than four septa. Additionally, the conidia of *A. heihuiensis* are obviously smaller than that of *A. scaphoides* (*A. heihuiensis*, 31–56 (45.4) × 6.5–14.5 (11.5) µm. versus *A. scaphoides*, 36.6–79.3 (57) × 11–17.5 (14) µm.); (3) *A. heihuiensis* produces clavate or drop-shaped, zero to two-septate microconidia, while *A. scaphoides* does not produce microconidia (Peach, 1952; Zhang et al., 2010Zhang & Hyde, 2014).

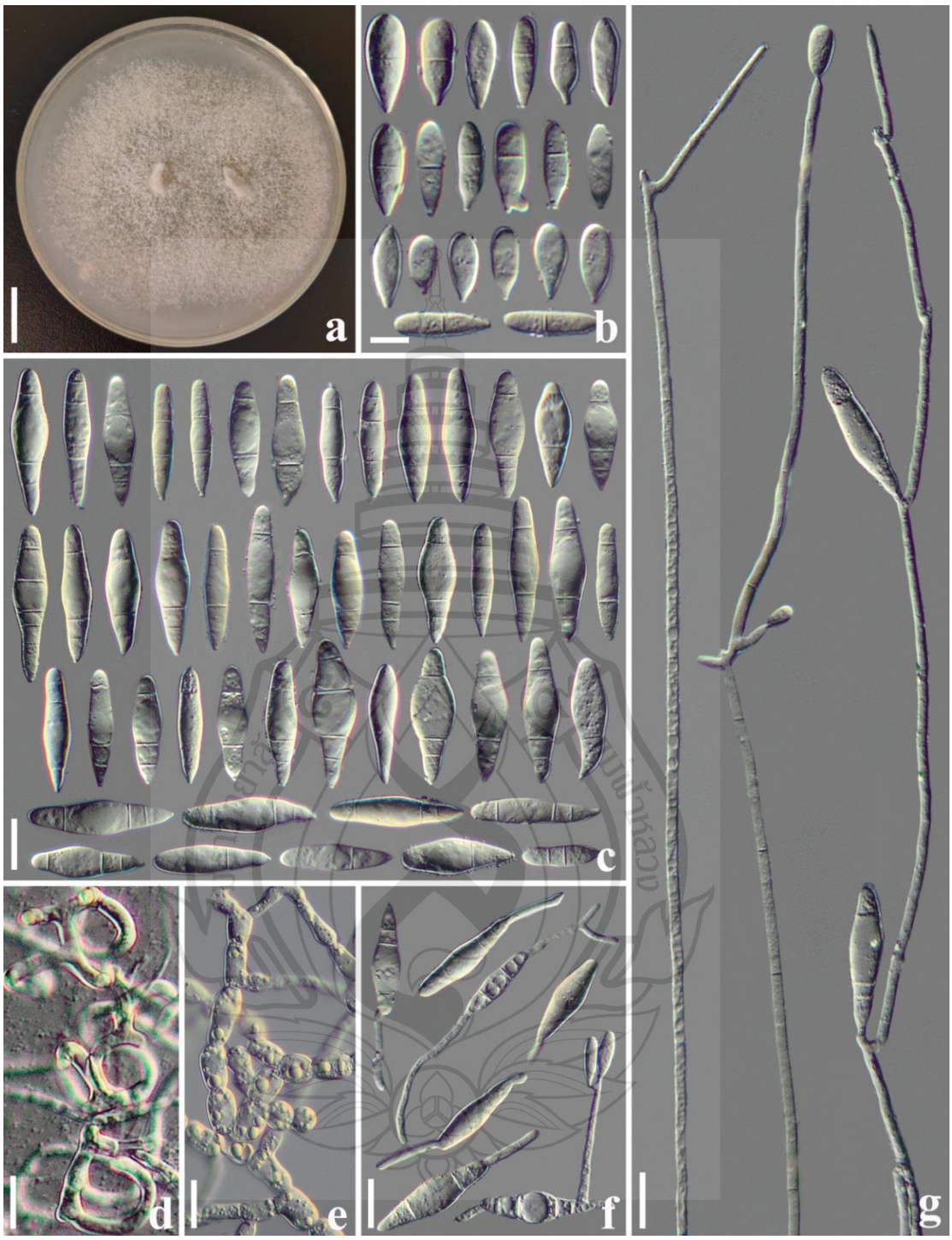

Figure 9.3 *Arthrobotrys heihuiensis* (CGMCC 3.20967). (a) Colony. (b) Microconidia. (c) Macroconidia. (d) Adhesive networks. (e) Chlamydospores. (f) Germinating conidia. (g) Conidiophores. Scale bars: (a) = 1 cm., (b) = 10 µm., (c–g) = 20 µm.

Arthrobotrys jinshaensis F. Zhang, S. Boonmee and X.Y. Yang sp. nov. (Figure 9.4)

Index Fungorum number: IF901489; Facesoffungi number: FOF14176

Etymology: The species name "*jinshaensis*" refers to the name of sample collection site: Jinsha River, Jinjiang Town, Shangri-La City, Yunnan Province, China.

Material examined: China, Yunnan Province, Shangri-La City, Jinjiang Town, Jinsha River, N 27°8′50.56″, E 99°49′39.43″, from freshwater sediment, 9 July 2014, F. Zhang. Holotype CGMCC 3.20969, preserved in the China General Microbiological Culture Collection Center. Ex-type culture DLUCC 133, preserved in the Dali University Culture Collection. Additional specimen examined: China, Yunnan Province, Shangri-La City, Jinjiang Town, N 27°8′50.56″, E 99°49′39.43″, from freshwater sediment, 9 July 2014, F. Zhang. Living culture MA142, preserved in germplasm resources center of Institute of Eastern-Himalaya Biodiversity Research, Dali University.

Culture characteristics: *Colonies* on PDA white, cottony, reaching 55 mm diameter after 10 days at 26°C. *Hypha* composed of septate, branched, smooth, hyaline. *Conidiophores* erect, septate, hyaline, unbranched or occasionally producing one to four short branches near the apex and bearing one to four conidia, 130–357 µm. long ($\bar{x}$ = 246.3 µm., n = 50), 3.5–6 µm. ($\bar{x}$ = 4.8 µm., n = 50) wide at the base, 2–4 µm. ($\bar{x}$ = 3.1 µm., n = 50) wide at the apex. *Conidia* smooth-faced and hyaline, rounded at the apex and truncated at the base, 14.5–57 × 7.5–23 µm. ($\bar{x}$ = 36.6 × 14.7 µm, n = 50), immature conidia drop-shaped, obovate, clavate, with a super cell at the apex and one to two septa (mostly two-septate) at the base; mature conidia sub-fusiform, clavate, two to four-septate (mostly three-septate, one septum located at the apex and two septa at the base of the conidia), with a super cell at the middle of the conidia. Conidia germinate from the small cells at both ends, and the super cells never germinate. Catching nematodes with *adhesive networks*. *Chlamydospores* 9.5–21.5 × 5.5–9 µm. ($\bar{x}$ = 14.8 × 7.2 µm, n = 50), smooth-faced and hyaline, cylindrical, globose or ellipsoidal, in chains when present.

Notes: Phylogenetically, *A. jinshaensis* clusters together with *A. yangjiangensis*, *A. mangrovispora*, *A. thaumasia*, *A. eudermata*, and *A. janus* with 89% MLBS and 0.91 BYPP support (Figure 9.1). There are 7.9% (49/622 bp), 7.3% (43/586 bp), 7.6% (46/607 bp), 8.2% (50/611 bp), and 8% (46/577 bp) differences between *A. jinshaensis* and *A. yangjiangensis*, *A. mangrovispora*, *A. thaumasia*, *A. eudermata*, and *A. janus* in ITS sequences, respectively. Morphologically, *A. jinshaensis*, *A. mangrovispora*, *A.*

megalospora, *A. microscaphoides*, *A. obovata*, *A. oudemansii,* and *A. psychrophila* all produced conidiophores with short branches at the apex. However, *A. jinshaensis* can be easily distinguished from *A. megalospora*, *A. microscaphoides*, *A. obovata*, *A. oudemansii,* and *A. psychrophila* by its clavate, subfusiform, irregularly constricted, two to four-septate conidia (Zhang & Hyde, 2014). In comparison, *A. jinshaensis* is more similar to *A. mangrovispora* in its variable conidia. The main difference between *A. jinshaensis* and *A. mangrovispora* is that the conidia of *A. jinshaensis* are one to four-septate and mostly three-septate, while the conidia of *A. mangrovispora* are one to three-septate and mostly two-septate. Furthermore, a single conidiophores of *A. mangrovispora* may bear one to six conidia, while the conidiophore of *A. jinshaensis* bear no more than four conidia (Swe et al., 2008; Zhang & Hyde, 2014).

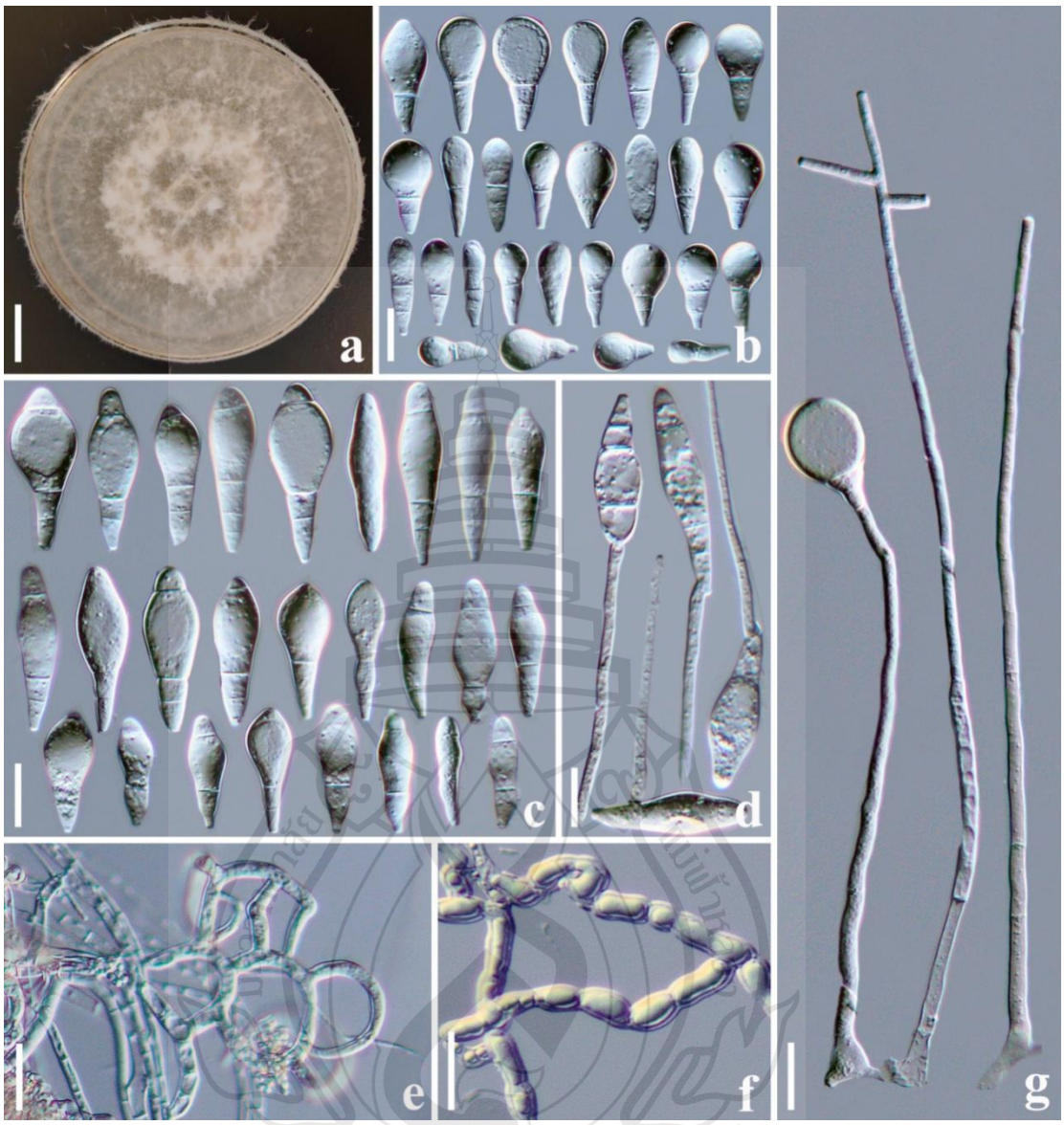

Figure 9.4 *Arthrobotrys jinshaensis* (CGMCC 3.20969). (a) Colony. (b) Immature conidia. (c) Mature conidia. (d) Germinating conidia. (e) Adhesive networks. (f) Chlamydospores. (g) Conidiophores. Scale bars: (a) = 1 cm., (b–g) = 20 µm.

Arthrobotrys yangbiensis F. Zhang, S. Boonmee, and X.Y. Yang sp. nov. (Figure 9.5)

Index Fungorum number: IF901487; Facesoffungi number: FOF14177

Etymology: The species name "*yangbiensis*" refers to the name of sample collection site: Yangbi County, Dali City, Yunnan Province, China.

Material examined: China, Yunnan Province, Dali City, Yangbi County, Yangbi River, N 25°42′37.94″, E 99°54′52.15″, from freshwater sediment, 4 April 2018, F. Zhang. Holotype CGMCC 3.24985, preserved in the China General Microbiological Culture Collection Center. Ex-type culture DLUCC 36-1, preserved in the Dali University Culture Collection. Additional specimen examined: China, Yunnan Province, Dali City, Yangbi County, Yangbi River, N 25°42′37.94″, E 99°54′52.15″, from freshwater sediment, 4 April 2018, F. Zhang. Living culture Y678, preserved in germplasm resources center of Institute of Eastern-Himalaya Biodiversity Research, Dali University.

Culture characteristics: *Colonies* on PDA white, cottony, reaching 40 mm diameter after 10 days at 26°C. *Hypha* composed of septate, branched, smooth, and hyaline. *Conidiophores* erect, septate, hyaline, unbranched or sometimes branched at the upper half part, producing a cluster of short denticles (2–5) at the apex or producing several clusters of short denticles by repeated elongation, 210–365 µm. long ($\bar{x}$ = 284.7 µm., n = 50), 3–5.5 µm. ($\bar{x}$ = 3.9 µm., n = 50) wide at the base, and 1.5–3.5 µm. ($\bar{x}$ = 2.4 µm., n = 50) wide at the apex. *Conidia* 40.5–73 × 8.5–18 µm. ($\bar{x}$ = 55.4 × 13.6 µm, n = 50), elongate–fusiform or clavate, some conidia curved, hyaline, smooth-faced, two to five-septate (mostly three or four-septate), with a super cell at the middle or apex of the conidia, and some conidia produce coiled filamentous appendages. Conidia germinate from the small cells at both ends and the super cells never germinate. They capture nematodes with *adhesive networks*. *Chlamydospore* not observed.

Notes: The phylogenetic analyses revealed that *A. yangbiensis* is sister to *A. gampsospora* with 99% MLBS and 0.97 BYPP support (Figure 9.1). *Arthrobotrys yangbiensis* is 14.7% (118/798 bp) different from *A. gampsospora* in ITS sequences. In morphology, *A. yangbiensis* shares some morphological features of short denticle conidiophores and sub-fusiform, curved conidia with *A. gampsospora* but they differ in shape and size of microconidia. In addition, the conidiophores of *A. yangbiensis* produce several clusters of short denticles by repeated elongation or geniculate branches of conidiophores, and bear several clusters of conidia, while *A. gampsospora* bears a single cluster of conidia at the apex of conidiophores (Drechsler, 1962; Zhang & Hyde, 2014).

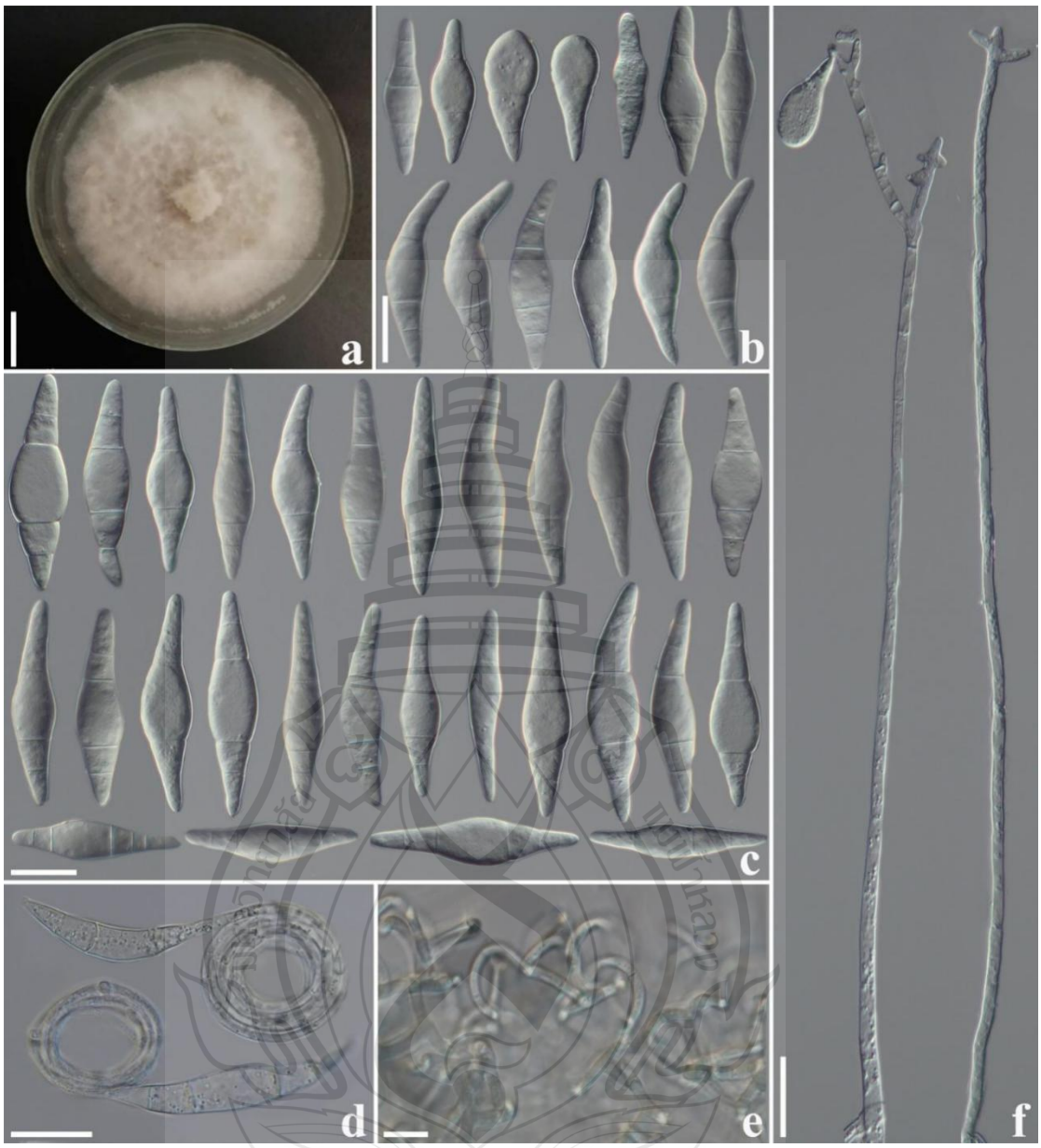

Figure 9.5 *Arthrobotrys yangbiensis* (CGMCC 3.20943). (a) Colony. (b, c) Conidia. (d) Conidia with filamentous appendages. (e) Adhesive networks. (f) Conidiophores. Scale bars: (a) = 1 cm., (b–f) = 20 μm.

Arthrobotrys yangjiangensis F. Zhang, S. Boonmee, and X.Y. Yang sp. nov. (Figure 9.6)

Index Fungorum number: IF901488; Facesoffungi number: FOF14178

Etymology: The species name "*yangjiangensis*" refers to the name of the sample collection site: Yangjiang Town, Yangbi County, Dali City, Yunnan Province, China.

Material examined: China, Yunnan Province, Dali City, Yangbi County, Yangjiang Town, Yangbi River, N 25°45′52.11″, E 99°54′46.43″, from freshwater sediment, 14 May 2018, F. Zhang. Holotype CGMCC 3.20968, preserved in the China General Microbiological Culture Collection Center. Ex-type culture DLUCC 124, preserved in the Dali University Culture Collection. Additional specimen examined: China, Yunnan Province, Dali City, Yangbi County, Yangjiang Town, Yangbi River, N 25°45′52.11″, E 99°54′46.43″, from freshwater sediment, 14 May 2018, F. Zhang. Living culture YB19, preserved in germplasm resources center of Institute of Eastern-Himalaya Biodiversity Research, Dali University.

Culture characteristics: *Colonies* on PDA white, cottony, reaching 55 mm diameter after 10 days in the incubator at 26°C. *Hypha* composed of septate, branched, smooth, and hyaline. *Conidiophores* erect, septate, hyaline, unbranched, bearing a single conidium at the apex, 198–537 µm. long ($\bar{x}$ = 409.4 µm., n = 50), 3–5.5 µm. ($\bar{x}$ = 4.7 µm., n = 50) wide at the base, and 2–3.5 µm. ($\bar{x}$ = 2.6 µm., n = 50) wide at the apex. *Conidia* smooth-faced and hyaline, rounded at the apex and truncated at the base, 24.5–47 × 14.5–29.5 µm. ($\bar{x}$ = 36.2 × 23.2 µm, n = 50), immature conidia drop-shaped, obovate, with a super cell at the apex and one to two septa (mostly two-septate) at the base; mature conidia broad fusiform, two to three-septate (mostly three-septate, one septum at the apex and two septa at the base), with a super cell at the middle of the conidia. Conidia germinate from the only small cells at both ends, and the super cells never germinate. Catching nematodes with *adhesive networks*. *Chlamydospores* 8.5–24 × 7–13.5 µm. ($\bar{x}$ = 14 × 10 µm, n = 50), smooth-faced and hyaline, cylindrical, globose or ellipsoidal, hyaline, and in chains when present.

Notes: Phylogenetically, *A. yangjiangensis* formed a basal lineage with *A. jinshaensis* (another new species reported in this study), *A. mangrovispora*, *A. thaumasia*, *A. eudermata*, and *A. janus* with 89% MLBS and 0.91 BYPP support (Figure 9.1). A comparison of ITS nucleotides reveled *A. yangjiangensis* was 7.9% (49/622 bp), 12.2%

(92/754 bp), 7% (42/604 bp), 9.4% (75/795 bp), and 6.3% (36/573 bp) different from *A. jinshaensis*, *A. mangrovispora*, *A. thaumasia*, *A. eudermata,* and *A. janus*, respectively. Morphologically, *A. yangjiangensis* can be easily distinguished from *A. jinshaensis* and *A. janus* by its conidial shape with drop-shaped, broad fusiform, two to three-septate conidia (Li et al., 2003; Zhang & Hyde, 2014). The distinguishing characteristics between *A. yangjiangensis*, *A. mangrovispora*, and *A. thaumasia* is that the conidiophores of *A. yangjiangensis* bear only one single conidium at the apex, while the conidiophores of the latter two species produce several short denticles at the apex and bear multiple conidia (Drechsler, 1937; Swe et al., 2008; Zhang & Hyde, 2014). By contrast, *A. yangjiangensis* is more similar to *A. eudermata* in its simple conidiphores and broad fusiform conidia. However, the conidia of *A. yangjiangensis* are noticeably smaller than those of *A. eudermata* (*A. yangjiangensis*, 2.5–4 (36.2) × 14.5–29.5 (23.2) µm. versus *A. eudermata*, 37–55 (49) × 17.5–35 (28) µm.). Furthermore, *A. eudermata* produces ellipsoid, aseptate microconidia, whereas *A. yangjiangensis* does not (Drechsler, 1950; Zhang & Hyde, 2014).

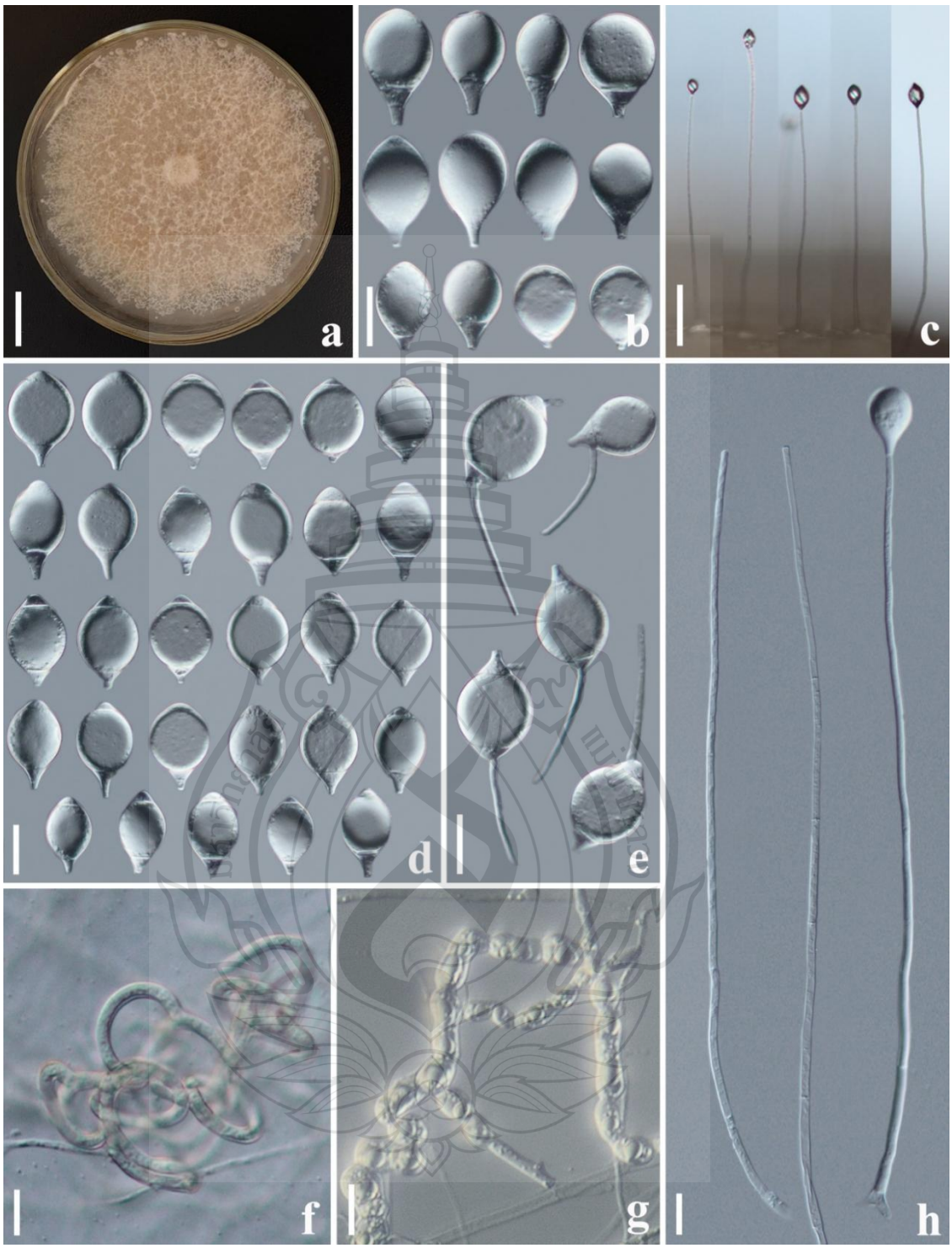

Figure 9.6 *Arthrobotrys yangjiangensis* (CGMCC 3.20968). (a) Colony. (b) Immature conidia. (d) Mature conidia. (e) Germinating conidia (f) Adhesive networks. (g) Chlamydospores. (c, h) Conidiophores. Scale bars: (a) = 1 cm., (b, d–h) = 20 µm., (c) = 100 µm.

9.4 Discussion

Among the 130 species (plus our five new species) of *Orbiliomycetes* nematode-trapping fungi (NTF), 61 species have distribution records in freshwater habitats. Among these species, 17 species were first isolated from freshwater habitats. To date, *A. hyrcanus*, *A. blastospora*, *A. dainchiensis*, *A. eryuanensis*, *A. hengjiangensis* and five new species reported in this study were exclusively found in freshwater environments (Hao et al., 2004, 2005; Swe et al., 2009; Liu et al., 2014; Tarigan et al., 2020; Zhang et al., 2022). These findings collectively emphasize that freshwater NTF are an important component of NTF diversity. Hence, future studies on NTF diversity should fully consider the significance of freshwater habitats.

The five newly identified species presented were all derived from sediment samples in water depths of less than 2 m. Previous investigations have demonstrated the absence of NTF beyond a water depth of 4 m (Hao et al., 2005). However, abundant aquatic nematodes still exist in deeper waters (Ptatscheck & Traunspurger, 2020; de Jesús-Navarrete et al., 2022). At such depths, there must be other nematode regulators to perform the function of aquatic nematode population regulation instead of NTF. Accordingly, it is speculated that more novel nematophagous microorganisms may be discovered in deeper waters employing efficacious research methodologies. The exploration and examination of these enigmatic nematophagous microorganisms hold the potential to provide valuable insights into the origins and evolutionary processes of carnivorous microorganisms, while also offering promising prospects for the biological control of detrimental nematodes.

It is generally believed that aquatic NTF originate from terrestrial ecosystems. However, unlike terrestrial environments, NTF face numerous challenges in aquatic habitats. For instance, the interaction between NTF and nematodes relies on processes such as host recognition, generation of trapping structures, invasion and digestion of nematode, etc. These processes are more or less dependent on the transmission of extracellular signaling factors (Tunlid & Ahrén, 2011; Hsueh et al., 2013; Kuo et al., 2020). However, in aquatic environments, these extracellular signaling molecules are likely to be diluted and lose their corresponding functions. Consequently, how aquatic NTF prey on nematodes in water, how they maintain osmotic balance in water, and how they reproduce and spread in

water remain unresolved questions in the field. Investigating these questions cannot only deepen our understanding of fungal adaptive evolution but also constitutes an important aspect of the study on the origin and evolution of these extraordinary organisms.

CHAPTER 10

BURNED FORESTS AS POTENTIAL SITES FOR DISCOVERY OF NEW FUNGI: MORPHO-PHYLOGENETIC EVIDENCE WITH FIFTEEN NEW SPECIES OF NEMATODE-TRAPPING FUNGI (*ORBILIOMYCETES*)

10.1 Introduction

Fungi, integral components of ecosystems, hold a crucial role in ecological processes, including the cycling of materials and energy, preservation of ecological balance, and driving the evolution of plants and animals (Dix, 2012; Krings et al., 2012; Treseder & Lennon, 2015, Lindahl & Clemmensen, 2016; Niego et al., 2023a). Simultaneously, fungi function as significant pathogens for animals and plants, potential agents for pest and disease control, and vital sources of human food and medicine. Therefore, fungi are intricately linked with human production and livelihoods (Butt et al., 2001; Grau et al., 2004; Bongomin et al., 2017; Strong et al., 2022; Niego et al., 2023b). Hence, a comprehensive understanding of fungal diversity serves as a basis for preserving ecological stability, managing detrimental fungi, and engaging in the sustainable utilization of beneficial fungal resources.

Approximately 2.2–3.8 million fungal species are believed to exist (Hawksworth & Lücking, 2017). So far, only around 160,000 species have been described (Hyde et al., 2020; Bhunjun et al., 2022). This indicates that our knowledge on over 95% of fungi is limited or nonexistent. The exploration of these undiscovered species poses a considerable challenge for mycologists and biodiversity experts. One key issue is how and where to discover these undescribed species (Hawksworth & Rossman, 1997; Troussellier et al., 2017). Generally, fungi that can be easily isolated tend to belong to dominant groups characterized by higher biomass, whereas a

substantial portion of the 95% of unidentified fungi appear to be rare species. The lower population densities of these uncommon species make them challenging to isolate and cultivate, primarily because dominant species suppress them through competition (Foster & Bell, 2012). From an ecological standpoint, unlocking the competitive suppression imposed by dominant groups on these apparently rare species could be the pivotal factor in accessing a greater abundance of uncommon fungi.

Soil is one of the largest reservoirs of microorganisms and harbours an incredibly rich fungal resource (Serna-Chavez et al., 2013; Fierer, 2017). In soil, dominant fungi typically inhabit the upper layers, where essential resources like nutrients, water, and air are plentiful, whereas rare fungi are distributed in the lower layers (She et al., 2020). The inherent vertical distribution disparity offers a natural advantage in mitigating the competitive suppression exerted by dominant groups on rare species. Forest fires, common natural occurrences on Earth, play a crucial role as ecological regulators (Giglio et al., 2006). During a fire, the soil's surface temperature can reach as high as 50–1500°C (Bruns et al., 2020), rapidly eliminating dominant microorganisms in the top-soil. Due to the low thermal conductivity of soil, rare microorganisms in the lower soil layers are less affected by the high temperatures and are thus preserved (Certini et al., 2021). Therefore, forest fires serve as an effective method for alleviating the competitive suppression of rare fungi by dominant ones.

From the aforementioned information, we hypothesize that samples obtained from burned forests may exhibit a higher prevalence of rare fungi and harbour novel species. To verify this hypothesis, we focused on nematode-trapping fungi (NTF, *Orbilimycetes*, *Orbiliaceae*), a group characterized by moderate taxonomic diversity (3 genera, 130 species) and well-established research methods, demonstrating substantial application and research significance (Yang et al., 2007; Zhang & Hyde, 2014; Jiang et al., 2017; Soliman et al., 2021). We isolated and identified NTF from three burned forests, resulting in the identification of 21 novel species of rare NTF, six of which have been published in previous studies (Zhang et al., 2020b; Zhang et al., 2022b; Zhang et al., 2023b), and the remaining 15 new species are described in detail herein. In addition, the fungal diversity in burned forests is discussed, highlighting a promising avenue for discovering more rare microorganisms.

10.2 Material and Methods

10.2.1 Soil Sample Collection

The soil samples used in this study were collected from three burned forests located in Yunnan Province, China (Wanqiao, Yunlong and Yushan) (Table 10.1). The surface litter and large particles were removed prior to collecting soil cores. A soil core (0–20 cm. deep) was collected with a sterilized soil borer (50 mm-diameter). Each soil core was divided into two distinct samples: the first sample represented the upper 10 cm., while the second sample represented the lower 10–20 cm.. These samples were placed into separate sterile sample bags with identifying marks. All collected samples were transported to the laboratory, and subsequent processing was finalized within a week.

Table 10.1 Sampling area information

Sample area	Coordinate	Ignition time	Burned area (acre)	Original vegetation	Sampling time	Sampling sites number	Samples number
Wanqiao	N 25°47'58.48" E 100°6'11.48"	May 2021	720	Yunnan pines	June 16, 2021	10	20
Yunlong	N 25°51'22.50" E 99°13'38.43"	March 2014	4200	Yunnan pines	March 6, 2018	160	320
Yushan	N 25°37'09.37" E 100°09'02.39"	April 2017	500	Yunnan pines	March 24, 018	14	28

10.2.2 Fungal Isolation and Purification

The soil samples underwent a thorough mixing process, and 3–5 g of the sample was evenly spread on the surface of a corn meal agar plate (CM.A) using sterile toothpicks following previous studied (Drechsler, 1941; Duddington, 1955; Eren & Pramer, 1965; Zhang & Hyde, 2014). *Panagrellus redivivus* Goodey (free-living nematodes) cultured on oatmeal medium (Zhang & Hyde, 2014) were isolated using the Baermann Funnel method (Staniland, 1954) and the concentration was adjusted with sterile water to 4000–5000 nematodes per milliliter. 1 ml of nematode suspension

were added to each plate to stimulate the germination of nematode-trapping fungi (NTF) in the soil (Zhang & Hyde, 2014). The plates were then placed in a light-free incubator at 26°C. Over the course of 3rd, 4th, and 5th weeks, the plates were examined under a stereomicroscope to locate the spores of NTF. Single spore of NTF was transferred to a fresh CM.A plate using a sterile toothpick (Zhang et al., 2022a), and incubated at 26 °C for one week. The process of single spore isolation was repeated until a pure culture was obtained (Figure 10.1).

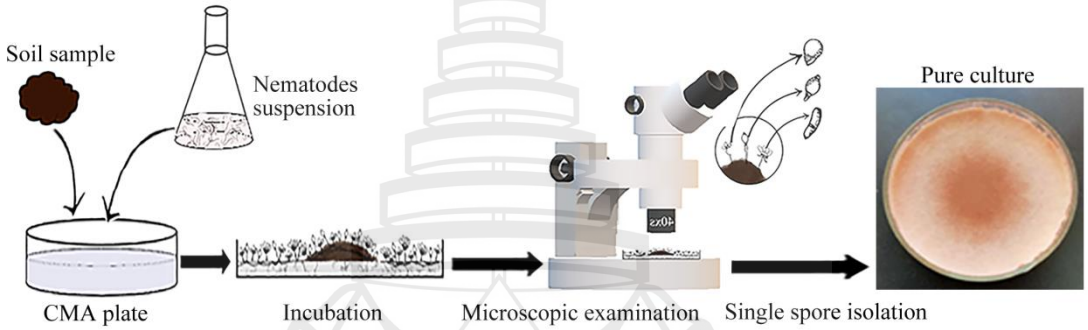

Figure 10.1 NTF isolation and purification processes

10.2.3 Morphological Observation

The pure culture was transferred onto fresh potato dextrose agar (PDA) and CM.A plates (with a sterile cover glass inserted obliquely and a 2 × 2 cm. observation well was created by removing agar from the center of the plate) using sterile toothpicks and incubate at 26℃. Once the mycelia overspread the cover glass, the cover glass was gently removed with tweezers and a temporary slide was prepared using sterile water. Morphological characteristics such as conidia, conidiophores and chlamydospores were photographed and measured with an Olympus BX53 microscope under differential interference mode (Olympus Corporation, Japan). Once the mycelia overspread the observation well, a drop of nematode suspension (*P. redivivus*, 500–1000 nematodes) was added to the center of the well to induce the formation of trapping structures. After incubating at 26℃ for 2–5 days, the types of trapping structure were checked and photographed using an Olympus BX53 microscope (Olympus Corporation, Japan).

10.2.4 DNA Extraction, PCR Amplification, and Sequencing

The pure culture was inoculated onto a fresh PDA plate and incubated at 26°C. The mycelia was harvested using a sterile scalpel. Genomic DNA extraction was performed using a rapid fungal genomic DNA isolation kit (Sangon Biotech Company, Limited, Shanghai, China). The primers pairs ITS4-ITS5 (White et al., 1990), 526F-1567R (O'Donnell et al., 1998), and 6F-7R (Liu et al., 1999) were respectively used to amplify the ITS, TEF, and RPB2 regions with reaction conditions and systems described in previous publications (Zhang et al., 2023a). The PCR products were then purified using a DiaSpin PCR Product Purification Kit (Sangon Biotech Company, Limited, Shanghai, China). The ITS and RPB2 regions were sequenced in the forward and reverse directions using PCR primers, while the TEF region was sequenced using the 247F-609R (Yang et al., 2007) primer pair (BioSune Biotech Company, Limited, Shanghai, China).

10.2.5 Phylogenetic Analysis

The newly generated sequences were checked, edited and assembled using SeqMan v. 7.0 (DNASTAR, Madison, Wisconsin, USA) (Swindell & Plasterer, 1997). They were then deposited in the GenBank database at the National Center for Biotechnology Information (NCBI; https://www.ncbi.nlm.nih.gov/, accessed on 4 December 2023) and compared against the database using BLASTn (https://blast.ncbi.nlm.nih.gov/, accessed on 13 February 2024). Initial BLASTn searches indicated that all newly generated DNA sequences belong to *Dactylellina* in *Orbiliaceae* (*Orbiliomycetes*) (Yang et al., 2007; Zhang & Hyde, 2014). Consequently, *Dactylellina* was searched in the Species Fungorum (http://www.speciesfungorum.org, accessed on 18 February 2024), and all relevant records were checked individually according to the relevant literatures to ensure that all *Dactylellina* species were considered in this study (Li et al., 2006; Su et al., 2008; Zhang & Hyde, 2014; Kavitha et al., 2020; Zhang et al., 2020b; Crous et al., 2022). All reliable ITS, TEF, and RPB2 sequences of *Dactylellina* species, as well as some related taxa were downloaded from the Genbank database (Table 10.2). The sequence alignments of the three genes were generated using MAFFT v.7 (http://mafft.cbrc.jp/alignment/server/, accessed on 21 February 2024) (Katoh & Standley, 2013). MEGA6.0 (Tamura et al., 2013) was utilized

to check, adjust and link the three alignments into a multigene dataset. *Vermispora fusarina* YXJ 02-13-5 and *V. leguminacea* CGMCC 6.0291 were selected as outgroups. Phylogenetic trees were constructed using both maximum likelihood (ML), and Bayesian inference (BI) methods. New species are established based on guidelines provided by Jeewon and Hyde (2016).

Table 10.2 The GenBank accession number of the isolates included in this study

Taxon	Strain	GenBank accession no.		
		ITS	TEF	RPB2
Arthrobotrys cookedickinson	YMF 1.00024	MF948393	MF948550	MF948474
Arthrobotrys eryuanensis	CGMCC 3.19715	MT612105	OM850307	OM850301
Arthrobotrys eudermata	SDT24	AY773465	AY773407	AY773436
Arthrobotrys gongshanensis	CGMCC 3.23753	OM801277	OM809162	OM809163
Arthrobotrys lunzhangensis	CGMCC 3.20941	OK643973	OM621809	OM621810
Dactylellina appendiculata	CBS 206.64	AF106531	DQ358227	DQ358229
Dactylellina arcuata	CBS 174.89	AF106527	DQ999852	DQ999799
Dactylellina asthenopaga	CBS 917.85	U51962	-	-
Dactylellina candida	YMF 1.00036	AY965749	-	-
Dactylellina cangshanensis	CGMCC 3.19714	MK372062	MN915115	MN915114
Dactylellina cionopaga	SQ 27-3	AY773467	AY773409	AY773438
Dactylellina cionopaga	XJ 03-9-3	AY773473	AY773415	AY773444
Dactylellina copepodii	CBS 487.90	U51964	DQ999835	DQ999816
Dactylellina dashabaensis	DLUCC146	PP971320	PP707964	PP707949
Dactylellina dashabaensis	WQ07	OR866260	OR902052	OR902037
Dactylellina dongxi	DLUCC150	PP971324	PP707968	PP707953
Dactylellina dongxi	YL209	OR866264	OR902056	OR902041
Dactylellina drechsleri	CBS 549.63	DQ999819	DQ999840	DQ999810
Dactylellina dulongensis	CGMCC 3.20945	OM956085	OP477093	OP477094
Dactylellina ellipsospora	YNWS 02-8-1	AY773458	AY773400	AY773429
Dactylellina entomopaga	CBS 642.80	AY965758	DQ358228	DQ358230
Dactylellina erhaiensis	DLUCC153	PP971327	PP707971	PP707956
Dactylellina erhaiensis	YS03	OR866267	OR902059	OR902044
Dactylellina fodingensis	DLUCC149	PP971323	PP707967	PP707952
Dactylellina fodingensis	YS79	OR866263	OR902055	OR902040
Dactylellina formosana	CCRC 32740	U51956	-	-
Dactylellina gephyropaga	CBS 585.91	AY965756	DQ999846	DQ999801
Dactylellina gephyropaga	CBS 178.37	U51974	DQ999847	DQ999802
Dactylellina haptospora	CBS 100520	DQ999820	DQ999850	DQ999814

Table 10.2 (continued)

Taxon	Strain	GenBank accession no.		
		ITS	TEF	RPB2
Dactylellina haptotyla	SQ 95-2	AY773470	AY773412	AY773441
Dactylellina haptotyla	XJ 03-96-1	DQ999827	DQ999849	DQ999804
Dactylellina hertziana	CBS 395.93	AF106519	-	-
Dactylellina huisuniana	CCRC 33444	U51965	-	-
Dactylellina lancangensis	DLUCC148	PP971322	PP707966	PP707951
Dactylellina lancangensis	YL165	OR866262	OR902054	OR902039
Dactylellina leptospora	SHY 6-1	AY773466	AY773408	AY773437
Dactylellina lobata	CBS 329.94	KT215196	-	-
Dactylellina lysipaga	YMF 1.00535	MF948399	-	MF948479
Dactylellina maerensis	DLUCC141	PP971315	PP707959	PP707944
Dactylellina maerensis	YS14	OR866255	OR902047	OR902032
Dactylellina mammillata	CBS 229.54	AY902794	DQ999843	DQ999817
Dactylellina mazongensis	DLUCC151	PP971315	PP707969	PP707954
Dactylellina mazongensis	YL264	OR866265	OR902057	OR902042
Dactylellina miaoweiensis	DLUCC145	PP971319	PP707963	PP707948
Dactylellina miaoweiensis	YL94	OR866259	OR902051	OR902036
Dactylellina miltoniae	CBS:148270	NR_185432	-	ON803537
Dactylellina multiseptatum	YMF 1.00127	AY965751	-	-
Dactylellina nanzhaoensis	DLUCC152	PP971326	PP707970	PP707955
Dactylellina nanzhaoensis	YS22	OR866266	OR902058	OR902043
Dactylellina niuzidengensis	DLUCC143	PP971317	PP707961	PP707946
Dactylellina niuzidengensis	YL39	OR866257	OR902049	OR902034
Dactylellina parvicollis	XSBN 22–1	AY804215	DQ999854	DQ999798
Dactylellina phymatopaga	CBS 325.72	KT215204	DQ999834	DQ999815
Dactylellina quercus	6175	AY773453	AY773395	AY773424
Dactylellina robusta	CBS 110125	DQ999821	DQ999851	DQ999800
Dactylellina sichuanensis	YMF 1.00023	AY902795	-	-
Dactylellina tingmingensis	DLUCC142	PP971316	PP707960	PP707945
Dactylellina tingmingensis	YS28	OR866256	OR902048	OR902033
Dactylellina varietas	YMF 1.00118	AY902805	-	-
Dactylellina wanqiaoensis	DLUCC144	PP971318	PP707962	PP707947
Dactylellina wanqiaoensis	WQ54	OR866258	OR902050	OR902035
Dactylellina wubaoshanensis	DLUCC154	PP971328	PP707972	PP707957
Dactylellina wubaoshanensis	YL349	OR866268	OR902060	OR902045
Dactylellina xinjuanii	DLUCC155	PP971329	PP707973	PP707958
Dactylellina xinjuanii	YL531	OR866269	OR902061	OR902046
Dactylellina yangxiensis	DLUCC147	PP971321	PP707965	PP707950

Table 10.2 (continued)

Taxon	Strain	GenBank accession no.		
		ITS	TEF	RPB2
Dactylellina yangxiensis	WQ114	OR866261	OR902052	OR902038
Dactylellina yunnanensis	CBS 615.95	AY965757	-	-
Dactylellina yushanensis	CGMCC 3.19713	MK372061	MN915113	MN915112
Drechslerella dactyloides	expo-5	AY773463	AY773405	AY773434
Drechslerella daliensis	CGMCC 3.20131	MT592896	OK556701	OK638157
Drechslerella pengdangensis	DL53	OQ946588	OQ989313	OQ989303
Drechslerella stenobrocha	YNWS 02-9-1	AY773460	AY773402	AY773431
Drechslerella tianchiensis	XJ353	OQ946590	OQ989315	OQ989305
Vermispora fusarina	YXJ 02-13-5	AY773447	AY773389	AY773418
Vermispora leguminacea	CGMCC 6.0291	DQ494376	-	-

JModelTest v2.1.10 (Posada, 2008) was used to assess the best-fit optimal substitution models for ITS (GTR+I+G), TEF (SYM+I), and RPB2 (GTR+I+G) genes.

Maximum likelihood (ML) analysis was performed using PhyloSuite v1.2.3 (Zhang et al., 2020a). The dataset was partitioned, and each gene was analyzed with the corresponding model. The statistical bootstrap support values (BS) were computed using rapid bootstrapping with 1000 replicates (Felsenstein, 1985).

MrBayes v. 3.2.6. (Huelsenbeck & Ronquist, 2001) was used to conduct the Bayesian inference (BI) analysis. MEGA 6.0 (Tamura et al., 2013) was used to convert the multiple sequence alignment fasta file into a MrBayes-compatible NEXUS file. The dataset was partitioned, and six simultaneous Markov chains were run for 10,000,000 generations, and trees were sampled every 100 generations. The first 25% trees were discarded, and the remaining trees were used to calculate the posterior probabilities (PP) in the majority rule consensus tree. All above parameters were edited in the MrBayes block in the NEX file.

The resulting tree was visualized with FigTree (Rambaut, 2010). The backbone tree was further edited and reorganized using Microsoft PowerPoint (2013) and Adobe Photoshop CS6 software (Adobe Systems, USA).

10.2.6 Establishing a Comprehensive Morphological Framework to Classify *Dactylellina* Species

Establishment of an appropriate taxonomic framework can enable rapid species identification, especially under circumstances where there is taxonomic confusion regarding to the use of specific morphs in species delineation. Accuracy and usability (user friendly) are two primary criteria for evaluating the quality of any taxonomic scheme to be implemented to differentiate species. Conventional taxonomy has relied upon the use of keys (especially dichotomous keys) to segregate and assist in species identification. This has previously been convenient when dealing with few species at a certain taxonomic hierarchy. However, with the discovery of more species, keys are not always appropriate and practical when dealing with speciose genera characterized by inadequate morphological variants, species that exhibit high degree of morphological similarities and overlap and where morphologies have undergone convergent evolution (especially asexual species). Species keys are occasionally complex with lengthy descriptions, often lead to subjective interpretations or misidentification especially when species do not fit into the key, cannot be used for new species and does not reflect or take evolutionary relationships into account (Zhang & Hyde, 2014; Zhang et al., 2022a).

In this study, we aimed to construct a highly accurate and user-friendly morphological taxonomy framework to *Dactylellina* species in tabular form. The logical framework for its construction is as follows: Firstly (step 1), all morphological characteristics of *Dactylellina* species that can be used for species identification were tabulated (such as trapping structure, conidiophore and conidia). Secondly (step 2), all *Dactylellina* species are classified into several groups based on clearly differentiating features. For example, all *Dactylellina* species can be divided into three groups according to their trapping structures: capture nematodes with adhesive knobs, capture nematodes with adhesive branches, and catch nematodes using non-constricting rings (which coexist with adhesive knobs). Among the group that captures nematodes with adhesive knobs, the growth pattern of conidia on the conidiophore (clustered or dispersed) can be used to differentiate them further. In this way, all *Dactylellina* species can be eventually divided into several subclasses by several well-defined morphological characteristics (each subclass may contain a single or multiple species).

Lastly (step 3), the detailed description of each species that was not detailed in step 2 was attached to each subclass to facilitate a precise comparison of all the detailed characteristics and improve the identification accuracy. Throughout the different stages of developing the taxonomic framework, it has been ensured that morphological descriptions are precise, accurate and devoid of subjective descriptions and judgments.

10.3 Results

10.3.1 Phylogenetic Analyses

Based on the records from Species Fungorum and relevant literatures (http://www.speciesfungorum.org, accessed on 18 February 2024, Li et al., 2006; Su et al., 2008; Zhang & Hyde, 2014; Kavitha et al., 2020; Zhang et al., 2020b; Crous et al., 2022), *Dactylellina* comprises a total of 36 valid species, of which molecular data is available for 31 species. Therefore, the molecular dataset used in this study include ITS (76), TEF (63), and RPB2 (65) sequences from 64 isolates representing 46 *Dactylellina* species (plus our 30 isolates of 15 new species) and related taxa in *Orbiliomycetes* (five *Arthrobotrys* species and five *Drechslerella* species). The final concatenated alignment comprised a total of 1665 characteristics (507 for ITS, 440 for TEF, and 718 for RPB2), including 843 conserved sites, 812 variable sites, and 684 parsimony informative sites.

The Maximum Likelihood (ML) analysis yielded a best-scoring tree, with a final ML optimization likelihood value of -6734.326751. For the Bayesian analysis (BI), the consensus tree was calculated using the remaining 75% of trees, and the Bayesian posterior probabilities were evaluated with a final average standard deviation of the split frequency of 0.009196. While there are slight topological differences between the ML and BI trees regarding the phylogenetic positions of *Arthrobotrys* species and certain *Dactylellina* species, both trees consistently show that all species that capture nematodes using adhesive branches within *Dactylellina* clustered together with support. Furthermore, the position of species within the subclades containing the new species remain consistent, indicating that the above mentioned minor discrepancies between the ML and BI trees did not affect the phylogenetic placement of our new species (Figure 10.2).

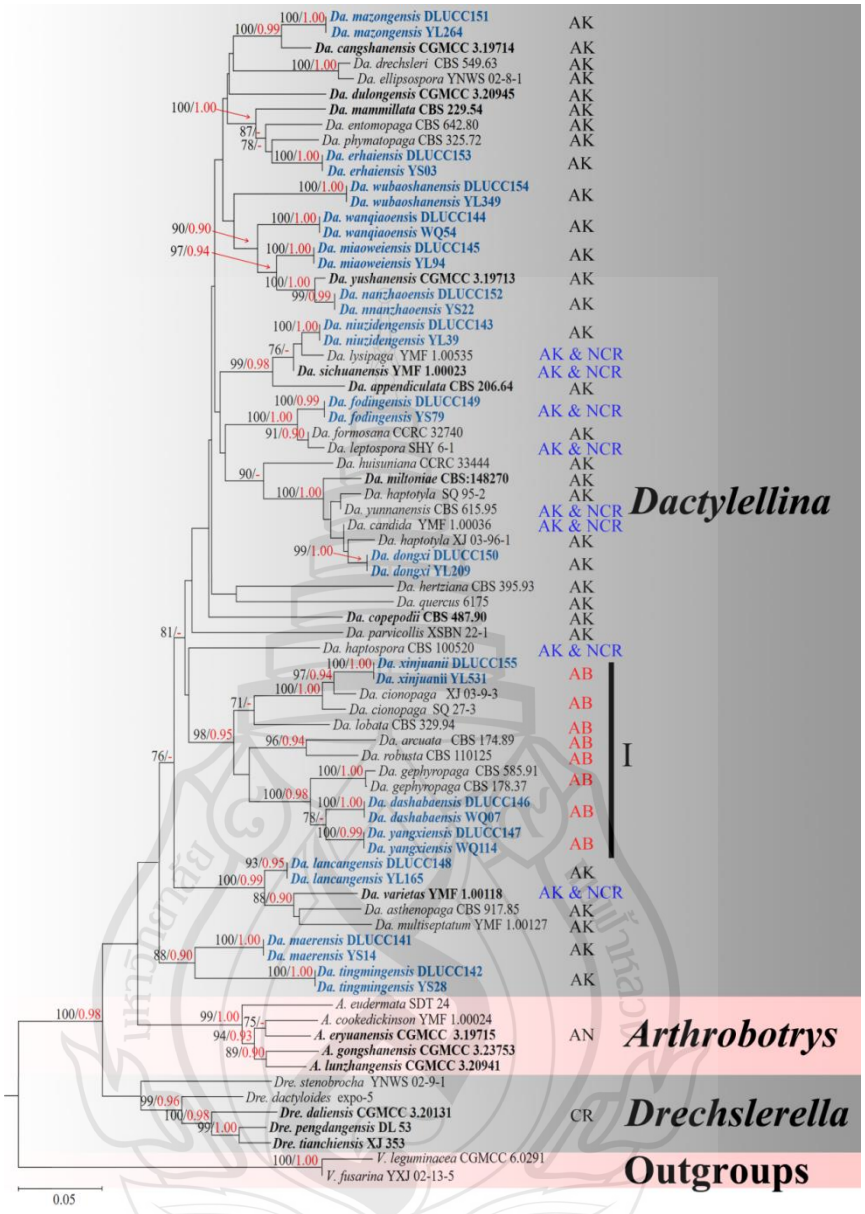

Figure 10.2 Maximum likelihood tree based on a combined ITS, TEF, and RPB2 sequence from 56 species of *Orbiliaceae* nematode-trapping fungi. Bootstrap support values for maximum likelihood (black) greater than 70% and Bayesian posterior probabilities values (red) greater than 0.90 are indicated above the nodes. The new isolates are in blue; type strains are in bold. The tree is rooted with *Vermispora fusarina* YXJ02-13-5 and *V. leguminaceae* CGMCC 6.0291. Different trapping structures labeled on tree are defined as: adhesive knobs (AK), non-constricting rings (NCR), adhesive branches (AB), adhesive networks (AN), and constricting rings (CR)

10.3.2 Taxonomy

Orbiliomycetes O.E. Erikss & Baral, Myconet 9: 96 (2003)

Orbiliales O.E. Erikss & Baral, Myconet 9: 96 (2003)

Note – *Orbiliales* is the sole order in *Orbiliomycetes* and contains a single family, *Orbiliaceae* Nannfeldt. The molecular phylogenetic studies demonstrated that *Orbiliaceae* is a monophyletic group and shares a parallel branch relationship with *Pezizales*. Eriksson et al. (2003) discovered that all *Orbiliaceae* species possess six specific signature nucleotides (CTAACC) in their SSU rDNA sequences. These findings led to the establishment of *Orbiliales* and *Orbiliomycetes* (Pfister, 1997; Eriksson et al., 2003).

Orbiliaceae Nannfeldt, Nova Acta R. Soc. Scient. upsal. Ser. 48(2): 250 (1932)

Type genus – *Orbilia* Fr. Scan. 1835

Note – *Orbiliaceae* was established by Nannfeldt in 1932 and was initially classified under *Helotiales* (Nannfeldt, 1932). According to molecular phylogenetic analyses and the identification of specific nucleotides in the SSU rDNA sequence data, *Orbiliaceae* was reclassified into the order *Orbiliales* and this reclassification restricted the family within this order (Pfister, 1997; Eriksson et al., 2003). Members of *Orbiliaceae* are a group of small cup fungi characterized by a high dioptric and morphologically diverse (spherical, teardrop-shaped, ellipsoid, or vermiform) spore body appears in the ascospore, unitunicate asci, brightly coloured, small, waxy, and translucent apothecium (Nannfeldt, 1932). *Orbiliaceae* species exhibit strong adaptability and can be found in various environments ranging from deserts and steppes to rainforests, from decaying wood and fallen leaves to the surfaces of animal dung (Liu et al., 2006; Zhang et al., 2009; Gou et al., 2014; Pfister, 2015; Shao et al., 2018; Baral et al., 2022). Currently, *Orbiliaceae* comprises three sexual genera: *Hyalorbilia* Baral & G. Morson (Eriksson et al., 2003; Baral et al., 2018), *Orbilia* Fries (Fries, 1849), and *Pseudorbilia* Zhang (Zhang et al., 2007), as well as at least ten asexual genera, including *Arthrobotrys* Corda, *Dactylellina* Morelet, *Drechslerella* Subram, *Dactylella* Grove, and *Dicranodion* Harkness, etc (Baral et al., 2018). Initially, this fungal group was considered insignificant due to their unclear ecological and application values. It was not until Pfister (1994) reported that the anamorph of *Orbilia fimicola* is *Arthrobotrys* species, a group of nematode-trapping fungi (NTF) with significant

research, application, and ecological stability value, that this group of fungi gained attention from mycologists. Currently, sexual-asexual connections have been established between *Orbiliaceae* species and three NTF genera, *Arthrobotrys*, *Drechslerella* and *Dactylellina* (Pfister, 1994; Zhang & Hyde, 2014; Baral et al., 2018). *Arthrobotrys* is the largest genus within *Orbiliomycetes* NTF and exhibits strong saprobic growth, reproductive capability, and adaptability, making it dominant across various habitats (Swe et al., 2011; Zhang & Hyde, 2014). *Dactylellina* demonstrates significant potential in the biological control of harmful nematodes because of its strong nematode-trapping ability (Zhang & Hyde, 2014). However, *Dactylellina* species are uncommon in most habitats and belong to rare taxa due to their weak saprobic growth and sporulation ability. Species in *Drechslerella* generally exhibit weaker nematode-trapping ability, which are clearly different from the mechanisms employed by *Arthrobotrys* and *Dactylellina* (Zhang & Hyde, 2014; Su et al., 2017). Their unique nematode-trapping mechanism makes them suitable fungi to study evolutionary mechanisms.

Dactylellina M. Morelet, Bull. Soc. Sci. nat. Arch. Toulon et du Var 178: 6 (1968)

Type species – *Dactylellina leptospora* M. Morelet

Note – *Dactylellina*, one of the three genera of *Orbiliomycetes* NTF, was initially established by Morelet (1968) with *Da. leptospora* M. Morelet as the type species. This genus was primordially defined by elongate, fusoid conidia, while microconidia were rarely formed. Scholler et al. (1999) revised the taxonomy of this genus with stalked adhesive knobs or non-constricting rings based on phylogenetic analysis. Further molecular data have validated the idea of dividing *Orbiliomycetes* NTF based on their trapping structures, resulting in the attributes of *Dactylellina* being revised again to capture nematodes using adhesive knobs, adhesive branches, and non-constricting rings (Li et al., 2005; Yang et al., 2007). *Dactylellina* comprises 51 species (plus our 15 new species, 34 species catch nematodes with adhesive knobs, seven with adhesive branches, and ten with both adhesive knobs and non-constricting rings) (Li et al., 2006; Zhang & Mo, 2006; Su et al., 2008; Zhang & Hyde, 2014; Kavitha et al., 2020; Zhang et al., 2020b; Crous et al., 2022). Because of its varied trapping structures and superior ability to catch nematodes, *Dactylellina* possesses considerable potential value in investigating the origin and evolution of specialized organisms, as well as in

the biological control of detrimental nematodes (Ji et al., 2020; Yang et al., 2020; Kumar et al., 2024a, 2024b).

Dactylellina dashabaensis F. Zhang, K.D. Hyde & X.Y. Yang, sp. nov. (Figure 10.3)

Index Fungorum number: IF901498; Facesoffungi number: FoF 15751.

Etymology: The specific epithet refers to the location "Dashaba Mountain, Wanqiao Town, Dali City, Yunnan Province, China", where the species was first collected.

Material examined – China, Yunnan Province, Dali City, Wanqiao Town, Dashaba Mountain, from the soil collected in burned forest (10–20 cm. depth), 16 June 2021, F. Zhang, ZX29-2. Holotype DLUCC146. Dali City, Wanqiao Town, Dashaba Mountain, from the soil collected in burned forest (10–20 cm. depth), 16 June 2021, F. Zhang, ZX4-2. Paratype WQ07.

Saprobic on soil. *Sexual morph*: Undetermined. *Colonies* on PDA white, villiform, growing slowly, reaching 35 mm diameter after 15 days in the incubator at 26 °C. *Mycelium* partly superficial, partly immersed, *hyphae* septate, branched, smooth and hyaline. *Conidiophores* 191.5–344 µm. long ($\bar{x}$ = 294.8 µm., n = 100), 3–5 µm. wide ($\bar{x}$ = 4.4 µm., n = 100) at the base, gradually tapering upwards to the apex, 2–3.5 µm. wide ($\bar{x}$ = 2.7 µm., n = 100) at the apex, erect, septate, hyaline, unbranched, bearing a single conidium at apex. *Conidia* 47–72 × 14.5–25.5 µm. ($\bar{x}$ = 59 × 21 µm., n = 100), smooth and hyaline, rounded at the apex and truncate at the base; immature conidia drop-shaped, obovate, with a super cell (the later cell in the conidia significantly larger than other cells) at the apex and 0–3 septa at the base; mature conidia subfusiform, 3–5-septate (mostly 4-septate, 1–2 septa at the apex and 1–3 septa at the base), with a super cell at the middle, the small cells at both ends are slender. No microconidia was observed. Conidia germinating from the small end cells, the super cell usually do not germinate. Catching nematodes with adhesive branches, with adjacent branches often fusing at the apex to form a two-dimensional adhesive network, and sometimes even a three-dimensional network structure. *Chlamydospores* not observed.

Notes: *Dactylellina dashabaensis* is related to *Da. yangxiensis* (another new species reported in this study) and *Da. gephyropaga* with 100% MLBS and 0.98 BYPP support. *Dactylellina dashabaensis* differs from *Da. yangxiensis* and *Da. gephyropaga* in ITS sequence by 3.2% (17/532 bp) and 4.6% (23/496 bp), respectively. *Dactylellina*

includes nine adhesive branching producing species (Zhang & Mo, 2006; Zhang & Hyde, 2014). Among them, *Da. dashabaensis* along with five other species (*Da. cionopaga*, *Da. gephyropaga*, *Da. shuzhengsum*, *Da. yangxiensis* and *Da. xinjuanii*) produce nearly spindle-shaped conidia (Zhang & Mo, 2006; Zhang & Hyde, 2014). However, *Da. dashabaensis* can be readily differentiated from them by the distinctive constriction of the septa at both ends of the conidia, as well as the slender small cells at both ends of the conidia.

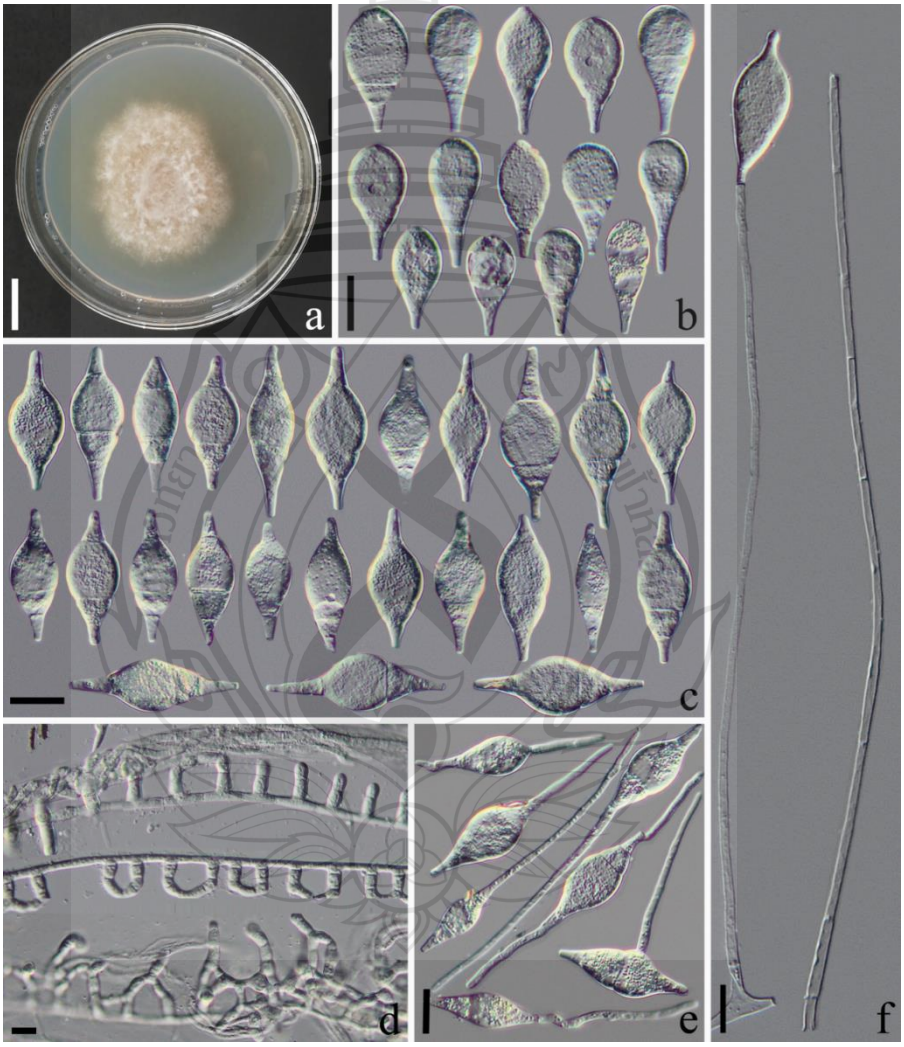

Figure 10.3 *Dactylellina dashabaensis* (DLUCC146). (a) Culture colony on PDA medium. (b, c) Conidia. (d) Trapping structure: adhesive branches. (e) Germinating conidia. (f) Conidiophores. Scale bars: (a) = 1 cm.., (b, c, e, f) = 20 µm., (d) = 10 µm.

Dactylellina dongxi F. Zhang, K.D. Hyde & X.Y. Yang, sp.nov. (Figure 10.4)

Index Fungorum number: IF902019; Facesoffungi number: FoF 15752

Etymology: The specific epithet “dongxi” is the Chinese abbreviation of the Institute of Eastern-Himalaya Biodiversity Research, Dali University that supports this study.

Material examined: China, Yunnan Province, Dali City, Yunlong County, Miaowei Town, Niuzideng Mountain, from the soil collected in burned forest (0–10 cm. depth), 6 March 2018, F. Zhang, BF135-1. Holotype DLUCC150. Dali City, Yunlong County, Miaowei Town, Niuzideng Mountain, from the soil collected in burned forest (10–20 cm. depth), 6 March 2018, F. Zhang, BF102-2. Paratype YL209.

Saprobic on soil. *Sexual morph*: Undetermined. *Colonies* on PDA white, cottony, growing slowly, reaching 51 mm diameter after 15 days in the incubator at 26 °C. *Mycelium* partly superficial, partly immersed. *Hyphae* septate, branched, smooth and hyaline. *Conidiophores* 145–304.5 µm. long ($\bar{x}$ = 257.1 µm., n = 100), 2.5–5 µm. wide ($\bar{x}$ = 4 µm., n = 100) at the base, gradually tapering upwards to the apex, 1.5–3 µm. wide ($\bar{x}$ = 2.1 µm., n = 100) at the apex, erect, septate, hyaline, unbranched or occasionally producing a long branch near the apex, producing a cluster of short denticles (2–6) at the apex of each branch, sometimes can also producing several clusters of short denticles by repeated elongation, each short denticle bearing a single conidium. *Conidia* two types: *macroconidia* 30–56.5 × 8–16 µm. ($\bar{x}$ = 40.6 × 12.8 µm., n = 100), smooth and hyaline, rounded at the apex and truncated at the base; immature macroconidia drop-shaped, clavate, 1–3 septate, with a super cell at the apex or middle; mature macroconidia subfusiform, 3–4-septate (mostly 4-septate, 1–2 septa at the apex and 1–3 septa at the base), with a super cell at the middle; *microconidia* 20–27.5 × 4–7.5 µm. ($\bar{x}$ = 24.7 × 5.3 µm., n = 100), smooth and hyaline, clavate or lanceolate, rounded at the apex and truncated at the base, producing with micro-cycle conidiation mode, 0–1-septate. Macroconidia germinating from the small end cells, and the super cell usually do not germinate. Catching nematodes with adhesive knobs, 4.5–6.5 µm. ($\bar{x}$ = 5.2 µm., n = 100) diameter. *Chlamydospores* not observed.

Notes: Phylogenetically, *Dactylellina dongxi*, *Da. miltoniae*, *Da. haptotyla*, *Da. yunnanensis* and *Da. candida* cluster in a same clade, although their relationship is unclear. There are differences of 5.7% (31/542 bp) and 1.9% (9/486 bp) in the ITS

sequences between *Da. dongxi* and *Da. miltoniae*, *Da. haptotyla*, respectively. The ITS sequences of *Da. dongxi*, *Da. yunnanensis* and *Da. candida* are almost identical (with differences of 0 and 1 base, respectively). However, there are distinct morphological differences between *Da. dongxi* and *Da. yunnanensis*, *Da. candida*: *Da. dongxi* captures nematodes only with adhesive knobs, while *Da. yunnanensis* and *Da. candida* capture nematodes with both adhesive knobs and non-constricting rings. The conidiophore of *Da. dongxi* can extend upwards to produce multiple clusters of short denticles and bear multiple clusters of conidia, while those of *Da. yunnanensis* and *Da. candida* only bear a single cluster of conidia at the apex. *Da. dongxi* produces microconidia, while *Da. yunnanensis* and *Da. candida* do not (von Esenbeck, 1817; Zhang et al., 1996; Zhang & Mo, 2006; Zhang & Hyde, 2014). In comparison, *Da. dongxi* is more similar to *Da. miltoniae* and *Da. haptotyla* in terms of trapping structures and conidia, but there are still two differences between them: (1) The conidiophores of *Da. dongxi* sometime branch and produce multiple clusters of short denticles by repeated elongation, while those of *Da. miltoniae* and *Da. haptotyla* are unbranched and only bear a single cluster of conidia at the apex; (2) *Da. dongxi* produces microconidia, while *Da. miltoniae* and *Da. haptotyla* do not (Drechsler, 1950; Zhang & Mo, 2006; Zhang & Hyde, 2014; Crous et al., 2022).

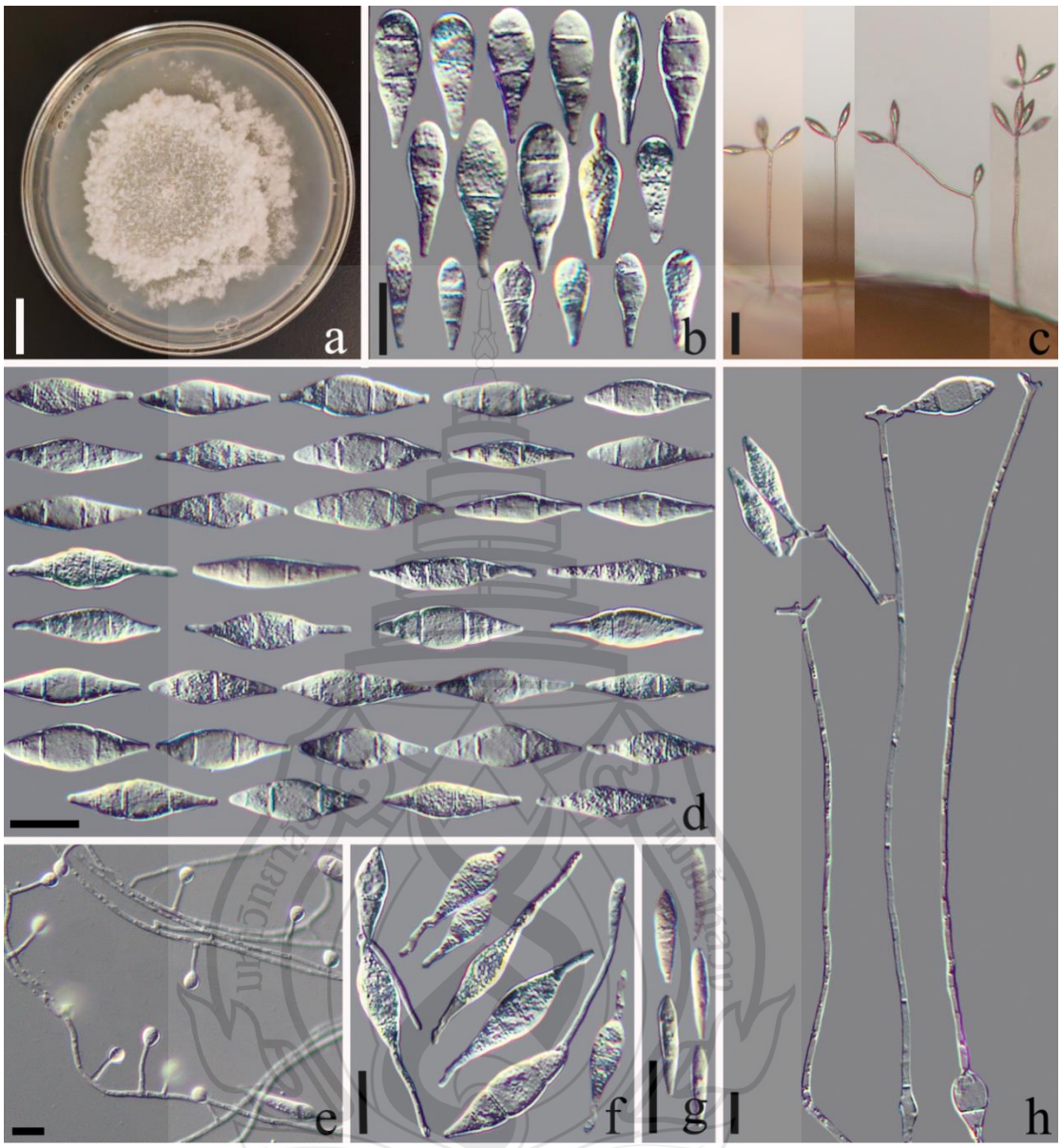

Figure 10.4 *Dactylellina dongxi* (DLUCC150). (a) Culture colony on PDA medium. (b, d) Macroconidia. (e) Trapping structure: adhesive knobs. (f) Germinating conidia. (g) Microconidia. (c, h) Conidiophores. Scale bars: (a) = 1 cm.., (b, d, f, g, h) = 20 µm., (e) = 10 µm., (c) = 50 µm.

Dactylellina erhaiensis F. Zhang, K.D. Hyde & X.Y. Yang, sp. nov. (Figure 10.5)

Index Fungorum number: IF902029; Facesoffungi number: FoF 15753

Etymology: The species name “erhaiensis” refers to the Erhai Lake watershed where the sampling site is located.

Material examined: China, Yunnan Province, Dali City, Cangshan Mountain, Maer Peak (Yushan Mountain), from the soil collected in burned forest (0–10 cm. depth), 24 March 2018, F. Zhang, L1-1. Holotype DLUCC153. Cangshan Mountain, Maer Peak, from the soil collected in burned forest (10–20 cm. depth), 24 March 2018, F. Zhang, L2-1. Paratype YS03.

Saprobic on soil. *Sexual morph*: Undetermined. *Colonies* on PDA white, villiform, growing slowly, reaching 53 mm diameter after 15 days in the incubator at 26 °C. *Mycelium* partly superficial, partly immersed. *Hyphae* septate, branched, smooth and hyaline. *Conidiophores* 106–264.5 µm. long ($\bar{x}$ = 203.9 µm., n = 100), 2.5–6 µm. wide ($\bar{x}$ = 4.6 µm., n = 100) at the base, gradually tapering upwards to the apex, 1.5–3.5µm. wide ($\bar{x}$ = 2.2 µm., n = 100) at the apex, erect, septate, hyaline, unbranched, bearing a single conidium at the apex. *Conidia* two types: *macroconidia* 21–39 × 8.5–16.5 µm. ($\bar{x}$ = 27.8 × 12.9 µm., n = 100), smooth and hyaline, rounded at the apex and truncated at the base; immature macroconidia drop-shaped, obovate, with a super cell at the apex and 1–2 septa at the base; mature macroconidia subfusiform, 3–4-septate (mostly 3-septate, 1–2 septa at both end), with a super cell at the middle. *Microconidia* are rare, 11–20.5 × 4.5–8.5 µm. ($\bar{x}$ = 14.4 × 6.4 µm., n = 100), smooth and hyaline, clavate or lanceolate, rounded at the apex and truncated at the base, 0–1-septate (mostly 1-septate). *Macroconidia* germinating from the small end cells, and the super cell usually do not germinate. Catching nematodes with adhesive knobs, 4.4–7.5 µm. ($\bar{x}$ = 5.3 µm., n = 100) diameter. *Chlamydospores* not observed.

Notes: Phylogenetically, *Dactylellina erhaiensis* clusters together with *Da. mammillata*, *Da. entomopaga* and *Da. phymatopaga*. *Dactylellina erhaiensis* has 5.4% (27/497 bp), 4.2% (21/495 bp) and 3.2% (16/495 bp) differences from *Da. mammillata*, *Da. entomopaga* and *Da. phymatopaga* in its ITS sequence. Based solely on the shape and septa number of conidia, *Da. erhaiensis* (subfusiform, mostly 3-septate, with a super cell at the middle of the conidia) can be easily distinguished from *Da. entomopaga* (cylindrical or clavate, lacking super cell, with a single septum) (Drechsler, 1944; Zhang & Hyde, 2014). There are adequate differences in the conidial size between *Da. erhaiensis* and *Da. mammillata*, *Da. phymatopaga* [*Da. erhaiensis*, 21–39 (27.8) × 8.5–16.5 (12.9) µm. versus *Da. mammillata*, 30–60 × 9–17µm., *Da. phymatopaga*, 46–71 (62.3) × 21–29 (24.7) µm.]. In addition, *Da. erhaiensis* produces

clavate or lanceolate microcinidia, while *Da. mammillata* and *Da. phymatopaga* do not (Drechsler, 1954; Zhang & Hyde, 2014).

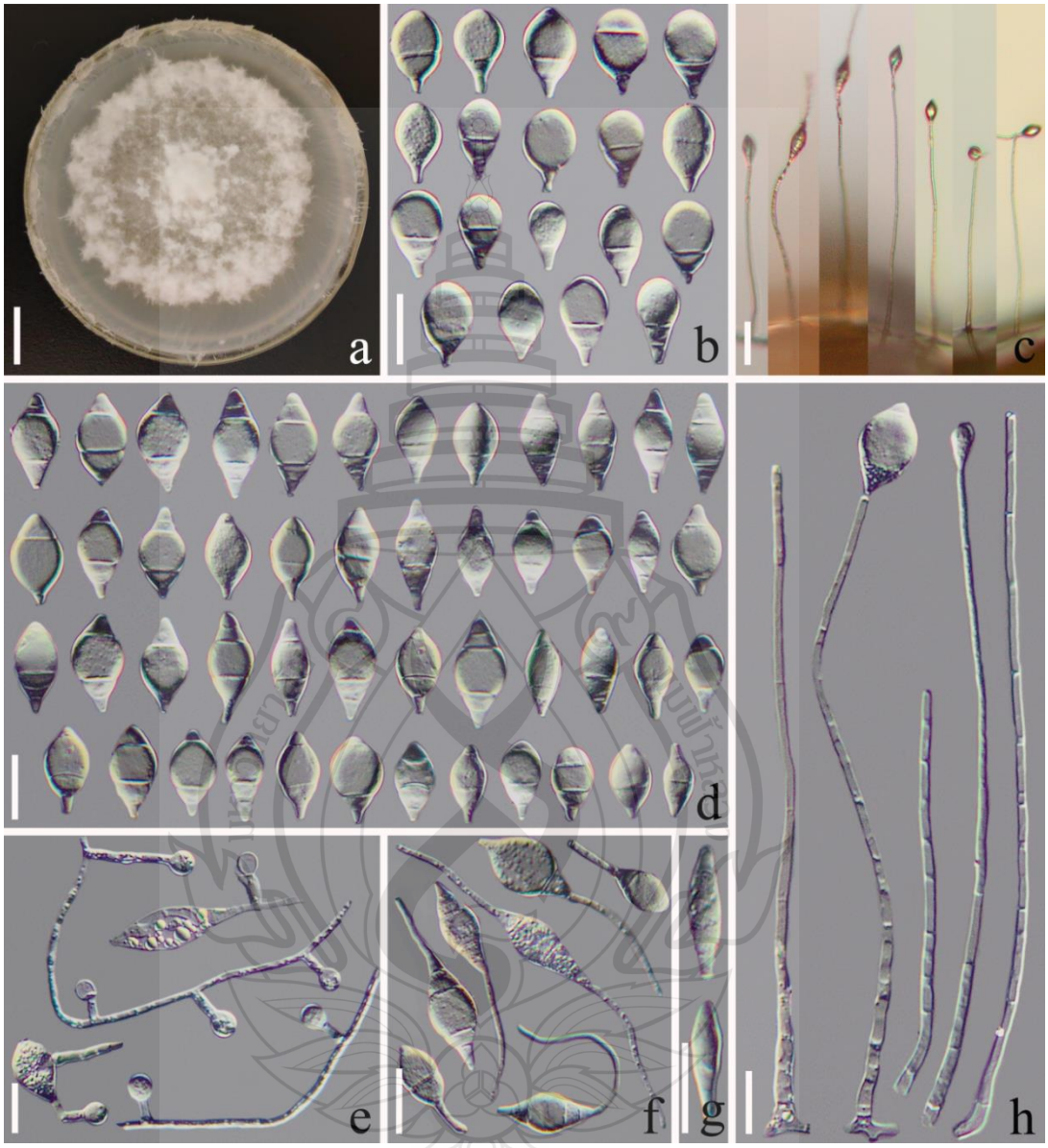

Figure 10.5 *Dactylellina erhaiensis* (DLUCC153). (a) Culture colony on PDA medium. (b, d) Macroconidia. (e) Trapping structure: adhesive knobs. (f) Germinating conidia. (g) Microconidia. (c, h) Conidiophores. Scale bars: (a) = 1 cm.., (b, d, f, h) = 20 µm., (e, g) = 10 µm., (c) = 50 µm.

Dactylellina fodingensis F. Zhang, K.D. Hyde & X.Y. Yang, sp. nov. (Figure 10.6)

Index Fungorum number: IF901501; Facesoffungi number: FoF 15754

Etymology: The species name "fodingensis" refers to Foding Peak where the samples collected, which is one of the famous 19 Peak in Cangshan Mountain.

Material examined: China, Yunnan Province, Dali City, Cangshan Mountain, Maer Peak (Yushan Mountain), from the soil collected in burned forest (0–10 cm. depth), 24 March 2018, F. Zhang, H1-3. Holotype DLUCC149. Cangshan Mountain, Maer Peak, from the soil collected in burned forest (10–20 cm. depth), 24 March 2018, F. Zhang, F2-2. Paratype YS79.

Saprobic on soil. *Sexual morph*: Undetermined. *Colonies* on PDA white, cottony, growing slowly, reaching 45 mm diameter after 15 days in the incubator at 26 °C. *Mycelium* partly superficial, partly immersed. *Hyphae* septate, branched, smooth and hyaline. *Conidiophores* 97.5–182.5 µm. long ($\bar{x}$ = 143.7 µm., n = 100), 2.5–5 µm. wide ($\bar{x}$ = 3.6 µm., n = 100) at the base, gradually tapering upwards to the apex, 1.5–3 µm. wide ($\bar{x}$ = 2.2 µm., n = 100) at the apex, erect, septate, hyaline, producing several clusters of short denticles by repeated elongation or branching of conidiophores, with each denticle bearing a single conidium (usually 5–22 conidia are gathered into a cluster). *Conidia* 28–70.5 × 4–6 µm. ($\bar{x}$ = 48.6 × 5.1 µm., n = 100), smooth and hyaline, clavate, lanceolate, with some conidia slightly curved, rounded at the apex and truncated at the base, with 2–10 septa evenly distributed in the conidia. No microconidia was observed. Capturing nematodes using non-constricting rings and adhesive knobs, adhesive knobs rare and can grow directly on the conidia (conidia traps, CT), 4.5–7.5 µm. ($\bar{x}$ = 5.9 µm., n = 100) diameter; the non-constricting ring easily fall off, with outer diameter 14.5–19.5 µm. ($\bar{x}$ = 16.6 µm., n = 100), the inner diameter 9–13 µm. ($\bar{x}$ = 10.7 µm., n = 100). *Chlamydospores* not observed.

Notes: Phylogenetically, *Dactylellina fodingensis* clusters together with *Da. formosana* and *Da. leptospora* (100% MLBS and 1.00 BYPP). *Dactylellina fodingensis* is 1.5% (7/493 bp) different from *Da. formosana* in ITS. There are 1% (5/492 bp), 15% (77/512 bp) and 1.8% (10/554 bp) difference in ITS, TEF and RPB2 between *Da. fodingensis* and *Da. leptospora.* Morphologically, *Da. fodingensis* can be easily distinguished from *Da. formosana* by their trapping structures (*Da. fodingensis*

captures nematode with adhesive knobs and non-constricting rings, while *Da. formosana* produces only adhesive knobs) and conidiophores (*Da. fodingensis* produces branched, 97.5–182.5 (143.7) µm. long conidiophore bearing multiple conidia, while *Da. formosana* produces unbranched 17–90µm. long conidiophores bearing a single conidium) (Liou et al., 1995; Zhang & Hyde, 2014). The main difference between *Da. fodingensis* and *Da. leptospora* is that the conidiophores of *Da. fodingensis* typically produce 5 to 22 short denticles at the apex (5–22 conidia clusters borne on the conidiophore), and the conidiophores can produce several multiple clusters of short denticles by repeated elongation. While, the conidiophores of *Da.leptospora* usually produce only 1–3 short denticles at the apex (bearing 1–3 conidia). In addition, the conidia of *Da. leptospora* are longer than those of *Da. fodingensis* [*Da. leptospora*, 30–92 (64) µm versus *Da. fodingensis*, 28–70.5 (48.6) µm] (Drechsler 1937; Zhang & Hyde, 2014). *Da. fodingensis* is more similar to *Da. haptospora* in their trapping structures, conidiophores and the shape of conidia. However, the conidia of *Da. haptospora* typically bear an adhesive knob at the apex, and they are noticeably finer than those of *Da. fodingensis* [*Da. haptospora*, 2.2–3.7 µm versus *Da. fodingensis*, 4–6 (5.1) µm] (Drechsler, 1940; Zhang & Hyde, 2014).

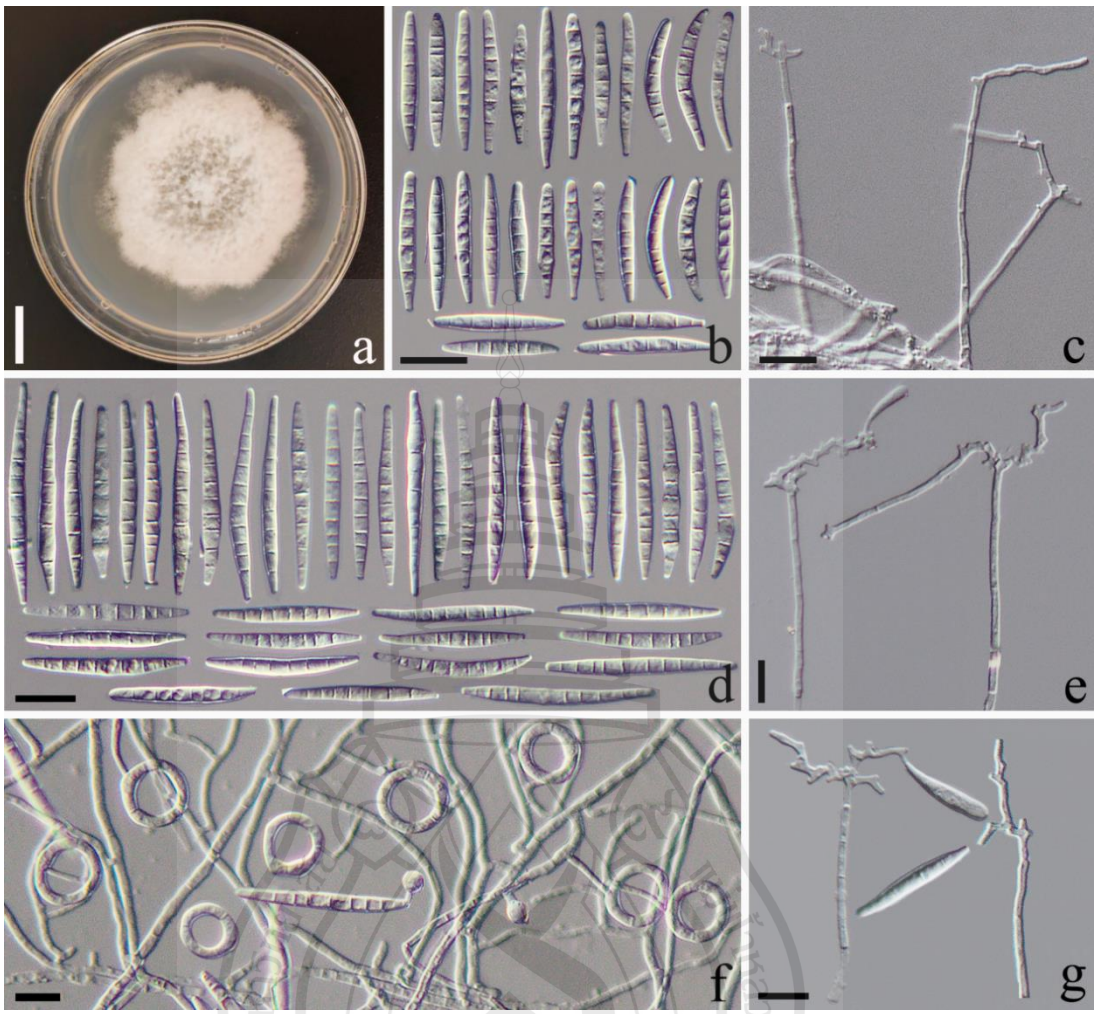

Figure 10.6 *Dactylellina fodingensis* (DLUCC149). (a) Culture colony on PDA medium. (b, d) Conidia. f Trapping structure: adhesive knobs and non-constricting rings. (**c, e, g**) Conidiophores. Scale bars: (**a**) = 1 cm., (b, c, d, e, g) = 20 µm., (f) = 10 µm.

Dactylellina lancangensis F. Zhang, K.D. Hyde & X.Y. Yang, sp. nov. (Figure 10.7)

Index Fungorum number: IF902018; Facesoffungi number: FoF 15755

Etymology: The species name “lancangensis” refers to the Lancang River watershed where the sample area is located.

Material examined: China, Yunnan Province, Dali City, Yunlong County, Miaowei Town, Niuzideng Mountain, from the soil collected in burned forest (10–20 cm. depth), 6 March 2018, F. Zhang, BF114-2. Holotype DLUCC148. Dali City,

Yunlong County, Miaowei Town, Niuzideng Mountain, from the soil collected in burned forest (10–20 cm. depth), 6 March 2018, F. Zhang, BF131-2. Paratype YL165.

Saprobic on soil. *Sexual morph*: Undetermined. *Colonies* on PDA white, cottony, growing slowly, reaching 53 mm diameter after 15 days in the incubator at 26 °C. *Mycelium* partly superficial, partly immersed. *Hyphae* septate, branched, smooth and hyaline. *Conidiophores* 164.5–297 µm. long ($\overline{x}$ = 241.3 µm., n = 100), 2.5–5 µm. wide ($\overline{x}$ = 3.8 µm., n = 100) at the base, gradually tapering upwards to the apex, 1.5–3 µm. wide ($\overline{x}$ = 2.4 µm., n = 100) at the apex, erect, septate, hyaline, unbranched or producing a short branch near the apex, bearing a single conidium at the apex of each branch. *Conidia* 30.5–56 × 8.5–17.5 µm. ($\overline{x}$ = 42.1 × 12.3 µm., n = 100), smooth and hyaline, rounded at the apex and truncated at the base; immature conidia drop-shaped, obovate, clavate, 1–3 septate, with a super cell at the apex or middle; mature conidia clavate or subfusiform, 3–5-septate (mostly 4-septate, 1–2 septa at the apex and 1–3 septa at the base of the conidia), with a super cell at the middle. No microconidia was observed. Conidia germinating from the small end cells, and the super cell usually do not germinate. Catching nematodes with *adhesive knobs*, 4.5–7 µm. ($\overline{x}$ = 5.6 µm., n = 100) diameter. *Chlamydospores* not observed.

Notes: The phylogenetic analyses revealed that *Da. lancangensis* is related to *Da. varietas*, *Da. asthenopaga* and *Da. multiseptatum*. There are 11% (56/513 bp), 13.3% (70/527 bp) and 14.9% (72/519 bp) differences between *Da. lancangensis* and *Da. varietas*, *Da. asthenopaga*, *Da. multiseptatum* in ITS sequence, respectively. Morphologically, *Da. lancangensis* differs from *Da. varietas* and *Da. asthenopaga*. *Da. lancangensis* captures nematodes with adhesive knobs alone and produces conidia with a super cell, whereas *Da. varietas* captures nematodes with both adhesive knobs and non-constricting rings, and both *Da. varietas* and *Da. asthenopaga* produce conidia without super cell (the septa are evenly distributed in the conidia) (Drechsler, 1937; Li et al., 2006; Zhang & Hyde, 2014). The main difference between *Da. lancangensis* and *Da. multiseptatum* is that the conidia of former are smaller than those of the latter [*Da. lancangensis*, 30.5–56 (42.1) × 8.5–17.5 (12.3) µm. versus *Da. multiseptatum*, 67.5–132.5 (91.6) × 3.8–17.5 (15.5) µm.]. In addition, *Da. multiseptatum* produces 4–9-septate conidia, while the conidia of *Da. lancangensis* has no more than 5 septa (Su et al., 2005; Zhang & Hyde, 2014).

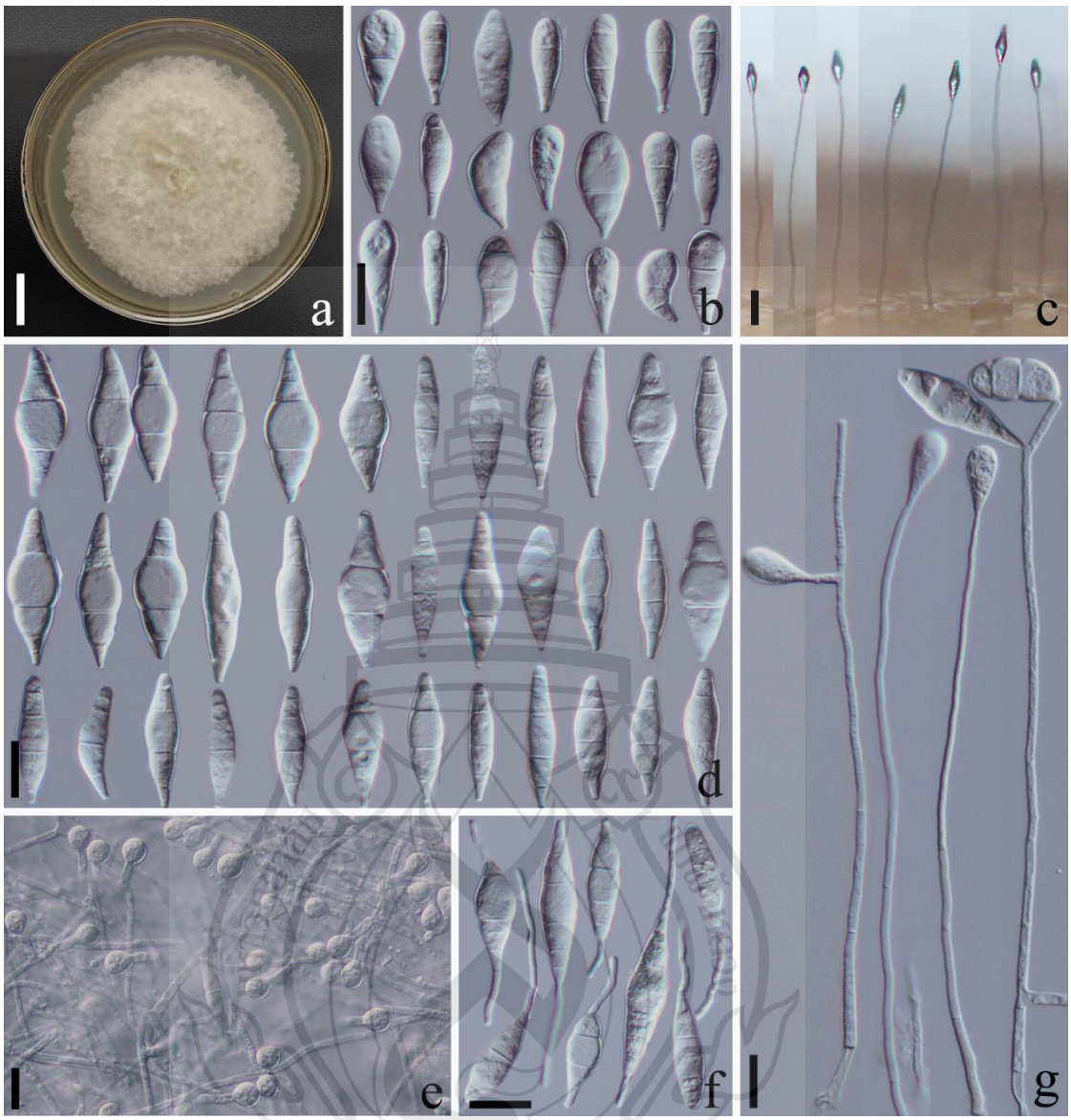

Figure 10.7 *Dactylellina lancangensis* (DLUCC148). (a) Culture colony on PDA medium. (b, d) Conidia. e Trapping structure: adhesive knobs. (f) Germinating conidia. (c, g) Conidiophores. Scale bars: (a) = 1 cm., (b, d, f, g) = 20 µm., (e) = 10 µm., (c) = 50 µm.

Dactylellina maerensis F. Zhang, K.D. Hyde & X.Y. Yang, sp. nov. (Figure 10.8)

Index Fungorum number: IF902012; Facesoffungi number: FoF 15756

Etymology: The species name “maerensis” refers to the location “Maer Peak, Cangshan Mountain, Dali City, Yunnan Province, China” where the species was first

collected.

Material examined – China, Yunnan Province, Dali City, Cangshan Mountain, Maer Peak (Yushan Mountain), from the soil collected in burned forest (10–20 cm. depth), 24 March 2018, F. Zhang, A2-1. Holotype DLUCC141. Cangshan Mountain, Maer Peak, from the soil collected in burned forest (0–10 cm. depth), 24 March 2018, F. Zhang, B1-3. Paratype YS14.

Saprobic on soil. *Sexual morph*: Undetermined. *Colonies* on PDA white, cottony, growing slowly, reaching 50 mm diameter after 15 days in the incubator at 26 °C. *Mycelium* partly superficial, partly immersed. *Hyphae* septate, branched, smooth and hyaline. *Conidiophores* 160–320 µm. long ($\bar{x}$ = 236 µm., n = 100), 4–6.5 µm. wide ($\bar{x}$ = 4.6 µm., n = 100) at the base, gradually tapering upwards to the apex, 2–3.5 µm. wide ($\bar{x}$ = 2.7 µm., n = 100) at the apex, erect, septate, hyaline, unbranched or occasionally producing a long branch near the apex, bearing a single conidium at the apex of each branch. *Conidia* 30–49.5 × 9.5–16.5 µm. ($\bar{x}$ = 40.8 × 12.6 µm., n = 100), smooth and hyaline, rounded at the apex and truncated at the base; immature conidia drop-shaped, obovate, with a super cell at the apex and 0–3 septa at the base; mature conidia clavate or subfusiform, 2–4-septate (mostly 3-septate, 1–2 septa at both end of the conidia), with a super cell at the middle. No microconidia was observed. Conidia germinating from the small end cells, and the super cell usually do not germinate. Catching nematodes with *adhesive knobs,* 4.5–7.5 µm. ($\bar{x}$ = 5.3 µm., n = 100) diameter. *Chlamydospores* not observed.

Notes: Phylogenetic analysis showed that *Dactylellina maerensis* is sister to *Da.tingmingensis*. However, its phylogenetic position is uncertain due to lower support value (88% MLBS, 0.90 BYPP). There are 3.7% (21/563 bp), 5.4% (28/516 bp), and 21% (119/571 bp) difference in ITS, TEF and RPB2 between *Da. maerensis* and *Da. tingmingensis*. Morphologically, *Da. maerensis* can be easily distinguished from *Da. tingmingensis* in their conidiophores. The conidiophores of *Da. maerensis* are dispersed, unbranched or occasionally produce a branch near the apex, and is longer (160–320 µm. ($\bar{x}$ =236 µm., n = 100)), while the conidiophores of *Da. tingmingensis* grow in clusters, and often produce branches near the base with 55–180 µm. ($\bar{x}$ =120 µm., n = 100) long. *Dactylellina maerensis* is more similar to *Da. dulongensis* and *Da. yushanensis*. However, the conidia of both *Da. dulongensis* and *Da. yushanensis* predominantly

feature 4-septate, while those of *Da. maerensis* primarily with 3 septa, and the apices of conidia from the first two species are more pointed than those of *Da. maerensis*. Furthermore, the branches of conidiophores produced by *Da. maerensis* are typically longer, while those of *Da. dulongensis* and *Da. yushanensis* are often characterized by shorter denticles (Zhang et al., 2020b).

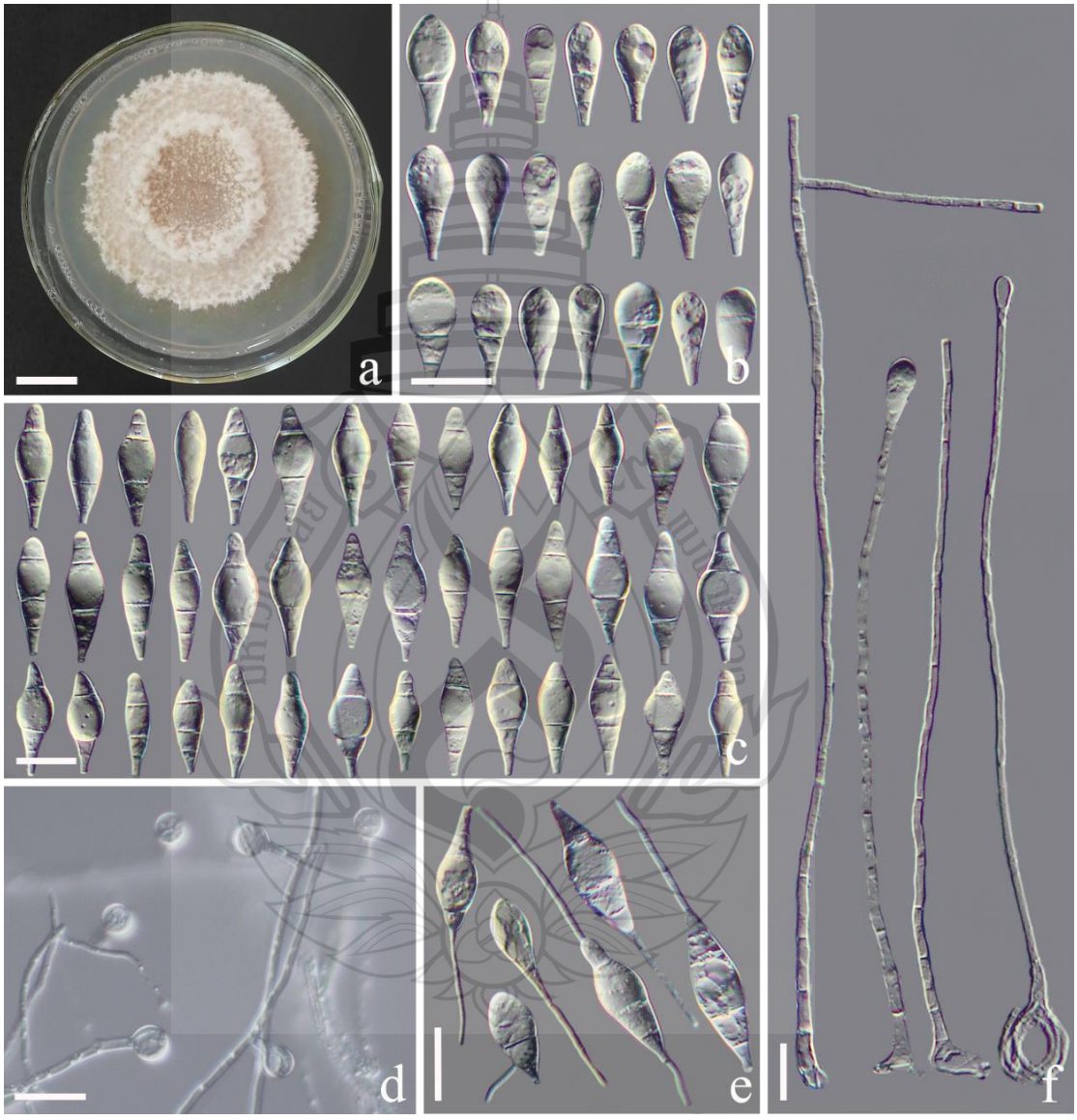

Figure 10.8 *Dactylellina maerensis* (DLUCC141). (a) Culture colony on PDA medium. (b, c) Conidia. (d) Trapping structure: adhesive knobs. (e) Germinating conidia. (f) Conidiophores. Scale bars: (a) = 1 cm., (b, c, e, f) = 20 µm., (d) = 10 µm.

Dactylellina mazongensis F. Zhang, K.D. Hyde & X.Y. Yang, sp. nov. (Figure 10.9)

Index Fungorum number: IF902020; Facesoffungi number: FoF 15757

Etymology: The species name “mazongensis” refers to Mazong Ridge, a ridge where Niuzideng Mountain (where the species was first collected) is located.

Material examined: China, Yunnan Province, Dali City, Yunlong County, Miaowei Town, Niuzideng Mountain, from the soil collected in burned forest (10–20 cm. depth), 6 March 2018, F. Zhang, BF147-2. Holotype DLUCC151. Dali City, Yunlong County, Miaowei Town, Niuzideng Mountain, from the soil collected in burned forest (10–20 cm. depth), 6 March 2018, F. Zhang, BF95-2. Paratype YL264.

Saprobic on soil. *Sexual morph*: Undetermined. *Colonies* on PDA white, cottony, growing slowly, reaching 48 mm diameter after 15 days in the incubator at 26 °C. *Mycelium* partly superficial, partly immersed. *Hyphae* septate, branched, smooth and hyaline. *Conidiophores* 127.5–386.5 µm. long ($\bar{x}$ = 225.7 µm., n = 100), 3–6.5 µm. wide ($\bar{x}$ = 4.1 µm., n = 100) at the base, gradually tapering upwards to the apex, 1.5–3.5µm. wide ($\bar{x}$ = 2 µm., n = 100) at the apex, erect, septate, hyaline, unbranched, bearing a single conidium at the apex. *Conidia* 26.5–53 × 6–16.5 µm. ($\bar{x}$ = 39.2 × 9.9 µm., n = 100), smooth and hyaline, rounded at the apex and truncated at the base; immature conidia drop-shaped, clavate, 0–3 septate, with a super cell at the apex or middle; mature conidium clavate or subfusiform, 3–5-septate (mostly 4-septate, 1–2 septa at both end of conidia), with a super cell at the middle. No microconidia was observed. Conidia germinating from the small end cells, and the super cell usually do not germinate. Catching nematodes with adhesive knobs, 4.5–6.5 µm. ($\bar{x}$ = 5.1 µm., n = 100) diameter. *Chlamydospores* not observed.

Notes: *Dactylellina mazongensis* is a phylogenetically distinct species that is most closely related to *Da. cangshanensis* with 100% MLBS and 0.99 BYPP support. There is a difference of 3.6% (18/494 bp) in ITS sequence between *Da. mazongensis* and *Da. cangshanensis*. Morphologically, the main difference between *Da. mazongensis* and *Da. cangshanensis* lies in their conidia. The conidia of *Da. cangshanensis* are mostly spindle-shaped with 2–4 septa, and nearly all the conidia possess a super cell (Zhang et al., 2020b). In contrast, the conidia of *Da. mazongensis* exhibits a greater variety (spindle-shaped, clavate, or lanceolate). Some conidia of *Da. mazongensis* are 5-septate and lack the distinct super cell.

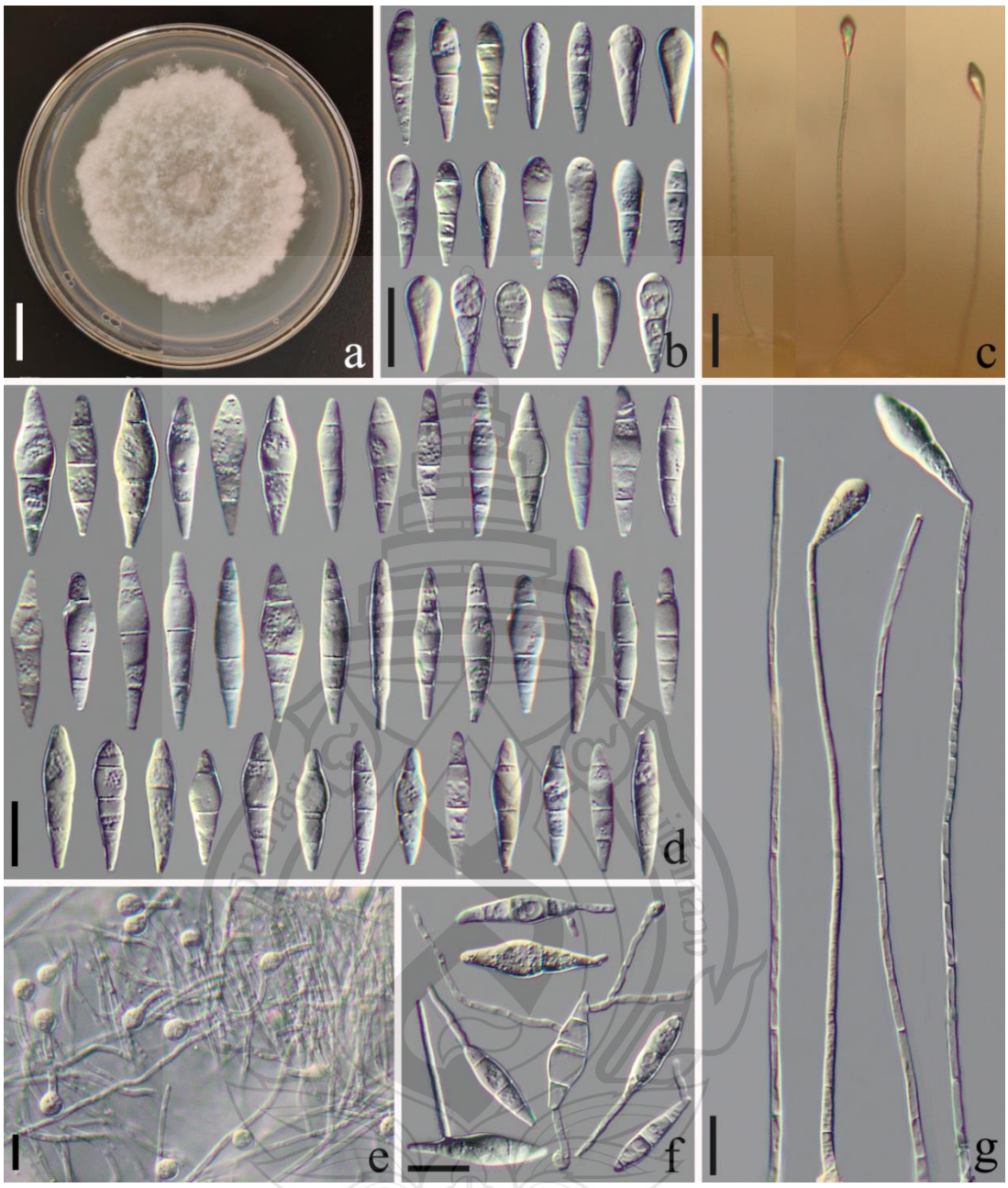

Figure 10.9 *Dactylellina mazongensis* (DLUCC151). (a) Culture colony on PDA medium. (b, d) Conidia. e Trapping structure: adhesive knobs. (f) Germinating conidia. (c, g) Conidiophores. Scale bars: (a) = 1 cm., (b, d, f, g) = 20 µm., (e) = 10 µm., (c) = 50 µm.

Dactylellina miaoweiensis F. Zhang, K.D. Hyde & X.Y. Yang, sp. nov. (Figure 10.10)

Index Fungorum number: IF902016; Facesoffungi number: FoF 15758

Etymology: The species name "miaoweiensis" refers to the location "Miaowei Town, Yunlong County, Dali City, Yunnan Province, China" where the species was first collected.

Material examined: China, Yunnan Province, Dali City, Yunlong County, Miaowei Town, Niuzideng Mountain, from the soil collected in burned forest (10–20 cm. depth), 6 March 2018, F. Zhang, BF46-2. Holotype DLUCC145. Dali City, Yunlong County, Miaowei Town, Niuzideng Mountain, from the soil collected in burned forest (0–10 cm. depth), 6 March 2018, F. Zhang, BF72-1. Paratype YL94.

Saprobic on soil. *Sexual morph*: Undetermined. *Colonies* on PDA white, villiform, growing slowly, reaching 52 mm diameter after 15 days in the incubator at 26 °C. *Mycelium* partly superficial, partly immersed. *Hyphae* septate, branched, smooth and hyaline. *Conidiophores* 145–301 µm. long ($\bar{x}$ = 224.2 µm., n = 100), 3–5.5 µm. wide ($\bar{x}$ = 4.2 µm., n = 100) at the base, gradually tapering upwards to the apex, 2–3 µm. wide ($\bar{x}$ = 2.5 µm., n = 100) at the apex, erect, septate, hyaline, unbranched, bearing a single conidium at the apex. *Conidia* 32–49.5 × 10.5–18.5 µm. ($\bar{x}$ = 38.6 × 13.5 µm., n = 100), smooth and hyaline, rounded at the apex and truncated at the base; immature conidia drop-shaped, obovate, with a super cell at the apex and 0–2 septa at the base; mature conidia subfusiform, 3–4-septate (mostly 3-septate, 1–2 septa at both end of the conidia), with a super cell at the middle. No microconidia was observed. Conidia germinating from the small end cells, and the super cell never germinating. Catching nematodes with adhesive knobs, 4.5–6.5 µm. ($\bar{x}$ = 5.1 µm., n = 100) diameter. *Chlamydospores* not observed.

Notes: Phylogenetically, *Dactylellina miaoweiensis* is related to *Da. yushanensis* and *Da. nanzhaoensis*. *Dactylellina miaoweiensis* is 6.7% (34/511 bp) and 4.6% (24/523 bp) different from *Da. yushanensis* and *Da. nanzhaoensis* in ITS sequence. Morphologically, there are sufficient differences between the conidia of *Da. miaoweiensis* and *Da. nanzhaoensis*. The conidia of *Da. miaoweiensis* are mostly spindle-shaped with 3–4 septa, and each conidium has a distinct super cell. In contrast, the conidia of *Da. nanzhaoensis* are elongate spindle-shaped, fusiform, or lanceolate, with 2–5 septa, and some conidia lack obvious super cell. Additionally, *Da.*

nanzhaoensis produces microconidia, while *Da. miaoweiensis* does not. The main differences between *Da. miaoweiensis* and *Da. yushanensis* are as follows: The conidiophores of *Da. miaoweiensis* are unbranched and bear a single conidium, whereas those of *Da. yushanensis* produce a geniculate branch and bear two conidia. The small cells at both ends of the conidia produced in *Da. yushanensis* are slenderer compared to *Da. miaoweiensis*. Additionally, *Da. yushanensis* produces microconidia, while *Da. miaoweiensis* does not (Zhang et al., 2020b).

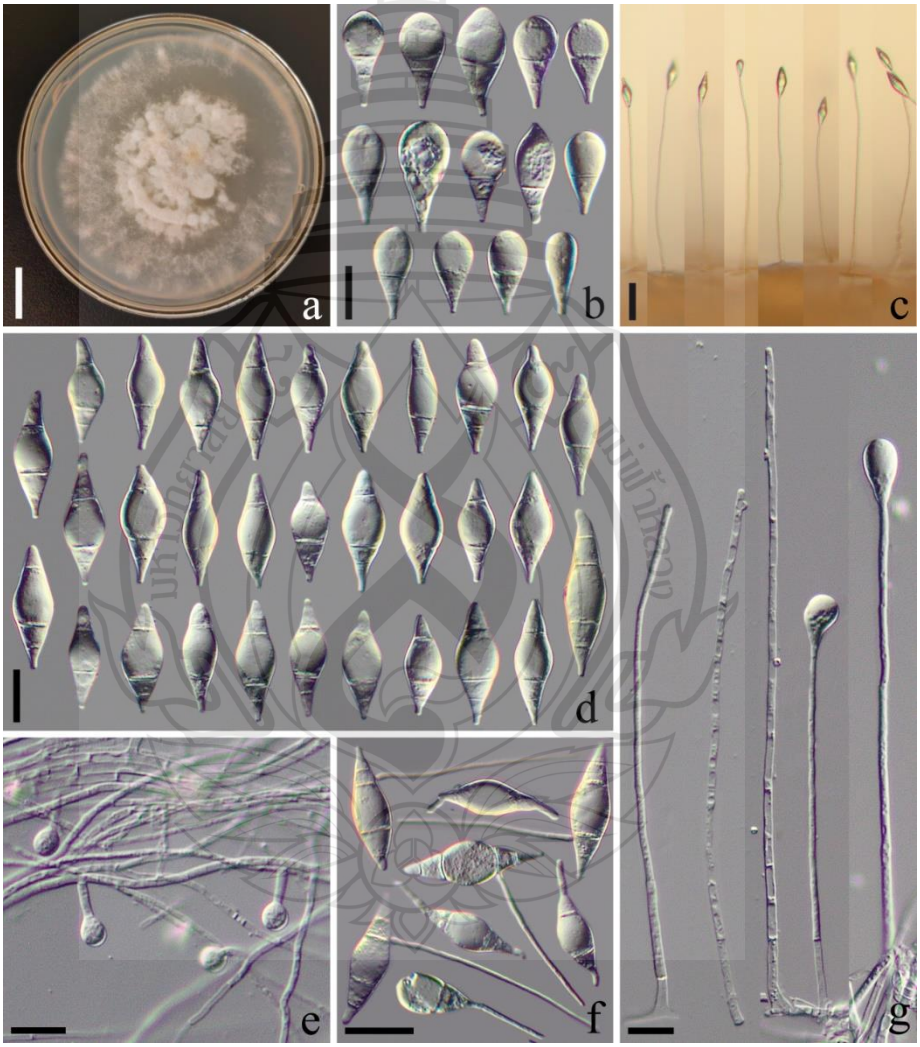

Figure 10.10 *Dactylellina miaoweiensis* (DLUCC145). (a) Culture colony on PDA medium. (b, d) Conidia. e Trapping structure: adhesive knobs. (f) Germinating conidia. (c, g) Conidiophores. Scale bars: (a) = 1 cm., (b, d, f, g) = 20 µm., (e) = 10 µm., (c) = 50 µm.

Dactylellina nanzhaoensis F. Zhang, K.D. Hyde & X.Y. Yang, sp. nov. (Figure 10.11)

Index Fungorum number: IF902021; Facesoffungi number: FoF 15758

Etymology: The species name "nanzhaoensis" refers to the ancient name of Dali City, Yunnan Province, China, where the soil sample were collected.

Material examined – China, Yunnan Province, Dali City, Cangshan Mountain, Maer Peak (Yushan Mountain), from the soil collected in burned forest (10–20 cm. depth), 24 March 2018, F. Zhang, L2-2. Holotype DLUCC152. Cangshan Mountain, Maer Peak, from the soil collected in burned forest (0–10 cm. depth), 24 March 2018, F. Zhang, D1-3. Paratype YS22.

Saprobic on soil. *Sexual morph*: Undetermined. *Colonies* on PDA white to yellowish, cottony, growing slowly, reaching 50 mm diameter after 15 days in the incubator at 26 °C. *Mycelium* partly superficial, partly immersed. *Hyphae* septate, branched, smooth and hyaline. *Conidiophores* 126–298.5 µm. long ($\bar{x}$ = 209.6 µm., n = 100), 2.5–5 µm. wide ($\bar{x}$ = 4.2 µm., n = 100) at the base, gradually tapering upwards to the apex, 1.5–3 µm. wide ($\bar{x}$ = 2 µm., n = 100) at the apex, erect, septate, hyaline, unbranched, bearing a single conidium at the apex. *Conidia* two types: *macroconidia* 30.5–59 × 6–16.5 µm. ($\bar{x}$ = 47.7 × 11.6 µm., n = 100), smooth and hyaline, clavate, long-fusiform, lanceolate, usually with a super cell at the middle, rounded at the apex and truncated at the base, 2–5-septate (1–2 septa at the apex and 1–3 septa at the base of the conidia),; *microconidia* 20.5–38.5 × 6–8.5 µm. ($\bar{x}$ = 30.4 × 7.4 µm., n = 100), smooth and hyaline, clavate, subfusiform, lanceolate, 0–2-septate. Macroconidia germinating from the small end cells, and the super cell usually do not germinate. Catching nematodes with adhesive knobs, 4.5–6.5 µm. ($\bar{x}$ = 5.1 µm., n = 100) diameter. *Chlamydospores* not observed.

Notes: Phylogenetically, *Dactylellina nanzhaoensis* is the closest species of *Da. yushanensis* (100% MLBS and 1.00 BYPP). Although there is only 1.6 % (8/509 bp) difference in their ITS sequences, they can be clearly distinguished morphologically. The conidiophores of *Da. nanzhaoensis* are unbranched, bearing a single conidium, while those of *Da. yushanensis* occasionally produce a geniculate branch and bear two conidia. The macroconidia of *Da. nanzhaoensis* exhibit greater morphological diversity (clavate, long-fusiform, lanceolate), with some macroconidia lack the super cells. In

contrast, the large conidia of *Da. yushanensis* are mostly spindle-shaped with pointed ends and a super cell (Zhang et al., 2020b). In comparison, *Da. nanzhaoensis* is morphologically more similar to another newly reported species (*Da. mazongensis*) in this study. However, the macroconidia of *Da. nanzhaoensis* are longer than those of *Da. mazongensis* [*Da. nanzhaoensis*, 30.5–59 (47.7) µm. versus *Da. mazongensis*, 26.5–53(39.2) µm.]. Additionally, *Da. nanzhaoensis* produces microconidia, whereas *Da. mazongensis* does not. Furthermore, there is a lower sequence similarity between them, *Da. nanzhaoensis* is 9.1% (46/506 bp), 6.5% (30/460 bp) and 11.9% (64/537 bp) different from *Da. mazongensis* in ITS, TEF and RPB2 sequences.

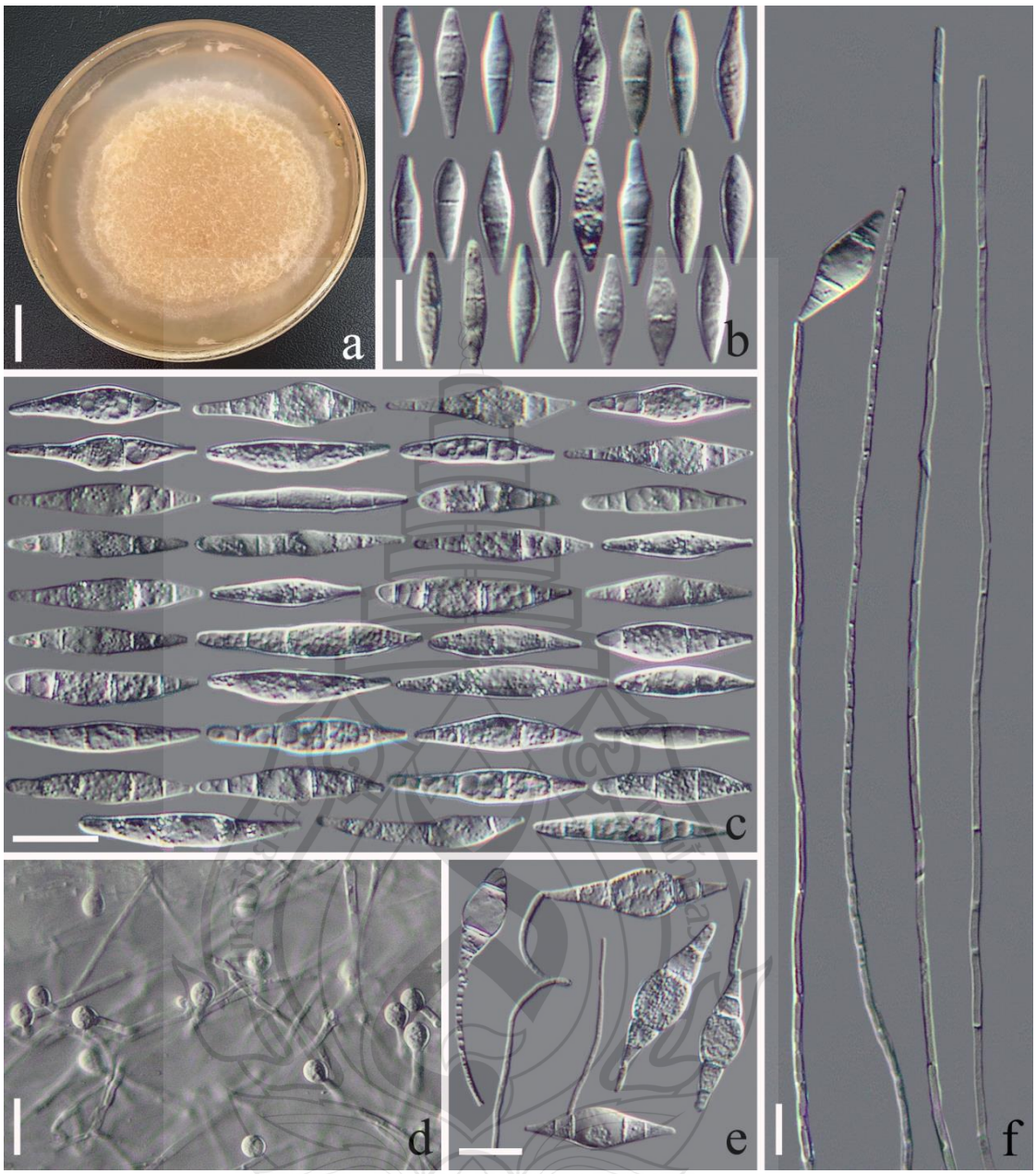

Figure 10.11 *Dactylellina nanzhaoensis* (DLUCC152). (a) Culture colony on PDA medium. (b) Microconidia. (c) Macroconidia. (d) Trapping structure: adhesive knobs. (e) Germinating conidia. (f) Conidiophores. Scale bars: (a) =1 cm., (b, c, e, f) =20 µm., (d) =10 µm.

Dactylellina niuzidengensis F. Zhang, K.D. Hyde & X.Y. Yang, sp. nov. (Figure 10.12)

Index Fungorum number: IF902014; Facesoffungi number: FoF 15759

Etymology: The species name niuzidengensis" refers to the location "Niuzideng Mountain, Miaowei Town, Yunlong County, Dali City, Yunnan Province, China" where the species was first collected.

Material examined: China, Yunnan Province, Dali City, Yunlong County, Miaowei Town, Niuzideng Mountain, from the soil collected in burned forest (0–10 cm. depth), 6 March 2018, F. Zhang, BF09-1. Holotype DLUCC143. Dali City, Yunlong County, Miaowei Town, Niuzideng Mountain, from the soil collected in burned forest (0–10 cm. depth), 6 March 2018, F. Zhang, BF99-1. Paratype YL39.

Saprobic on soil. *Sexual morph*: Undetermined. *Colonies* on PDA white, villiform, growing slowly, reaching 55 mm diameter after 15 days in the incubator at 26 °C. *Mycelium* partly superficial, partly immersed. *Hyphae* septate, branched, smooth and hyaline. *Conidiophores* 86–225.5 µm. long ($\bar{x}$ = 164.6 µm., n = 100), 3.5–6 µm. wide ($\bar{x}$ = 4.5 µm., n = 100) at the base, gradually tapering upwards to the apex, 2–3.5 µm. wide ($\bar{x}$ = 2.6 µm., n = 100) at the apex, erect, septate, hyaline, producing several branches in the middle and upper part of the conidiophores, each branch bear a single conidium at the apex or produce several short denticles near the apex (each denticle bear a single conidium). *Conidia* two types: *macroconidia* 40–88 × 9.5–17.5 µm. ($\bar{x}$ = 54.5 × 12.8 µm., n = 100), smooth and hyaline, diverse in form, clavate, botuliform, subfusiform, usually with a super cell at the middle, rounded at the apex and truncated at the base, some conidia slightly curved, 3–6-septate; *microconidia* 22–35 × 7.8–14.5 µm. ($\bar{x}$ = 29.3 × 11.8 µm., n = 100), smooth and hyaline, diverse in form, drop-shaped, obovate, clavate, subfusiform, subelliptic, rounded at the apex and truncated at the base, some microconidia slightly curved, 0–4-septate (mostly 2-septate). Macroconidia germinating from the small end cells, and the super cell usually do not germinate. Catching nematodes with adhesive knobs, 4.5–6.5 µm. ($\bar{x}$ = 5.4 µm., n = 100) diameter. *Chlamydospores* not observed.

Notes: Phylogenetically, *Dactylellina niuzidengensis* clusters together with *Da. lysipaga*, *Da. sichuanensis* and *Da. appendiculata* with 99% MLBS and 0.98 BYPP support. There is 6.5% (32/495 bp) difference in the ITS region between *Da.*

niuzidengensis and *Da. appendiculata*, whereas *Da. niuzidengensis* differs from *Da. lysipaga* and *Da. sichuanensis* by only 2 and 9 bases in the ITS region. Nevertheless, there are still morphological differences between *Da. niuzidengensis* and *Da. lysipaga*, *Da. sichuanensis*. For instance, *Da. niuzidengensis* captures nematodes using adhesive knobs alone, while *Da. lysipaga* and *Da. sichuanensis* capture nematodes using adhesive knobs and non-constricting rings. The conidiophore of *Da. niuzidengensis* typically produces long branches, which can also generate short denticles, in contrast, the conidiophore of *Da. lysipaga* and *Da. sichuanensis* unbranched. The conidia of *Da. lysipaga* and *Da. sichuanensis* are mostly spindle-shaped, whereas *Da. niuzidengensis* exhibits a greater diversity in conidia morphology, including clavate, botuliform, or subfusiform. *Dactylellina niuzidengensis* produces microconidia with 0–3 (2) septa, while *Da. lysipaga* and *Da. sichuanensis* do not produce microconidia (Drechsler, 1937; Li et al., 2006; Zhang & Hyde, 2014). The differences between *Da. niuzidengensis* and *Da. appendiculata* are also evident. The conidiophores of *Da. appendiculata* typically do not branch and bear a single conidium at the apex. In contrast, the conidiophore of *Da. niuzidengensis* usually branches, bearing multiple conidia. The conidia of *Da. appendiculata* are mostly spindle-shaped, while *Da. niuzidengensis* exhibits a greater diversity in conidial morphology (Drechsler, 1937; Zhang & Hyde, 2014).

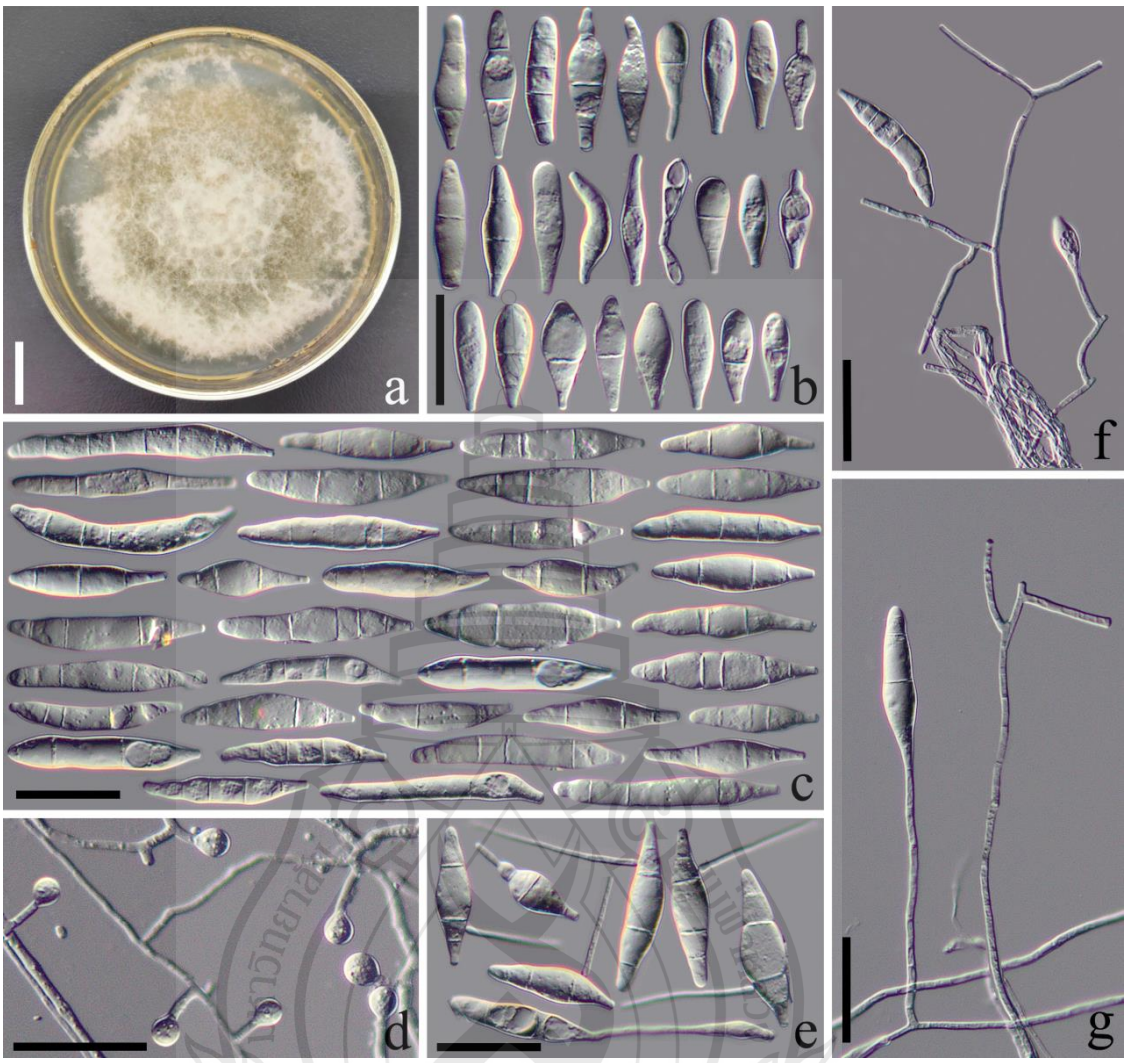

Figure 10.12 *Dactylellina niuzidengensis* (DLUCC143). (a) Culture colony on PDA medium. (b) Microconidia. (c) Macroconidia. (d) Trapping structure: adhesive knobs. (e) Germinating conidia. (f, g) Conidiophores. Scale bars: (a) = 1 cm., (b, c, e, f, g) =20 µm., (d) =10 µm.

Dactylellina tingmingensis F. Zhang, K.D. Hyde & X.Y. Yang, sp. nov. (Figure 10.13)

Index Fungorum number: IF902013; Facesoffungi number: FoF 15760

Etymology: The specific epithet “tingmingensis” refers to a stream (Mingting Stream) next to the sample collection site, which is one of the famous 18 streams in Cangshan Mountain.

Material examined: China, Yunnan Province, Dali City, Cangshan Mountain, Maer Peak (Yushan Mountain), from the soil collected in burned forest (0–10 cm. depth), 24 March 2018, F. Zhang, F1-2. Holotype DLUCC142. Cangshan Mountain, Maer Peak, from the soil collected in burned forest (0–10 cm. depth), 24 March 2018, F. Zhang, E1-3. Paratype YS28.

Saprobic on soil. *Sexual morph*: Undetermined. *Colonies* on PDA white, cottony, growing slowly, reaching 45 mm diameter after 15 days in the incubator at 26 °C. *Mycelium* partly superficial, partly immersed. *Hyphae* septate, branched, smooth and hyaline. *Conidiophores* 55–180 µm. long ($\bar{x}$ =120 µm., n = 100), 4–6.5 µm. wide ($\bar{x}$ = 5 µm., n = 100) at the base, gradually tapering upwards to the apex, 2–3.5 µm. wide ($\bar{x}$ = 2.8 µm., n = 100) at the apex, erect, septate, hyaline, usually grows in clusters, unbranched or branched at the base, bearing a single conidium at the apex or a second conidium at the subapical. *Conidia* 32.5–56 × 10.5–18 µm. ($\bar{x}$ = 43.9 × 14.9 µm., n = 100), smooth and hyaline, rounded at the apex and truncated at the base; immature conidia drop-shaped, obovate, with a super cell at the apex and 0–2 septa at the base; mature conidia subfusiform, 3–4-septate (mostly 4-septate, 1–2 septate at both ends of the conidia), with a super cell at the middle. No microconidia was observed. Conidia germinating from the small end cells, and the super cell usually do not germinate. Catching nematodes with adhesive knobs, 4.5–7.5 µm. ($\bar{x}$ = 5.3 µm., n = 100) diameter. *Chlamydospores* not observed.

Notes: Phylogenetically, *Da. tingmingensis* is sister to *Da. maerensis* (another new species described in this paper) and forms an independent lineage (88% MLBS, 0.90 BYPP). In morphology, *Da. tingmingensis* can be easily distinguished from all *Dactylellina* species by its shorter conidiophores growing in clusters and branching at the base (the conidiophore of all other *Dactylellina* species grow individually and dispersedly) (Zhang & Mo, 2006; Zhang & Hyde, 2014).

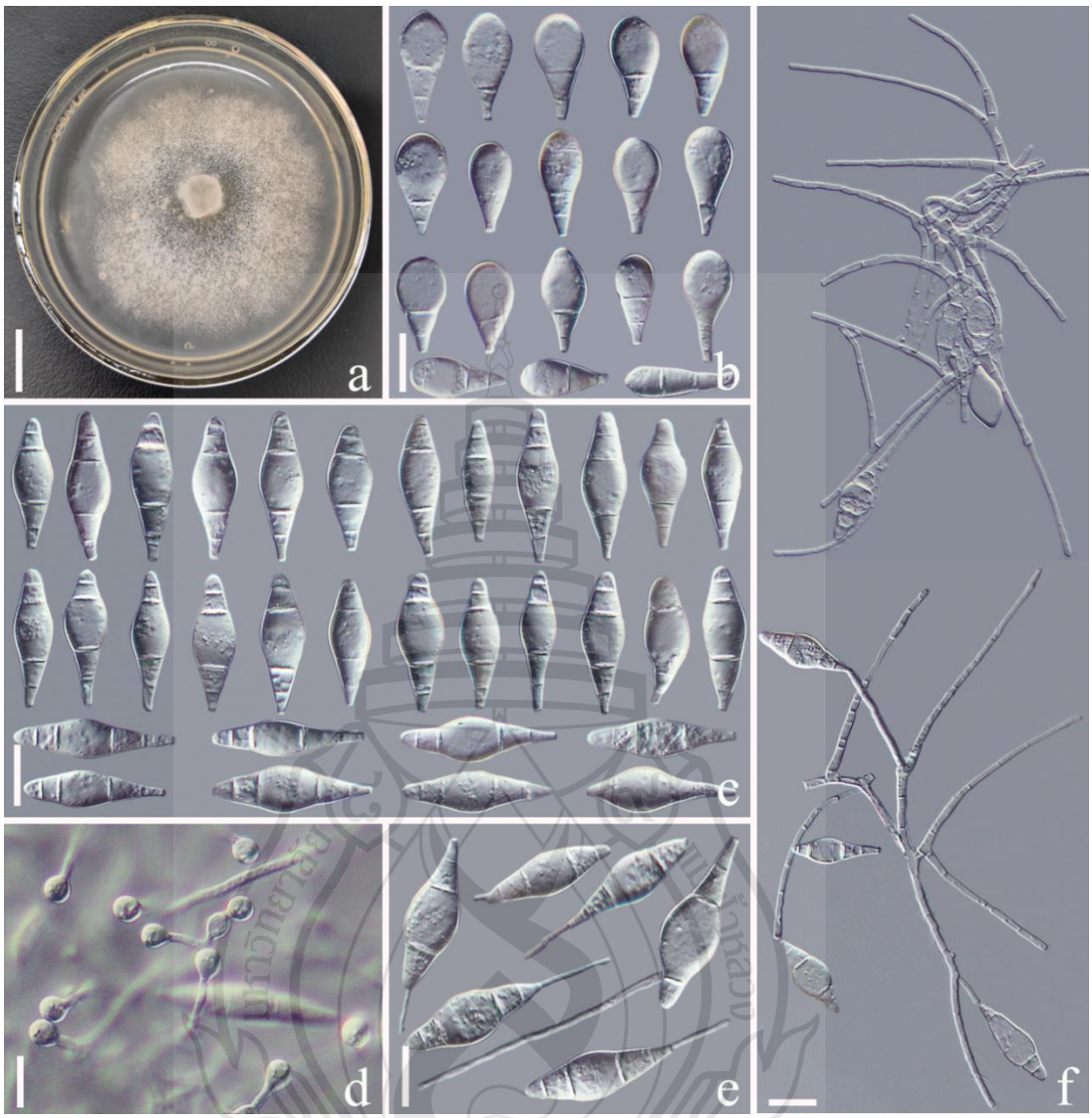

Figure 10.13 *Dactylellina tingmingensis* (DLUCC142). (a) Culture colony on PDA medium. (b, c) Conidia. (d) Trapping structure: adhesive knobs. (e) Germinating conidia. (f) Conidiophores. Scale bars: (a) = 1 cm., (b, c, e, f) = 20 µm., (d) = 10 µm.

Dactylellina wanqiaoensis F. Zhang, K.D. Hyde & X.Y. Yang, sp. nov. (Figure 10.14)

Index Fungorum number: IF902015; Facesoffungi number: FoF 15761

Etymology: The specific epithet refers to the location “Wanqiao Town, Dali City, Yunnan Province, China”, where the species was first collected.

Material examined: China, Yunnan Province, Dali City, Wanqiao Town, Dashaba Mountain, from the soil collected in burned forest (0–10 cm. depth), 16 June 2021, F. Zhang, ZX6-1. Holotype DLUCC144. Dali City, Wanqiao Town, Dashaba Mountain, from the soil collected in burned forest (10–20 cm. depth), 16 June 2021, F. Zhang, ZX18-2. Paratype WQ54.

Saprobic on soil. *Sexual morph*: Undetermined. *Colonies* on PDA white, cottony, growing slowly, reaching 45 mm diameter after 15 days in the incubator at 26°C. *Mycelium* partly superficial, partly immersed. *Hyphae* septate, branched, smooth and hyaline. *Conidiophores* 110.5–251 µm. long ($\bar{x}$ =183.2 µm., n = 100), 3–5.5 µm. wide ($\bar{x}$ = 3.9 µm., n = 100) at the base, gradually tapering upwards to the apex, 2–3.5 µm. ($\bar{x}$ = 2.6 µm., n = 100) wide at the apex, erect, septate, hyaline, unbranched, bearing 1–4 conidia per conidiophore (a single conidium is born at apex, while the rest are usually scattered on the conidiophore). *Conidia* 27.5–45.5 × 11–14.5 µm. ($\bar{x}$ = 37.9 × 13.2 µm., n = 100), smooth and hyaline, rounded at the apex and truncated at the base; immature conidia drop-shaped, obovate, with a super cell at the apex and 0–3 septa at the base; mature conidium subfusiform, 3–5-septate (1–2 septa at apex and 1–3 septa at base of the conidia), with a super cell at the middle. No microconidia was observed. Conidia germinating from the small end cells, and the super cell never germinating. Catching nematodes with adhesive knobs, 4.5–6.5 µm. ($\bar{x}$ = 5.3 µm., n = 100) diameter. *Chlamydospores* not observed.

Notes: Phylogenetically, *Dactylellina wanqiaoensis* clusters together with *Da. yushanensis* and two other new species reported in this study *Da. miaoweiensis* and *Da. nanzhaoensis* (90% MLBS and 0.90 BYPP). *Dactylellina wanqiaoensis* is 6.5% (33/510 bp), 7.5% (67/897 bp) and 7% (40/604 bp) different from *Da. yushanensis*, *Da. miaoweiensis* and *Da. nanzhaoensis* in ITS sequences. Morphologically, the conidial shape of *Da. wanqiaoensis* resemble those of several species, such as *Da.cangshanensis*, *Da. mutabilis*, and *Da. robusta*. However, the distinctive feature of *Da. wanqiaoensis* is the presence of 1–4 conidia borne on a conidiophore, and after the conidia detach from the conidiophore, the latter does not exhibit any protruding structure (such as short denticles or nodes). This characteristic is absent in other similar species (Zhang & Mo, 2006; Zhang & Hyde, 2014).

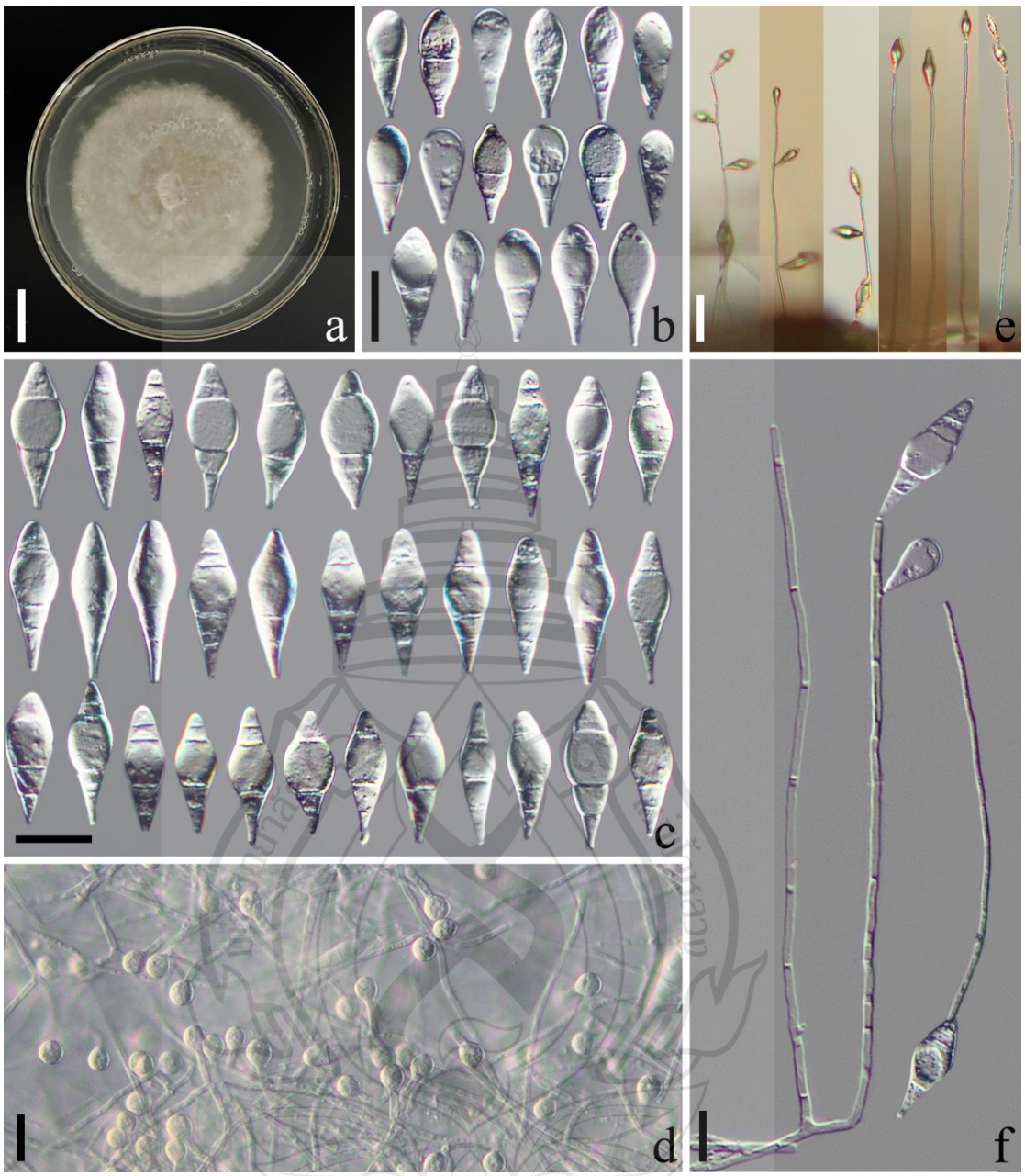

Figure 10.14 *Dactylellina wanqiaoensis* (DLUCC144). (a) Culture colony on PDA medium. (b, c) Conidia. (d) Trapping structure: adhesive knobs. (e, f) Conidiophores. Scale bars: (a) = 1 cm., (b, c, f) = 20 µm., (d) = 10 µm., (e) = 50 µm.

Dactylellina wubaoshanensis F. Zhang, K.D. Hyde & X.Y. Yang, sp. nov. (Figure 10.15)

Index Fungorum number: IF902030; Facesoffungi number: FoF 15762

Etymology: The species name "wubaoshanensis" refers to a peak (Wubaoshan Peak) next to the sample collection site.

Material examined – China, Yunnan Province, Dali City, Yunlong County, Miaowei Town, Niuzideng Mountain, from the soil collected in burned forest (0–10 cm. depth), 6 March 2018, F. Zhang, BF159-1. Holotype DLUCC154. Dali City, Yunlong County, Miaowei Town, Niuzideng Mountain, from the soil collected in burned forest (10–20 cm. depth), 6 March 2018, F. Zhang, BF160-2. Paratype YL349.

Saprobic on soil. *Sexual morph*: Undetermined. *Colonies* on PDA white, cottony, growing slowly, reaching 36 mm diameter after 15 days in the incubator at 26 °C. *Mycelium* partly superficial, partly immersed. *Hyphae* septate, branched, smooth and hyaline. *Conidiophores* 71–249 µm. long ($\bar{x}$ = 158.4 µm., n = 100), 2.5–7 µm. wide ($\bar{x}$ = 4.4 µm., n = 100) at the base, gradually tapering upwards to the apex, 1.5–3 µm. ($\bar{x}$ = 2.5 µm., n = 100) wide at apex, erect, septate, hyaline, unbranched, bearing a single conidium at the apex, occasionally a second conidium is born in the lower middle part of the conidiophore. *Conidia* 30–51.5 × 9.5–16 µm. ($\bar{x}$ = 39.5 × 12.2 µm., n = 100), smooth and hyaline, rounded at the apex and truncated at the base; immature conidia drop-shaped, with a super cell at the apex and 1–3 septa at the base; mature conidium subfusiform, 3–4-septate (1–2 septa at both end of the conidia), with a super cell at the middle. No microconidia was observed. Conidia germinating from the small end cells, and the super cell usually do not germinate. Catching nematodes with adhesive knobs, 4–6.5 µm. ($\bar{x}$ = 5.2 µm., n = 100) diameter. *Chlamydospores* not observed.

Notes: Phylogenetic analysis revealed that the systematic position of *Dactylellina wubaoshanensis* is uncertain but showed distinction from known species. *Dactylellina wubaoshanensis* is morphologically similar to *Da. ellipsospora* and *Da. maerensis* (the other new species reported in this study). There are two main differences between *Da. wubaoshanensis* and *Da. ellipsospora*: 1) The former occasionally bears two conidia on a single conidiophore, while the latter only bears a single conidium per conidiophore; 2) The conidia of *Da. wubaoshanensis* are smaller than those of *Da. ellipsospora* [*Da. wubaoshanensis*, 30–51.5 (39.5) × 9.5–16 (12.2) µm. versus *Da. ellipsospora*, 40–57.5

(48.3) × 10–17.5 (13) µm.], and *Da. ellipsospora* produces 2–4-septa conidia, whereas *Da. wubaoshanensis* can produce 5-septate conidia (Zhang & Mo, 2006; Zhang & Hyde, 2014). *Dactylellina wubaoshanensis* can be distinguished from *Da. maerensis* based on the morphology of their conidiophores: the second conidia of the former typically develops on the lower middle part of the conidiophore, while the second conidia of the latter usually bear on a branch near the apex of the conidiophore. Furthermore, the base and apex of the conidia produced by *Da. wubaoshanensis* are nearly symmetrical, whereas in *Da. maerensis*, the base and apex of the conidia are noticeably asymmetrical.

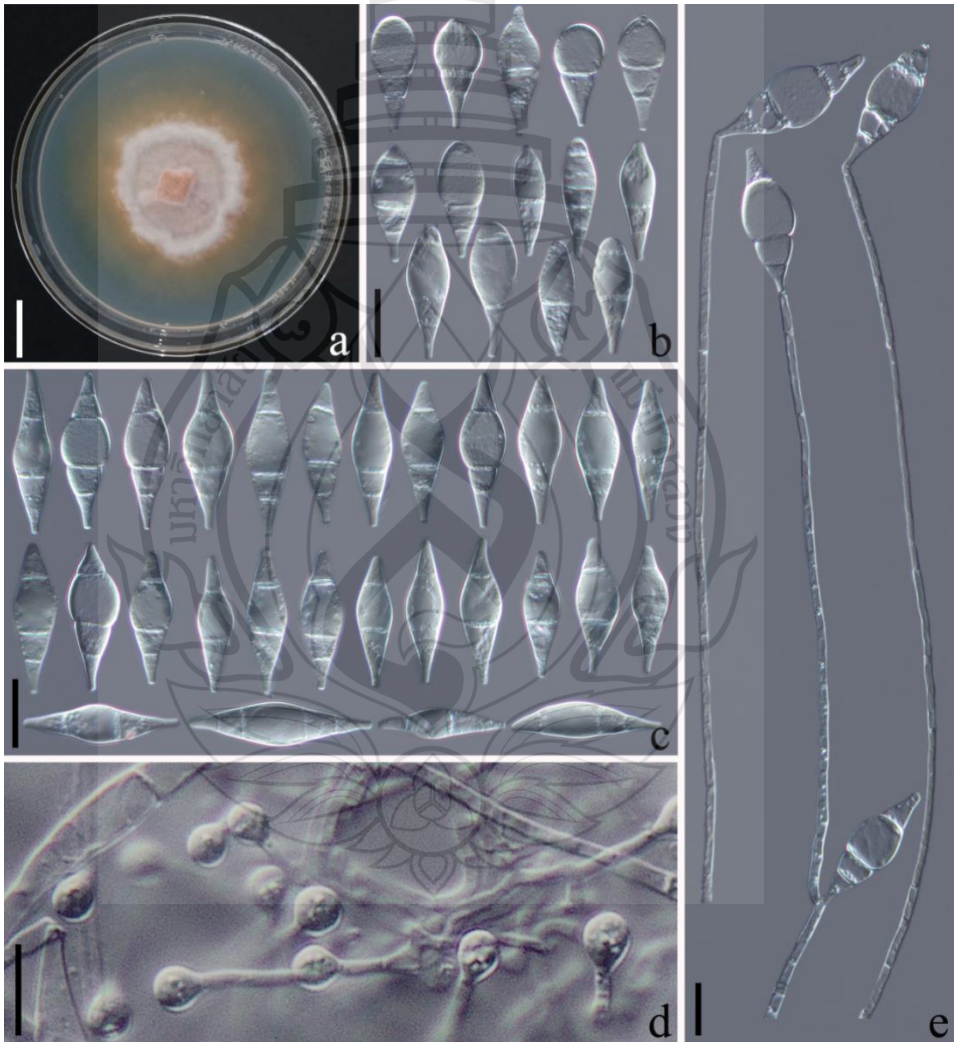

Figure 10.15 *Dactylellina wubaoshanensis* (DLUCC154). (a) Culture colony on PDA medium. (b, c) Conidia. (d) Trapping structure: adhesive knobs. (e) Conidiophores. Scale bars: (a) =1 cm., (b, c, e) =20 µm., (d) =10 µm.

Dactylellina xinjuanii F. Zhang, K.D. Hyde & X.Y. Yang, sp. nov. (Figure 10.16)

Index Fungorum number: IF902031; Facesoffungi number: FoF 15763

Etymology: The specific epithet "xinjuanii" comes from Xinjuan Zhou, one of the main collectors of this batch of soil samples.

Material examined: China, Yunnan Province, Dali City, Yunlong County, Miaowei Town, Niuzideng Mountain, from the soil collected in burned forest (10–20 cm. depth), 6 March 2018, F. Zhang, BF119-2. Holotype DLUCC155. Dali City, Yunlong County, Miaowei Town, Niuzideng Mountain, from the soil collected in burned forest (10–20 cm. depth), 6 March 2018, F. Zhang, BF101-2. Paratype YL531.

Saprobic on soil. *Sexual morph*: Undetermined. *Colonies* on PDA white, villiform, growing slowly, reaching 55 mm diameter after 15 days in the incubator at 26 °C. *Mycelium* partly superficial, partly immersed. *Hyphae* septate, branched, smooth and hyaline. *Conidiophores* 68–281 µm. long ($\bar{x}$ = 177.9 µm., n = 100), 4.4–7.5 µm. ($\bar{x}$ = 6 µm., n = 100) wide at the base, gradually tapering upwards to the apex, 2–4.5 µm. wide ($\bar{x}$ = 3.5 µm., n = 100) at the apex, erect, septate, hyaline, unbranched, bearing a single conidium at the apex. *Conidia* 40–58 × 14.5–21 µm. ($\bar{x}$ = 50.2 × 16.7 µm., n = 100), smooth and hyaline, rounded at the apex and truncated at the base; immature conidia drop-shaped or clavate, 1–3-septate, with a super cell at the apex or middle; mature conidium subfusiform, 3–5-septate (mostly 4-septate, 1–2 septa at apex and 2–3 at base of the conidia), with a super cell at the middle. No microconidia was observed. Conidia germinating from the small end cells, and the super cell usually do not germinate. Catching nematodes with adhesive branches, adjacent branches often fuse at the apex to form a two-dimensional adhesive network. *Chlamydospores* not observed.

Notes: *Dactylellina xinjuanii* is phylogenetically related to *Da. cionopaga* (100% MLBS and 1.00 BYPP). They show difference of 4.6% (23/495 bp), 5.2% (27/517 bp), and 3.3% (18/547 bp) in ITS, TEF and RPB2 sequences. Morphologically, *Da. xinjuanii* and *Da. cionopaga* are difficult to distinguish at first sight. However, the former produces unbranched conidiophores and bear a single conidium at the apex, while the latter sometimes produces branched conidiophores and bear multiple conidia. In addition, the top and base of the conidia of the former are asymmetrical, while those of the latter are generally symmetrical. Furthermore, the conidia of *Da. cionopaga* are constricted significantly at the septa, while the conidia of *Da. xinjuanii* do not have any constrictions

(Drechsler, 1950; Zhang & Mo, 2006).

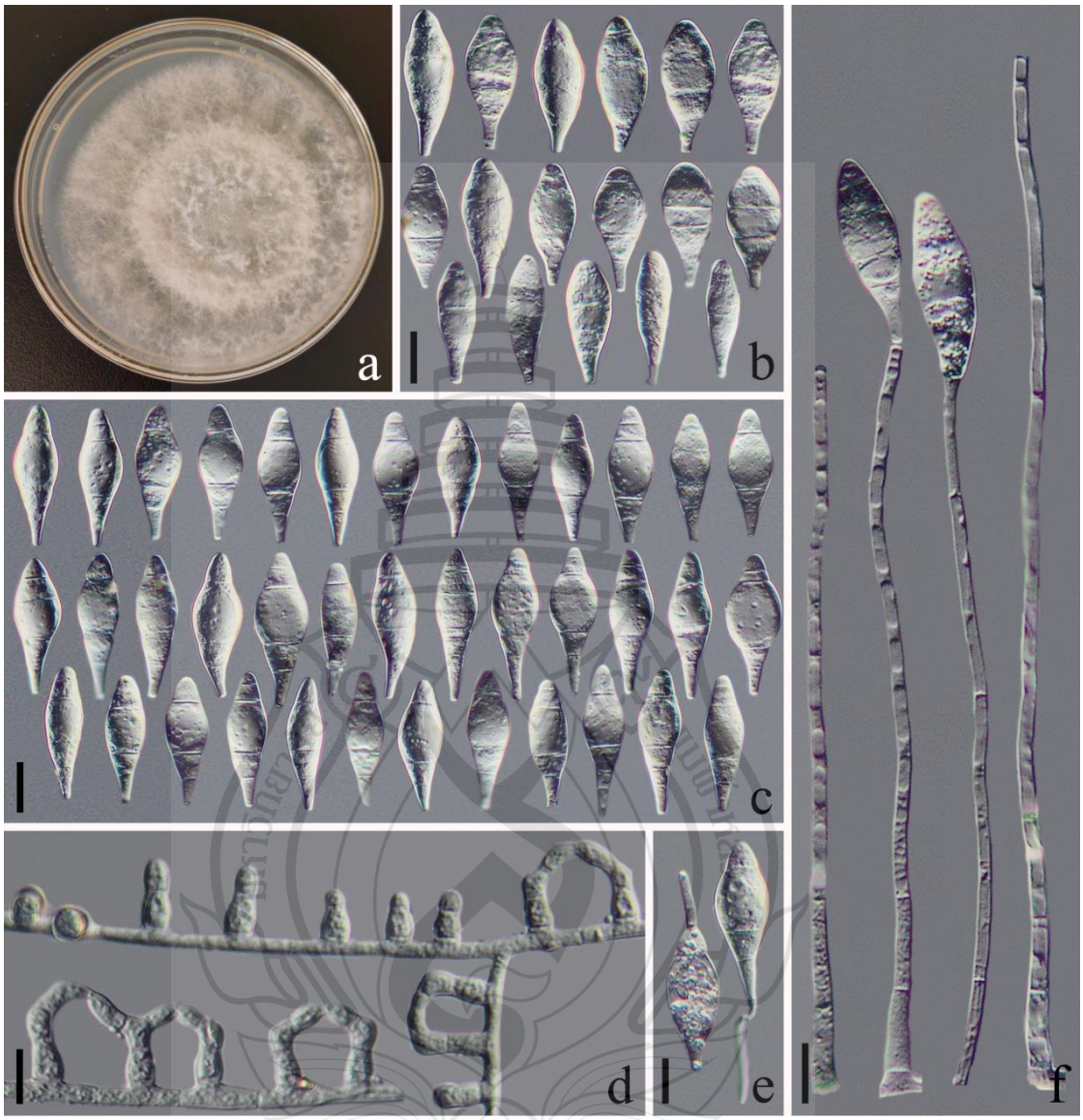

Figure 10.16 *Dactylellina xinjuanii* (DLUCC155). (a) Culture colony on PDA medium. (b, c) Conidia. (d) Trapping structure: adhesive branches. (e) Germinating conidia. (**f**) Conidiophores. Scale bars: (a) = 1 cm., (b, c, e, f) = 20 µm., (d) = 10 µm.

Dactylellina yangxiensis F. Zhang, K.D. Hyde & X.Y. Yang, sp. nov. (Figure 10.17)

Index Fungorum number: IF902017; Facesoffungi number: FoF 15764

Etymology: The specific epithet "yangxiensis" refers to a stream (Yangxi Stream) next to the sample collection site, which is one of the famous 18 streams in Cangshan Mountain.

Material examined: China, Yunnan Province, Dali City, Wanqiao Town, Dashaba Mountain, from the soil collected in burned forest (0–10 cm. depth), June 2021, F. Zhang, ZX14-1. Holotype DLUCC147. Dali City, Wanqiao Town, Dashaba Mountain, from the soil collected in burned forest (0–10 cm. depth), June 2021, F. Zhang, ZX9-1. Paratype WQ114.

Saprobic on soil. *Sexual morph*: Undetermined. *Colonies* on PDA white, cottony, growing slowly, reaching 38 mm diameter after 15 days in the incubator at 26 °C. *Mycelium* partly superficial, partly immersed. *Hyphae* septate, branched, smooth and hyaline. *Conidiophores* 185.5–304 µm. long ($\bar{x}$ = 261.8 µm., n = 100), 3–6 µm. wide ($\bar{x}$ = 4.6 µm., n = 100) at the base, gradually tapering upwards to the apex, 1.5–3 µm. wide ($\bar{x}$ = 2.3 µm., n = 100) at the apex, erect, septate, hyaline, unbranched, bearing a single conidium at the apex. *Conidia* 25.5–49 × 10–20 µm. ($\bar{x}$ = 39.2 × 15.3 µm., n = 100), smooth and hyaline, subfusiform, some conidia slightly curved, rounded at the apex and truncated at the base, with a super cell at the middle, 1–4-septate (mostly 3-septate). No microconidia was observed. Conidia usually germinating from the small cells at both ends. Catching nematodes with adhesive branches, adjacent branches often fuse at the apex to form a two-dimensional adhesive network. *Chlamydospores* not observed.

Notes: Phylogenetically, *Dactylellina yangxiensis* clusters together with *Da. dashabaensis* (other new species reported in this study) and *Da. gephyropaga* with 100% MLBS and 0.98 BYPP support. *Dactylellina yangxiensis* is 3% (16/529 bp) and 5% (25/496 bp) different from *Da. dashabaensis* and *Da. gephyropaga* in ITS sequences. In morphology, *Da. yangxiensis* is more similar to *Da. shuzhengsum* in the terms of conidiophore (unbranched, bearing a single conidium at the apex), the shape and septa of conidia (subfusiform, 2–4-septate, with a super cell at the middle of the conidia). However, the trapping structure (adhesive branches) of *Da. shuzhengsum* typically have

a short stalk connected to the mycelium at its base, which is absent in *Da. yangxiensis*. Furthermore, the conidia of *Da. yangxiensis* are noticeably wider than those of *Da. shuzhengsum* [*Da. yangxiensis*, 10–20 (15.3) µm. versus *Da. shuzhengsum*, 5–12.5 (8.3) µm.] (Zhang & Mo, 2006).

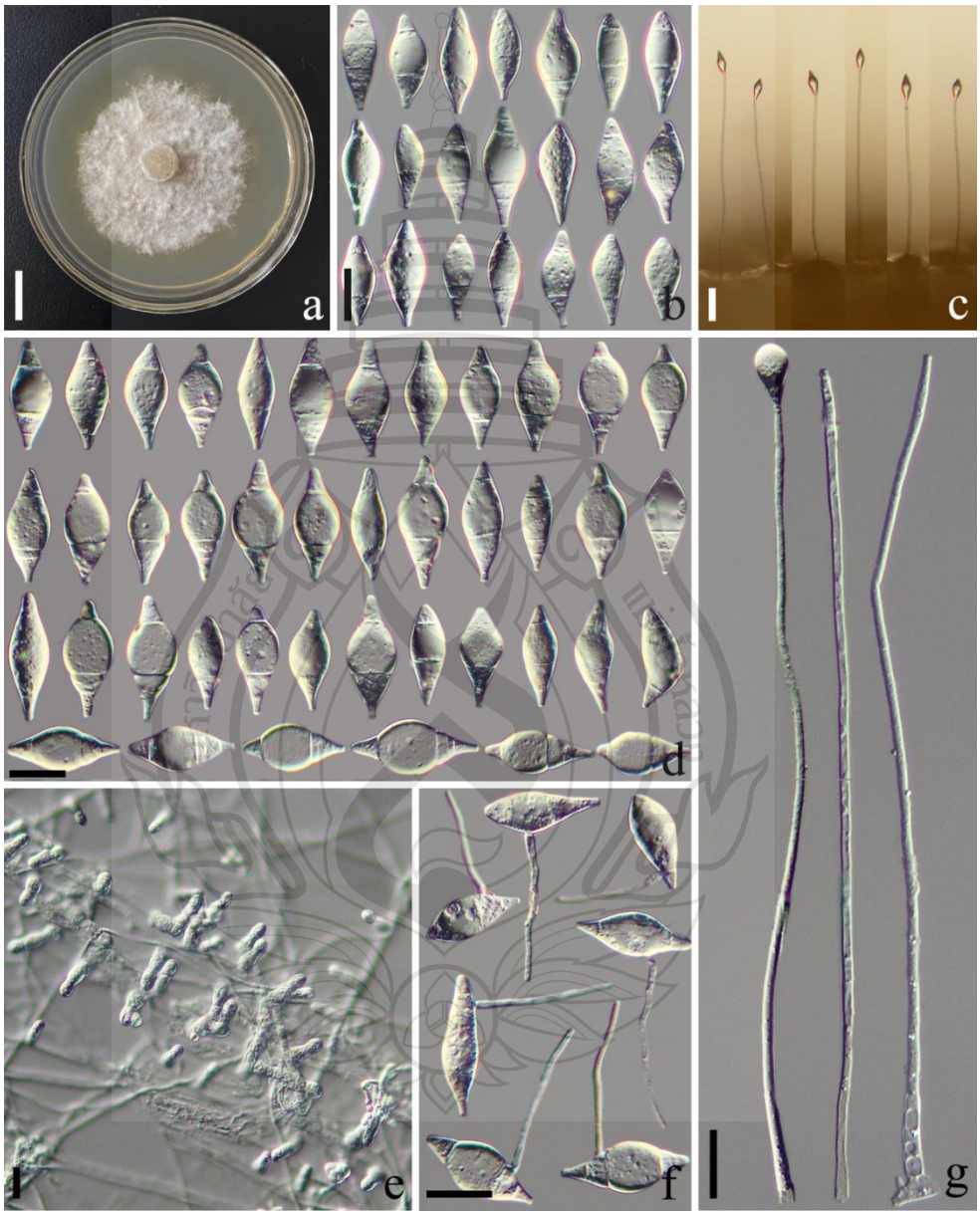

Figure 10.17 *Dactylellina yangxiensis* (holotype DLUCC147). (a) Culture colony on PDA medium. (b, d) Conidia. (e) Trapping structure: adhesive branches. (f) Germinating conidia. (c, g) Conidiophores. Scale bars: (a) = 1 cm., (b, d, f, g) = 20 µm., (e) = 10 µm., (c) = 50 µm.

10.3.3 Comprehensive Morphological Framework of *Dactylellina* Species

The comprehensive morphological framework of *Dactylellina* species we provide here consists of three modules (we divided the framework of *Dactylellina* into two figures according to their trapping structures due to the table being too large to put in the text) (Figure 10.18, 10.19). The first module is the preliminary classification part (columns 1–3), which utilizes features that are clearly differentiated and can be clearly discerned through preliminary observation (such as the type of trapping structures, the characteristics of conidiophores, the shape, septa and super cell of conidia) to divide 51 *Dactylellina* species into several categories. When identifying an unknown strain, it can be classified into a specific category based on these characteristics. The second module is the detail description part (column 4), which supplements the features not mentioned in the first module, aids in further species identification and facilitates comparison of similar species. This section allows for a more detailed comparison of strains that cannot be identified using the first module. The third module is the species name part (column 5), which corresponds one-to-one with the aforementioned species features.

Compared with the traditional dichotomous species key, the key of *Dactylellina* species we provide here demonstrates the following advantages. Firstly, it includes various morphological features of each species, accurately representing the appearance of each species in the table. This facilitates the comparison of similar species, improving the accuracy of species identification and further providing a comprehensive understanding of the morphological features of this group of fungi. Secondly, most of the features listed in the table are objective descriptions, reducing the subjective judgments often seen in traditional dichotomous species keys (such as “the conidia of A are longer” or “the conidia of A are rounded”), thus increasing the accuracy and usability of the key. Thirdly, due to the limited number of features available for species identification and the high number of similar species, the result may correspond to multiple possible species when using this species key for strain identification. Although this table may not be able to identify an unknown strain to an exact species accurately, it can accurately bring the unknown strain close to several possible species, and further accurate identification can be made based on other features (such as detailed morphological comparisons and even molecular biology identification). When there are many similar species, compared with traditional dichotomous species key that forcefully assign a species, this identification method is also

an effective way to improve accuracy.

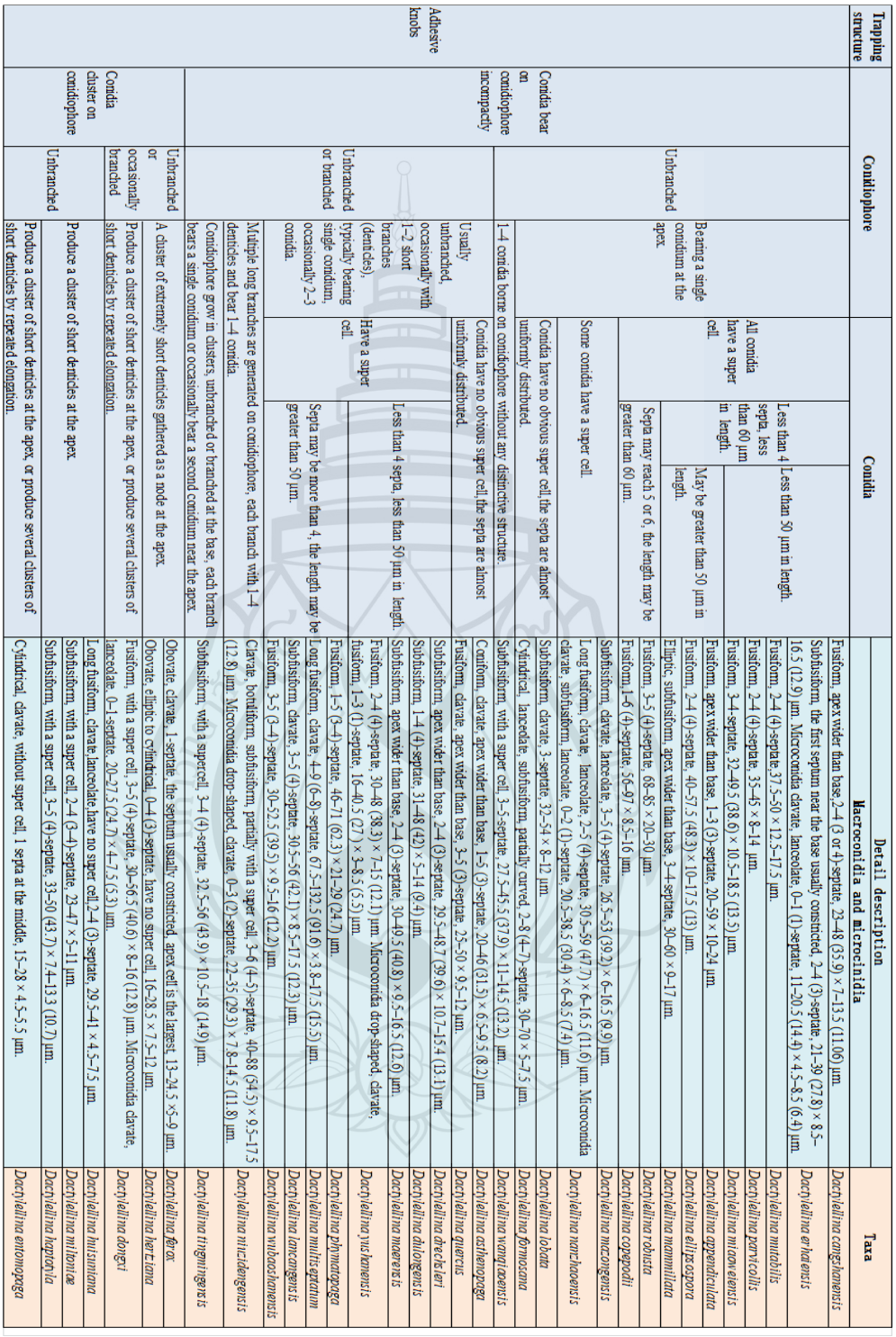

Trapping structure	Conidiophore	Conidia	Detail description	Taxa
			Macroconidia and microcinidia	
Adhesive knobs	Unbranched	All conidia have a super cell. Less than 4 septa, less than 60 μm in length.	Fusiform, apex wider than base,2–4 (3 or 4)-septate, 23–48 (35.9) × 7–13.5 (11.06) μm.	*Dactylellina congjiahensis*
			Subfusiform, the first septum near the base usually constricted, 2–4 (3)-septate, 21–39 (27.8) × 8.5–16.5 (12.9) μm. Microconidia clavate, lanceolate, 0–1 (1)-septate, 11–20.5 (14.4) × 4.5–8.5 (6.4) μm.	*Dactylellina erbaensis*
			Fusiform, 2–4 (4)-septate,37.5–50 × 12.5–17.5 μm.	*Dactylellina mutabilis*
			Fusiform, 2–4 (4)-septate, 35–45 × 8–14 μm.	*Dactylellina parvicolla*
			Fusiform, 3–4-septate, 32–49.5 (38.6) × 10.5–18.5 (13.5) μm.	*Dactylellina microcienisis*
		Less than 4 septa, less than 60 μm in length. May be greater than 50 μm in length.	Fusiform, apex wider than base, 1–3 (3)-septate, 20–59 × 10–24 μm.	*Dactylellina appendiculata*
			Fusiform, 2–4 (4)-septate, 40–57.5 (48.3) × 10–17.5 (13) μm.	*Dactylellina ellipsospora*
			Elliptic, subfusiform, apex wider than base, 3–4-septate, 30–60 × 9–17 μm.	*Dactylellina mammillata*
			Fusiform, 3–5 (4)-septate, 68–85 × 20–30 μm.	*Dactylellina robusta*
		Septa may reach 5 or 6, the length may be greater than 60 μm.	Fusiform,1–6 (4)-septate, 56–97 × 8.5–16 μm.	*Dactylellina copepodii*
	Conidia bear on conidiophore incompactly	Some conidia have a super cell.	Subfusiform, clavate, lanceolate, 3–5 (4)-septate, 26.5–53 (39.2) × 6–16.5 (9.9) μm.	*Dactylellina macongensis*
			Long fusiform, clavate, lanceolate, 2–5 (4)-septate, 30.5–59 (47.7) × 6–16.5 (11.6) μm. Microconidia clavate, subfusiform, lanceolate, 0–2 (1)-septate, 20.5–38.5 (30.4) × 6–8.5 (7.4) μm.	*Dactylellina nonchaoensis*
		Conidia have no obvious super cell,the septa are almost uniformly distributed.	Subfusiform, clavate, 3-septate, 32–54 × 8–12 μm.	*Dactylellina lobata*
			Cylindrical, lanceolate, subfusiform, partially curved, 2–8 (4–7)-septate, 30–70 × 5–7.5 μm.	*Dactylellina formosana*
		1–4 conidia borne on conidiophore without any distinctive structure.	Subfusiform, with a super cell, 3–5-septate, 27.5–45.5 (37.9) × 11–14.5 (13.2) μm.	*Dactylellina wangtaoensis*
		Conidia have no obvious super cell,the septa are almost uniformly distributed.	Conifom, clavate, apex wider than base, 1–5 (3)-septate, 20–46 (31.5) × 6.5–9.5 (8.2) μm.	*Dactylellina asthenopaga*
			Fusiform, clavate, apex wider than base, 3–5 (3)-septate, 25–50 × 9.5–12 μm.	*Dactylellina quercus*
			Subfusiform, apex wider than base, 2–4 (3)-septate, 29.5–48.7 (39.6) × 10.7–15.4 (13.1) μm.	*Dactylellina drechsleri*
			Subfusiform, 1–4 (4)-septate, 31–48 (42) × 5–14 (9.4) μm.	*Dactylellina duiongensis*
		Less than 4 septa, less than 50 μm in length.	Subfusiform, apex wider than base, 2–4 (3)-septate, 30–49.5 (40.8) × 9.5–16.5 (12.6) μm.	*Dactylellina macrensis*
		Have a super cell.	Fusiform, 2–4 (4)-septate, 30–48 (38.3) × 7–15 (12.1) μm. Microconidia drop-shaped, clavate,	*Dactylellina yuxiensis*
	Unbranched or branched	Multiple long branches (denticles), typically bearing single conidium, occasionally 2–3 conidia.	fusiform, 1–3 (1)-septate, 16–40.5 (27) × 3–8.5 (5.5) μm.	
			Fusiform, 1–5 (3–4)-septate, 46–71 (62.3) × 21–29 (24.7) μm.	*Dactylellina phymatopaga*
		Septa may be more than 4, the length may be greater than 50 μm.	Long fusiform, clavate, 4–9 (6–8)-septate, 67.5–192.5 (91.6) × 3.8–17.5 (15.5) μm.	*Dactylellina multiseptatum*
			Subfusiform, clavate, 3–5 (4)-septate, 30.5–56 (42.1) × 8.5–17.5 (12.3) μm.	*Dactylellina ioncongensis*
			Fusiform, 3–5 (3–4)-septate, 30–52.5 (39.5) × 9.5–16 (12.2) μm.	*Dactylellina wuboochomensis*
		Multiple long branches are generated on conidiophore, each branch with 1–4 denticles and bear 1–4 conidia.	Clavate, bottleform, subfusiform, partially with a super cell, 3–6 (4–5)-septate, 40–88 (54.5) × 9.5–17.5 (12.8) μm. Microconidia drop-shaped, clavate, 0–3 (2)-septate, 22–35 (29.3) × 7.8–14.5 (11.8) μm.	*Dactylellina nicidiengensis*
		Conidiophore grow in clusters, unbranched or branched at the base, each branch bears a single conidium or occasionally bear a second conidium near the apex.	Subfusiform, with a supercell, 3–4 (4)-septate, 32.5–56 (43.9) × 10.5–18 (14.9) μm.	*Dactylellina tingmingensis*
	Unbranched or occasionally branched	A cluster of extremely short denticles gathered as a node at the apex.	Obovate, clavate, 1-septate, the septum usually constricted, apex cell is the largest, 13–24.5 ×5–9 μm.	*Dactylellina foro*
		Produce a cluster of short denticles at the apex, or produce several clusters of short denticles by repeated elongation.	Obovate, elliptic to cylindrical, 0–4 (3)-septate, have no super cell, 16–28.5 × 7.5–12 μm.	*Dactylellina hertona*
			Fusiform, with a super cell, 3–5 (4)-septate, 30–56.5 (40.6) × 8–16 (12.8) μm. Microconidia clavate, lanceolate, 0–1-septate, 20–27.5 (24.7) × 4–7.5 (5.3) μm.	*Dactylellina donggi*
	Conidia cluster on conidiophore	Produce a cluster of short denticles at the apex.	Long fusiform, clavate,lanceolate,have no super cell,2–4 (3)-septate, 29.5–41 × 4.5–7.5 μm.	*Dactylellina huisuniana*
			Subfusiform, with a super cell, 2–4 (3–4)-septate, 23–47 × 5–11 μm.	*Dactylellina mibonicae*
	Unbranched	Produce a cluster of short denticles at the apex, or produce several clusters of short denticles by repeated elongation.	Subfusiform, with a super cell, 3–5 (4)-septate, 33–50 (43.7) × 7.4–13.3 (10.7) μm.	*Dactylellina haptotyla*
			Cylindrical, clavate, without super cell, 1 septa at the middle, 15–28 × 4.5–5.5 μm.	*Dactylellina entomopaga*

Figure 10.18 The comprehensive morphological framework of adhesive Knobs produce species in *Dactylellina*

Trapping structure	Conidiophore	Conidia	Detail description Macroconidia	Taxa
Adhesive branches	Conidia cluster on conidiophore	Unbranched,produce a cluster of short denticles at the apex, bear 1–8 conidia.	Long fusiform, without super cell, 3 septa are evenly distributed, 30–54 × 4–6 μm.	*Dactylellina arcuata*
	Conidia bear on conidiophore incompactly	Unbranched, occasionally produce 1–2 short branches (short denticles), bear 1–3conidia.	Fusiform, with a super cell, 2–6 (3–4)-septate, 35–60 × 13–21 μm.	*Dactylellina clonopaga*
		Unbranched, bear a single conidium at the apex. Less than 4 septa, less than 50 μm in length.	Fusiform, with a super cell, 2–6 (3–4)-septate, 30–67.5 (45) × 10–23.5 (16) μm.	*Dactylellina gephyropaga*
			Fusiform, with a super cell, 1–4 (3–4)-septate, 25–45 (32.4) × 5–12.5 (8.3) μm. Adhesive branches with a short stalk.	*Dactylellina shuchengsum*
			Subfusiform, with a super cell, 2–4 (3)-septate, 25.5–49 (39.2) × 10–20 (15.3) μm.	*Dactylellina yangxiensis*
		Septa may reach 5 or 6, the length may be greater than 50 μm.	Subfusiform, with a super cell, 3–6 (4–5)-septate, 40–58 (50.2) × 14.5–21 (16.7) μm.	*Dactylellina xinjiangi*
			Subfusiform, with a super cell, the septa of the small cells at both ends is clearly constricted, 3–5 (4)-septate, 47–72 (59) × 14.5–25.5 (21) μm.	*Dactylellina dashiboensis*

Trapping structure	Conidiophore	Conidia	Detail description Macroconidia and conidiophore	Taxa
Adhesive knobs and non-constricting rings	Conidia cluster on conidiophore	Have a obvious super cell	Fusiform, partially curved, 3–9 (4–6)-septate, 34–81 (47.3) × 8.5–12.5 (10.2) μm. Conidiophore produce 1–5 short branches at the apex, bear 1–5 conidia.	*Dactylellina yunnanensis*
			Long fusiform, partially curved, 2–5 (4)-septate, 27.5–57.5 (35) × 7.5–12.5 (9) μm. Conidiophore Produce 1–12 short branches at the apex, bear 1–12 (3–5) conidia.	*Dactylellina candida*
			Fusiform, clavate, lanceolate, partially curved, 1–13 (6–8)-septate, 28.7–51.5 (40.8) × 3.2–5.2 (4.2) μm. Conidiophore unbranched or produce long branches, each branch produce 1–7 short denticles, bear 1–7 conidia.	*Dactylellina daliensis*
		Have no obvious super cell,septa was almost uniformly distributed.	Long columnar, lanceolate, apex usually attached a adhesive knob, 5–8-septate, 35–60 × 2.2–3.7 μm.Conidiophore produce a cluster of denticles (1–15) near the apex, bear 1–15 conidia.	*Dactylellina haptospora*
			Long fusiform, partially curved, 1–9 (7–8)-septate, 25–61.5 (46.5) × 6.5–10 (9) μm. Conidiophore produce long branches in the lower part of the middle, each branch with 1–5 short denticles,bear 1–5 conidia.	*Dactylellina varietas*
			Clavate, lanceolate, partially curved, 4–10-septate, 28–70.5 (48.6) × 4–6 (5.1) μm. Conidiophore branched, each branch with a cluster of short denticles (5–22), or produce several clusters by repeated elongation.	*Dactylellina fodingensis*
	Conidia bear on conidiophore incompactly	Unbranched, bear a single conidium at the apex.	Fusiform, partially curved, with a super cell, 3–6 (4)-septate, 35–82.5 (53.5) × 7.5–17.5 (13) μm.	*Dactylellina sichuanensis*
			Fusiform, with a super cell, 3–8 (5)-septate, 25.5–117.5 (66.5) × 5.5–15.2 (14.1) μm.	*Dactylellina tilaqueata*
		Unbranched, occasionally produce 1–2 short branches (short denticles),bear 1–3 conidia	Subfusiform, with a super cell, 2–4 (3–4)-septate, 27.5–85 (40.7) × 9–17.5 (11) μm.	*Dactylellina hysipaga*
			Long fusiform, long columnar, lanceolate, clavate, apex usually attached a adhesive knob, without super cell, 4–15-septate, 30–92 (64) × 4–6 (4.5) μm .Microconidia subfusiform, lanceolate,3–8-septate,10–35 × 4–5.8 μm.	*Dactylellina leptospora*

Figure 10.19 The comprehensive morphological framework of adhesive branches and non-constricting rings produce species in *Dactylellina*

10.4 Discussion

10.4.1 The Phylogenetic Relationships of Trapping Structure in *Dactylellina*

As a group of fungi capable of forming specialized structures to capture nematodes, *Orbiliomycetes* nematode-trapping fungi (NTF) have received extensive attention as typical representatives of carnivorous fungi due to their unique survival strategies, diverse morphological structures, rich species diversity, and potential value in the biological control of harmful nematodes (Zhang & Hyde, 2014; Jiang et al., 2017; Soliman et al., 2021). One of the most important research directions in the field of NTF is to explore the evolution of these unique fungi, and the emergence of predation function is usually considered as the main reason for the wide distribution of this group fungi. Thus, trapping structures are mainly considered in evolutionary studies, and understanding the phylogenetic relationships among species that produce different trapping structures is a key basis for exploring the evolution of NTF. Presently, the phylogenetic relationships within NTF have been partially resolved, For instance, species employing constricting rings to capture nematodes form a distinct clade (*Drechslerella*), and diverged from other species that trap nematodes with four kinds of adhesive trapping structures. Among four adhesive trapping structures, species produce adhesive networks cluster together (*Arthrobotrys*), and diverged from the remaining three types of adhesive trapping structures. However, the phylogenetic relationships among these three adhesive trapping structure, grouped as *Dactylellina*, remain unclear (Ahrén et al., 1998; Li et al., 2005; Yang et al., 2007; Yang et al., 2012). The scarcity of research material is a major factor impeding progress in understanding the phylogenetic relationships of these three trapping structures within the *Dactylellina*. *Dactylellina* exhibits low diversity in common habitats (such as forest or farmland soil, sediment, animal waste), with most species being exceedingly rare, particularly those capture nematodes with adhesive branches (only four species reported globally) and those producing non-constricting-ring (only nine species reported globally). This study reports eleven new species employing adhesive knobs to capture nematodes, one species utilizing non-constricting rings, and three species utilizing adhesive branches, thus providing additional data for intrageneric taxonomic studies of *Dactylellina*.

Furthermore, this study found that all tested species that produce adhesive branches (8 species) formed a stable clade (Clade I, 98% MLBS and 0.95 BYPP support) (Figure 10.2). This result demonstrates the monophyly of species that produce adhesive branches and partially clarifies the phylogenetic relationships within the genus *Dactylellina*. However, the phylogenetic relationships among *Dactylellina* species that produce adhesive knobs and non-constricting rings have not yet been fully resolved and more research is needed.

10.4.2 The Contribution of Wildfire to Microbial Diversity

The history of NTF diversity research can be divided into three periods. Only five species were discovered in the initial phase of nearly 90 years (from 1839 to 1929). The rich phase (from 1931 to 2009), nearly 90 species were described over 80 years. In the recent period over ten years (from 2010 to 2019), only four species were discovered (http://www.speciesfungorum.org (accessed on 10 January 2024), Zhang et al., 2022a). This trend might have been indicative that there remain little to be discovered more in terms of novel species. However, we have investigated NTF in Yunnan Province in recent years, resulting in the discovery of 36 new species. Among these, 13 new *Arthrobotrys* (a dominant genus in most habitats) species and two new *Drechslerella* species were found in typical habitats such as forest soil and freshwater sediments (Zhang et al., 2022a; Zhang et al., 2022c; Yang et al., 2023; Zhang et al., 2023a; Zhang et al., 2023b). The discovery of these species was on the expected line because of our large-scale survey, which involved 3,346 samples from across Yunnan Province. However, what was unexpected is that 21 rare and new NTF species (18 *Dactylellina* and 3 *Drechslerella* species) were isolated from 420 soil samples collected from three burnt forests in Dali City, Yunnan Province (Zhang et al., 2020b; Zhang et al., 2022b; Zhang et al., 2023b). The isolation of such a significant number of rare and new NTF species in such a small area and with such a limited sample size is highly unusual.

We also propose a hypothesis to explain this unusual phenomenon: the majority of species commonly isolated are dominant taxa within their habitats. In a typical habitat, *Arthrobotrys* species are dominant and usually found in resource-rich upper soil due to their strong saprophytic growth and reproduction ability. In contrast, *Dactylellina* and *Drechslerella* species are rare and usually found in subsoils that lack resources due

to their weak saprophytic and reproductive ability (Mo et al., 2008; Swe et al., 2009; Deng et al., 2020; Dackman et al., 2021). When a fire occurs, *Arthrobotrys* species in the upper soil become more susceptible to the impact of the fire and are eliminated, resulting in the formation of habitat gaps in the upper soil. However, the rare species in the lower layer are protected by the upper soil, allowing them to remain intact. During the subsequent recovery phase, after the competitive suppression imposed by *Arthrobotrys* on rare species is lifted, the surviving *Dactylellina* and *Drechslerella* species can grow abundantly and occupy the habitat gaps in the surface soil, forming dominant groups in the area and more likely to be isolated. Based on this principle, we speculate that other microbial groups with vertical distribution differences in the soil may also exhibit similar patterns and yield many rare species in burned forests (She et al., 2020; She et al., 2022). Further studies focusing on other groups are currently underway, and their findings will form the subject for future reports.

The formation and maintenance of biodiversity are central topics in ecological research (Zhihua et al., 2002; Vandermeer, 2006; Chisholm et al., 2016). With increasing global climate change and the intensification of human activities in recent years, forest fires have become more frequent and severe, attracting widespread attention to their impact on biodiversity (Bowman & Murphy, 2010; He et al., 2019; Kelly et al., 2020). On one hand, the high temperatures generated by forest fires and the resulting environmental disturbances can cause devastating damage to vegetation and animals. On the other hand, our research indicates that fire-affected forests harbour a more significant number of rare species, and previous studies have also confirmed the high species diversity and endemism often found in fire-prone areas (Bond & Parr, 2010; Fernandes et al., 2018; She et al., 2020; She et al., 2022). Based on the hypothesis we proposed above, we can further speculate that one of the contribution of forest fires to biodiversity may be in the creation of habitat gaps in the surface soil and the elimination of competitive suppression exerted by dominant taxa (*Arthrobotry* species) on rare taxa (*Dactylellina* and *Drechslerella* species). This expands the diversity of previously rare *Dactylellina* and *Drehslerella* species. Further reasoning, if a region has not experienced a forest fire for an extended period, rare species within the region may be continuously suppressed by dominant species due to their weaker competitive abilities. Over time, this competition may lead to a gradual reduction in the population size of

the rare species and eventually their extinction. Environmental disturbance factors, such as forest fires, can initiate the reconfiguration of the local biological community and create opportunities for rare species to thrive. Therefore, we propose that forest fires may play a critical role in enabling the survival of rare and vulnerable species and serve as an essential mechanism for maintaining biodiversity in ecosystems. It is unclear at the moment if any of the isolated species from the lower strata of the soil are pyrophiles.

The role of rare microorganisms in ecosystems has long intrigued ecologists (Sutherland et al., 2013). This study offers some insights into this matter. Nematodes, as the most abundant animals in soil ecosystems, directly or indirectly participate in nearly all soil ecological processes. Therefore, the stability of their populations is crucial for normal functioning of ecosystems (Bongers & Bongers, 1998; Semprucci et al., 2012, Mekonen et al., 2017). NTF serve as essential regulators of nematode populations within the ecosystem (Liu et al., 2009; Zhang et al., 2020c). In undisturbed habitats, *Arthrobotrys* species which have high population densities, play a dominant role in balancing nematode populations. However, when a fire occurs, *Arthrobotrys* is eliminated, and the previously rare genera *Dactylellina* and *Drechslerella* become more abundant, thereby replacing *Arthrobotrys* in performing the ecological function of regulating nematode populations. Based on above, it can be inferred that one function of rare microorganisms is to act as alternative members, performing similar ecological functions when ecosystems undergo severe disturbances that prevent dominant taxa from fulfilling their ecological roles. These rare microorganisms contribute to the stability and functioning of ecosystems during periods of disruption. And burned forest is undoubtedly an ideal habitat for the discovery of new species and rare fungi.

CHAPTER 11

CONCLUSIONS

11.1 Overall Conclusion

The comprehensive suite of studies presented here has markedly enriched the field of mycology by illuminating the diversity, ecological significance, and evolutionary biology of nematode-trapping fungi (NTF), particularly within the diverse genus *Arthrobotrys* and its relatives in the *Orbiliomycetes*. These studies conducted in the biologically rich province of Yunnan, China, have not only expanded the taxonomic breadth with the discovery of numerous new fungal species but also highlighted their nuanced ecological roles and potential applications in bio-control within various ecosystems.

The identification of these new species, such as *Arthrobotrys blastospora*, which shows morphological traits akin to ancient carnivorous fungi, offers a profound glimpse into the evolutionary dynamics of carnivorous fungi. Such findings have implications far beyond taxonomy, suggesting mechanisms of ancient survival and adaptation that could be harnessed in modern agricultural practices.

These studies have utilized cutting-edge multilogues phylogenetic analysis to establish robust evolutionary relationships between newly discovered fungi and their more well-known counterparts. This detailed genetic scrutiny has confirmed that the newly identified species are distinct, clarifying their positions within the complex phylogenetic tree of the fungal kingdom and revealing how these species have diverged from common ancestors.

Furthermore, the ecological insights provided by these studies are invaluable. The fungi's diverse nematode-trapping mechanisms ranging from adhesive networks to mechanical constricting rings, illustrate a fascinating array of evolutionary adaptations that enable these fungi to thrive in competitive environments. This ecological versatility

underscores the potential of NTF to act as natural bio-control agents, capable of reducing harmful nematode populations in a way that is both effective and environmentally sustainable.

Importantly, the research conducted on these fungi has shown their ability to inhabit and function effectively in diverse environments, from terrestrial to aquatic systems. This adaptability makes them particularly valuable for developing biological control strategies in a variety of agricultural settings, offering a promising alternative to chemical pesticides.

In conclusion, the detailed exploration of these new species has not only provided critical taxonomic additions to the field of mycology but has also opened new avenues for research into the ecological applications of NTF. The implications of this work extend into ecological management, where these fungi could play pivotal roles in sustainable agriculture, highlighting the importance of preserving fungal biodiversity as a reservoir of biological tools for enhancing food security and ecosystem health. This body of research lays a foundational stone for future studies aimed at harnessing the power of biological processes to foster a more sustainable and resilient agricultural system globally.

11.2 Research Advantages

11.2.1 Diversity and Novelty: The identification of multiple new species of NTF, including those with unique aquatic adaptations, adds valuable entries to the global fungal taxonomy. This expands our understanding of fungal biodiversity, especially in less-studied aquatic environments.

11.2.2 Methodological Rigor: Employing multilogues phylogenetic analyses alongside detailed morphological characterizations ensures robust species identification and evolutionary insights, setting a high standard for fungal taxonomy research.

11.2.3 Ecological Insights: The research provides critical insights into the ecological roles of NTF, demonstrating their potential in biological control and their

mechanisms of nematode predation, which are crucial for sustainable agricultural practices.

11.2.4 Geographical and Ecological Range: Focusing on a biodiversity hotspot like Yunnan allows for the exploration of unique ecological niches, leading to the discovery of species with potentially unique genetic and ecological traits.

11.3 Future Work

11.3.1 Deeper Ecological Interactions: Future studies should aim to uncover the detailed mechanisms of interaction between NTF and their nematode hosts, especially in aquatic environments where extracellular signaling plays a critical role. Understanding these interactions will enhance the application of NTF in bio-control.

11.3.2 Broader Geographic Sampling: Expanding research to other diverse regions globally could uncover more species and provide a comparative analysis of NTF diversity and functionality across different ecological zones.

11.3.3 Long-term Ecological Impact Studies: Investigating the long-term effects of introducing NTF into new environments is crucial for assessing their impact on native species and ecosystems. This is particularly important for their application in biological control.

11.3.4 Technological Integration: Utilizing emerging technologies such as genomic sequencing and CRISPR-Cas systems could provide deeper insights into the genetic basis of predation and resistance in NTF, paving the way for genetically enhanced bio-control agents.

11.3.5 Conservation and Sustainable Use: As new species are discovered, particularly in regions undergoing rapid environmental changes, there is a pressing need to understand their roles in ecosystems and how they can be conserved and sustainably utilized.

By continuing to explore these avenues, we can not only advance our fundamental understanding of fungal ecology and evolution but also harness the potential of NTF in addressing agricultural and environmental challenges.

11.4 Publications

Nine papers as the first author, and three papers as co-author in collaboration, were published in SCI journals. The first and co-author publications are listed below and are appended to the thesis.

First author publications

Zhang, F., Zhou, X. J., Monkai, J., Li, F. T., Liu, S. R., Yang, X. Y., . . . Hyde, K. D. (2020). Two new species of nematode-trapping fungi (*Dactylellina*, *Orbiliaceae*) from burned forest in Yunnan, China. *Phytotaxa, 452*(1), 65–74. https://doi.org/10.11646/phytotaxa.452.1.6

Zhang, F., Liu, S. R., Zhou, X. J., Monkai, J., Hongsanan, S., Shang, Q. J., . . . Yang, X. Y. (2020). *Fusarium xiangyunensis* (*Nectriaceae*), a remarkable new species of nematophagous fungi from Yunnan, China. *Phytotaxa, 450*(3), 273–284. https://doi.org/10.11646/phytotaxa.450.3.3

Zhang, F., Boonmee, S., Bhat, J. D., Xiao, W., & Yang, X. Y. (2022). New *Arthrobotrys* nematode-trapping species (*Orbiliaceae*) from terrestrial soils and freshwater sediments in China. *Journal of Fungi, 8*(7), 671. https://doi.org/10.3390/jof8070671

Zhang, F., Boonmee, S., Monkai, J., Yang, X. Y, & Xiao, W. (2022). *Drechslerella daliensis* and *D. xiaguanensis* (*Orbiliales*, *Orbiliaceae*), two new nematode-trapping fungi from Yunnan, China. *Biodiversity Data Journal, 2022,* 10. https://doi.org/10.3897/BDJ.10.e96642

Zhang, F., Yang, Y. Q., Zhou, F. P, Xiao, W., Boonmee, S., & Yang, X. Y. (2023). Morphological and Phylogenetic Characterization of Five Novel Nematode-Trapping Fungi (*Orbiliomycetes*) from Yunnan, China. *Journal of Fungi, 9*(7), 735. https://doi.org/10.3390/jof9070735

Zhang, F., Boonmee, S., Yang, Y. Q., Zhou, F. P., Xiao, W., & Yang, X. Y. (2023). *Arthrobotrys blastospora* sp. nov.(*Orbiliomycetes*): A living fossil displaying morphological traits of mesozoic carnivorous fungi. *Journal of Fungi, 9*(4), 451. https://doi.org/10.3390/jof9040451

Zhang, F., Yang, Y. Q., Zhou, F. P, Xiao, W., Boonmee, S., & Yang, X. Y. (2024). Multilocus Phylogeny and Characterization of Five Undescribed Aquatic Carnivorous Fungi (*Orbiliomycetes*). *Journal of Fungi, 10*(1), 81. https://doi.org/10.3390/jof10010081

Zhang, F., Huang, S. Y., Yang, Y. Q., Zhou, F. P., Boonmee, S., Yang, X. Y., . . . Xiao, W. (In press). Urea regulates soil nematode population by enhancing the insecticidal ability of nematode-trapping fungi. *Scientific Reports*.

Zhang, F., Zhou, F. P., Yang, Y. Q., Boonmee, S., Yu, Z. F., Bhat, D. J., . . . Xiao, W. (In press). Burned forests as excellent area for the discovery of new fungal: Hints from fifteen rare novel carnivorous fungi in *Orbiliomycete*. *Mycosphere*.

Co-author publications

Yang, X., Zhang, F., Yang, Y., Zhou, F., Boonmee, S., Xiao, W., . . . Yang, X. (2023). Conidia Fusion: A Mechanism for Fungal Adaptation to Nutrient-Poor Habitats. *Journal of Fungi, 9*(7), 755. ttps://doi.org/10.3390/jof9070755

Hyde, K. D., Norphanphoun, C., Ma, J., Yang, H. D., Zhang, J. Y., Du, T. Y., . . . Zhao, Q. (2023) Mycosphere notes 387–412-novel species of funga taxa from around the world. *Mycosphere, 14*(1), 663–744.

Ishara, S. M., Kevin, D. H., Dhanushka, N. W., Samantha, C. K., Milan, C. S., Sajeewa S. N. M., . . . Zhang, F. (In prep). Fungal diversity notes 1818–1917: taxonomic and phylogenetic contributions on genera and species of fungi. *Fungal Diversity*.

REFERENCES

REFERENCES

Ahmad, F., Saeed, Q., Shah, S. M., Gondal, M. A., & Mumtaz, S. (2022). Environmental sustainability: Challenges and approaches. *Natural Resources Conservation and Advances for Sustainability, 1*, 243–270. https://doi.org/10.1016/B978-0-12-822976-7.00019-3

Ahmad, G., Khan, A., Khan, A. A., Ali, A., & Mohhamad, H. I. (2021). Biological control: A novel strategy for the control of the plant parasitic nematodes. *Antonie van Leeuwenhoek, 114*(7), 885–912. https://doi.org/10.1007/s10482-021-01577-9

Ahman, J., Johansson, T., Olsson, M., Punt, P. J., van den Hondel, C. A., & Tunlid, A. (2002). Improving the pathogenicity of a nematode-trapping fungus by genetic engineering of a subtilisin with nematotoxic activity. *Applied and Environmental Microbiology, 68*(7), 3408–3415. https://doi.org/10.1128/AEM.68.7.3408-3415.2002

Ahrén, D., & Tunlid, A. (2003). Evolution of parasitism in nematode-trapping fungi. *Journal of Nematology, 35*(2), 194.

Ahren, D., & Ursing, B., & Tunlid, A. (1998). Phylogeny of nematode-trapping fungi based on 18S rDNA sequences. *FEMS Microbiology Letters, 158*(2), 179–184. https://doi.org/10.1016/S0378-1097(97)00519-3

Akers, D., & McCrystal, R. (2014). *Integration of crop and soil insect management in sweetpotato*. HAL Project VG09052 Australian Sweetpotato Growers Inc.

Akhtar, M. S., Panwar, J., Abdullah, S. N., Siddiqui, Y., Swamy, M. K., & Ashkani, S. (2015). Biocontrol of plant parasitic nematodes by fungi: Efficacy and control strategies. *Organic Amendments and Soil Suppressiveness in Plant Disease Management, 2015*, 219–247. https://doi.org/10.1007/978-3-319-23075-7_11

Akladious, S. A., & Abbas, S.M. (2014). Application of *Trichoderma harzianum* T22 as a biofertilizer potential in maize growth. *Journal of Plant Nutrition, 37*(1), 30–49. https://doi.org/10.1080/01904167.2013.829100

Albertini, J. B., & Schweinitz, L. D. (1805). *Conspectus fungorum in Lusatiae Superioris agro Niskiensi crescentium, emethodo Persooniana*. Lipsiae, Sumtibus Kummerianis. https://doi.org/10.5962/bhl.title.3601

Ali, S., Ullah, M. I., Sajjad, A., Shakeel, Q., & Hussain, A. (2021). Environmental and health effects of pesticide residues. In M. I. Inamuddin, Ahamed & E. Lichtfouse (Eds.), *Sustainable agriculture reviews 48. Sustainable Agriculture Reviews* (vol. 48, pp. 311-336). Springer. https://doi.org/10.1007/978-3-030-54719-6_8

Anderson, M. G., Jarman, T. B., & Rickards, R. W. (1995). Structures and absolute configurations of antibiotics of the oligosporon group from the nematode-trapping fungus *Arthrobotrys oligospora*. *The Journal of Antibiotics, 48*(5), 391–398. https://doi.org/10.7164/antibiotics.48.391

Aoki, T., O'Donnell, K., Homma, Y., & Lattanzi, A. R. (2003). Sudden-death syndrome of soybean is caused by two morphologically and phylogenetically distinct species within the *Fusarium solani* species complex—*F. virguliforme* in North America and *F. tucumaniae* in South America. *Mycologia, 95*(4), 660–684. https://doi.org/10.1080/15572536.2004.11833070

Arnaudow, N. (1923). Ein neuer Rädertiere (Rotatoria) fangender Pilz. (Sommerstorffia spinosa, nov. gen., nov. sp.). *Flora oder Allgemeine Botanische Zeitung, 116*(1-2), 109–113. https://doi.org/10.1016/S0367-1615(17)31135-7

Ashraf, M. S., & Khan, T. A. (2005). Effect of opportunistic fungi on the life cycle of the root-knot nematode (*Meloidogyne javanica*) on brinjal. *Archives of Phytopathology and Plant Protection, 38*(3), 227–233. https://doi.org/10.1080/03235400500094498

Balazy, S., Mietkiewski, R., Tkaczuk, C., Wegensteiner, R., & Wrzosek, M. (2008). Diversity of acaropathogenic fungi in Poland and other European countries. *Experimental and Applied Acarology, 46*, 53–70. https://doi.org/10.1007/s10493-008-9207-1

Baral, H. O., Weber, E., & Marson, G. (2020). *Monograph of Orbiliomycetes (Ascomycota) based on vital taxonomy. Part I + II*. National Museum of Natural History Luxembourg.

Baral, H. O., Weber, E., & Marson, G. (2022). Buchbesprechung–book review. Monograph of *Orbiliomycetes* (Ascomycota) based on vital taxonomy. *Part I+ II*, 1752.

Baral, H. O., Weber, E., Gams, W., Hagedorn, G., Liu, B., Liu, X., . . . Weiß, M. (2018). Generic names in the *Orbiliaceae* (Orbiliomycetes) and recommendations on which names should be protected or suppressed. *Mycological Progress, 7*, 5–31. https://doi.org/10.1007/s11557-017-1300-6

Barron, G. L. (1977). *The nematode-destroying fungi*. Canadian Biological Publications Ltd.

Barron, G. L. (1990). A new predatory hyphomycete capturing copepods. *Can. J. Bot, 68*, 691–696. https://doi.org/10.1139/b90-090

Barron, G. L. (2012). Predators and parasites of microscopic animals. In G. T. Cole & B. Kendrich (Eds.), *Biology of conidial fungi* (vol. 2, pp. 167-200). Academic Press. https://doi.org/10.1016/B978-0-12-179502-3.50013-3

Barron, G. L., & Percy, J. G. (1975). Nematophagous fungi: A new Myzocytium. *Canadian Journal of Botany, 53*(13), 1306–1309. https://doi.org/10.1139/b75-157

Basnet, D., Kandel, P., Chettri, N., Yang, Y., Lodhi, M. S., Htun, N. Z., . . . Sharma, E. (2019). Biodiversity research trends and gaps from the confluence of three global biodiversity hotspots in the Far-Eastern Himalaya. *Int. J. Ecol., 2019*, 1–14. https://doi.org/10.1155/2019/1323419

Benny, G. L., Ho, H. M., Lazarus, K.L., & Smith, M. E. (2016). Five new species of the obligate mycoparasite *Syncephalis* (Zoopagales, Zoopagomycotina) from soil. *Mycologia, 108*(6), 1114–1129.

Bernard, G. C., Egnin, M., & Bonsi, C. (2017). The impact of plant-parasitic nematodes on agriculture and methods of control. *Nematology-Concepts, Diagnosis and Control, 16*(1), 121–151. https://doi.org/10.5772/intechopen.68958

Bhunjun, C. S., Niskanen, T., Suwannarach, N., Wannathes, N., Chen, Y. J., McKenzie, E. H., . . . Zhang, J.Y. (2022). The numbers of fungi: Are the most speciose genera truly diverse? *Fungal Diversity, 114*(1), 387–462. https://doi.org/10.1007/s13225-022-00501-4

Blight, M. M., & Grove, J. F. (1974). New metabolic products of *Fusarium culmorum*: Toxic trichothec-9-en-8-ones and 2-acetylquinazolin-4 (3 H)-one. *Journal of the Chemical Society, Perkin Transactions, 1*, 1691–1693. https://doi.org/10.1039/p19740001691

Bond, W. J., & Parr, C. L. (2010). Beyond the forest edge: Ecology, diversity and conservation of the grassy biomes. *Biological conservation, 143*(10), 2395–2404. https://doi.org/10.1016/j.biocon.2009.12.012

Bongers, T., & Bongers, M. (1998). Functional diversity of nematodes. *Applied Soil Ecology, 10*(3), 239–251. https://doi.org/10.1016/S0929-1393(98)00123-1

Bongomin, F., Gago, S., Oladele, R. O., & Denning, D. W. (2017). Global and multi-national prevalence of fungal diseases—estimate precision. *Journal of Fungi, 3*(4), 57. https://doi.org/10.3390/jof3040057

Booth, B., & Mitchell, A. (2001). *Getting started with ArcGIS™*. ESRI.

Bowman, D. M. J. S., & Murphy, B. P. (2010). Fire and biodiversity. In N. S, Sodhi & P. R. Ehrlich (eds.), *Conservation biology for all* (pp. 163-180). Oxford University Press. https://doi.org/10.1093/acprof:oso/9780199554232.003.0010

Braga, F. R., & de Araújo, J. V. (2014). Nematophagous fungi for biological control of gastrointestinal nematodes in domestic animals. *Applied Microbiology and Biotechnology, 98*, 71–82. https://doi.org/10.1007/s00253-013-5366-z

Brian, P., Dawkins, A., Grove, J.F., Hemming, H., Lowe, D., & Norris, G. L. F. (1961). Phytotoxic compounds produced by *Fusarium equiseti*. *Journal of Experimental Botany, 12*(1), 1–12. https://doi.org/10.1093/jxb/12.1.1

Bruns, T. D., Chung, J. A., Carver, A. A., & Glassman, S. I. (2020). A simple pyrocosm for studying soil microbial response to fire reveals a rapid, massive response by *Pyronema* species. *PLoS One, 15*(3), e0222691. https://doi.org/10.1371/journal.pone.0222691

Burges, A., & Raw, F. (1967). *Soil biology*. Academic Press.

Butt, T. M., Jackson, C., & Magan, N. (2001). *Fungi as bio-control agents: Progress, problems and potential*. CABI Publishing. https://doi.org/10.1079/9780851993560.0000

Castaner, D. (1968). *Monacrosporium sphaeroides,* a new nematode-destroying hyphomycete from Iowa. *Am. Midl. Nat, 80*, 280–283. https://doi.org/10.2307/2423619

Certini, G., Moya, D., Lucas-Borja, M. E., & Mastrolonardo, G. (2021). The impact of fire on soil-dwelling biota: A review. *Forest Ecology and Management, 488*, 118989. https://doi.org/10.1016/j.foreco.2021.118989

Chehri, K., Salleh, B., & Zakaria, L. (2015). Morphological and phylogenetic analysis of *Fusarium solani* species complex in Malaysia. *Microbial Ecology*, *69*(3), 457–471. https://doi.org/10.1007/s00248-014-0494-2

Chen, J., Xu, L. L., Liu, B., & Liu, X. Z. (2007). Taxonomy of *Dactylella* complex and *Vermispora*. I. Generic concepts based on morphology and ITS sequences data. *Fungal Diversity*, *26*, 73–83.

Chen, P., Zhang, J., Li, M., Fang, F., Hu, J., Sun, Z., . . . Li, J. (2023). Synergistic effect of *Bacillus subtilis* and *Paecilomyces lilacinus* in alleviating soil degradation and improving watermelon yield. *Frontiers in Microbiology, 13,* 101975. https://doi.org/10.3389/fmicb.2022.1101975

Chethana, K. W., Manawasinghe, I. S., Hurdeal, V. G., Bhunjun, C. S., Appadoo, M. A., Gentekaki, E., . . . Hyde, K. D. (2021). What are fungal species and how to delineate them? *Fungal Diversity, 109*, 1–25. https://doi.org/10.1007/s13225-021-00483-9

Chisholm, R. A., Fung, T., Chimalakonda, D., & O'Dwyer, J. P. (2016). Maintenance of biodiversity on islands. *Proceedings of the Royal Society B: Biological Sciences, 283*(1829), 20160102. https://doi.org/10.1098/rspb.2016.0102

Chitwood, D. J. (2003). Research on plant-parasitic nematode biology conducted by the United States Department of Agriculture–Agricultural Research Service. *Pest Management Science: Formerly Pesticide Science*, *59*(6–7), 748–753. https://doi.org/10.1002/ps.684

Christensen, M. (1989). A view of fungal ecology. *Mycologia, 81*(1), 1–9. https://doi.org/10.1080/00275514.1989.12025620

Ciancio, A., Logrieco, A., Lamberti, F., & Bottalico, A. (1988). Nematicidal effects of some *Fusarium toxins*. *Nematologia Mediterranea*, *16*(1), 137–138.

Ciarmela, M., Arambarri, A., Basualdo, J., & Minvielle, M. (2010). Effect of saprotrophic soil fungi on *Toxocara canis* eggs. *Malaysian Journal of Microbiology*, *6*, 75–80. https://doi.org/10.21161/mjm.20809

Comans-Pérez, R. J., Sánchez, J. E., Al-Ani, L. K. T., González-Cortázar, M., Castañeda-Ramírez, G. S., Mendoza-de, G. P., . . . Aguilar-Marcelino, L. (2021). Biological control of sheep nematode *Haemonchus contortus* using edible mushrooms. *Biological Control*, *152*, 104420. https://doi.org/10.1016/j.biocontrol.2020.104420

Cooke, R. C. (1962). The ecology of nematode-trapping fungi in the soil. *Annals of Applied Biology*, *50*(3), 507–513. https://doi.org/10.1111/j.1744-7348.1962.tb06045.x

Cooke, R. C., & Dickinson, C. H. (1965). Nematode-trapping species of *Dactylella* and *Monacrosporium*. *Trans. Br. Mycol. Soc*, *48*, 621–629. https://doi.org/10.1016/S0007-1536(65)80040-7

Corda, A. K. J. (1839). *Pracht-Flora Europaeischer Schimmelbildungen*. G. Fleischer.

Crofton, H. D. (1963). *Nematode parasite population in sheep and on pasture*. Commonwealth Agricultural Bureaux.

Crous, P. W., Begoude, B. A. D., Boers, J., Braun, U., Declercq, B., Dijksterhuis, J., . . . Linde, C. C. (2022). New and interesting fungi. *Fungal Systematics and Evolution*, *10*(1), 19–90. https://doi.org/10.3114/fuse.2022.10.02

D'mello, J., Placinta, C., & Macdonald, A. (1999). *Fusarium* mycotoxins: a review of global implications for animal health, welfare and productivity. *Animal Feed Science and Technology*, *80*(3–4), 183–205. https://doi.org/10.1016/S0377-8401(99)00059-0

Dackman, C., Jansson, H. B., & Nordbring-Hertz, B. (2021). Nematophagous fungi and their activities in soil. In J. M. Bollag & G. Stotzky (eds.), *Soil biochemistry* (pp. 95–130). CRC Press. https://doi.org/10.1201/9781003210207-3

Dasika, R., Tangirala, S., & Naishadham, P. (2012). Pesticide residue analysis of fruits and vegetables. *Journal of Environmental Chemistry and Ecotoxicology*, *4*(2), 19–28. https://doi.org/10.5897/JECE11.072

Dayal, R. (1975). *Key to phycomycetes predaceous or parasitic in nematodes or amoebae I*. Zoopagales.

Dayi, M. (2024). Evolution of parasitism genes in the plant parasitic nematodes. *Scientific Reports, 14*(1), 3733. https://doi.org/10.1038/s41598-024-54330-3

de Jesús-Navarrete, A., Armenteros, M., Espositos, A. V., & Rocha-Olivares, A. (2022). Size spectra, biomass, and trophic groups of free-living marine nematodes along a water-depth gradient in the northwestern Gulf of Mexico. *Mar. Ecol., 43,* e12723. https://doi.org/10.1111/maec.12723

Degenkolb, T., & Vilcinskas, A. (2016). Metabolites from nematophagous fungi and nematicidal natural products from fungi as an alternative for biological control. Part I: metabolites from nematophagous ascomycetes. *Applied Microbiology and Biotechnology, 100,* 3799–3812. https://doi.org/10.1007/s00253-015-7233-6

Deng, W., Wang, J. L., Scott, M. B., Fang, Y. H., Liu, S. R., Yang, X. Y., . . . Xiao, W. (2020). Sampling methods affect nematode-trapping fungi biodiversity patterns across an elevational gradient. *BMC Microbiology, 20*, 1–11. https://doi.org/10.1186/s12866-020-1696-z

Deng, W., Zhang, F., Fornacca, D., Yang, X. Y., & Xiao, W. (2023). Those nematode-trapping fungi that are not everywhere: Hints towards soil microbial biogeography. *Journal of Microbiology, 61*(5), 511–523. https://doi.org/10.1007/s12275-023-00043-7

Deng, W., Zhang, F., Li, Y. P., Zhang, X., Fornacca, D., Yang, X. Y., . . . Wen, X. (2023). Uncovering the biogeographic pattern of the widespread nematode-trapping fungi *Arthrobotrys oligospora*: Watershed is the key. *Front. Microbiol, 14*, 1152751. https://doi.org/10.3389/fmicb.2023.1152751

Desai, M., Shah, H., & Pillai, S. (1972). Effect of *Aspergillus niger* on root-knot nematode, *Meloidogyne incognita*. *Indian Journal of Nematology, 2*(2), 210–214.

Dighton, J., & White, J. F. (2017). *The fungal community: Its organization and role in the ecosystem*. CRC press. https://doi.org/10.1201/9781315119496

Dijksterhuis, J., Veenhuis, M., & Harder, W. (1993). Conidia of the nematophagous fungus *Drechmeria coniospora* adhere to but barely infect *Acrobeloides buetschilii*. *FEMS Microbiology Letters, 113*(2), 183–188. https://doi.org/10.1111/j.1574-6968.1993.tb06511.x

Dix, N. J. (2012). *Fungal ecology*. Springer Science & Business Media.

Drechsler, C. (1933). Morphological diversity among fungi capturing and destroying nematodes. *Journal of the Washington Academy of Sciences, 23*, 138–141.

Drechsler, C. (1933). Morphological features of some more fungi that capture and kill nematodes. *Journal of the Washington Academy of Sciences, 23*, 267–270.

Drechsler, C. (1934). Organs of capture in some fungi preying on nematodes. *Mycologia, 26*, 135–144. https://doi.org/10.1080/00275514.1934.12020709

Drechsler, C. (1935). Some conidia hyphomycetes destructive to terricolous amoebe. *Mycologia, 27*, 6–40. https://doi.org/10.1080/00275514.1935.12017059

Drechsler, C. (1936). A fusarium-like species of *Dactylella* capturing and consuming testaceous rhizopods. *J. Wash. Acad. Sci, 26*, 397–404.

Drechsler, C. (1937). Some hyphomycetes that prey on free-living terricolous nematodes. *Mycologia, 29*(4), 447–552. https://doi.org/10.1080/00275514.1937.12017222

Drechsler, C. (1939). Five new Zoopagaceae destructive to rhizopods and nematodes. *Mycologia, 31*(4), 388–415. https://doi.org/10.1080/00275514.1939.12017354

Drechsler, C. (1940). Three fungi destructive to free-living terricolous nematodes. *Journal of the Washington Academy of Sciences, 30*(6), 240–254.

Drechsler, C. (1940). Three new hyphomycetes preying on free-living terricolous nematodes. *Mycologia, 32*, 448–470. https://doi.org/10.1080/00275514.1940.12017423

Drechsler, C. (1941). Four phycomycetes destructive to nematodes and rhizopods. *Mycologia, 33*(3), 248–269. https://doi.org/10.1080/00275514.1941.12020814

Drechsler, C. (1941). Predaceous fungi. *Biological Reviews, 16*(4), 265–290. https://doi.org/10.1111/j.1469-185X.1941.tb01104.x

Drechsler, C. (1944). A species of *Arthrobotrys* that captures springtails. *Mycologia, 36*(4), 382–399. https://doi.org/10.1080/00275514.1944.12017561

Drechsler, C. (1946). A species of *Harposporium* invading its nematode host from the stoma. *Bulletin of the Torrey Botanical Club*, 557–564. https://doi.org/10.2307/2481340

Drechsler, C. (1947). A Nematode-Strangling *Dactylella* with Broad Quadriseptate Conidia. *Mycologia, 39*, 5–20. https://doi.org/10.1080/00275514.1947.12017587

Drechsler, C. (1950). Several species of *Dactylellina* and *Dactylaria* that capture freeliving nematode. *Mycologia, 42*, 1–79. https://doi.org/10.1080/00275514.1950.12017816

Drechsler, C. (1952). Another nematode-strangulating *dactylella* and some related hyphomycetes. *Mycologia, 44*, 533–556. https://doi.org/10.1080/00275514.1952.12024214

Drechsler, C. (1954). Production of aerial arthrospores by *Harposporium bysmatosporum*. *Bulletin of the Torrey Botanical Club, 81*, 411–413. https://doi.org/10.2307/2482283

Drechsler, C. (1954). Some hyphomycetes that capture eelworms in southern states. *Mycologia, 46*(6), 762–782. https://doi.org/10.1080/00275514.1954.12024413

Drechsler, C. (1961). Some clampless hyphomycetes predaceous on nematodes and rhizopods. *Sydowia, 15*, 762–782.

Drechsler, C. (1962). Some clampless hyphomycetes predacious on nematodes and rhizopods. *Sydowi Annal. Mycol. Ser. II, 15*, 9–24.

Drechsler, C. (1963). A slender-spored *Dactylella* parasitic on zoospores. *Phytotholigy, 53*, 993–994.

Drechsler, C. (1968). A new nematode-destroying *Harposporium* with slender helicoid conidia. *Sydowia, 22*, 189–193.

Duddington, C. L. (1955). Notes on the technique of handling predacious fungi. *Transactions of the British Mycological Society, 38*(2), 97–103. https://doi.org/10.1016/S0007-1536(55)80021-6

Duddington, C. L. (1940). Predaceous phycomycetes from Cotswold leaf-mould. *Nature, 145*, 150–151. https://doi.org/10.1038/145150a0

Duddington, C. L. (1950). Further records of British predaceous fungi. *Trans. Brit. Mycol. Soc., 33*, 3–4. https://doi.org/10.1016/S0007-1536(50)80076-1

Duddington, C. L. (1951). *Dactylella lobata*, predacious on nematodes. *Transactions of the British Mycological Society, 34*, 489–491. https://doi.org/10.1016/S0007-1536(51)80032-9

Duddington, C. L. (1951). Two new predacious hyphomycetes. *Trans. Brit. Mycol. Soc.*, *34*, 598-603. https://doi.org/10.1016/S0007-1536(51)80044-5

Duddington, C. L. (1954). Nematode-destroying fungi in agricultural soils. *Nature*, *168*, 38–39. https://doi.org/10.1038/168038b0

Duddington, C. L. (1957). *The friendly fungi: A3 problem*. Faber and Faber.

Durschnerpelz, U. U. (1987). Traps of Nematoctonus leiosporus: An unusual feature of an endoparasitic nematophagous fungus. *Trans Br. Mycol. Soc.*, *88*, 129–130. https://doi.org/10.1016/S0007-1536(87)80198-5

El-Borai, F. E., Campos-Herrera, R., Stuart, R. J., & Duncan, L.W. (2011). Substrate modulation, group effects and the behavioral responses of entomopathogenic nematodes to nematophagous fungi. *Journal of Invertebrate Pathology, 106*(3), 347–356. https://doi.org/10.1016/j.jip.2010.12.001

Elshafie, A. E., Al-Mueini, R., Al-Bahry, S. N., Akindi, A. Y., Mahmoud, I., & Al-Rawahi, S. H. (2006). Diversity and trapping efficiency of nematophagous fungi from Oman. *Phytopathologia Mediterranea, 45,* 266–270.

Eren, J., & Pramer, D. (1965). The most probable number of nematode-trapping fungi in soil. *Soil Sci.*, *99*, 285. https://doi.org/10.1097/00010694-196504000-00013

Eriksson, O. E., Baral, H. O., Currah, R. S., & Hansen, K. (2003). Notes on ascomycete systematics Nos 3580–3623. *Myconet, 9*, 91–103.

Evans, H. C., Groden, E., & Bischoff, J. F. (2010). New fungal pathogens of the red ant, Myrmica rubra, in the UK and implications for ant invasions in the USA. *Fungal Biology*, *114,* 451–466. https://doi.org/10.1016/j.funbio.2010.03.007

Farrell, F., Jaffee, B., & Strong, D. (2006). The nematode-trapping fungi *Arthrobotrys oligospora* in soil of the Bodega marne reserve: Distribution and dependenceon nematode-parasitized moth larvae. *Soil Biol. Biochem.*, *38,* 1422–1429. https://doi.org/10.1016/j.soilbio.2005.10.019

Felsenstein, J. (1985). Confidence limits on phylogenies: An approach using the bootstrap. *Evolution, 39*, 783–791. https://doi.org/10.2307/2408678

Feng, B., Zhao, Q., Xu, J., Qin, J., & Yang, Z. L. (2016). Drainage isolation and climate change-driven population expansion shape the genetic structures of *Tuber indicum* complex in the Hengduan Mountains region. *Sci. Rep., 6*, 21811. https://doi.org/10.1038/srep21811

Fernandes, G. W., Barbosa, N. P. U., Alberton, B., & Barbieri, A. (2018). The deadly route to collapse and the uncertain fate of Brazilian rupestrian grasslands. *Biodiversity and Conservation, 27*, 2587–2603. https://doi.org/10.1007/s10531-018-1556-4

Fierer, N. (2017). Embracing the unknown: Disentangling the complexities of the soil microbiome. *Nat. Rev. Microbiol, 15*, 579–590. https://doi.org/10.1038/nrmicro.2017.87

Flynn, L. J. (2007). Origin and evolution of the Diatomyidae, with clues to paleoecology from the fossil record. *Bull. Carnegie Mus. Nat. Hist., 39*, 173–181. https://doi.org/10.2992/0145-9058(2007)39[173:OAEOTD]2.0.CO;2

Fornacca, D., Ren, G., & Xiao, W. (2018). Evaluating the best spectral indices for the detection of burn scars at several post-fire dates in a mountainous region of Northwest Yunnan, China. *Remote Sensing, 10*(8), 1196. https://doi.org/10.3390/rs10081196

Foster, K. R., & Bell, T. (2012). Competition, not cooperation, dominates interactions among culturable microbial species. *Current biology, 22*(19), 1845–1850. https://doi.org/10.1016/j.cub.2012.08.005

Fowler, M. (1970). New Zealand predaceous fungi. *N. Z. J. Bot., 8*, 283–302. https://doi.org/10.1080/0028825X.1970.10429129

Freitas Soares, F. E., Sufiate, B. L., & Queiroz, J.H. (2018). Nematophagous fungi: Far beyond the endoparasite, predator and ovicidal groups. *Agriculture and Natural Resources, 52*, 1–8. https://doi.org/10.1016/j.anres.2018.05.010

Freitas, D. F., da Rocha, I. M., Vieira-da-Motta, O., & de Paula Santos, C. (2021). The role of melanin in the biology and ecology of nematophagous Fungi. *Journal of Chemical Ecology, 47*(7), 597–613. https://doi.org/10.1007/s10886-021-01282-x

Fresenius, G. (1850). *Beiträge zur Mykologie: Mit 13 lithographierten Tafeln*. Brönner. https://doi.org/10.5962/bhl.title.51534

Fresenius, G. (1852). *Beitrage zur Mykologie (Heft 1–2)*. Brönner.

Fries, E. (1815). *Observationes mycologicae*. Gerhard Bonnieri. https://doi.org/10.5962/bhl.title.112534

Fries, E. M. (1849). *Summa vegetabilium Scandinaviae Vol. 2*. Sectio posterior.

Fu, G. L. (1987). *List of rare and endangered plants in China*. Information System of Chinese Rare and Endangered Plant ISCREP. http://www.iplant.cn/rep/news/32.

Fuller, V. L., Lilley, C. J., & Urwin, P. E. (2008). Nematode resistance. *New Phytologist, 180*(1), 27–44. https://doi.org/10.1111/j.1469-8137.2008.02508.x

Gams, W., & Zare, R. (2003). A taxonomic review of the clavicipitaceous anamorphs parasitizing nematodes and other microinvertebrates. *Clavicipitalean Fungi, 18*, 26–81. https://doi.org/10.1201/9780203912706.pt1

Gao, R. H., Lei, L. P., & Liu, X. Z. (1996). A simple method for inducing and observing predacious devices of nematode-trapping fungi. *Acta Mycol. Sin., 4*, 304–305+326.

Garcia-Bustos, J. F., Sleebs, B. E., & Gasser, R. B. (2019). An appraisal of natural products active against parasitic nematodes of animals. *Parasites & Vectors*, *12*, 1–22. https://doi.org/10.1186/s13071-019-3537-1

Gicklhorn, J. (1922). Studien an *Zoophagus insidians* Som., einem *Tiere fangenden* Pilz. Glasn. *Soc. Sci. Nat. Croate., 34*, 198–229.

Giglio, L., van der Werf, G. R., Randerson, J. T., Collatz, G. J., & Kasibhatla, P. (2006). Global estimation of burned area using MODIS active fire observations. *Atmospheric Chemistry and Physics, 6*(4), 957–974. https://doi.org/10.5194/acp-6-957-2006

Gingerich, P. D., & Chaline, J. (1983). Origin and evolution of species: Evidence from the fossil record. In J. Chaline (Ed.), *Modalités, rythmes, mécanismes de l'évolution biologique: Gradualisme phylétique ou équilibres ponctués?*. Colloques Internationaux du Centre National de la Recherche Scientifique.

Girardi, N. S., Sosa, A. L., Etcheverry, M. G., & Passone, M. A. (2022). In vitro characterization bioassays of the nematophagous fungus *Purpureocillium lilacinum*: Evaluation on growth, extracellular enzymes, mycotoxins and survival in the surrounding agroecosystem of tomato. *Fungal Biology, 126*(4), 300–307. https://doi.org/10.1016/j.funbio.2022.02.001

Giuma, A. Y., & Cooke, R. C. (1972). Some endozoic fungi parasitic on soil nematodes. *Transactions of the British Mycological Society, 59*(2), 213–218. https://doi.org/10.1016/S0007-1536(72)80004-4

Gleason, F. H., & Lilje, O. (2009). Structure and function of fungal zoospores: Ecological implications. *Fungal Ecol.*, *2*, 53–59. https://doi.org/10.1016/j.funeco.2008.12.002

Glockling, S. L., & Beakes, G. W. (2000). A review of the taxonomy, biology and infection strategies of "biflagellate holocarpic" parasites of nematodes. *Fungal Diversity, 4*, 1–20.

Glockling, S. L., & Dick, M.W. (1994). *Dactylella megalobrocha*, a new species of nematophagous fungus with constricting rings. *Mycological Research, 98*(8), 845–853. https://doi.org/10.1016/S0953-7562(09)80252-9

González-Solís, D., & Jiménez-García, M. I. (2006). Parasitic nematodes of freshwater fishes from two Nicaraguan crater lakes. *Comp. Parasitol., 73*, 188–192. https://doi.org/10.1654/4195.1

Graminha, É. B., Costa, A. J., Oliveira, G. P., Monteiro, A. C., & Palmeira, S. B. (2005). Biological control of sheep parasite nematodes by nematode-trapping fungi: In vitro activity and after passage through the gastrointestinal tract. *World Journal of Microbiology and Biotechnology*, *21*, 717–722. https://doi.org/10.1007/s11274-004-4045-8

Grau, C. R., Dorrance, A. E., Bond, J., & Russin, J. S. (2004). Fungal diseases. *Soybeans: Improvement, Production, and Uses*, *16*, 679–763. https://doi.org/10.2134/agronmonogr16.3ed.c14

Gray, N. F. (1983). Ecology of nematophagous fungi: Distribution and habitat. *Annals of Applied Biology, 102*(3), 501–509. https://doi.org/10.1111/j.1744-7348.1983.tb02721.x

Gray, N. F., & Bailey, F. (1985). Ecology of nematophagous fungi: Vertical distribution in a deciduous woodland. *Plant and Soil, 86*(2), 217–223. https://doi.org/10.1007/BF02182896

Gronvold, J., Wolstrup, J., Nansen, P., Henriksen, S. A., Larsen, M., & Bresciani, J. (1993). Biological control of nematode parasites in cattle with nematode-trapping fungi: A survey of Danish studies. *Veterinary Parasitology*, *48*(1-4), 311–325. https://doi.org/10.1016/0304-4017(93)90165-J

Grossart, H. P., Wyngaert, S. V. D., Kagami, M., Wurzbacher, C., Cunliffe, M., & Rojas-Jimenez, K. (2019). Fungi in aquatic ecosystems. *Nat. Rev. Genet.*, *17*, 339–354. https://doi.org/10.1038/s41579-019-0175-8

Grube, M., Gaya, E., Kauserud, H., Smith, A. M., Avery, S. V., Fernstad, S. J., . . . Bendiksby, M. (2017). The next generation fungal diversity researcher. *Fungal Biology Reviews, 31*(3), 124–130. https://doi.org/10.1016/j.fbr.2017.02.001

Guevara-Suarez, M., Cano-Lira, J. F., De García, M. C. C., Sopo, L., De Bedout, C., Cano, L. E., . . . Celis, A. (2016). Genotyping of *Fusarium* isolates from onychomycoses in Colombia: Detection of two new species within the *Fusarium solani* species complex and in vitro antifungal susceptibility testing. *Mycopathologia, 181*(3–4), 165–174. https://doi.org/10.1007/s11046-016-9983-9

Guo, J., Li, S., Yang, L., Yang, J., Ye, T., & Yang, L. (2014). New records and new distribution of known species in the family *Orbiliaceae* from China. *African Journal of Microbiology Research, 8*(34), 3178–3190. https://doi.org/10.5897/AJMR2013.6589

Haard, K. (1968). Taxonomic studies on the genus *Arthrobotrys* Corda. *Mycotaxon, 16,* 107–113. https://doi.org/10.2307/3757214

Hagedorn, G., & Scholler, M. (1999). A reevaluation of predatory *orbiliaceous* fungi. I. phylogenetic analysis using rDNA sequence data. *Sydowiahorn, 51,* 27–48.

Hall, B. (2005). Phylogenetic trees made easy: A how-to manual, 2nd ed. *Journal of Heredity, 96*(4), 469–470. https://doi.org/10.1093/jhered/esi046

Hall, B. G. (2007). *Phylogenetic trees made easy: A how-to manual*. Sinauer Associates Sunderland.

Hall, T. A. (1999). BioEdit: A user-friendly biological sequence alignment editor and analysis program for Windows 95/98/NT. *Nucleic Acids Aymposium Aeries, 41*(41), 95–98.

Hallmann, J., & Sikora, R. (1994). Occurrence of plant parasitic nematodes and non-pathogenic species of *Fusarium* in tomato plants in Kenya and their role as mutualistic synergists for biological control of root-knot nematodes. *International Journal of Pest Management, 40*(4), 321–325. https://doi.org/10.1080/09670879409371907

Hao, Y. E., Luo, J., & Zhang, K. Q. (2004). A new aquatic nematode trapping hyphomycete. *Mycotaxon, 89*, 235–239.

Hao, Y., Mo, M., Su, H., & Zhang, K. Q. (2005). Ecology of aquatic nematode-trapping hyphomycetes in southwestern China. *Aquat. Microb. Ecol., 40*, 175–181. https://doi.org/10.3354/ame040175

Hastuti, L. D. S., Berliani, K., & Mulya, M. B. (2018). Inventarization of nematode-trapping fungi in terrestrial area of Deli Serdang Regency, North Sumatera. In *Proceedings of the International Conference of Science, Technology, Engineering, Environmental and Ramification Researches*—ICOSTEERR, Medan, Indonesia. https://doi.org/10.5220/0010095010271030

Hawksworth, D. L., & Lücking, R. (2017). Fungal diversity revisited: 2.2 to 3.8 million species. *Microbiology Spectrum, 5*(4), 10–1128. https://doi.org/10.1128/microbiolspec.FUNK-0052-2016

Hawksworth, D. L., & Rossman, A. Y. (1997). Where are all the undescribed fungi?. *Phytopathology, 87*(9), 888–891. https://doi.org/10.1094/PHYTO.1997.87.9.888

Hawksworth, D. L. (2004). Fungal diversity and its implications for genetic resource collections. *Studies in Mycology, 50*(1), 9–17.

Haydock, P. P., Woods, S. R., Grove, I. G., & Hare, M. C. (2006). Chemical control of nematodes. In R. N. Perry & M. Moens (Eds.), *Plant nematology* (pp. 392-410). CABI Digital Library. https://doi.org/10.1079/9781845930561.0392

He, T., Lamont, B. B., & Pausas, J. G. (2019). Fire as a key driver of earth's biodiversity. *Biological Reviews, 94*(6), 1983–2010. https://doi.org/10.1111/brv.12544

Herrera-Estrella, A., Casas-Flores, S., & Kubicek, C. P. (2016). Nematophagous Fungi. *Environmental and Microbial Relationships, 2016*, 247–467. https://doi.org/10.1007/978-3-319-29532-9_13

Hillis, D. M., & Bull, J. J. (1993). An empirical test of bootstrapping as a method for assessing confidence in phylogenetic analysis. *Systematic Biology*, *42*(2), 182. https://doi.org/10.1093/sysbio/42.2.182

Hofstetter, V., Miadlikowska, J., Kauff, F., & Lutzoni, F. (2007). Phylogenetic comparison of protein-coding versus ribosomal RNA-coding sequence data: A case study of the *Lecanoromycetes* (Ascomycota). *Molecular Phylogenetics and Evolution, 44*(1), 412–426. https://doi.org/10.1016/j.ympev.2006.10.016

Hoste, H., & Torres-Acosta, J. F. J. (2011). Non chemical control of helminths in ruminants: Adapting solutions for changing worms in a changing world. *Veterinary Parasitology*, *180*(1–2), 144–154. https://doi.org/10.1016/j.vetpar.2011.05.035

Hsueh, Y. P., Mahanti, P., Schroeder, F. C., & Sternberg, P.W. (2013). Nematode-trapping fungi eavesdrop on nematode pheromones. *Curr. Biol.*, *23*, 83–86. https://doi.org/10.1016/j.cub.2012.11.035

Huelsenbeck, J. P., & Ronquist, F. (2001). MRBAYES: Bayesian inference of phylogenetic trees. *Bioinformatics, 17*, 754–755. https://doi.org/10.1093/bioinformatics/17.8.754

Hugot, J. P., Baujard, P., & Morand, S. (2001). Biodiversity in helminths and nematodes as a field of study: An overview. *Nematology, 3*, 199–208. https://doi.org/10.1163/156854101750413270

Husman, S., McClure, M., Lambeth, J., Dennehy, T., & Deeter, B. (1995). *Telone II® and Temike® efficacy on rootknot nematodes in cotton*. University of Arizona.

Hussain, M., Zouhar, M., & Rysanek, P. (2017). Comparison between biological and chemical management of root knot nematode, *Meloidogyne Hapla*. *Pakistan Journal of Zoology*, *49*(1), 205-210. https://doi.org/10.17582/journal.pjz/2017.49.1.205.210

Hyde, K. D., Jeewon, R., Chen, Y. J., Bhunjun, C. S., Calabon, M. S., Jiang, H. B., . . . Tibpromma, S. (2020). The numbers of fungi: Is the descriptive curve flattening?. *Fungal Diversity*, *103*, 219–271. https://doi.org/10.1007/s13225-020-00458-2

Jaffee, B., Ferris, H., & Scow, K. (1998). Nematode-trapping fungi in organic and conventional cropping systems. *Phytopathology*, *88*(4), 344–350. https://doi.org/10.1094/PHYTO.1998.88.4.344

Jaffee, B., Tedford, E., & Muldoon, A. (1993). Tests for density-dependent parasitism of nematodes by nematode-trapping and endoparasitic fungi. *Biological Control*, *3*(4), 329–336. https://doi.org/10.1006/bcon.1993.1043

Jansson, H. B., & Autery, C. L. (1961). An *Arthrobotrys* from brackish water. *Mycologia*, *53*, 432–433. https://doi.org/10.2307/3756586

Jansson, H. B., & Poinar, G. O. (1986). Some possible fossil *nematophagous* fungi. *Trans. Br. Mycol. Soc.*, *87*, 471–474. https://doi.org/10.1016/S0007-1536(86)80227-3

Jasmer, D. P., Goverse, A., & Smant, G. (2003). Parasitic nematode interactions with mammals and plants. *Annual Review of Phytopathology*, *41*(1), 245–270. https://doi.org/10.1146/annurev.phyto.41.052102.104023

Jeewon, R., & Hyde, K. D. (2016). Establishing species boundaries and new taxa among fungi: Recommendations to resolve taxonomic ambiguities. *Mycosphere*, *7*(11), 1669–1677. https://doi.org/10.5943/mycosphere/7/11/4

Jeewon, R., Liew, E. C., & Hyde, K. D. (2002). Phylogenetic relationships of *Pestalotiopsis* and allied genera inferred from ribosomal DNA sequences and morphological characters. *Molecular Phylogenetics and Evolution, 25*(3), 378–392. https://doi.org/10.1016/S1055-7903(02)00422-0

Ji, X. L., Yu, Z. F., Yang, J. K., Xu, J. P., Zhang, Y., Liu, S. Q., . . . Zhang, K. Q. (2020). Expansion of adhesion genes drives pathogenic adaptation of nematode-trapping fungi. *IScience, 23*(5), 101057. https://doi.org/10.1016/j.isci.2020.101057

Jiang, X., Xiang, M., & Liu, X. (2017). Nematode-trapping fungi. *Microbiology Spectrum, 5*(1), 10–1128. https://doi.org/10.1128/microbiolspec.FUNK-0022-2016

Jones, J. T., Haegeman, A., Danchin, E. G., Gaur, H. S., Helder, J., Jones, M. G., . . . Perry, R. N. (2013). Top 10 plant-parasitic nematodes in molecular plant pathology. *Molecular Plant Pathology, 14*(9), 946–961. https://doi.org/10.1111/mpp.12057

Júnior, A. D., Ferreira, V. M., de Carvalho, L. M., Álvares, F. B. V., Vilela, V. L. R., Ferraz, C. M., . . . de Araújo, J. V. (2021). Association of the *nematophagous* fungi *Arthrobotrys musiformis* and *Monacrosporium sinense* in vitro and in vivo for biological control of equine cyathostomins. *Braz. J. Vet. Med., 43*, e003021. https://doi.org/10.29374/2527-2179.bjvm003021

Kang, H., Choi, I., Park, N., Bae, C., & Kim, D. (2019). Nematode-Trapping Fungi Showed Different Predacity among Nematode Species. *Research in Plant Disease, 25*(3), 149–155. https://doi.org/10.5423/RPD.2019.25.3.149

Katoh, K., & Standley, D. M. (2013). MAFFT multiple sequence alignment software version 7: Improvements in Performance and Usability. *Mol. Biol. Evol., 30*, 772–780. https://doi.org/10.1093/molbev/mst010

Kavitha, T. R., Priya, R. U., & Sunitha, T. R. (2020). *Dactylella*. In N. Amaresan, M. S. Kumar, K. Annapurna, K. Kumar & A. Sankaranarayanan (Eds.), *Beneficial microbes in agro-ecology* (pp. 809–816). Academic Press. https://doi.org/10.1016/B978-0-12-823414-3.00042-3

Kelly, L. T., Giljohann, K. M., Duane, A., Aquilué, N., Archibald, S., Batllori, E., Bennett, A. F., . . . Fortin, M. J. (2020). Fire and biodiversity in the Anthropocene. *Science, 370*(6519), eabb0355. https://doi.org/10.1126/science.abb0355

Kennedy, D., & Norman, C. (2005). What Don't We Know?. *Science, 309*, 75. https://doi.org/10.1126/science.309.5731.75

Khan, A., Williams, K. L., & Nevalainen, H. K. (2006). Infection of plant-parasitic nematodes by *Paecilomyces lilacinus* and *Monacrosporium lysipagum*. *BioControl, 51*(5), 659–678. https://doi.org/10.1007/s10526-005-4242-x

Kim, B. N., Kim, J. H., Ahn, J. Y., Kim, S., Cho, B. K., Kim, Y. H., . . . Min, J. (2020). A short review of the pinewood nematode, *Bursaphelenchus xylophilus*. *Toxicology and Environmental Health Sciences, 12,* 297–304. https://doi.org/10.1007/s13530-020-00068-0

Kim, D. G., Bae, S. G., & Shin, Y. S. (2001). Distribution of nematophagous fungi under different habitats. *Korean J. Mycol., 29,* 123–126.

Kimbrough, J. W. (1970). Current trends in the classification of discomycetes. *The Botanical Review, 36,* 91–161. https://doi.org/10.1007/BF02858958

Kirk, P. M., Cannon, P. F., Minter, D. W., & Stalpers, J. A. (2008). *Dictionary of the Fungi.* CAB International.

Kishino, H., & Hasegawa, M. (1989). Evaluation of the maximum likelihood estimate of the evolutionary tree topologies from DNA – sequence data, and the branching order in Hominoidea. *Journal of Molecular Evolution, 29,* 170–179. https://doi.org/10.1007/BF02100115

Koziak, A. T., Cheng, K. C., & Thorn, R. G. (2007). Phylogenetic analyses of *Nematoctonus* and *Hohenbuehelia* (Pleurotaceae). *Botany*, *85*(8), 762–773. https://doi.org/10.1139/B07-083

Krauss, G. J., Solé, M., Krauss, G., Schlosser, D., Wesenberg, D., & Bärlocher, F. (2011). Fungi in freshwaters: Ecology, physiology and biochemical potential. *FEMS Microbiol. Rev.*, *35*, 620–651. https://doi.org/10.1111/j.1574-6976.2011.00266.x

Krings, M., Taylor, T. N., & Dotzler, N. (2012). Fungal endophytes as a driving force in land plant evolution: Evidence from the fossil record. In D. Southworth (Ed.), *Biocomplexity of plant–fungal interactions* (pp. 5–27). Wiley. https://doi.org/10.1002/9781118314364.ch1

Kühn, J. (1877). Vorläufiger Bericht über die bisherigen Ergebnisse der seit dem Jahre 1875 im Auftrage des Vereins für Rübenzucker-Industrie ausgeführten Versuche zur Ermittlung der Ursache der Rübenmüdigkeit des Bodens und zur Erforschung der Natur der Nematoden. *Zeitschrift des Vereins für die Rübenzucker-Industrie des Duetschen Reich (ohne Band)*, *27*, 452–457.

Kukalova-Peck, J. (1978). Origin and evolution of insect wings and their relation to metamorphosis, as documented by the fossil record. *J. Morphol.*, *156*, 53–125. https://doi.org/10.1002/jmor.1051560104

Kumar, D. (2024) – Evaluation of nematophagous and bio-control efficacy of *Dactylellina phymatopaga* against *Meloidogyne graminicola* on rice (*Oryza sativa* L.). *Biological Control*, *188*, 105425. https://doi.org/10.1016/j.biocontrol.2023.105425

Kumar, D. (2024). Effectiveness of various nematode-trapping fungi for bio-control of the *Meloidogyne incognita* in tomato (*Lycopersicion esculentum* Mill.). *Rhizosphere, 29,* 100845. https://doi.org/10.1016/j.rhisph.2023.100845

Kumar, D., Maurya, N., Kumar, P., Singh, H., & Addy, S. K. (2015). Assessment of germination and carnivorous activities of a nematode-trapping fungus *Arthrobotrys dactyloides* in fungistatic and fungicidal soil environment. *Biological Control, 82,* 76–85. https://doi.org/10.1016/j.biocontrol.2014.12.014

Kumar, N., Singh, R., & Singh, K. (2011). Occurrence and colonization of nematophagous fungi in different substrates, agricultural soils and root galls. *Archives of Phytopathologyand Plant Protection, 44*(12), 1182–1195. https://doi.org/10.1080/03235408.2010.484945

Kuo, T. H., Yang, C. T., Chang, H. Y., Hsueh, Y. P., & Hsu, C. C. (2020). Nematode-trapping fungi produce diverse metabolites during predator–prey interaction. *Metabolites*, *10*, 117. https://doi.org/10.3390/metabo10030117

Kurihara, Y., Shirouzu, T., Tokumasu, S., & Harayama, S. (2009). *Hirsutella proturicola* sp. nov. isolated from a proturan, *Baculentulus densus* (Protura, Hexapoda). *Mycoscience, 50*, 56–62. https://doi.org/10.1007/S10267-008-0443-3

Lafta, A. A., & Kasim, A. A. (2019). Effect of nematode-trapping fungi, *Trichoderma harzianum* and *Pseudomonas fluorescens* in controlling *Meloidogyne* spp. *Plant Archives, 19*(1), 1163-1168.

Lamberti, F., D'Addabbo, T., Sasanelli, N., Carella, A., & Greco, P. (2000). Chemical control of root-knot nematodes. *Acta Hortic., 532*, 183-188. https://doi.org/10.17660/ActaHortic.2000.532.23.

Lamovšek, J., Gregor, U. R., & Trdan, S. (2013). Biological control of root-knot nematodes (*Meloidogyne* spp.): Microbes against the pests. *Acta Agriculturae Slovenica, 101*(2), 263–275. https://doi.org/10.14720/aas.2013.101.2.14917

Larson, A. J., Cansler, C. A., Cowdery, S. G., Hiebert, S., Furniss, T. J., Swanson, M. E., . . . Lutz, J. A. (2016). Post-fire morel (*Morchella*) mushroom abundance, spatial structure, and harvest sustainability. *Forest Ecology and Management, 377*, 16–25. https://doi.org/10.1016/j.foreco.2016.06.038

Lazarova, S., Coyne, D., Rodriguez, M. G., Peteira, B., & Ciancio, A. (2021). Functional diversity of soil nematodes in relation to the impact of agriculture—a review. *Diversity*, *13*(2), 64. https://doi.org/10.3390/d13020064

Lechenet, M., Bretagnolle, V., Bockstaller, C., Boissinot, F., Petit, M. S., Petit, S., . . . Munier-Jolain, N. M. (2014). Reconciling pesticide reduction with economic and environmental sustainability in arable farming. *PloS One*, *9*(6), e97922. https://doi.org/10.1371/journal.pone.0097922

Lee, J. P., Sekhon, S. S., Kim, J. H., Kim, S. C., Cho, B. K., Ahn, J. Y., . . . Kim, Y. H. (2021). The pine wood nematode *Bursaphelenchus xylophilus* and molecular diagnostic methods. *Molecular & Cellular Toxicology*, *17*, 1–3. https://doi.org/10.1007/s13273-020-00110-9

Leslie, J. F., & Summerell, B. A. (2006). *The Fusarium laboratory manual*. Blackwell Publishing Asia. https://doi.org/10.1002/9780470278376

Li, C. R., Chen, M. J., Wang, M., Lin, Y. R., Fan, M. Z., & Li, Z. Z. (2006). *Hirsutella heteropoda* sp. nov. and its teleomorph, new variety of *Cordyceps heteropoda*. *Mycosystema*, *25*, 163–168.

Li, J. W. (2009). A review of plant diversity and characteristics on three parallel rivers. *Sci. Technol. Inf.*, *15*, 59–64.

Li, J., Liu, Y., Zhu, H., & Zhang, K.Q. (2016). Phylogenic analysis of adhesion related genes Mad1 revealed a positive selection for the evolution of trapping devices of nematode-trapping fungi. *Scientific Reports*, *6*(1), 22609. https://doi.org/10.1038/srep22609

Li, J., Qian, W., Qiao, M., Bai, Y., & Yu, Z. (2013). A new *Drechslerella* species from Hainan, China. *Mycotaxon ,125,* 183–188. https://doi.org/10.5248/125.183

Li, J., Zou, C., Xu, J., Ji, X., Niu, X., Yang, J., . . . Zhang, K. Q. (2015). Molecular mechanisms of nematode-nematophagous microbe interactions: Basis for biological control of plant-parasitic nematodes. *Annual Review of Phytopathology*, *53,* 67–95. https://doi.org/10.1146/annurev-phyto-080614-120336

Li, J., Liu, Y., Zhu, H., & Zhang, K.Q. (Phylogenic analysis of adhesion related genes Mad1 revealed a positive selection for the evolution of trapping devices of nematode-trapping fungi. *Scientific Reports*, *6,* 22609. https://doi.org/10.1038/srep22609

Li, R. S., Liu, W., & Chen, H. (2001). *Three parallel rivers*. China Translation and Publication Corporation.

Li, S. D., Miao, Z. Q., Zhang, Y. H., & Liu, X. Z. (2003). *Monacrosporium janus* sp. nov., a new nematode-trapping hyphomycete parasitizing sclerotia and hyphae of *Sclerotinia sclerotiorum*. *Mycol. Res., 107,* 888–894. https://doi.org/10.1017/S0953756203008165

Li, S., Yu, Z., Zhang, Y., Qiao, M., Guo, J., & Zhang, K. (2009). *Arthrobotrys nonseptata*, a new anamorph from an Orbilia species. *Mycotaxon*, *109*, 247–254. https://doi.org/10.5248/109.247

Li, T. F., Zhang, K. Q., & Liu, X. Z. (2000). *Taxonomy of Nematophagous fungi*. Chinese Scientific and Technological Publication.

Li, Y., Hyde, K. D., Jeewon, R., Cai, L., Vijaykrishna, D., & Zhang, K. (2005). Phylogenetics and evolution of nematode-trapping fungi (*Orbiliales*) estimated from nuclear and protein coding genes. *Mycologia*, *97*(5), 1034–1046. https://doi.org/10.1080/15572536.2006.11832753

Li, Y., Jeewon, R., Hyde, K. D., Mo, M., & Zhang, K. (2006). Two new species of nematodetrapping fungi: Relationships inferred from morphology, rDNA and protein gene sequence analyses. *Mycological Research, 110*(7), 790–800. https://doi.org/10.1016/j.mycres.2006.04.011

Liang, Z. Q., Han, Y. F., Liu, A. Y., & Huang, J. Z. (2006). Some entomogenous fungi from Wuyishan and Zhangjiajie Nature Reserves. Three new species of the genus *Hirsutella*. *Mycotaxon*, *94*, 349–355

Lin, H. B., Li, Y. P., Duan, J. X., Xia, F. Y., Xiong, H. J., Wang, J. B., . . . Xiao, W. (2016). Screening of nematode-trapping fungi for biocontrol intestinal parasitic nematode of Yunnan snub-nosed monkey. *Sichuan Journal of Zoology*, *35*(1), 31–37.

Lin, S., Wu, R., Yang, F., Wang, J., & Wu, W. (2018). Spatial trade-offs and synergies among ecosystem services within a global biodiversity hotspot. *Ecol. Indic.*, *84*, 371–381. https://doi.org/10.1016/j.ecolind.2017.09.007

Lindahl, B. D., & Clemmensen, K. E. (2016). Fungal ecology in boreal forest ecosystems. In F. Martin (ed.), *Molecular mycorrhizal symbiosis* (pp. 387–404). Wiley. https://doi.org/10.1002/9781118951446.ch21

Lindau, G. (1904). Die Pilze Deutschlands, Oesterreichs und der Schweiz. VIII. Abteilung: Fungi imperfecti: Hyphomycetes (erste Hälfte). *Rabenhorst L. Kryptogamen-Flora. Ed.*, *2*, 1904–1907.

Linford, M., Yap, F., & Oliveira, J. M. (1938). Reduction of soil populations of the root-knot nematode during decomposition of organic matter. *Soil Sci.*, *45*, 127–142. https://doi.org/10.1097/00010694-193802000-00004

Link, H. F. (1809). Observationes in ordines plantarum naturales. Dissertatio I. *Magazin der Gesellschaft Naturforschenden Freunde Berlin, 3*(1), 3–42.

Liou, G. Y., & Tzean, S. S. (1997). Phylogeny of the genus *Arthrobotrys* and allied nematodetrapping fungi based on rDNA sequences. *Mycologia, 89*(6), 876–884. https://doi.org/10.1080/00275514.1997.12026858

Liou, J. Y., & Tzean, S. S. (1992). Stephanocysts as nematode-trapping and infecting propagules. *Mycologia, 84*(5), 786–790. https://doi.org/10.1080/00275514.1992.12026205

Liou, J. Y., Liou, G. Y., & Tzean, S. S. (1995). *Dactylella formosana*, a new nematode-traping fungus from Taiwan. *Mycological Research, 99*(6), 751–755. https://doi.org/10.1016/S0953-7562(09)80540-6

Liu, B., Liu, X. Z., & Zhuang, W. Y. (2005). *Orbilia querci* sp. nov. and its knob-forming nematophagous anamorph. F*EMS Microbiology Letters, 245*(1), 99–105. https://doi.org/10.1016/j.femsle.2005.02.027

Liu, B., Liu, X. Z., Zhuang, W. Y., & Baral, H. O. (2006). Orbiliaceous fungi from Tibet, China. *Fungal Diversity, 22*(1), 107–120.

Liu, S., Su, H., Su, X., Zhang, F., Liao, G., & Yang, X. (2014). *Arthrobotrys xiangyunensis*, a novel nematode-trapping taxon from a hot-spring in Yunnan Province, China. *Phytotaxa, 174*(2), 89–96. https://doi.org/10.11646/phytotaxa.174.2.3

Liu, X. Z., & Zhang, K. Q. (1994). Nematode-trapping species of *Monacrosporium* with special reference to two new species. *Mycological Research, 98*(8), 862–868. https://doi.org/10.1016/S0953-7562(09)80255-4

Liu, X. Z., Gao, R. H., Zhang, K. Q., & Cao, L. (1996). *Dactylella tenuifusaria* sp. nov., a rhizopod-capturing hyphomycete. *Mycol. Res., 100*, 236–238. https://doi.org/10.1016/S0953-7562(96)80129-8

Liu, X., Xiang, M., & Che, Y. (2009). The living strategy of nematophagous fungi. *Mycoscience, 50*(1), 20–25. https://doi.org/10.1007/S10267-008-0451-3

Liu, Y. J., Whelen, S., & Hall, B. D. (1999). Phylogenetic relationships among ascomycetes: Evidence from an RNA polymerse II subunit. *Molecular Biology and Evolution, 16*(12), 1799–1808. https://doi.org/10.1093/oxfordjournals.molbev.a026092

Liu., X., & Zhang, K. (2003). *Dactylella shizishanna* sp. nov., from Shizi Mountain, China. *Fungal Divers.*, *14*, 103–107.

Lohde, G. (1874). Ueber einige neue parasitische pilze. Tagebl Versamml Deut. Naturforsch. *Aerzte, 47*, 203–206.

Lombard, L., van der Merwe, N., Groenewald, J., & Crous, P.W. (2015). Generic concepts in Nectriaceae. *Studies in Mycology, 80,* 189–245. https://doi.org/10.1016/j.simyco.2014.12.002

Luo, H., Mo, M., Huang, X., Li, X., & Zhang, K. (2004). *Coprinus comatus*: A basidiomycete fungus forms novel spiny structures and infects nematode. *Mycologia, 96*(6), 1218–1224. https://doi.org/10.1080/15572536.2005.11832870

Madeira, F., Pearce, M., Tivey, A. R., Basutkar, P., Lee, J., Edbali, O., . . . Lopez, R. (2022). Search and sequence analysis tools services from EMBL-EBI in 2022. *Nucleic Acids Research, 50*(W1), W276-W279. https://doi.org/10.1093/nar/gkac240

Maia Filho, F. D. S., Vieira, J. N., Berne, M. E. A., Stoll, F. E., Nascente, P. D. S., Pötter, L., . . . Pereira, D. I. B. (2013). Fungal ovicidal activity on *Toxocara canis* eggs. *Revista Iberoamericana de Micología*, *30*(4), 226–230. https://doi.org/10.1016/j.riam.2012.12.009

Mani, A., & Sethi, C. (1984). Some characteristics of culture filtrate of *Fusarium solani* toxic to *Meloidogyne incognita*. *Nematropica, 14*(2), 121–129.

Masigol, H., Rezakhani, F., Pourmoghaddam, M. J., Khodaparast, S. A., & Grossart, H. P. (2022). The introduction of two new species of aquatic fungi from Anzali Lagoon, Northern Iran. *Diversity*, *14*, 889. https://doi.org/10.3390/d14100889

Mathivanan, N., Kabilan, V., & Murugesan, K. (1998). Purification, characterization, and antifungal activity of chitinase from *Fusarium chlamydosporum*, a mycoparasiteto groundnut rust, *Puccinia arachidis*. *Microbiology, 44*(7), 646–651. https://doi.org/10.1139/w98-043

McCulloch, J. S. (1977). New species of nematophagous fungi from Queensland. *Trans. Br. Mycol. Soc.*, *68*, 173–179. https://doi.org/10.1016/S0007-1536(77)80005-3

McInnes, S. J. (2003). A predatory fungus (Hyphomycetes: *Lecophagus*) attacking Rotifera and Tardigrada in maritime Antarctic lakes. *Polar Biol*, *26*, 79–82. https://doi.org/10.1007/s00300-002-0449-9

Meier, R., Blaimer, B., Buenaventura, E., Hartop, E., von Rintelen, T., Srivathsan, A., . . . Yeo, D. (2022). A re-analysis of the data in Sharkey et al.'s (2021) minimalist revision reveals that BINs do not deserve names, but BOLD systems needs a stronger commitment to open science. *Cladistics*, *38*, 264–275. https://doi.org/10.1111/cla.12489

Mekonen, S., Petros, I., Hailemariam, M., & Conservation, B. (2017). The role of nematodes in the processes of soil ecology and their use as bioindicators. *Agric. Biol. JN Am.*, *8*(4), 132–140.

Midha, S. K. (1997). The all India coordinated research project on nematode pests and their control: A possible model for other countries. In *Diagnosis of key nematode pests of chickpea and pigeonpea and their management: Proceedings of a Regional Training Course* (pp. 40-46). International Crops Research Institute for the Semi-Arid Tropics.

Miller, M., Pfeiffer, W., & Schwartz, T. (2010). *Creating the CIPRES Science Gateway for inference of large phylogenetic trees*. IEEE. https://doi.org/10.1109/GCE.2010.5676129

Mo, M. H., Chen, W. M., Su, H. Y., Zhang, K. Q., Duan, C. Q., & He, D. M. (2006). Heavy metal tolerance of nematode-trapping fungi in lead-polluted soils. *Applied Soil Ecology*, *31*(1–2), 11–19. https://doi.org/10.1016/j.apsoil.2005.04.008

Mo, M. H., Chen, W. M., Yang, H. R., & Zhang, K. Q. (2008). Diversity and metal tolerance of nematode-trapping fungi in Pb-polluted soils. *The Journal of Microbiology*, *46*(1), 16. https://doi.org/10.1007/s12275-007-0174-8

Mo, M., Su, H., & Zhang, K. (2005). Ecology of aquatic nematode-trapping hyphomycetes in southwestern China. *Aquatic Microbial Ecology*, *40*(2), 175–181. https://doi.org/10.3354/ame040175

Mo., M., Huang, X., Zhou, W., Huang, Y., Hao, Y. E., & Zhang, K. (2005). *Arthrobotrys yunnanensis* sp. nov., the fourth anamorph of *Orbilia auricolor*. *Fungal Divers.*, *18*, 107–115.

Moens, M., & Hendrickx, G. (1998). Effect of long term aldicarb applications on the development of field populations of some endoparasitic nematodes. *Fundamental and Applied Nematology*, *21*(2), 199–204.

Moliszewska, E. B., Nabrdalik, M., & Kudrys, P. (2022). Nematicidal potential of nematophagous fungi. In S. K. Deshmukh, K. R. Sridhar & S. M. Badalyan (Eds.), *Fungal biotechnology* (pp. 409–434). CRC Press. https://doi.org/10.1201/9781003248316-22

Moosavi, M. R., & Zare, R. (2020). Fungi as biological control agents of plant-parasitic nematodes. In J. Mérillon & K. Ramawat (Eds.), *Plant defence: Biological control* (pp. 67-107). Springer. https://doi.org/10.1007/978-94-007-1933-0_4

Morales, A., Alvear, M., Valenzuela, E., Castillo, C. E., & Borie, F. (2011). Screening, evaluation and selection of phosphate-solubilising fungi as potential biofertiliser. *Journal of Soil Science and Plant Nutrition, 11*(4), 89–103. https://doi.org/10.4067/S0718-95162011000400007

Morelet, M. (1968). De aliquibus in Mycologia novitatibus. *Bulletin de la Société des Sciences naturelles et d'Archéologie de Toulon et du Var, 175*, 5–6.

Morikawa, C., Saikawa, M., & Barron, G. L. (1993). Fungal predators of rotifers-a comparative study of Zoophagus, Lecophagus and Cephaliophora. *Mycological Research, 97*(4), 421–428. https://doi.org/10.1016/S0953-7562(09)80129-9

Morris, E. E., & Hajek, A. E. (2014). Eat or be eaten: Fungus and nematode switch off as predator and prey. *Fungal Ecology, 11*, 114–121. https://doi.org/10.1016/j.funeco.2014.05.006

Morton, C. O., Mauchline, T. H., Kerry, B. R., & Hirsch, P. R. (2003). PCR-based DNA fingerprinting indicates host-related genetic variation in the nematophagous fungus *Pochonia chlamydosporia*. *Mycological Research, 107*(2), 198–205. https://doi.org/10.1017/S0953756203007251

Mueller, J. D. (2011). The use of Temike 15G on cotton and soybean in the southeast. In *Proceedings of the Beltwide Cotton Conferences* (vol. 1, pp. 208-214). The National Cotton Council.

Nannfeldt, J. A. (1932). Studien uber die Morphologie und Systematik der nicht-lichenisierten inoperculaten Discomyceten. *Nova Acta Regiae Soc. Sci. Upsal. Ser*., 8, 1–368.

Nguyen, L. T., Jang, J. Y., Kim, T. Y., Yu, N. H., Park, A. R., Lee, S., . . . Kim, J. C. (2018). Nematicidal activity of verrucarin A and roridin A isolated from M*yrothecium verrucaria* against *Meloidogyne incognita*. *Pesticide Biochemistry and Physiology, 148*, 133–143. https://doi.org/10.1016/j.pestbp.2018.04.012

Nguyen, L. T., Schmidt, H. A., Haeseler, A., & Minh, B. Q. (2014). IQ-TREE: A fast and effective stochastic algorithm for estimating maximum-likelihood phylogenies. *Molecular Biology and Evolution, 32*(1), 268–274. https://doi.org/10.1093/molbev/msu300

Nicol, J. M., Turner, S. J., Coyne, D. L., den Nijs, L. J. M. F., Hockland, S., & Maafi, Z. T. (2011). Current nematode threats to world agriculture. In J. Jones, G. Gheysen & C. Fenoll (Eds.), *Genomics and molecular genetics of plant-nematode interactions* (pp. 21–43). Springer. https://doi.org/10.1007/978-94-007-0434-3_2

Niego, A. G. T., Lambert, C., Mortimer, P., Thongklang, N., Rapior, S., Grosse, M., . . . Stadler, M. (2023). The contribution of fungi to the global economy. *Fungal Diversity, 121*, 95–137. https://doi.org/10.1007/s13225-023-00520-9

Niego, A. G. T., Rapior, S., Thongklang, N., Raspé, O., Hyde, K. D., & Mortimer, P. (2023). Reviewing the contributions of macrofungi to forest ecosystem processes and services. *Fungal Biology Reviews, 44*, 100294. https://doi.org/10.1016/j.fbr.2022.11.002

Norabadi, M. T., Sahebani, N., & Etebarian, H. R. (2014). Biological control of root-knot nematode (*Meloidogyne javanica*) disease by *Pseudomonas fluorescens* (Chao). *Archives of Phytopathology and Plant Protection, 47*(5), 615–621. https://doi.org/10.1080/03235408.2013.816102

Nordbring-Hertz, B., Jansson, H., & Tunlid, A. (2006). Nematophagous fungi. *eLS, 1*, 1–11. https://doi.org/10.1038/npg.els.0004293

Norton, D. C., & Niblack, T. L. (2020). Biology and ecology of nematodes. In W. R. Nickle (ed.), *Manual of agricultural nematology* (pp. 47–72). CRC Press. https://doi.org/10.1201/9781003066576-2

Norvell, L. L. (2011). Fungal nomenclature. 1. Melbourne approves a new Code. *Mycotaxon, 116*(1), 481–490. https://doi.org/10.5248/116.481

O'Donnell, K., Kistler, H. C., Cigelnik, E., & Ploetz, R. C. (1998). Multiple evolutionary origins of the fungus causing Panama disease of banana: Concordant evidence from nuclear and mitochondrial gene genealogies. *Proc. Natl. Acad. Sci., 95,* 2044–2049. https://doi.org/10.1073/pnas.95.5.2044

O'Donnell, K., Rooney, A. P., Proctor, R. H., Brown, D. W., McCormick, S. P., Ward, T. J., . . . David, M. G. (2013). Phylogenetic analyses of RPB1 and RPB2 support a middle Cretaceous origin for a clade comprising all agriculturally and medically important fusaria. *Fungal Genetics and Biology, 52,* 20–31. https://doi.org/10.1016/j.fgb.2012.12.004

Okada, H., Harada, H., & Kadota, I. (2005). Fungal-feeding habits of six nematode isolates in the genus *Filenchus*. *Soil Biology and Biochemistry, 37*(6), 1113–1120. https://doi.org/10.1016/j.soilbio.2004.11.010

Onofri, S., & Tosi, S. (1992). *Arthrobotrys ferox* sp. nov., a springtail-capturing hyphomycete from continental Antarctica. *Mycotaxon, 44*(2), 445–451.

Pfister, D. H. (1997). Pollux and life histories of fungi. *Mycologia, 89*(1), 1–23. https://doi.org/10.1080/00275514.1997.12026750

Owen, R. B. (2005). Physical geography and geology: Imprints on a landscape, Yunnan, China. *Geography, 90*(3), 279–287. https://doi.org/10.1080/00167487.2005.12094140

Page, R. D. M. (1996). TreeView: An application to display phylogenetic trees on personal computers. *Computer Applications in the Biosciences, 12,* 357–358. https://doi.org/10.1093/bioinformatics/12.4.357

Pandey, V. S. (1973). Predatory activity of nematode trapping fungi against the larvae of *Trichostrongylus axei* and *Ostertagia ostertagi:* A possible method of biological control. *Journal of Helminthology, 47*(1), 35–48. https://doi.org/10.1017/S0022149X00023725

Pandit, R. J., Kunjadia, P. D., Mukhopadhyaya, P. N., Joshi, C. G., & Nagee, A. H. (2014). Isolation, molecular characterization and predatory activity of two Indian isolates of nematode-trapping fungi. *Applied Biological Research, 16*(1), 10–20. https://doi.org/10.5958/0974-4517.2014.00042.1

Pausas, J. G., & Ribeiro, E. (2017). Fire and plant diversity at the global scale. *Global Ecology and Biogeography, 26*(8), 889–897. https://doi.org/10.1111/geb.12596

Peach, M. (1950). Aquatic predacious fungi. *Trans. Br. Mycol. Soc., 33*, 148–153. https://doi.org/10.1016/S0007-1536(50)80058-X

Peach, M. (1952). Aquatic predacious fungi. II. *Trans. Br. Mycol. Soc., 35*, 19–23. https://doi.org/10.1016/S0007-1536(52)80002-6

Peiris, P. U. S., Li, Y., Brown, P., & Xu, C. (2020). Fungal bio-control against *Meloidogyne* spp. in agricultural crops: A systematic review and meta-analysis. *Biological Control*, *144*, 104235. https://doi.org/10.1016/j.biocontrol.2020.104235

Persoon, C. H. (1801). *Synopsis Methodica Fungorum*. Henricus Dieterich.

Pfister, D. H. (1994). *Orbilia fimicola*, a nematophagous discomycete and its *Arthrobotrys* anamorph. *Mycologia*, *86*, 451–453. https://doi.org/10.1080/00275514.1994.12026433

Pfister, D. H. (1997). Castor, pollux and life histories of fungi. *Mycologia, 89*, 1–23. https://doi.org/10.1080/00275514.1997.12026750

Pfister, D. H. (2015). Pezizomycotina: Pezizomycetes, Orbiliomycetes. *Systematics and Evolution, Part B*, 35–55. https://doi.org/10.1007/978-3-662-46011-5_2

Pfister, D. H., & Liftik, M. E. (1995). Two *Arthrobotrys* anamorphs from *Orbilia auricolor*. *Mycologia*, *87*(5), 684–688. https://doi.org/10.1080/00275514.1995.12026584

Poloczek, E., & Webster, J. (1994). Conidial traps in *Nematoctonus* (nematophagous Basidiomycetes). *Nova Hedwig.*, *59*, 201–205.

Posada, D. (2008). jModelTest: Phylogenetic model averaging. *Mol. Biol. Evol.*, *25*, 1253–1256. https://doi.org/10.1093/molbev/msn083

Pramer, D. (1964). Nematode-trapping fungi. *Science, 144*, 382–388. https://doi.org/10.1126/science.144.3617.382

Ptatscheck, C., & Traunspurger, W. (2020). The ability to get everywhere: Dispersal modes of free-living, aquatic nematodes. *Hydrobiologia*, *847*, 3519–3547. https://doi.org/10.1007/s10750-020-04373-0

Quijada, L., Baral, H., Beltran-Tejera, E., & Pfister, D. (2020). *Orbilia jesu-laurae* (Ascomycota, Orbiliomycetes), a new species of neotropical nematode-trapping fungus from Puerto Rico, supported by morphology and molecular phylogenetics. *Willdenowia*, *50*(2), 241–251. https://doi.org/10.3372/wi.50.50210

R Core Team. (2014). *R: A language and environment for statistical computing*. R Foundation for Statistical Computing.

Rahman, L., Chan, K. Y., & Heenan, D. P. (2007). Impact of tillage, stubble management and crop rotation on nematode populations in a long-term field experiment. *Soil and Tillage Research*, *95*(1-2), 110–119. https://doi.org/10.1016/j.still.2006.11.008

Rahman, M. U., Chen, P., Zhang, X., & Fan, B. (2023). Predacious strategies of nematophagous fungi as bio-control agents. *Agronomy*, *13*(11), 2685. https://doi.org/10.3390/agronomy13112685

Rambaut, A. (2010). *FigTree v1. 3.1*. http://tree. bio. ed. ac. uk/software/figtree/

Rannala, B., & Yang, Z. (1996). Probability distribution of molecular evolutionary trees: A new method of phylogenetic inference. *Journal of Molecular Evolution, 43*, 304–311. https://doi.org/10.1007/BF02338839

Rezakhani, F., Khodaparast, S. A., Masigol, H., Roja-Jimenez, K., Grossart, H. P., & Bakhshi, M. (2019). A preliminary report of aquatic hyphomycetes isolated from Anzali lagoon (Gilan province, North of Iran). *Rostaniha*, *20*, 123–143.

Rong, S., Xin-Juan, Z., Hai-Qing, W., Fa, Z., Xiao-Yan, Y., & Wen, X. (2020). Succession of soil nematode-trapping fungi following fire disturbance in forest. *Journal of Forest Research*, *25*(6), 433–438. https://doi.org/10.1080/13416979.2020.1793465

Rubner, A. (1996). Revision of predacious hyphomycetes in the *Dactylella-Monacrosporium* complex. *Stud. Mycol.*, *39*, 1–134.

Saccardo, P. (1880). Fungi Veneti novi vel critici v. mycologiae Veneti addendi XI. *Michelia*, *2*, 154–176.

Saikawa, M. (2011). Ultrastructural studies on zygomycotan fungi in the Zoopagaceae and Cochlonemataceae. *Mycoscience*, *52*, 83–90. https://doi.org/10.1007/S10267-010-0083-2

Santamaria, B., Verbeken, A., & Haelewaters, D. (2023). Mycophagy: A global review of interactions between invertebrates and fungi. *Journal of Fungi*, *9*(2), 163. https://doi.org/10.3390/jof9020163

Saxena, G. (2018). Biological control of root-knot and cyst nematodes using nematophagous fungi. In B. Giri, R. Prasad & A. Varma (eds.), *Root biology* (pp. 221–237). Springer. https://doi.org/10.1007/978-3-319-75910-4_8

Schenck, S., Kendrick, W. B., & Pramer, D. (1977). A new nematode-trapping hyphomycete and a reevaluation of *Dactylaria* and *Arthrobotrys*. *Can. J. Bot.*, *55*, 977–985. https://doi.org/10.1139/b77-115

Schmidt, A. R., Dorfelt, H., & Perrichot, V. (2007). Carnivorous fungi from cretaceous amber. *Science*, *318*, 1743. https://doi.org/10.1126/science.1149947

Schmidt, A. R., Dörfelt, H., & Perrichot, V. (2008). *Palaeoanellus dimorphus* gen. et sp. nov. (Deuteromycotina): A Cretaceous predatory fungus. *Am. J. Bot.*, *95*, 1328–1334. https://doi.org/10.3732/ajb.0800143

Schmidt, A. R., Dörfelt, H., & Perrichot, V. (2009). Palaeomycology: Do we consider extinct lineages in the evaluation of fossil fungi?. *Mycol. Res.*, *113*, 275–276.

Scholler, M., Hagedorn, G., & Rubner, A. (1999). A reevaluation of predatory orbiliaceous fungi. II. A new generic concept. *Sydowia*, *51*, 89–113.

Schroers, H. J., Samuels, G. J., Zhang, N., Short, D. P., Juba, J., & Geiser, D. M. (2016). Epitypification of *Fusisporium* (*Fusarium*) *solani* and its assignment to a common phylogenetic species in the *Fusarium solani* species complex. *Mycologia*, *108*(4), 806–819. https://doi.org/10.3852/15-255

Semprucci, F., & Balsamo, M. (2012). Key role of free-living nematodes in the marine ecosystem. In F. Boari & J. A. Chung (Eds.), *Nematodes: Morphology, functions and management strategies* (pp. 109-134). NOVA Science Publishers.

Serna-Chavez, H. M., Fierer, N., & van Bodegom, P. M. (2013). Global drivers and patterns of microbial abundance in soil. *Glob. Ecol. Biogeogr*, *22*, 1162–1172. https://doi.org/10.1111/geb.12070

Serra, E. F., Silva, A. L., Ripoll, M. K., Tavares, N. C., Waller, S. B., Osório, L. D. G., . . . Meireles, M. C. A. (2017). Nematode-trapping fungi in soil samples from Alegrete-RS. *Sci. Anim. Health*, *5*, 21–34. https://doi.org/10.15210/sah.v5i1.9135

Shang, Q. J., Phookamsak, R., Camporesi, E., Khan, S., Lumyong, S., & Hyde, K. D. (2018). The holomorph of *Fusarium celtidicola* sp. nov. from *Celtis australis*. *Phytotaxa*, *361*(3), 251–265. https://doi.org/10.11646/phytotaxa.361.3.1

Shao, Y., Baral, H. O., Ou, X., Wu, H., Huang, F., Zheng, H., . . . Liu, B. (2018). New species and records of orbiliaceous fungi from Georgia, USA. *Mycological Progress, 17*, 1225–1235. https://doi.org/10.1007/s11557-018-1438-x

She, R., Zhou, X. J., Wang, H. Q., Zhang, F., Yang, X. Y., & Xiao, W. (2020). Succession of soil nematode-trapping fungi following fire disturbance in forest. *Journal of Forest Research*, *25*(6), 433–438. https://doi.org/10.1080/13416979.2020.1793465

She, R., Zhou, X. J., Wang, H. Q., Zhang, F., Yang, X. Y., & Xiao, W. (2022). Natural recovery from fire disturbance is more favorable than assisted recovery for the restoration of soil nematode-trapping fungi. *Canadian Journal of Microbiology*, *68*(5), 329–339. https://doi.org/10.1139/cjm-2021-0237

Shepherd, A. M. (1955). *Some observations on the distribution andbiology of fungi Predaceouson Nematodes* (Doctoral dissertation). University of London.

Sherbakoff, C. D. (1933). A new fungus parasitic on nematodes. *Mycologia*, *25*, 258. https://doi.org/10.1080/00275514.1933.12020665

Short, D. P., O'Donnell, K., Thrane, U., Nielsen, K. F., Zhang, N., Juba, J. H., . . . Geiser, D. M. (2013). Phylogenetic relationships among members of the *Fusarium solani* species complex in human infections and the descriptions of *F. keratoplasticum sp. nov.* and *F. petroliphilum stat. nov*. *Fungal Genetics and Biology, 53*, 59–70. https://doi.org/10.1016/j.fgb.2013.01.004

Singh, R. K., Pandey, S. K., & Chattopadhyay A. (2014). Biodiversity and periodical/seasonal distribution of nematode trapping fungi from different habitats. *J. Pure Appl. Microbiol, 9*(1), 767–776.

Šišić, A., Al-Hatmi, A. M., Baćanović-Šišić, J., Ahmed, S. A., Dennenmoser, D., de Hoog, G. S., . . . Finckh, M. R. (2018). Two new species of the *Fusarium solani* species complex isolated from compost and hibiscus (*Hibiscus* sp.). *Antonie van Leeuwenhoek, 111*(10), 1785–1805. https://doi.org/10.1007/s10482-018-1068-y

Sivanandhan, S., Khusro, A., Paulraj, M. G., Ignacimuthu, S., & Al-Dhabi, N. A. (2017). Biocontrol properties of basidiomycetes: An overview. *Journal of Fungi, 3*(1), 2. https://doi.org/10.3390/jof3010002

Smith, M. E., & Jaffee, B. A. (2009). PCR primers with enhanced specificity for nematodetrapping fungi (Orbiliales). *Microbial Ecology*, *58*(1), 117–128. https://doi.org/10.1007/s00248-008-9453-0

Soliman, M. S., El-Deriny, M. M., Ibrahim, D. S. S., Zakaria, H., & Ahmed, Y. (2021). Suppression of root-knot nematode Meloidogyne incognita on tomato plants using the nematode trapping fungus *Arthrobotrys oligospora* Fresenius. *Journal of Applied Microbiology, 131*(5), 2402–2415. https://doi.org/10.1111/jam.15101

Sommerstorff, H. (1911). Ein Tiere fangender Pilz. (*Zoophagus insidians*, nov. gen., nov. spec.). *Österreichische Botanische Zeitschrift, 61*, 361–373. https://doi.org/10.1007/BF01643971

Soprunov, F. F., & Galiulina, Z. A. (1951). Predaceous hyphomycetes from Turkmenistan soil. *Mikorobiologiya, 20*, 489–499.

Sorokin, N. (1876). Note sur les vegetaux parasites des Anguillulae. *Annales des Sciences Naturalles Botanique Ser., 64*, 62–71.

Speijer, P. R. & Sikora, R. A. (1993). Influence of a complex disease involving *Pratylenchus goodeyi* and non-pathogenic strain of *Fusarium oxysporum* on banana root health. In C. S. Gold (Ed.), *Biological and integrated control of highland banana and plantain pests and diseases* (pp. 231–239). International Institute of Tropical Agriculture.

Staniland, L. N. (1954). A modification of the Baermann funnel technique for the collection of nematodes from plant material. *J Helminthol, 28*(1–2), 115–117. https://doi.org/10.1017/S0022149X00032739

Stiller, J. W., & Hall, B. D. (1997). The origin of red algae: implications for plastid evolution. *Proceedings of the National Academy of sciences, 94*(9), 4520–4525. https://doi.org/10.1073/pnas.94.9.4520

Stirling, G. R. (2018). Biological control of plant-parasitic nematodes. In K. Davies & Y. Spiegel (Eds.), *Diseases of nematodes* (pp. 103–150). CRC Press. https://doi.org/10.1201/9781351071468-9

Strong, P. J., Self, R., Allikian, K., Szewczyk, E., Speight, R., O'Hara, I., . . . Harrison, M. D. (2022). Filamentous fungi for future functional food and feed. *Current Opinion in Biotechnology, 76*, 102729. https://doi.org/10.1016/j.copbio.2022.102729

Su, H. Y., Hao, Y. E., Mo, M., & Zhang, K. Q. (2007). The ecology of nematode-trapping hyphomycetes in cattle dung from three plateau pastures. *Veterinary Parasitology, 144*, 293–298. https://doi.org/10.1016/j.vetpar.2006.10.012

Su, H. Y., Hao, Y. E., Yang, X., Yu, Z. F., Deng, J., & Mo, M. (2008). A new species of *Dactylellina* producing adhesive knobs and non-constricting rings to capture nematodes. *Mycotaxon, 105*, 313.

Su, H. Y., Li, M., & Liu, X. X. (2006). Improvement of the slide making method of nematode trapping fungi. *J. Dali Univ., 6*, 25–26+30.

Su, H., Li, Y., Mo, M., & Zhang, K. (2005). *Monacrosporium multiseptatum*, a new predacious fungus from China. *Mycotaxon, 92*, 193–196.

Su, H., Zhao, Y., Zhou, J., Feng, H., Jiang, D., Zhang, K. Q., . . . Yang, J. (2017). Trapping devices of nematode-trapping fungi: Formation, evolution, and genomic perspectives. *Biological Reviews, 92*(1), 357–368. https://doi.org/10.1111/brv.12233

Subramanian, C. V. (1963). *Dactylella*, *Monacrosporium* and *Dactylina*. *Journal of the Indian Botanical Society, 42*, 291–300.

Subramanian, C. V. (1977). Revision of hyphomycetes 1. *Kawaka, 5*, 93–98.

Sun, H. (2002). Evolution of arctic-tertiary fora in himalayan-hengduan mountains. *Acta Bot. Yunnanica, 24*, 671–688.

Sun, H., & Li, Z. M. (2003). Qinghai-Tibet Plateau uplift and its impact on Tethys fora. *Adv. Earth Sci.*, *18*, 852–862.

Sutherland, W. J., Freckleton, R. P., Godfray. H. C. J., Beissinger, S. R., Benton, T., Cameron, D. D., . . . Hails, R. S. (2013). Identification of 100 fundamental ecological questions. *Journal of Ecology, 101*(1), 58–67. https://doi.org/10.1111/1365-2745.12025

Swe, A., Jeewon, R., & Hyde, K. D. (2008). Nematode-trapping fungi from mangrove habitats. *Cryptogamie, 29*(4), 333.

Swe, A., Jeewon, R., Pointing, S. B., & Hyde, K. D. (2008). Taxonomy and molecular phylogeny of *Arthrobotrys mangrovispora*, a new marine nematode-trapping fungal species. *Bot. Mar., 51*, 331–338. https://doi.org/10.1515/BOT.2008.043

Swe, A., Jeewon, R., Pointing, S. B., & Hyde, K. D. (2009). Diversity and abundance of nematode-trapping fungi from decaying litter in terrestrial, freshwater and mangrove habitats. *Biodiversity and Conservation, 18*(6), 1695–1714. https://doi.org/10.1007/s10531-008-9553-7

Swe, A., Li, J., Zhang, K. Q., Pointing, S. B., Jeewon, R., & Hyde, K. D. (2011). Nematode-trapping fungi. *Current Research in Environmental & Applied Mycology, 1*(1), 1–26.

Swindell, S. R., & Plasterer, T. N. (1997). Seqman. In S. R. Swindell (ed.), *Sequence data analysis guidebook* (pp. 75–89). Springer. https://doi.org/10.1385/0-89603-358-9:75

Swofford, D. L. (2002). *PAUP*: Phylogenetic analysis using parsimony (*and other methods), version 4*. Sinauer.

Szabó, M., Csepregi, K., Gálber, M., Virányi, F., & Fekete, C. (2012). Control plant-parasitic nematodes with *Trichoderma* species and nematode-trapping fungi: The role of chi18-5 and chi18-12 genes in nematode egg-parasitism. *Biological Control, 63*(2), 121–128. https://doi.org/10.1016/j.biocontrol.2012.06.013

Tahseen, Q. (2012). Nematodes in aquatic environments: Adaptations and survival strategies. *Biodivers. J., 3*, 13–40.

Tamura, K., Stecher, G., Peterson, D., Filipski, A., & Kumar, S. (2013). MEGA6: molecular evolutionary genetics analysis version 6.0. *Molecular Biology and Evolution, 30*(12), 2725–2729. https://doi.org/10.1093/molbev/mst197

Tanabe, Y., O'Donnell, K., Saikawa, M., & Sugiyama, J. (2000). Molecular phylogeny of parasitic Zygomycota (Dimargaritales, Zoopagales) based on nuclear small subunit ribosomal DNA sequences. *Molecular Phylogenetics and Evolution, 16*(2), 253–262. https://doi.org/10.1006/mpev.2000.0775

Tarigan, W. E., Munir, E. Hastuti, L. D. S., & Hartanto, A. (2020). Occurrence of nematophagous fungi in freshwater samples of Toba Lake, North Sumatra, Indonesia. *J. Phys. Conf. Ser., 1462*, 012052. https://doi.org/10.1088/1742-6596/1462/1/012052

Tewoldemedhin, Y. T., Lamprecht, S. C., Vaughan, M. M., Doehring, G., & O'Donnell, K. (2017). Soybean SDS in South Africa is caused by *Fusarium brasiliense* and a novel undescribed *Fusarium* Sp. *Plant Disease, 101*(1), 150–157. https://doi.org/10.1094/PDIS-05-16-0729-RE

Thaler, L. (1986). Origin and evolution of mice: An appraisal of fossil evidence and morphological traits. *Poxviruses, 127*, 3–11. https://doi.org/10.1007/978-3-642-71304-0_1

Thorn, R. G., & Barron, G. L. (1984). Carnivorous mushrooms. *Science, 224*, 76–78. https://doi.org/10.1126/science.224.4644.76

Thorn, R. G., Moncalvo, J. M., Reddy, C. A., & Vilgalys, R. (2000). Phylogenetic analyses and the distribution of nematophagy support a monophyletic *Pleurotaceae* within the polyphyletic pleurotoid-lentinoid fungi. *Mycologia, 92*, 241–252. https://doi.org/10.1080/00275514.2000.12061151

Thorn, R. G., Scholler, M., & Gams, W. (2008). Mycological research news. *Mycol. Res., 112*, 611–612.

Timper, P. (2014). Conserving and enhancing biological control of nematodes. *Journal of Nematology, 46*(2), 75.

Treseder, K. K., & Lennon, J. T. (2015). Fungal traits that drive ecosystem dynamics on land. *Microbiology and Molecular Biology Reviews, 79*(2), 243–262. https://doi.org/10.1128/MMBR.00001-15

Troussellier, M., Escalas, A., Bouvier, T., & Mouillot, D. (2017). Sustaining rare marine microorganisms: macroorganisms as repositories and dispersal agents of microbial diversity. *Frontiers in Microbiology, 8*, 947. https://doi.org/10.3389/fmicb.2017.00947

Trudgill, D. L. (1991). Resistance to and tolerance of plant parasitic nematodes in plants. *Annual Review of Phytopathology, 29*(1), 167–192. https://doi.org/10.1146/annurev.py.29.090191.001123

Tunlid, A., & Ahrén, D. (2011). Molecular mechanisms of the interaction between nematode-trapping fungi and nematodes: Lessons from genomics. In K. Davies & Y. Spiegel (Eds.), *Biological control of plant-parasitic nematodes: Building coherence between microbial ecology and molecular mechanisms* (pp. 145–169). Springer. https://doi.org/10.1007/978-1-4020-9648-8_6

Tzean, S. S., & Liou, J. Y. (1993). Nematophagous resupinate basidiomycetous fungi. *Phytopathology, 83*, 1015–1020. https://doi.org/10.1094/Phyto-83-1015

Ulzurrun, G., & Hsueh, Y. P. (2018). Predator-prey interactions of nematode-trapping fungi and nematodes: Both sides of the coin. *Applied Microbiol Biotechnol, 102*, 3939–3949. https://doi.org/10.1007/s00253-018-8897-5

Valkanov, A. (1931). Über die Morphologie und Systematik der rotatorienbefallenden Oomyceten. *Godishnik na Sofiiskiya Universitet (Jahrbuch der Sofiana Universitat), 27*, 215–233.

Van Vooren, N., & Audibert, C. (2005). Révision du complexe "*Cordyceps sphecocephala". 1re partie: les guêpes végétales. Bulletin mensuel de la Société Linnéenne de Lyon, 74*, 221–254. https://doi.org/10.3406/linly.2005.13604

Vandermeer, J. (2006). Oscillating populations and biodiversity maintenance. *Bioscience, 56*(12), 967–975. https://doi.org/10.1641/0006-3568(2006)56[967:OPABM]2.0.CO;2

Vidal-Diez de Ulzurrun, G., & Hsueh, Y. P. (2018). Predator-prey interactions of nematode-trapping fungi and nematodes: Both sides of the coin. *Applied Microbiology and Biotechnology, 102,* 3939–3949. https://doi.org/10.1007/s00253-018-8897-5

Vilela, V. L. R., Feitosa, T. F., Braga, F. R., de Araújo, J. V., dos Santos, A., de Morais, D. F., . . . Athayde, A. C. R. (2016). Coadministration of nematophagous fungi for biological control over gastrointestinal helminths in sheep in the semiarid region of northeastern Brazil. *Veterinary Parasitology, 221*, 139–143. https://doi.org/10.1016/j.vetpar.2016.03.027

Vilela, V., Feitosa, T., Braga, F., Araujo, J., Oliveira, S., Silva, S., . . . Athayde, A. (2012). Biological control of goat gastrointestinal helminthiasis by *Duddingtonia flagrans* in a semi-arid region of the northeastern Brazil. *Veterinary Parasitology, 188*(1-2), 127–133. https://doi.org/10.1016/j.vetpar.2012.02.018

Von Esenbeck, C. G. N. (1817). *Das system der pilze und schwämme: Ein versuch*. In der Stahelschen buchhandlung.

Voronin, M. (1870). *Sphaeria lemneae, Sordaria coprophila, Arthrobotrys oligospora*. *Beitrgge Zur Morphologie Und Physiologie Der Pilze*, *1870*, 325–360.

Vu, D., Groenewald, M., De Vries, M., Gehrmann, T., Stielow, B., Eberhardt, U., . . . Boekhout, T. (2019). Large-scale generation and analysis of filamentous fungal DNA barcodes boosts coverage for kingdom fungi and reveals thresholds for fungal species and higher taxon delimitation. *Stud. Mycol*, *92*, 135–154. https://doi.org/10.1016/j.simyco.2018.05.001

Wachira, P., Mibey, R., Okoth, S., Kimenju, J., & Kiarie, J. (2009). Diversity of nematode destroying fungi in Taita Taveta, Kenya. *Fungal Ecology*, *2*(2), 60–65. https://doi.org/10.1016/j.funeco.2008.11.002

Wang, C., Mo, M., Li, X., Tian, B., & Zhang, K. (2007). Morphological characteristics and infection processes of nematophagous *Harposporium* with reference to two new species. *Fungal Diversity*, *26*(1), 287–304.

Wang, J. X., Peng, X. F., & Yang, S. Y. (2005). Analysis of tourism resources and environmental vulnerability in three Parallel Rivers World Natural Heritage Site. *J. Yunnan Norm. Univ. Nat. Sci.*, *25*, 59–64.

Wang, X., Li, G. H., Zou, C. G., Ji, X. L., Liu, T., Zhao, P. J., . . . Qin, Y. K. (2014). Bacteria can mobilize nematode-trapping fungi to kill nematodes. *Nat. Commun.*, *5*, 5776. https://doi.org/10.1038/ncomms6776

White, T. J., Bruns, T., Lee, S., & Taylor, J. (1990). Amplification and direct sequencing of fungal ribosomal RNA genes for phylogenetics. *PCR Protocols: A Guide to Methods and Applications*, *18*(1), 315–322. https://doi.org/10.1016/B978-0-12-372180-8.50042-1

Williamson, V. M., & Hussey, R. S. (1996). Nematode pathogenesis and resistance in plants. *The Plant Cell, 8*(10), 1735. https://doi.org/10.2307/3870226

Wingfield, M. J., De Beer, Z. W., Slippers, B., Wingfield, B. D., Groenewald, J. Z., Lombard, L., . . . Crous, P. W. (2012). One fungus, one name promotes progressive plant pathology. *Mol. Plant Pathol, 13*, 604–613. https://doi.org/10.1111/j.1364-3703.2011.00768.x

Wolstrup, J., Nansen, P., Gronvold, J., Henriksen, S., & Larsen, M. (1996). Toward practical biological control of parasitic nematodes in domestic animals. *Journal of Nematology, 28*(2), 129.

Wu, H. Y., Kim, D. G., Ryu, Y. H., & Zhou, X. B. (2012). *Arthrobotrys koreensis*, a new nematodetrapping species from Korea. *Sydowia, 64*(1), 129–136.

Yadav, B., Singh, U. B., Malviya, D., Vishwakarma, S. K., Ilyas, T., Shafi, Z., . . . Singh, H. V. (2023). Nematophagous fungi: Biology, ecology and potential application. In U. B. Singh, R. Kumar & H. B. Singh (Eds.), *Detection, diagnosis and management of soil-borne phytopathogens* (pp. 309–328). Springer Singapore. https://doi.org/10.1007/978-981-19-8307-8_12

Yang, C. T., Vidal-Diez de Ulzurrun, G., Gonçalves, A. P., Lin, H. C., Chang, C. W., Huang, T. Y., . . . Stajich, J. E. (2020). Natural diversity in the predatory behavior facilitates the establishment of a robust model strain for nematode-trapping fungi. *Proceedings of the National Academy of Sciences, 117*(12), 6762–6770. https://doi.org/10.1073/pnas.1919726117

Yang, E., Xu, L., Yang, Y., Zhang, X., Xiang, M., Wang, C., . . . Liu, X. (2012). Origin and evolution of carnivorism in the Ascomycota (fungi). *Proceedings of the National Academy of Sciences, 109*(27), 10960–10965. https://doi.org/10.1073/pnas.1120915109

Yang, H., Yang, D., & Zhou, J. (2008). Diversity of nematode-trapping fungi in soil of eucalyptus. *Journal-Yunnan University Natural Sciences, 30*(1), 101.

Yang, J., & Zhang, K. Q. (2014). Biological control of plant-parasitic nematodes by nematophagous fungi. In K.-Q. Zhang & K. D. Hyde (Eds.), *Nematode-trapping fungi* (pp. 231–262). Springer. https://doi.org/10.1007/978-94-017-8730-7_5

Yang, X. Y., Liu, L. P., Su, X. J., Ye, Y. B., Huang, A. Y., & Su, H. Y. (2011). Study on the biological diversity of nematode-trapping fungi in Erhai Lake. *Agricultural Science & Technology*, *12*(8), 1100–1102.

Yang, Y. Q., Li, F. T., Li, Y. P., She, R., & Yang, X. Y. (2023). Research progress of biological control of nematodes based on citespace. *Chinese Agricultural Science Bulletin, 39*(4), 139–148.

Yang, Y. Q., Zhang, F., Li, Z. Q., Zhou, F. P., Yang, X. Y., & Xiao, W. (2023). Morphological and multigene phylogenetic analyses reveal two new nematode-trapping fungi (*Arthrobotrys*, Orbiliaceae) from Yunnan, China. *Phytotaxa, 591*(4), 263–272. https://doi.org/10.11646/phytotaxa.591.4.3

Yang, Y., Yang, E., An, Z., & Liu, X. Z. (2007). Evolution of nematode-trapping cells of predatory fungi of the Orbiliaceae based on evidence from rRNA-encoding DNA and multiprotein sequences. *Proceedings of the National Academy of Sciences, 104*(20), 8379–8384. https://doi.org/10.1073/pnas.0702770104

Yang, Y., Tian, K., Hao, J., Pei, S., & Yang, Y. (2004). Biodiversity and biodiversity conservation in Yunnan, China. B*iodiversity & Conservation, 13*, 813–826. https://doi.org/10.1023/B:BIOC.0000011728.46362.3c

Yeates, G. W., Ferris, H., Moens, T., & Putten, W. V. D. (2009). The role of nematodes in ecosystems (pp. 1–44). Nematodes as Environmental Indicators. https://doi.org/10.1079/9781845933852.0001

Yu, Z., Qin, L., Zhang, Y., Qiao, M., Kong, Y., & Zhang, K. (2009). A new *Drechslerella* species isolated from *Orbilia cf. orientalis*. *Mycotaxon, 110*(1), 253–259. https://doi.org/10.5248/110.253

Yu, Z., Zhang, Y., Qiao, M., Baral, H. O., Weber, E., & Zhang, K. (2006). *Drechslerella brochopaga*, the anamorph of *Orbilia (Hyalinia) orientalis*. *Mycotaxon, 96,* 163–168.

Zare, R., Gam, W., & Evans, H. C. (2000). A revision of *Verticillium* section Prostrata.V. The genus Pochonia, with notes on Rotiferophthora. *Nova Hedwigia, 73,* 51–86. https://doi.org/10.1127/nova.hedwigia/73/2001/51

Zareen, A., Siddiqui, I., Aleem, F., Zaki, M., & Shaukat, S. S. (2001). Observations on the nematicidal effect of *Fusarium solani* on the rootknot nematode, *Meloidogyne javanica. Journal of Plant Pathology, 83*(3), 207–214.

Zarrin, M., Rahdar, M., Poormohamadi, F., & Rezaei-Matehkolaei, A. (2017). In vitro nematophagous activity of predatory fungi on infective nematodes larval stage of strongyloidae family. *Macedonian Journal of Medical Sciences, 5*(3), 281. https://doi.org/10.3889/oamjms.2017.064

Zhang, D. C., Zhang, Y. H., Boufford, D. E., & Sun, H. (2009). Elevational patterns of species richness and endemism for some important taxa in the Hengduan Mountains, southwestern China. *Biodivers. Conserv., 18,* 699–716. https://doi.org/10.1007/s10531-008-9534-x

Zhang, D., Gao, F.L., Jakovlić, I., Zou, H., Zhang, J., Li, W. X., . . . Wang, G. T. (2020). PhyloSuite: An integrated and scalable desktop platform for streamlined molecular sequence data management and evolutionary phylogenetics studies. *Molecular Ecology Resources, 20*(1), 348–355. https://doi.org/10.1111/1755-0998.13096

Zhang, F., Boonmee, S., Bhat, J. D., Xiao, W., & Yang, X. Y. (2022). New *Arthrobotrys* nematode-trapping species (Orbiliaceae) from terrestrial soils and freshwater sediments in China. *Journal of Fungi, 8*(7), 671. https://doi.org/10.3390/jof8070671

Zhang, F., Boonmee, S., Monkai, J., Yang, X. Y., & Xiao, W. (2022). *Drechslerella daliensis* and *D. xiaguanensis* (Orbiliales, Orbiliaceae), two new nematode-trapping fungi from Yunnan, China. *Biodivers Data J., 10*, e96642. https://doi.org/10.3897/BDJ.10.e96642

Zhang, F., Boonmee, S., Yang, Y. Q., Zhou, F. P., Xiao, W., & Yang, X. Y. (2023). *Arthrobotrys blastospora* sp. nov. (Orbiliomycetes): A living fossil displaying morphological traits of mesozoic carnivorous fungi. *Journal of Fungi, 9*(4), 451. https://doi.org/10.3390/jof9040451

Zhang, F., Liu, S. R., Zhou, X. J., Monkai, J., Hongsanan, S., Shang, Q. J., . . . Yang, X. Y. (2020). *Fusarium xiangyunensis* (Nectriaceae), a remarkable new species of nematophagous fungi from Yunnan, China. *Phytotaxa, 450*, 273–284. https://doi.org/10.11646/phytotaxa.450.3.3

Zhang, F., Yang, Y. Q., Zhou, F. P., Xiao, W., Boonmee, S., & Yang, X. Y. (2024). Multilocus phylogeny and characterization of five undescribed aquatic carnivorous fungi (Orbiliomycetes). *Journal of Fungi, 10*(1), 81. https://doi.org/10.3390/jof10010081

Zhang, F., Yang, Y. Q., Zhou, F. P., Xiao, W., Boonmee, S., Yang, X. Y. (2023). Morphological and phylogenetic characterization of five novel nematode-trapping fungi (orbiliomycetes) from Yunnan, China. *Journal of Fungi, 9*(7), 735. https://doi.org/10.3390/jof9070735

Zhang, F., Zhou, X. J., Monkai, J., Li, F. T., Liu, S. R., Yang, X. Y., . . . Hyde, K. D. (2020). Two new species of nematode-trapping fungi (*Dactylellina*, Orbiliaceae) from burned forest in Yunnan, China. *Phytotaxa, 452*(1), 65–74. https://doi.org/10.11646/phytotaxa.452.1.6

Zhang, H., Wei, Z., Zhang, J., & Liu, X. (2021). Classification of dendrocola nematode-trapping fungi. *Journal of Forestry Research, 32*(3), 295–304. https://doi.org/10.1007/s11676-020-01159-x

Zhang, K. Q., & Hyde, K. D. (2014). *Nematode-trapping fungi*. Springer Science & Business. https://doi.org/10.1007/978-94-017-8730-7

Zhang, K. Q., & Mo, M. H. (2006). *Flora fungorum sinicorum (Vol. 33): Arthrobotrys et gengra cetera cognata*. Science Press.

Zhang, K. Q., Li, T. F., & Liu, X. Z. (2001). *Biology of nematophagous fungi*. China Science & Technology Press.

Zhang, K., Liu, X., & Cao, L. (1996). Nematophagous species of *Monacrosporium* from China. *Mycological Research, 100*(3), 274–276. https://doi.org/10.1016/S0953-7562(96)80153-5

Zhang, N., O'Donnell, K., Sutton, D. A., Nalim, F. A., Summerbell, R. C., Padhye, A. A., . . . Geiser, D. M. (2006). Members of the *Fusarium solani* species complex that cause infections in both humans and plants are common in the environment. *Journal of Clinical Microbiology, 44*(6), 2186–2190. https://doi.org/10.1128/JCM.00120-06

Zhang, S. Y., Hao, Y. E., & Zhang, K. Q. (2007). Freshwater nematophagous fungi of Yunnan Province and Guizhou Province, China. *Journal-Yunnan University Natural Sciences, 29*(2), 199.

Zhang, X., Zhang, F., Jiang, L., Yang, Y. Q., Yang, X. Y., & Xiao, W. (2022). Two new nematode-trapping fungi (*Arthrobotrys*, Orbiliaceae) from Yunnan, China. *Phytotaxa, 568*(3), 255–266. https://doi.org/10.11646/phytotaxa.568.3.2

Zhang, Y., Li, G., & Zhang, K. (2011). A review on the research of nematophagous fungal species. *Mycosystema, 30*, 836–845.

Zhang, Y., Li, S., Li, H., Wang, R., Zhang, K. Q., & Xu, J. (2020). Fungi–nematode interactions: Diversity, ecology, and bio-control prospects in agriculture. *Journal of Fungi, 6*(4), 206. https://doi.org/10.3390/jof6040206

Zhang, Y., Qiao, M., Baral, H. O., Xu, J., Zhang, K. Q., & Yu, Z. F. (2020). Morphological and molecular characterization of *Orbilia pseudopolybrocha* and *O. tonghaiensis*, two new species of Orbiliaceae from China. *International Journal of Systematic and Evolutionary Microbiology, 70*(4), 2664–2676. https://doi.org/10.1099/ijsem.0.004088

Zhang, Y., Qiao, M., Weber, E., Baral, H. O., Hagedorn, G., & Yu, Z. F. (2010). *Arthrobotrys scaphoides* from China and Europe with a phylogenetic analysis including the type strain. *Mycotaxon*, *111*, 291. https://doi.org/10.5248/111.291

Zhang, Y., Yang, G., Fang, M., Deng, C., Zhang, K. Q., Yu, Z., . . . Xu, J. (2020). Comparative analyses of mitochondrial genomes provide evolutionary insights into nematode-trapping fungi. *Frontiers in Microbiology, 11*, 617. https://doi.org/10.3389/fmicb.2020.00617

Zhang, Y., Yu, Z. F., Baral, H. O., Mo, M. H., & Zhang, K. Q. (2009). New species and records of *Orbilia* (Orbiliaceae, Ascomycota) from China. *Fungal Diversity*, *36*, 141–153.

Zhang, Y., Yu, Z. F., Baral, H. O., Qiao, M., & Zhang, K. Q. (2007). *Pseudorbilia* gen. nov. (Orbiliaceae) from Yunnan, China. *Fungal Diversity, 26*, 305–312.

Zhang, Y., Zhang, K. Q., & Hyde, K. D. (2014). The ecology of nematophagous fungi in natural environments. In K.-Q. Zhang & K. D. Hyde (Eds.), *Nematode-trapping fungi* (pp. 211–229). Springer. https://doi.org/10.1007/978-94-017-8730-7_4

Zhao, J., Huang, J., Yan, J., & Fang, G. (2020). Economic loss of pine wood nematode disease in mainland China from 1998 to 2017. *Forests., 11*(10), 1042. https://doi.org/10.3390/f11101042

Zhaxybayeva, O., & Gogarten, J. P. (2002). Bootstrap, bayesian probability and maximum likelihood mapping: Exploring new tools for comparative genome analyses. *Genomics, 3*, 1–15. https://doi.org/10.1186/1471-2164-3-4

Zhihua, G., Runguo, Z., & Youxu, J. (2002). The formation and maintenance mechanisms of biodiversity and the research techniques for biodiversity. *Scientia Silvae Sinicae*, *38*(6), 116–124.

Zhou, B. (2010). Revising the Yunnan key protected wild plants list. *Acta Bot. Yunnanica*, *32*, 221–226. https://doi.org/10.3724/SP.J.1143.2010.09255

Zhu, M. C., Li, X. M., Zhao, N., Yang, L., Zhang, K. Q., & Yang, J. K. (2022). Regulatory mechanism of trap formation in the nematode-trapping fungi. *Journal of Fungi*, *8*(4), 406. https://doi.org/10.3390/jof8040406

Zopf, W. (1888). *Zur Kenntniss der Infections-Krankheiten niederer Thiere und Pflanzen*. E. Blochmann.

Zouhar, M., Douda, O., Nováková, J., Doudová, E., Mazáková, J., Wenzlová, J., . . . Renčo, M. (2013). First report about the trapping activity of *Stropharia rugosoannulata* acanthocytes for Northern Root Knot Nematode. *Helminthologia*, *50*, 127–131. https://doi.org/10.2478/s11687-013-0120-8

APPENDICES

APPENDIX A

CHEMICAL REAGENTS AND MEDIA

1. Lactoglycerol used for mounting semi-permanent slides.

Lactic acid 10 ml

Glycerol 10 ml

Distilled water 10 ml

Mix 10 ml lactic acid, 10 ml glycerol, and add 10 ml distilled water.

2. Lactophenol-Cotton Blue used to highlight fungal structures for viewing with the compound light microscope. Cotton blue is the most popular stain for observing pseudoparaphyses, septa or ascus walls. This gives excellent clarity and is also suitable for most fungal groups .

Phenol (crystals) 20 g

Lactic acid 16 ml

Glycerol 31 ml

Dissolve phenol in distilled water, add lactic acid, glycerol and 0.05 g of Poirrier's (cotton) blue or acid fuchsin.

3. Corn Meal Agar (CMA) used for fungal culturing

Corn meal 30 g

Dextrose 20 g

Agar 18 g

Boiling 30 g corn meal in 800 ml of distilled water for 20 minutes and filtering the mixtures through four layers of gauze, supplementing the filtrates to 1000 ml with distilled water, and adjusting the pH to 7, then adding 18 g of agar. Autoclaving at 121℃ for 20 minutes, pouring the mixtures into 60 mm plates to create CMA plates.

4. Potato Dextrose Agar (PDA) used for fungal culturing.

Fresh potato 200 g

Dextrose 20 g

Agar 18 g

Boiling 200 g fresh potato in 800 ml of distilled water for 20 minutes and filtering the mixtures through four layers of gauze, supplementing the filtrates to 1000 ml with distilled water, and adjusting the pH to 7, then adding 18 g of agar and 20 g of dextrose. Autoclaving at 121℃ for 20 minutes, pouring the mixtures into 60 mm plates to create PDA plates.

.

APPENDIX B

ABSTRACT OF PUBLICATIONS

Phytotaxa 452 (1): 065–074
https://www.mapress.com/j/pt/

Article

ISSN 1179-3155 (print edition)
PHYTOTAXA
ISSN 1179-3163 (online edition)

https://doi.org/10.11646/phytotaxa.452.1.6

Two new species of nematode-trapping fungi (*Dactylellina*, Orbiliaceae) from burned forest in Yunnan, China

FA ZHANG[1,2,6], XIN-JUAN ZHOU[1,5,7], JUTAMART MONKAI[2,8], FEI-TENG LI[1,5,9], SHUO-RAN LIU[1,3,4,10], XIAO-YAN YANG[1,3,4,11]*, XIAO WEN[1,3,4,12] & KEVIN D. HYDE[2,13]

[1] *Institute of Eastern-Himalaya Biodiversity Research, Dali University, Dali, Yunnan 671003, P.R. China.*
[2] *Centre of Excellence in Fungal Research, Mae Fah Luang University, Chiang Rai 57100, Thailand.*
[3] *Key Laboratory of Yunnan State Education Department on Er 'hai Lake Basin Protection and the Sustainable Development Research, Dali University, Dali, Yunnan 671003, P.R. China.*
[4] *The provincial innovation team of biodiversity conservation and utility of the three parallel rivers from Dali University, Dali University, Dali, Yunnan 671003, P.R. China.*
[5] *School of Public Health, Dali University, Dali, Yunnan 671003, P.R. China.*
[6] *zhanglieasternhimalaya@gmail.com; https://orcid.org/0000-0002-3749-2948*
[7] *1391890018@qq.com; https://orcid.org/0000-0002-8119-9167*
[8] *mjutamart@gmail.com; https://orcid.org/0000-0001-6043-0625*
[9] *m18323032954@163.com; https://orcid.org/0000-0001-7105-0468*
[10] *46795859@qq.com; https://orcid.org/0000-0003-3983-9949*
[11] *yangxy@eastern-himalaya.cn; https://orcid.org/0000-0002-9304-308X*
[12] *xiaow@eastern-himalaya.cn; https://orcid.org/0000-0002-4951-7524*
[13] *kdhyde3@gmail.com; https://orcid.org/0000-0002-2191-0762*
**Corresponding author*

Abstract

Two new *Dactylellina* (nematode-trapping fungi) species, *D. yushanensis* and *D. cangshanensis* from the burned forest soil in Cangshan Mountain, Yunnan Province, China are introduced in this paper based on morphology and phylogenetic analysis. Their descriptions and illustrations are provided. *Dactylellina yushanensis* is characterized by its geniculate branched conidiophore, two types conidia and fusiform, clavate or drop-shaped microconidia grown in conidiophore or produced by macroconidia with micro-cycle conidiation pathway. *Dactylellina cangshanensis* is characterized by its fusiform, spindle-shaped, clavate or drop-shaped conidia with 2-4-septate. Phylogenetic analysis based on combined ITS, EF1-α and RPB2 sequence showed that these two species cluster together with *D. ellipsospora* with obvious genetic differentiation.

Keywords: Burned forest, New species, Morphology, Orbiliaceae, Phylogeny

Phytotaxa 450 (3): 273–284
https://www.mapress.com/j/pt/

Article

ISSN 1179-3155 (print edition)
PHYTOTAXA
ISSN 1179-3163 (online edition)

https://doi.org/10.11646/phytotaxa.450.3.3

Fusarium xiangyunensis (Nectriaceae), a remarkable new species of nematophagous fungi from Yunnan, China

FA ZHANG[1,2,8], SHUO-RAN LIU[1,3,4,9], XIN-JUAN ZHOU[1,5,10], JUTAMART MONKAI[2,11], SINANG HONGSANAN[6,7,12], QIU-JU SHANG[2,13], KEVIN D. HYDE[2,14] & XIAO-YAN YANG[1,3,4,15*]

[1] *Institute of Eastern-Himalaya Biodiversity Research, Dali University, Dali, Yunnan 671003, P.R. China.*
[2] *Centre of Excellence in Fungal Research, Mae Fah Luang University, Chiang Rai 57100, Thailand.*
[3] *Key Laboratory of Yunnan State Education Department on Er'hai Lake Basin Protection and the Sustainable Development Research, Dali University, Dali, Yunnan 671003, P.R. China.*
[4] *The provincial innovation team of biodiversity conservation and utility of the three parallel rivers from Dali University, Dali University, Dali, Yunnan 671003, China.*
[5] *School of Public Health, Dali University, Dali, Yunnan 671003, P.R. China.*
[6] *Shenzhen Key Laboratory of Microbial Genetic Engineering, College of Life Sciences and Oceanography, Shenzhen University, Shenzhen 518060, P.R. China.*
[7] *Shenzhen Key Laboratory of Laser Engineering College of Optoelectronic Engineering Shenzhen University, Shenzhen, 518060, P. R. China.*
[8] *zhanglieasternhimalaya@gmail.com; https://orcid.org/0000-0002-3749-2948*
[9] *46795859@qq.com; https://orcid.org/0000-0003-3983-9949*
[10] *1391890018@qq.com; https://orcid.org/0000-0002-8119-9167*
[11] *mjutamart@gmail.com; https://orcid.org/0000-0001-6043-0625*
[12] *sinang333@gmail.com; https://orcid.org/0000-0003-0550-3152*
[13] *sqj1094860574@163.com; https://orcid.org/0000-0002-2861-3058*
[14] *kdhyde3@gmail.com; https://orcid.org/0000-0002-2191-0762*
[15] *yangxy@eastern-himalaya.cn; https://orcid.org/0000-0002-9304-308X*
**Corresponding author's email*

Abstract

Fusarium xiangyunensis sp. nov., isolated from hot-spring waterlogged soil in China, which is an endoparasitic fungus of nematodes, is described and illustrated. Evidence for the new species is provided by morphology and phylogenetic analyses of combined ITS, EF-1α and RPB1 sequence data. Phylogenetic analyses showed that *F. xiangyunensis* clustered with those species belonging to the *F. solani* species complex and grouped together with *F. witzenhausenense*. This species differs from *F. witzenhausenense* in habitat (parasitic on *Hibiscus* sp.), conidia and chlamydospores. Furthermore, the nematicidal activity of its microconidia was determined and causes infection and death of nematodes in both sterile water and solid medium.

Keywords: 1 new species, Adhesive microconidia, Endoparasitic nematodes, Phylogeny

Journal of *Fungi*

MDPI

Article

New *Arthrobotrys* Nematode-Trapping Species (Orbiliaceae) from Terrestrial Soils and Freshwater Sediments in China

Fa Zhang [1,2,3], Saranyaphat Boonmee [2,3], Jayarama D. Bhat [4], Wen Xiao [1,5,6] and Xiao-Yan Yang [1,5,*]

1 Institute of Eastern-Himalaya Biodiversity Research, Dali University, Dali 671003, China; zhangf@eastern-himalaya.cn (F.Z.); xiaow@eastern-himalaya.cn (W.X.)
2 Center of Excellence in Fungal Research, Mae Fah Luang University, Chiang Rai 57100, Thailand; saranyaphat.boo@mfu.ac.th
3 School of Science, Mae Fah Luang University, Chiang Rai 57100, Thailand
4 Department of Botany, Goa University, Taleigao 403206, India; bhatdj@gmail.com
5 Key Laboratory of Yunnan State Education Department on Er'hai Lake Basin Protection and the Sustainable Development Research, Dali University, Dali 671003, China
6 Yunling Back-and-White Snub-Nosed Monkey Observation and Research Station of Yunnan Province, Dali 671003, China
* Correspondence: yangxy@eastern-himalaya.cn

Abstract: *Arthrobotrys* is the most complex genus of Orbiliaceae nematode-trapping fungi. Its members are widely distributed in various habitats worldwide due to their unique nematode-trapping survival strategies. During a survey of nematophagous fungi in Yunnan Province, China, twelve taxa were isolated from terrestrial soil and freshwater sediment habitats and were identified as six new species in *Arthrobotrys* based on evidence from morphological and multigene (ITS, TEF, and RPB2) phylogenetic analyses. These new species i.e., *Arthrobotrys eryuanensis*, *A. jinpingensis*, *A. lanpingensis*, *A. luquanensis*, *A. shuifuensis*, and *A. zhaoyangensis* are named in recognition of their places of origin. Morphological descriptions, illustrations, taxonomic notes, and a multilocus phylogenetic analysis are provided for all new taxa. In addition, a key to known species in *Arthrobotrys* is provided, and the inadequacies in the taxonomic study of nematode-trapping fungi are also discussed.

Keywords: 6 new taxa; molecular phylogeny; morphological; nematode-trapping hyphomycetes; taxonomy

Citation: Zhang, F.; Boonmee, S.; Bhat, J.D.; Xiao, W.; Yang, X.-Y. New *Arthrobotrys* Nematode-Trapping Species (Orbiliaceae) from Terrestrial Soils and Freshwater Sediments in China. *J. Fungi* **2022**, *8*, 671. https://doi.org/10.3390/jof8070671

Biodiversity Data Journal 10: e96642
doi: 10.3897/BDJ.10.e96642

open access

Taxonomy & Inventories

Drechslerella daliensis and *D. xiaguanensis* (Orbiliales, Orbiliaceae), two new nematode-trapping fungi from Yunnan, China

Fa Zhang[‡,§,|], Saranyaphat Boonmee[§,|], Jutamart Monkai[§], Xiao-Yan Yang[‡,¶,#], Wen Xiao[‡,¶,#]

‡ Institute of Eastern-Himalaya Biodiversity Research, Dali University, Dali, China
§ Center of Excellence in Fungal Research, Mae Fah Luang University, Chiang Rai, Thailand
| School of Science, Mae Fah Luang University, Chiang Rai, Thailand
¶ Key Laboratory of Yunnan State Education Department on Er'hai Lake Basin Protection and the Sustainable Development Research, Dali University, Dali, China
# The provincial innovation team of biodiversity conservation and utility of the three parallel rivers from Dali University, Dali University, Dali, China

Corresponding author: Xiao-Yan Yang (yangxy@eastern-himalaya.cn)

Academic editor: Ning Jiang

Received: 23 Oct 2022 | Accepted: 02 Dec 2022 | Published: 16 Dec 2022

Citation: Zhang F, Boonmee S, Monkai J, Yang X-Y, Xiao W (2022) *Drechslerella daliensis* and *D. xiaguanensis* (Orbiliales, Orbiliaceae), two new nematode-trapping fungi from Yunnan, China. Biodiversity Data Journal 10: e96642. https://doi.org/10.3897/BDJ.10.e96642

Abstract

Background

Nematode-trapping fungi are a highly specialised group in fungi and are essential regulators of natural nematode populations. At present, more than 130 species have been discovered in Zygomycota (Zoopagaceae), Basidiomycota (*Nematoctonus*), and Ascomycota (Orbiliaceae). Amongst them, nematode-trapping fungi in Orbiliaceae have become the research focus of carnivorous fungi due to their abundant species. During the investigation of carnivorous fungi in Yunnan, China, four fungal strains isolated from burned forest soil were identified as two new nematode-trapping species in *Drechslerella* (Orbiliaceae), based on multigene phylogenetic analysis and morphological characters.

Journal of *Fungi*

MDPI

Article

Morphological and Phylogenetic Characterization of Five Novel Nematode-Trapping Fungi (Orbiliomycetes) from Yunnan, China

Fa Zhang [1,2,3], Yao-Quan Yang [2], Fa-Ping Zhou [2], Wen Xiao [2,4,5], Saranyaphat Boonmee [1,3,*] and Xiao-Yan Yang [2,4,*]

1 Center of Excellence in Fungal Research, Mae Fah Luang University, Chiang Rai 57100, Thailand; zhangf@eastern-himalaya.cn
2 Institute of Eastern-Himalaya Biodiversity Research, Dali University, Dali 671003, China; yangyaoquan0519@outlook.com (Y.-Q.Y.); 1572180239@163.com (F.-P.Z.); xiaow@eastern-himalaya.cn (W.X.)
3 School of Science, Mae Fah Luang University, Chiang Rai 57100, Thailand
4 The Provincial Innovation Team of Biodiversity Conservation and Utility of the Three Parallel Rivers Region, Dali University, Dali 671003, China
5 Yunling Back-and-White Snub-Nosed Monkey Observation and Research Station of Yunnan Province, Dali 671003, China
* Correspondence: saranyaphat.boo@mfu.ac.th (S.B.); yangxy@eastern-himalaya.cn (X.-Y.Y.)

Abstract: Nematode-trapping fungi are widely studied due to their unique morphological structure, survival strategy, and potential value in the biological control of harmful nematodes. During the identification of carnivorous fungi preserved in our laboratory, five novel nematode-trapping fungi were established and placed in the genera *Arthrobotrys* and *Drechslerella* based on morphological and multigene (*ITS*, *TEF*, and *RPB2*) phylogenetic analyses. *A. hengjiangensis* sp. nov. and *A. weixiensis* sp. nov. are characterized by producing adhesive networks to catch nematodes. *Dr. pengdangensis* sp. nov., *Dr. tianchiensis* sp. nov., and *Dr. yunlongensis* sp. nov. are characterized by producing constricting rings. Morphological descriptions, illustrations, taxonomic notes, and phylogenetic analysis are provided for all new taxa; a key for *Drechslerella* species is listed; and some deficiencies in the taxonomy and evolution study of nematode-trapping fungi are also discussed herein.

Citation: Zhang, F.; Yang, Y.-Q.; Zhou, F.-P.; Xiao, W.; Boonmee, S.;

Keywords: carnivorous fungi; new species; Orbiliaceae; phylogeny; trapping structure

Journal of *Fungi*

MDPI

Article

Arthrobotrys blastospora sp. nov. (Orbiliomycetes): A Living Fossil Displaying Morphological Traits of Mesozoic Carnivorous Fungi

Fa Zhang [1,2,3], Saranyaphat Boonmee [2,3], Yao-Quan Yang [1], Fa-Ping Zhou [1], Wen Xiao [1,4,5,6] and Xiao-Yan Yang [1,4,*]

1 Institute of Eastern-Himalaya Biodiversity Research, Dali University, Dali 671003, China; zhangf@eastern-himalaya.cn
2 Center of Excellence in Fungal Research, Mae Fah Luang University, Chiang Rai 57100, Thailand
3 School of Science, Mae Fah Luang University, Chiang Rai 57100, Thailand
4 Key Laboratory of Yunnan State Education Department on Er'hai Lake Basin Protection and the Sustainable Development Research, Dali University, Dali 671003, China
5 The Provincial Innovation Team of Biodiversity Conservation and Utility of the Three Parallel Rivers from Dali University, Dali University, Dali 671003, China
6 Yunling Black-and-White Snub-Nosed Monkey Observation and Research Station of Yunnan Province, Dali 671003, China
* Correspondence: yangxy@eastern-himalaya.cn

Abstract: The evolution of carnivorous fungi in deep time is still poorly understood as their fossil record is scarce. The approximately 100-million-year-old Cretaceous *Palaeoanellus dimorphus* is the earliest fossil of carnivorous fungi ever discovered. However, its accuracy and ancestral position has been widely questioned because no similar species have been found in modern ecosystems. During a survey of carnivorous fungi in Yunnan, China, two fungal isolates strongly morphologically resembling *P. dimorphus* were discovered and identified as a new species of *Arthrobotrys* (Orbiliaceae, Orbiliomycetes), a modern genus of carnivorous fungi. Phylogenetically, *Arthrobotrys blastospora* sp. nov. forms a sister lineage to *A. oligospora*. *A. blastospora* catches nematodes with adhesive networks and produces yeast-like blastospores. This character combination is absent in all other previously known modern carnivorous fungi but is strikingly similar to the Cretaceous *P. dimorphus*. In this paper, we describe *A. blastospora* in detail and discuss its relationship to *P. dimorphus*.

Keywords: blastospores; fossil fungi; nematode-trapping fungi; Orbiliaceae; relic species; trapping structures

Citation: Zhang, F.; Boonmee, S.; Yang, Y.-Q.; Zhou, F.-P.; Xiao, W.; Yang, X.-Y. *Arthrobotrys blastospora* sp. nov. (Orbiliomycetes): A Living Fossil Displaying Morphological Traits of Mesozoic Carnivorous Fungi.

Journal of *Fungi*

MDPI

Article

Multilocus Phylogeny and Characterization of Five Undescribed Aquatic Carnivorous Fungi (*Orbiliomycetes*)

Fa Zhang [1,2,3], Yao-Quan Yang [1], Fa-Ping Zhou [1], Wen Xiao [1,4,5], Saranyaphat Boonmee [2,3,*] and Xiao-Yan Yang [1,4,*]

1 Institute of Eastern-Himalaya Biodiversity Research, Dali University, Dali 671003, China; zhangf@eastern-himalaya.cn (F.Z.); yanyq@eastern-himalaya.cn (Y.-Q.Y.); zhoufp@eastern-himalaya.cn (F.-P.Z.); xiaow@eastern-himalaya.cn (W.X.)
2 Center of Excellence in Fungal Research, Mae Fah Luang University, Chiang Rai 57100, Thailand
3 School of Science, Mae Fah Luang University, Chiang Rai 57100, Thailand
4 The Provincial Innovation Team of Biodiversity Conservation and Utility of the Three Parallel Rivers Region, Dali University, Dali 671003, China
5 Yunling Back-and-White Snub-Nosed Monkey Observation and Research Station of Yunnan Province, Dali 671003, China
* Correspondence: saranyaphat.boo@mfu.ac.th (S.B.); yangxy@eastern-himalaya.cn (X.-Y.Y.)

Abstract: The diversity of nematode-trapping fungi (NTF) holds significant theoretical and practical implications in the study of adaptive evolution and the bio-control of harmful nematodes. However, compared to terrestrial ecosystems, research on aquatic NTF is still in its early stages. During a survey of NTF in six watersheds in Yunnan Province, China, we isolated 10 taxa from freshwater sediment. Subsequent identification based on morphological and multigene (*ITS*, *TEF1-α*, and *RPB2*) phylogenetic analyses inferred they belong to five new species within *Arthrobotrys*. This paper provides a detailed description of these five novel species (*Arthrobotrys cibiensis*, *A. heihuiensis*, *A. jinshaensis*, *A. yangbiensis*, and *A. yangjiangensis*), contributing novel insights for further research into the diversity of NTF and providing new material for the biological control of aquatic harmful nematodes. Additionally, future research directions concerning aquatic NTF are also discussed.

Keywords: aquatic habitat; *Arthrobotrys*; carnivorous fungi; new species; *Orbiliaceae*; phylogeny

Citation: Zhang, F.; Yang, Y.-Q.; Zhou, F.-P.; Xiao, W.; Boonmee, S.; Yang, X.-Y. Multilocus Phylogeny and

MYCOSPHERE X(X): X–X (2024) www.mycosphere.org ISSN 2077 7019
Doi 10.5943/mycosphere/X/X/X

ARTICLE

Burned forests may be excellent sites for discovery of new fungi: Tips from fifteen new species of rare Nematode-Trapping Fungi (Orbiliomycetes)

Zhang F[1,2,3], Zhou FP[1], Yang YQ[1], Boonmee S[2,3], Yu ZF[4], Bhat DJ[5], Jeewon R[6], Hyde KD[2,3]*, Yang XY[1,7]*, Xiao W[1,7,8]

[1] *Institute of Eastern-Himalaya Biodiversity Research, Dali University, Dali 671003, China.*
[2] *Center of Excellence in Fungal Research, Mae Fah Luang University, Chiang Rai 57100, Thailand.*
[3] *School of Science, Mae Fah Luang University, Chiang Rai 57100, Thailand.*
[4] *Laboratory for Conservation and Utilization of Bio-Resources, Key Laboratory for Microbial Resources of the Ministry of Education, Yunnan University, Kunming 650091, Yunnan, China.*
[5] *Department of Botany and Microbiology, College of Science, King Saud University, P.O. Box 2455, Riyadh 11451, Saudi Arabia*
[6] *Department of Health Sciences, Faculty of Medicine and Health Sciences, University of Mauritius, Reduit, Mauritius.*
[7] *The Provincial Innovation Team of Biodiversity Conservation and Utility of the Three Parallel Rivers Region, Dali University, Dali 671003, China.*
[8] *Yunling Back-and-White Snub-Nosed Monkey Observation and Research Station of Yunnan Province, Dali 671003, China.*

Citation – Zhang F, Zhou FP, Yang YQ, Boonmee S, Yu ZF, Bhat DJ, Jeewon R, Hyde KD, Yang XY, Xiao W 2024 – Burned forests may be excellent sites for discovery of new fungi: Tips from fifteen new species of rare Nematode-Trapping Fungi (Orbiliomycetes). Mycosphere X(X), X–X, Doi 10.5943/mycosphere/X/X/X

Abstract

Understanding the diversity in a given region is crucial for maintaining ecological stability and ensuring the sustainable utilization of fungal resources. Where and how undescovered fungi can be isolated is of concern to mycologists and biodiversity experts. During an investigation of nematode-trapping fungi (NTF) in three burned forests in Yunnan Province, China, we isolated 21 new species of rare NTF from 368 soil samples (18 *Dactylellina* and 3 *Drechslerella* species), which accounts for nearly 50% of the new species published in recent years (2010–2023). The discovery of numerous new and interesting fungal species in confined areas with limited samples is remarkable. This study reports 15 unpublished new NTF taxa isolated from burned forests, providing novel information and materials for application, diversity and evolutionary research of this group. More importantly, this paper extensively discusses the impact of forest fires on fungal diversity and further highlights a new pathway for the exploration of new and rare fungal resources.

Keywords – 15 new species – Burned forest – *Dactylellina* –Fungal diversity – Nematode-trapping fungi – Orbiliaceae – Pyrodiversity – Rare fungi

CURRICULUM VITAE

CURRICULUM VITAE

NAME Fa Zhang

EDUCATIONAL BACKGROUND

2015 Bachelor of Science
Biosciences
Dali University, China

WORK EXPERIENCE

2015-2017 Research assistant
Institution of Eastern Himalaya Research, China

PUBLICATION

First Author

Zhang, F., Zhou, X. J., Monkai, J., Li, F. T., Liu, S. R., Yang, X. Y., . . . Hyde, K. D. (2020). Two new species of nematode-trapping fungi (*Dactylellina*, Orbiliaceae) from burned forest in Yunnan, China. *Phytotaxa, 452*(1), 65–74. https://doi.org/10.11646/phytotaxa.452.1.6

Zhang, F., Liu, S. R., Zhou, X. J., Monkai, J., Hongsanan, S., Shang, Q. J., . . . Yang, X. Y. (2020). *Fusarium xiangyunensis* (Nectriaceae), a remarkable new species of nematophagous fungi from Yunnan, China. *Phytotaxa, 450*(3), 273–284. https://doi.org/10.11646/phytotaxa.450.3.3

Zhang, F., Boonmee, S., Bhat, J. D., Xiao, W., & Yang, X. Y. (2022). New *Arthrobotrys* nematode-trapping species (Orbiliaceae) from terrestrial soils and freshwater sediments in China. *Journal of Fungi, 8*(7), 671. https://doi.org/10.3390/jof8070671

Zhang, F., Boonmee, S., Monkai, J., Yang, X. Y, & Xiao, W. (2022). *Drechslerella daliensis* and *D. xiaguanensis* (Orbiliales, Orbiliaceae), two new nematode-trapping fungi from Yunnan, China. *Biodiversity Data Journal, 10*. https://doi.org/10.3897/BDJ.10.e96642

Zhang, F., Yang, Y. Q., Zhou, F. P, Xiao, W., Boonmee, S., & Yang, X. Y. (2023). Morphological and Phylogenetic Characterization of Five Novel Nematode-Trapping Fungi (Orbiliomycetes) from Yunnan, China. *Journal of Fungi, 9*(7), 735. https://doi.org/10.3390/jof9070735

Zhang, F., Boonmee, S., Yang, Y. Q., Zhou, F. P., Xiao, W., & Yang, X. Y. (2023). *Arthrobotrys blastospora* sp. nov.(Orbiliomycetes): A living fossil displaying morphological traits of mesozoic carnivorous fungi. *Journal of Fungi, 9*(4), 451. https://doi.org/10.3390/jof9040451

Zhang, F., Yang, Y. Q., Zhou, F. P, Xiao, W., Boonmee, S., & Yang, X. Y. (2024). Multilocus Phylogeny and Characterization of Five Undescribed Aquatic Carnivorous Fungi (Orbiliomycetes). *Journal of Fungi, 10*(1), 81. https://doi.org/10.3390/jof10010081

Zhang, F., Zhou F. P., Li, F. T., Yang, Y. Q., Yang, X. Y., & Xiao Wen. (In press). A potential strategy for pine wilt disease control: Promoting the growth of native nematophagous fungi. *Forest pathology*.

Zhang, F., Huang, S. Y., Yang, Y. Q., Zhou, F. P., Boonmee, S., Yang, X. Y., . . . Xiao, W. (In press). Urea regulates soil nematode population by enhancing the insecticidal ability of nematode-trapping fungi. *Scientific Reports*.

Zhang, F., Zhou, F. P., Yang, Y. Q., Boonmee, S., Yu, Z. F., Bhat, D. J., . . . Xiao, W. (In press). Burned forests as excellent area for the discovery of new fungal: Hints from fifteen rare novel carnivorous fungi in Orbiliomycete. *Mycosphere*.

Co-first author publications

Deng, W., Zhang, F., Li, Y. P., Zhang, X., Fornacca, D., Yang, X. Y., . . . Xiao, W. (2023). Uncovering the biogeographic pattern of the widespread nematode-trapping fungi *Arthrobotrys oligospora*: Watershed is the key. *Frontiers in Microbiology*, *14*, 1152751. https://doi.org/10.3389/fmicb.2023.1152751

Dou, Z. R., Zhang, F., Zhou, G. J., Gong, G. F., Ding, J. J, Fan, X. H., . . . Wang, K. L. (2023). *Varicosporellopsis shangrilaensis* sp. nov.(Nectriaceae, Hypocreales), a new terricolous species isolated from the rhizosphere soil of *Astragalus polycladus* in northwestern Yunnan, China. *Phytotaxa, 600*(4), 230–238. https://doi.org/10.11646/phytotaxa.600.4.2

Yang, X., Zhang, F., Yang, Y., Zhou, F., Boonmee, S., Xiao, W., . . . Yang, X. (2023). Conidia Fusion: A Mechanism for Fungal Adaptation to Nutrient-Poor Habitats. *Journal of Fungi, 9*(7), 755. ttps://doi.org/10.3390/jof9070755

Corresponding author publications

Zhao, E. M., Zhao, H. Y., Liu, G. Y., Jiang, J. B., Zhang, F., Zhang, J. L., . . . Yang, X. Y. (In press). Automated Recognition of Conidia of Nematode-Trapping Fungi Based on Improved YOLOv8. IEEE ACCESS.

Co-author publications

Rong, S., Zhou, X. J., Wang, H. Q., Zhang, F., Yang, X. Y., & Xiao, W. (2020). Succession of soil nematode-trapping fungi following fire disturbance in forest. *Journal of Forest Research*, *25*(6), 433–438. https://doi.org/10.1080/13416979.2020.1793465

Zhang, X., Zhang, F., Jiang, L., Yang, Y. Q., Yang, X. Y., & Xiao, W. (2022). Two new nematode-trapping fungi (*Arthrobotrys*, Orbiliaceae) from Yunnan, China. *Phytotaxa, 568*(3), 255–266. https://doi.org/10.11646/PHYTOTAXA.568.3.2

She, R., Zhou, X. J., Wang, H. Q., Zhang, F., Yang, X. Y., & Xiao, W. (2022). Natural recovery from fire disturbance is more favorable than assisted recovery for the restoration of soil nematode-trapping fungi. *Canadian Journal of Microbiology*, *68*(5), 329–339. https://doi.org/10.1139/cjm-2021-0237

Deng, W., Zhang, F., Fornacca, D., Yang, X. Y., & Xiao, W. (2023). Those nematode-trapping fungi that are not everywhere: Hints towards soil microbial biogeography. *Journal of Microbiology*, *61*(5), 511–523. https://doi.org/10.1007/s12275-023-00043-7

Yang, Y. Q., Zhang, F., Li, Z. Q., Zhou, F. P., Yang, X. Y., & Xiao, W. (2023). Morphological and multigene phylogenetic analyses reveal two new nematode-trapping fungi (*Arthrobotrys*, Orbiliaceae) from Yunnan, China. *Phytotaxa*, *591*(4), 263–272. https://doi.org/10.11646/PHYTOTAXA.591.4.3

Hyde, K. D., Norphanphoun, C., Ma, J., Yang, H. D., Zhang, J. Y., Du, T. Y., . . . Li, C. J. (2023). Mycosphere notes 387–412–novel species of fungal taxa from around the world. *Mycosphere*, *14*(1), 663–744.

She, R., Wang, H. Q., Fornacca, D., Li, F. T., Zhang, F., Yang, Y. Q., . . . Xiao, W. Independence and Synergy Effects of Heat and Ash on Forest Soil Nematode-Trapping Fungi Communities. Available at SSRN, 4102524. https://doi.org/10.3390/fire6010027